PHYSIOLOGICAL AND GENETIC DETERMINATION OF YIELD AND YIELD COMPONENTS IN A BREAD WHEAT × SPELT MAPPING POPULATION

By

QUAN XIE, BSc, MSc.

Thesis submitted to the University of Nottingham
for the degree of Doctor of Philosophy

MAY 2015

Abstract

A substantial increase in wheat yield is needed for global food security. This requires a comprehensive understanding of the physiological and genetic basis of yield determination. The present study aimed to dissect yield physiologically and genetically in a recombinant inbred line mapping population derived from bread wheat × spelt. A total of 201 traits were investigated in the field and glasshouse across three years, and these traits formed five themes: genetic variation in yield and yield components, and the usefulness of spelt as a genetic resource; tillering dynamics; biomass accumulation; flowering time and subsequent leaf senescence; and grain filling processes. Large genetic variation in all traits was found, and spelt showed many desirable traits and alleles independent of low threshability, so it can be used to broaden genetic diversity for yield improvement in bread wheat, while maintaining the free-threshing habit. Quantitative trait loci for tiller production and survival were identified, which were also affected by light environment under the canopy: low red:far red ratio (R:FR) led to early tillering cessation, few total shoots, high infertile shoot number and shoot abortion, probably resulting from an assimilate shortage due to early and enhanced stem growth induced by low R:FR. More fertile tillers normally contributed to plant yield and grain number, but reduced individual grain weight, partly because of smaller carpels and fewer stem water soluble carbohydrates at anthesis. In addition, preanthesis biomass accumulation increased yield and yield components. For grain weight, slightly early anthesis and delayed but fast leaf senescence were associated with larger grains. Carpel size at anthesis, grain dry matter and water accumulation, as well as grain morphological expansion, determined final grain weight, because of pleiotropy or tight gene linkages. These findings provide deeper insight into yield determination in wheat, and facilitate trait-based physiological and molecular breeding.

Acknowledgements

First, I would like to thank my supervisor Dr Debbie Sparkes, who is friendly, easy-going, patient and supportive at all times. I have received so much help from her: PhD application, settling down in UK and supervision for my study. During this project, she has given a lot of suggestions and assistance regarding experimental design, data collection and analysis, and feedback on different reports, conference abstracts, papers and thesis. The most impressive thing is the constant encouragement from her, with which I become more confident and brave about my study so that I am able to try many new ideas. I also thank my supervisor Dr Sean Mayes, who has taught me a lot about crop genetics.

This PhD project has been sponsored by the China Scholarship Council Research Excellence Scholarship, a joint funding from the China Scholarship Council (CSC) and University of Nottingham. I am very grateful to my sponsors, as this opportunity let me experience so many new things, both overseas life and academic research in a world-class institution.

I would like to thank Beat Keller (Institute of Plant Biology, University of Zurich, Switzerland) for providing the mapping population and Monika Messmer (Research Institute of Organic Agriculture, Switzerland) for providing the molecular marker data. I also thank John Alcock, Matthew Tovey, Fiona Wilkinson and Mark Meacham for their help with field trials, glasshouse experiments and laboratory work.

During this PhD, there was some hard time for me. Fortunately, my friends have always been with me. I wish to express appreciation to Menaka Fernando and her family, Ali Amamou, Thanita Boomsrangson, Yadgar Mahmood, Chuong Nguyen, Toby Townsend, Stephen Jones and Johar Roy for discussion, communications, and technical help. I thank Poh Ying Lim, Li Deng, Tingyan Peng, Ruoxin Liao and Yuqian Sun for their help and suggestions with data collection and compilation as well as statistical analysis. I also thank Chungui Lu, Guiping Sun, Valerie Owens, John Owens, Dave Sutcliffe, Jerry Griffiths and many others for their great friendship, which lets me have a wonderful life in Sutton Bonington Village in the past four years.

Finally, I am indebted to my parents and brother as well as my darling Shuyang Guo for their continuous supports and love, and they have always encouraged me to go through every hard time in my life.

Table of Contents

List of Abbreviations

Abbreviation	Full form
ADM	Accumulated dry matter
ANOVA	Analysis of variance
BC	Before Christ
c.	circa
C1	First carpel within a spikelet counting from rachis
C2	Second carpel within a spikelet counting from rachis
C3	Third carpel within a spikelet counting from rachis
CCI	Chlorophyll concentration index
CDMT	Contribution of dry matter translocation to yield
CGR	Crop growth rate
Chl	Chlorophyll
Chl_{accum}	Accumulated chlorophyll content
Chl_{loss}	Duration of rapid chlorophyll loss
Chl_{per}	Duration of chlorophyll persistence
Chl_{tot}	Total duration of chlorophyll persistence and loss
cM	centiMorgan
d	day
DAA	Degree days after anthesis
DMT	Dry matter translocation
DMTE	Dry matter translocation efficiency
DNA	Deoxyribonucleic acid
DW	Dry weight
e.g.	exempli gratia
et al	et alia
F_5	Fifth filial generation
FAO	Food and Agriculture Organization
Fig.	Figure
G1	First grain within a spikelet counting from rachis
G2	Second grain within a spikelet counting from rachis
G3	Third grain within a spikelet counting from rachis
GA	Green area
GA_{accum}	Accumulated green area
GA_{loss}	Duration of rapid green area loss
GA_{per}	Duration of green area persistence
GA_{tot}	Total duration of green area persistence and loss

Abbreviation	Full form
GF	Grain filling
GFR	Grain filling rate
GS	Growth stage
h	hour
H^2	Broad sense heritability
HI	Harvest index
i.e.	id est
K	Potassium
L/H	Grain length/height
L/W	Grain length/width
LI	Light interception
LOD	Logarithm of the odds
LSD	Least significant difference
MAS	Marker-assisted selection
Max chl	Maximum chlorophyll content
Max CLR	Maximum chlorophyll loss rate
Max GALR	Maximum green area loss rate
Mg	Magnesium
MQM	Multiple-QTL model
MWC	Maximum water content of grain
N	Nitrogen
NS	Not significant
^oC	degree Celsius
^oCd	degree day
P	Phosphorus
PAR	Photosynthetically active radiation
PGW	Potential grain weight
QTL	Quantitative trait locus
r	Correlation coefficient
R:FR	Red:far red ratio
R^2/r^2	Coefficient of determination
REML	Residual maximum likelihood
RFLP	Restriction fragment length polymorphism
RIL	Recombinant inbred line
RNA	Ribonucleic acid

Abbreviation	Full form
RUE	Radiation use efficiency
S.E.D./SED	Standard error of the difference of means
SEM	Standard error of the mean
SFI	Spike fertility index
SGR	Spike growth rate
SLA	Specific leaf area
SNP	Single nucleotide polymorphism
SPI	Spike partitioning index
spp.	species
SSR	Simple sequence repeat
T.	Triticum
TGW	Thousand grain weight
t_{max}	Time at maximum grain filling rate
t_{mwc}	Time at maximum grain water content
UK	United Kingdom
UN	United Nations
uon	University of Nottingham
USA	United States of America
USDA	United States Department of Agriculture
WAR	Water absorption rate of grain
WLR	Water loss rate of grain
WSC	Water soluble carbohydrate
YP	Yield partitioning within spike

List of Tables

(Table numbering: Table + chapter number + '-' + table number in that chapter)

List of Figures

(Figure numbering: Figure + chapter number + '-' + figure number in that chapter)

Chapter 1

General Introduction

Chapter 1 General introduction

1.1 Wheat origin and domestication

Wheat (Triticum spp.) was one of the Neolithic founder crops, and played an important role in the transition from hunter-gathering to a sedentary agrarian society approximately 12,000 years ago (Lev-Yadun et al., 2000; Abbo et al., 2013). The first wheat was diploid einkorn (T. boeoticum Boiss., genome A^bA^b), and grown in the Near-Eastern Fertile Crescent (Salamini et al., 2002; Kilian et al., 2007). Wild einkorn was then cultivated and produced the domesticated form (T. monococcum L.). Subsequently, a tetraploid wheat emmer (T. dicoccum Schübl., genome A^uA^uBB) became the most important crop in the Fertile Crescent. Emmer was domesticated from its wild progenitor, T. dicoccoides Koern., which was derived from the hybridisation between a wild diploid wheat (T. urartu Thum. ex Gandil., genome A^uA^u) and a relative of goat grass (Aegilops speltoides Tausch., genome SS, as the donor of the B genome) occurring during 300,000–500,000 years ago (Bottley et al., 2006; Peng et al., 2011). Next, expansion of domesticated tetraploid wheat resulted in sympatry with another goat grass (Ae. tauschii Coss., genome DD) and a spontaneous hybridisation between them took place about 9,000 years ago that gave rise to the emergence of hexaploid spelt (T. spelta L., genome A^uA^uBBDD) (McFadden and Sears, 1946; Dubcovsky and Dvorak, 2007; Peng et al., 2011). Finally, free-threshing forms (bread wheat T. aestivum L. and durum wheat T. durum Desf.) are usually considered as a result of mutations in spelt and emmer, respectively, about 8,500 years ago (Peng et al., 2011). However, the evolutionary sequence of spelt and bread wheat is still in debate. It has been proposed that spelt was derived from a hybridisation between free-threshing hexaploid wheat and hulled emmer (Blatter et al., 2004; Dvorak et al., 2012).

During wheat evolution, domestication was largely responsible for the appearance of current wheat. This process was a series of events for genetic selection to alter some key traits such as rachis fragility, glume tenacity and threshability, for better harvesting performance (Salamini et al., 2002). Wild einkorn and emmer have brittle spikes (spikes disarticulating into spikelets at maturity), and transformation of a brittle into non-brittle spike gave rise to domesticated forms (Salamini et al., 2002; Gill et al., 2007). The second domestication trait is tenacious glumes, which hinder the release of

seeds from spikelets. Einkorn and emmer (both wild and domesticated forms) as well as spelt, usually have tenacious glumes, whereas bread and durum wheats have soft ones. The free-threshing phenotype represents the final step of wheat domestication (Salamini et al., 2002). The most crucial gene governing this trait is Q, which is pleiotropic, not only conferring the free-threshing character but also influencing the threshability-related traits (e.g. glume tenacity and spike fragility) and spike morphology (e.g. spike shape, spike length, spikelet number and spike compactness) (Muramatsu, 1963; Jantasuriyarat et al., 2004; Simons et al., 2006).

1.2 Wheat cultivation today

On the basis of area grown, wheat is the most important crop in the world today; it ranks the 3rd behind maize and rice in terms of production (FAO, 2014). In 2014, it was globally grown on 222 million hectares of land, with a production of 723 million tonnes (Fig. 1-1) (FAO, 2014; USDA, 2015). The main type of wheat currently cultivated is hexaploid bread wheat, accounting for c. 95% of the total production; most of the remaining 5% is from tetraploid durum wheat (Shewry, 2009; Peng et al., 2011). Ancient wheats like einkorn, emmer and spelt, are grown as minor crops in some regions for use of traditional foods and organic farming (Konvalina et al., 2010; Zaharieva et al., 2010).

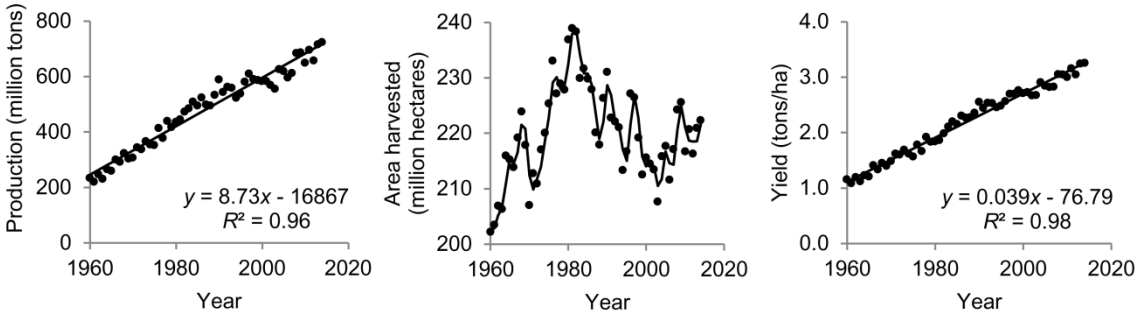

Fig. 1-1 Global wheat production, area harvested and yield from 1960 to 2014. Data sources from FAO and the United States Department of Agriculture (FAO, 2014; USDA, 2015).

Compared with other crops, wheat has a number of advantages contributing to its success: adaptability, productivity and end-use value. Wheat cultivation expands from South America and southern Oceania to North America, northern Europe and Asia, and from sea level to c. 3000 m (Slafer and Whitechurch, 2001). Adaptability to

diverse environments (latitude, radiation, temperature, water and soil) makes it serve as a key food source for humans worldwide. When grown under a broad range of environments, wheat can produce satisfactory yield, enabling it to provide 19% of the calories and 20% of the proteins to the world population (Braun et al., 2010). In addition, the unique properties of dough from wheat flour allow it to be processed into various foods such as bread, cake, noodle, dessert, pasta and biscuit (Shewry, 2009).

1.3 Challenges for wheat production

Since the Green Revolution, wheat production has increased greatly (Fig. 1-1), and played a key role in global food security. As a component of production, arable land area for wheat cultivation has decreased since the 1980s, although there seems a slight increase in recent years. Decline in land area predominantly results from urbanisation and land degradation in many countries, especially developing ones. During urbanisation, a large area of arable land is replaced with growing or new cities or towns, leading to irreversible land loss. Pollution from new cities, towns and factories worsens this process, making the nearby land unsuitable for cropping. Additionally, arable land degradation is accelerated, including erosion, desertification and salinisation, mainly as a result of the mismanagement of land and agricultural intensification. In future decades, increasing demands for meat and milk, as well as biofuels, will lead to a further competition for land to grow feed and biofuel crops.

While area under cultivation has decreased, wheat production has increased through the other component, i.e. yield, in the past 30 years. Yield has been increasing continuously, on average at a growth rate of 2.1% per year (USDA, 2015), benefiting from both plant genetic improvement and crop management. In 1960s, the dwarfing genes (Rht) were used to reduce plant height, leading to a substantial increase in grain number and harvest index (the proportion of grain weight to total plant biomass) (Brooking and Kirby, 1981; Youssefian et al., 1992; Flintham et al., 1997), and a reduced loss caused by lodging. Improvement of the post Green Revolution cultivars in resistance to diseases and pests has also contributed to yield gain (Singh and Trethowan, 2007). At the same time, wheat plants can grow under relatively favourable conditions by irrigation and applications of fertilisers (e.g. nitrogen, phosphate and potash) and biocides (e.g. pesticide, fungicide and herbicide), which reduces the gap between on-farm yields and yield potential.

A close look, however, reveals that yield progress has slowed down in the last two decades. Currently, annual yield growth rate is only around 1.0%, lower than that of demand (1.7%) (Reynolds et al., 2012; Ray et al., 2013; The Wheat Initiative, 2013). Rising demand for wheat production mainly stems from the increasing world population, predicted to exceed 9 billion by 2050 (United Nations, 2013), which, together with the changing dietary preferences, requires that global crop production is doubled by then (Ray et al., 2013). A further increase in wheat yield is essential to meet future food security. However, this is being challenged by global climate change. A warmer climate would result in high temperature and drought significantly influencing crop production, while an increase in frequency and magnitude of extreme weather makes crop production unpredictable. It has been predicted that there would be more frequent heat stress from booting to anthesis during wheat growth and development (Semenov et al., 2014), a key period to define grain number and potential grain size in wheat (Calderini et al., 2001; González et al., 2011). Heat stress occurring during this time decreases grain yield by 8–30%, due to reduction in both yield components (Lizana and Calderini, 2013; Semenov et al., 2014). Apart from global climate change, diminishing natural resources (e.g. fossil fuels) and rising prices for fertilisers, also limit yield advance in wheat (FAO, 2015).

1.4 Genetic improvement for wheat yield gain

As there is little new land to bring into production, future progress in wheat production will depend on improvement in grain yield. Genetic improvement of wheat plants has played a central role in boosting yield since the Green Revolution by changes in plant architecture (e.g. height) and increases in resistance to biotic and abiotic stresses. It is believed that this trend will continue, and that more efforts are needed to develop novel varieties with even higher yield (and quality). This is more important when considering environmental concerns from intensive agriculture. Ideal wheat varieties would require fewer fertilisers and biocides, minimising detrimental effects on agricultural ecosystems in a cost-effective way. Moreover, modifying key developmental periods and increased resistance to high temperature and drought, will enable wheat to grow and produce adequate yield under climate change. These can be achieved in conventional breeding by exploiting genetic variation in various agronomically important traits existing in elite varieties. There is much larger genetic variation in the Triticeae consisting of numerous relatives of wheat (approximately

350 species in 30 genera) (Feuillet and Muehlbauer, 2009). Desirable traits and genes in these relatives are able to be introduced into bread wheat by either traditional hybridisation (e.g. for hexaploid spelt), or wide crosses followed by cytogenetic techniques (e.g. for diploid rye).

1.5 Grain yield determination in wheat

To achieve genetic gain for wheat yield improvement, a first step is to understand its determination at genetic and physiological levels. Grain yield itself is an outcome of plant growth and development over the whole lifecycle, as well as interactions with environmental cues. Given its complexity, yield component approaches have long been used to dissect this trait. That is, yield can be divided into a number of relatively simpler components either numerically or physiologically (Slafer, 2007). Numerical components include grain number per unit land area and individual grain weight; the former has four sub-components, i.e. plants per unit land area, spikes per plant, spikelets per spike and grains per spikelet. The other approach is physiological, considering yield as a product of biomass and harvest index. Thus, factors affecting these components would determine final grain yield indirectly. Following this strategy, the next step is to identify the genetic and physiological basis underlying yield components and their secondary factors, taking account of trade-off between different traits.

For numerical components, plant number per unit land area depends on seed sown and establishment. Seed rates on farms are normally high (> 250 seeds m^{-2} in UK) to produce dense plant populations. Establishment includes seed germination, emergence and overwinter survival (if winter type), and is affected by sowing date, sowing depth, soil type (lower for loams and clays), soil moisture, overwinter weather (e.g. temperature), and pest and disease damage (Sylvester-Bradley et al., 2008). However, yield would not be reduced by slightly lower plant population due to compensatory tillering (Sylvester-Bradley et al., 2008). Tillering can occur from autumn to spring after plant emergence, depending on sowing time and temperature thereafter. A key function of tillering is to establish final spike number per plant. A plant can produce up to 35 shoots in total; however, not all tillers initiated finally form spikes: 10−80% usually die between the onset of stem elongation and anthesis, as affected by genotype, season, growing location, seeding rate and nutrient supply (Ishag and Taha, 1974; Hucl and Baker, 1989; Sharma, 1995; Berry et al., 2003; Sylvester-Bradley et al.,

2008). During tillering, spikelets are also being initiated (Slafer and Whitechurch, 2001), and a spike encompasses c. 16−25 spikelets. At the later stage of spikelet initiation, floret initiation takes place within spikelets. A spikelet has up to 10 florets, but fewer than five finally set grains (grains per spikelet); the remaining florets are aborted around anthesis (Kirby, 1988; González-Navarro et al., 2015). Different from grain number components, individual grain weight is mainly determined during postanthesis period, when the assimilates from current photosynthesis and vegetative organs are translocated and stored into grains until desiccation. It has been found that the preanthesis period (from booting to anthesis) is also critical for final grain weight. During this period, carpels grow rapidly, and may set an upper limit to grain weight (Calderini et al., 1999; Hasan et al., 2011).

Turning to physiological components, plant biomass is accumulated from emergence to whole-plant senescence via photosynthesis and resource capture from soil. Internally, plant biomass consists of different organs, including leaves, stems, spikes (plus grains), and roots. Externally, it is a product of light interception and radiation use efficiency (RUE, biomass per unit of radiation intercepted) (Reynolds et al., 2012). Canopy characteristics and photosynthetic capacity, therefore, are important traits increasing biomass. In addition, only grains are harvestable for direct food use. Harvest index (HI) has been used to describe the proportion of harvestable biomass. Current modern wheat varieties have HI of c. 0.45−0.50 (spring type) and 0.50−0.55 (winter type), approaching its theoretical maximum value (c. 0.64 in winter wheat) (Foulkes et al., 2011; Reynolds et al., 2012).

1.6 Objectives and hypotheses of this project

Despite many studies focusing on grain yield to date, how yield is determined at physiological and genetic levels is still unclear because of its complexity. As stated above, yield includes a number of components, and each component is formed through different physiological processes at different stages during plant growth and development. This requires that future studies should encompass all aspects of yield components to provide a comprehensive understanding of grain yield determination; at the same time, each aspect has to be demonstrated in detail to clarify the underlying mechanism, so that the knowledge can be transferred and realised in breeding. While analysing multiple yield components and their secondary traits, care must be taken to optimise any trade-offs between them to minimise negative effects.

Based on these concepts, this project was carried out to understand the physiological and genetic basis of yield and yield components of wheat. The specific objectives included:

- Determining the relationships between yield and yield components;
- Identifying a wide range of physiological traits associated with yield and yield components;
- Optimising the trade-offs between yield components and between the physiological traits;
- Understanding the genetic basis of the relationships between yield, yield components and associated physiological traits.

To achieve this, two field trials and one glasshouse experiment were conducted in three growing seasons, using a recombinant inbred line (RIL) mapping population. This population was derived from a cross between the Swiss winter bread wheat 'Forno' and Swiss winter spelt 'Oberkulmer', and consists of 226 F_5 RILs (Messmer et al., 1999). As a hexaploid relative and potential genetic resource of bread wheat, spelt Oberkulmer was deployed to introduce genetic variation in yield and yield components (e.g. larger but fewer grains) (Winzeler et al., 1994; Zanetti et al., 2001).

In this mapping population, a number of hypotheses were to be tested, each of which is presented in a chapter (**Chapters 2−6**).

Chapter 2: Spelt is a useful gene source to enlarge genetic variation in yield and yield components in the Forno × Oberkulmer mapping population; based on this variation, the relationships between yield and yield components are observed.

Chapter 3: Tillering dynamics determines final fertile shoots per plant, a major component of yield. Tiller production and survival are controlled by both genetic and environmental (e.g. light quality) factors.

Chapter 4: Biomass accumulation and partitioning, especially during preanthesis period, determine yield and yield components.

Chapter 5: Flowering time and subsequent leaf senescence affect individual grain weight.

Chapter 6: During grain filling, grain dry matter accumulation, grain water uptake and loss, and grain morphological expansion, are the physiological drivers of individual grain weight, and these traits share their genetic architectures to some extent.

As these chapters are prepared as journal papers, the references cited are included at the end of each chapter.

1.7 References

Abbo S, Lev-Yadun S, Heun M, Gopher A. 2013. On the 'lost' crops of the neolithic Near East. Journal of Experimental Botany **64**, 815-822.

Berry PM, Spink JH, Foulkes MJ, Wade A. 2003. Quantifying the contributions and losses of dry matter from non-surviving shoots in four cultivars of winter wheat. Field Crops Research **80**, 111-121.

Blatter R, Jacomet S, Schlumbaum A. 2004. About the origin of European spelt (Triticum spelta L.): allelic differentiation of the HMW Glutenin B1-1 and A1-2 subunit genes. Theoretical and Applied Genetics **108**, 360-367.

Bottley A, Xia GM, Koebner RMD. 2006. Homoeologous gene silencing in hexaploid wheat. The Plant Journal **47**, 897-906.

Braun HJ, Atlin G, Payne T. 2010. Multi-location testing as a tool to identify plant response to global climate change. In: Reynolds MP, ed. Climate Change and Crop Production. Surrey: CABI, 115-138.

Brooking IR, Kirby EJM. 1981. Interrelationships between stem and ear development in winter wheat: the effects of a Norin 10 dwarfing gene, Gai/Rht_2. Journal of Agricultural Science **97**, 373-381.

Calderini DF, Abeledo LG, Savin R, Slafer GA. 1999. Effect of temperature and carpel size during pre-anthesis on potential grain weight in wheat. Journal of Agricultural Science **132**, 453-459.

Calderini DF, Savin R, Abeledo LG, Reynolds MP, Slafer GA. 2001. The importance of the period immediately preceding anthesis for grain weight determination in wheat. Euphytica **119**, 199-204.

Dubcovsky J, Dvorak J. 2007. Genome plasticity a key factor in the success of polyploid wheat under domestication. Science **316**, 1862-1866.

Dvorak J, Deal KR, Luo M, You FM, von Borstel K, Dehghani H. 2012. The origin of spelt and free-threshing hexaploid wheat. Journal of Heredity **103**, 426-441.

FAO. 2014. FAOSTAT. http://faostat.fao.org/.

FAO. 2015. World Fertilizer Trends and Outlook to 2018. Rome: FAO.

Feuillet C, Muehlbauer GJ. 2009. Genetics and Genomics of the Triticeae. New York: Springer.

Flintham JE, Borner A, Worland AJ, Gale MD. 1997. Optimizing wheat grain yield: effects of Rht (gibberellin-insensitive) dwarfing genes. Journal of Agricultural Science **128**, 11-25.

Foulkes MJ, Slafer GA, Davies WJ, Berry PM, Sylvester-Bradley R, Martre P, Calderini DF, Griffiths S, Reynolds MP. 2011. Raising yield potential of wheat. III. Optimizing partitioning to grain while maintaining lodging resistance. Journal of Experimental Botany **62**, 469-486.

Gill BS, Li W, Sood S, Kuraparthy V, Friebe BR, Simons KJ, Zhang Z, Faris JD. 2007. Genetics and genomics of wheat domestication-driven evolution. Israel Journal of Plant Sciences **55**, 223-229.

González-Navarro OE, Griffiths S, Molero G, Reynolds MP, Slafer GA. 2015. Dynamics of floret development determining differences in spike fertility in an elite population of wheat. Field Crops Research **172**, 21-31.

González FG, Miralles DJ, Slafer GA. 2011. Wheat floret survival as related to pre-anthesis spike growth. Journal of Experimental Botany **62**, 4889-4901.

Hasan AK, Herrera J, Lizana C, Calderini DF. 2011. Carpel weight, grain length and stabilized grain water content are physiological drivers of grain weight determination of wheat. Field Crops Research **123**, 241-247.

Hucl P, Baker RJ. 1989. Tillering patterns of spring wheat genotypes grown in a semiarid environment. Canadian Journal of Plant Science **69**, 71-79.

Ishag HM, Taha MB. 1974. Production and survival of tillers of wheat and their contribution to yield. Journal of Agricultural Science **83**, 117-124.

Jantasuriyarat C, Vales M, Watson C, Riera-Lizarazu O. 2004. Identification and mapping of genetic loci affecting the free-threshing habit and spike compactness in wheat (Triticum aestivum L.). Theoretical and Applied Genetics **108**, 261-273.

Kilian B, Özkan H, Walther A, Kohl J, Dagan T, Salamini F, Martin W. 2007. Molecular diversity at 18 loci in 321 wild and 92 domesticate lines reveal no reduction of nucleotide diversity during Triticum monococcum (Einkorn) domestication:

implications for the origin of agriculture. Molecular Biology and Evolution **24**, 2657-2668.

Kirby EJM. 1988. Analysis of leaf, stem and ear growth in wheat from terminal spikelet stage to anthesis. Field Crops Research **18**, 127-140.

Konvalina P, Capouchova I, Stehno Z, Moudry J. 2010. Agronomic characteristics of the spring forms of the wheat landraces (einkorn, emmer, spelt, intermediate bread wheat) grown in organic farming. Journal of Agrobiology **27**, 9-17.

Lev-Yadun S, Gopher A, Abbo S. 2000. The cradle of agriculture. Science **288**, 1602-1603.

Lizana XC, Calderini DF. 2013. Yield and grain quality of wheat in response to increased temperatures at key periods for grain number and grain weight determination: considerations for the climatic change scenarios of Chile. Journal of Agricultural Science **151**, 209-221.

McFadden ES, Sears ER. 1946. The origin of Triticum spelta and its free-threshing hexaploid relatives. Journal of Heredity **37**, 107-116.

Messmer MM, Keller M, Zanetti S, Keller B. 1999. Genetic linkage map of a wheat × spelt cross. Theoretical and Applied Genetics **98**, 1163-1170.

Muramatsu M. 1963. Dosage effect of the spelta gene q of hexaploid wheat. Genetics **48**, 469-482.

Peng JH, Sun D, Nevo E. 2011. Domestication evolution, genetics and genomics in wheat. Molecular Breeding **28**, 281-301.

Ray DK, Mueller ND, West PC, Foley JA. 2013. Yield trends are insufficient to double global crop production by 2050. PLoS ONE **8**, e66428.

Reynolds M, Foulkes J, Furbank R, Griffiths S, King J, Murchie E, Parry M, Slafer G. 2012. Achieving yield gains in wheat. Plant Cell and Environment **35**, 1799-1823.

Salamini F, Özkan H, Brandolini A, Schäfer-Pregl R, Martin W. 2002. Genetics and geography of wild cereal domestication in the Near East. Nature Reviews Genetics **3**, 429-441.

Semenov MA, Stratonovitch P, Alghabari F, Gooding MJ. 2014. Adapting wheat in Europe for climate change. Journal of Cereal Science **59**, 245-256.

Sharma RC. 1995. Tiller mortality and its relationship to grain yield in spring wheat. Field Crops Research **41**, 55-60.

Shewry PR. 2009. Wheat. Journal of Experimental Botany **60**, 1537-1553.

Simons KJ, Fellers JP, Trick HN, Zhang Z, Tai YS, Gill BS, Faris JD. 2006. Molecular characterization of the major wheat domestication gene Q. Genetics **172**, 547-555.

Singh RP, Trethowan R. 2007. Breeding Spring Bread Wheat for Irrigated and Rainfed Production Systems of the Developing World. Iowa, USA: Blackwell Publishing.

Slafer GA. 2007. Physiology of determination of major wheat yield components. In: Buck HT, Nisi JE, Salomón N, eds. Wheat production in stressed environments. The Netherlands: Springer, 557-565.

Slafer GA, Whitechurch EM. 2001. Manipulating wheat development to improve adaptation. In: Reynolds MP, Ortiz-Monasterio JI, McNab A, eds. Application of Physiology in Wheat Breeding. Mexico: CIMMYT, 160-170.

Sylvester-Bradley R, Berry P, Blake J, Kindred D, Spink J, Bingham I, McVittie J, Foulkes J. 2008. The wheat growth guide. London: HGCA.

The Wheat Initiative. 2013. An International Vision for Wheat Improvement. Paris, France.

United Nations. 2013. World Population Prospects: the 2012 Revision. New York: United Nations.

USDA. 2015. World wheat supply and disapperance. http://www.ers.usda.gov/data-products/wheat-data.aspx.

Winzeler H, Schmid JE, Winzeler M. 1994. Analysis of the yield potential and yield components of F1 and F2 hybrids of crosses between wheat (Triticum aestivum L.) and spelt (Triticum spelta L.). Euphytica **74**, 211-218.

Youssefian S, Kirby EJM, Gale MD. 1992. Pleiotropic effects of the GA-insensitive Rht dwarfing genes in wheat. 2. Effects on leaf, stem, ear and floret growth. Field Crops Research **28**, 191-210.

Zaharieva M, Ayana N, Hakimi A, Misra S, Monneveux P. 2010. Cultivated emmer wheat (Triticum dicoccon Schrank), an old crop with promising future: a review. Genetic Resources and Crop Evolution **57**, 937-962.

Zanetti S, Winzeler M, Feuillet C, Keller B, Messmer M. 2001. Genetic analysis of bread-making quality in wheat and spelt. Plant Breeding **120**, 13-19.

Chapter 2

Physiological and Genetic Dissection of Grain Yield in the Bread Wheat Forno × Spelt Oberkulmer Mapping Population

2.1 Abstract

Novel germplasm resources are required to broaden the genetic diversity of bread wheat (Triticum aestivum L.) for further yield improvement. In this study, the usefulness of spelt (Triticum spelta L.) as a genetic resource to improve yield and yield components of bread wheat was determined. A recombinant inbred line mapping population of bread wheat cultivar Forno and spelt cultivar Oberkulmer was used to quantify the yield and yield components. Subsequently, quantitative trait loci (QTL) for the yield traits, together with grain threshability, were identified. Oberkulmer had larger grains (in 2012 season), more fertile tillers per plant, higher biomass, longer and laxer spikes than Forno. QTL analysis revealed six alleles for low threshability and two for tenacious glumes from the spelt, and the Q gene had major effects. Furthermore, 48 favourable alleles for yield and yield components were detected from Oberkulmer, and 85% of them were independent of those for low threshability and tenacious glumes. Therefore, spelt is a useful genetic resource for yield improvement of bread wheat, while maintaining the free-threshing habit. In addition, most of QTL for grain number components were coincident with those for grain weight. Analysis of allelic effects of the coincident QTL showed that increased grain number was associated with decreased grain weight, which explained their negative phenotypic relationships. Thus, the independent alleles of spelt could be used for simultaneous improvement of grain number and weight in bread wheat.

2.2 Introduction

Wheat is a dominant crop worldwide, providing 19% of the calories and 20% of the proteins consumed by humans (Braun et al., 2010). In the light of burgeoning world's population, 9.4 billion by 2050 as forecasted by the UN, a substantial increase in grain yield of wheat is needed to ensure global food security. The progress in grain yield, however, has fallen in the past 20 years (3.8% per annum from 1961 to 1989, but only 2% in 1990s and 1.6% in 2000s); should this trend continue over the next 30 years, the growth rate will drop to 1.1% per annum (FAO, 2014). Factors such as climate change, natural resource shortage and environmental pollution further threaten wheat productivity. Genetic improvement in wheat has greatly contributed to yield growth since the Green Revolution, and will still be the key requirement under environmental challenges in future decades. Grain yield is a complex trait, consisting of two major components, grain number per unit land area and individual grain weight. The former can be divided into four sub-components, i.e. plants per unit land area, spikes per plant, spikelets per spike, and grains per spikelet (Slafer, 2007). To further improve grain yield, both grain number and individual grain weight should be increased in parallel.

In empirical breeding, new varieties are usually selected from the progeny of the crosses of elite lines, with respective advantages of yield components or resistance to biotic or abiotic stresses. To hasten the development of new varieties, a limited number of currently used varieties are often adopted as parents. This strategy, however, has reduced genetic diversity in modern wheat, and made it harder to further raise yield potential. Exploitation of novel genetic resources has been considered as an alternative, as proposed by the international Wheat Yield Consortium (WYC) in 2009 (Reynolds et al., 2011). In the tribe Triticeae, the large number of relatives of wheat provide the potential to improve yield performance of bread wheat.

Spelt is an old-world crop cultivated since 5,000 BC; however, it currently remains a minor crop for the use of bread and feed in Europe and North America (Campbell, 1997). The height of cultivated spelts ranges from 90 to 130 cm, and the spikes are laxer and 4 to 7 cm longer than those of bread wheat (Campbell, 1997). As one of the hexaploid wheats, spelt has the same genome constitution as bread wheat (genome AABBDD). It can be hybridised with bread wheat easily, and their hybrids are fertile, which facilitates the transfer of desirable traits and genes to bread wheat. A high level of genetic diversity in spelt germplasm collections has been revealed by molecular

markers (Bertin et al., 2004). In addition, genetic variation in bread-making quality (Caballero et al., 2001, 2004; An et al., 2005), protein concentration (Stallknecht et al., 1996; Gomez-Becerra et al., 2010), lipid content (Ruibal-Mendieta et al., 2002) and mineral nutrient concentrations (for example, Zn, Fe and Se) (Ruibal-Mendieta et al., 2005; Zhao et al., 2009; Gomez-Becerra et al., 2010), has been reported. Spelt also shows resistance to abiotic and biotic stresses, such as aluminium (Raman et al., 2009), flooding (Burgos et al., 2001b), leaf rust (Dyck and Sykes, 1994; Wang et al., 2010; Mohler et al., 2012), yellow rust (Sun et al., 2002), leaf and glume blotch (Aguilar et al., 2005; Simon et al., 2010). Many genes and quantitative trait loci (QTL) associated with bread-making quality and stress resistance have been identified from spelt (Burgos et al., 2001a; Zanetti et al., 2001; Aguilar et al., 2005; Guzman et al., 2012; Mohler et al., 2012).

In contrast, only a few studies have focused on the yield and yield components of spelt, mainly because of its tenacious glumes and low threshability that make it difficult to separate grains from chaff. Significant genetic variation in yield and yield components has been observed in spelt: 4.2−6.0 t ha^{-1} for grain yield, 0.8−2.0 g for grain weight per spike, 15.3−47.1 mg for individual grain weight, 20−30 grains per spike, 18−33 spikelets per spike, 1.1−1.6 grains per spikelet, 10−47 tillers per plant, 6−24 spikes per plant, 14.3−15.7 t ha^{-1} for above-ground biomass, and 0.3−0.4 for harvest index (HI, the ratio of total grain to total shoot dry weight) (Winzeler et al., 1994; Stallknecht et al., 1996; Troccoli and Codianni, 2005; Hou et al., 2010; Konvalina et al., 2010; Koutroubas et al., 2012). Compared with bread wheat, spelt tends to have larger but fewer grains, and higher biomass but lower HI, resulting in less or comparable yield (Stallknecht et al., 1996; Abdel-Aal et al., 1997; Campbell, 1997; Konvalina et al., 2010; Koutroubas et al., 2012). Crosses between bread wheat and spelt have been made, and the F_1 hybrids show large heterosis effects on grain yield per spike, individual grain weight, and grain number per spike (Schmid and Winzeler, 1990; Winzeler et al., 1994), indicating different genetic architectures between the two hexaploid wheats. This genetic difference implies that spelt may provide a new gene source for yield improvement in bread wheat.

In this study, we aimed to investigate the usefulness of spelt as a genetic resource to improve yield and yield components of bread wheat, while avoiding its non-free-threshing habit. To achieve this, a recombinant inbred line mapping population,

derived from a cross between the bread wheat cultivar ‘Forno’ and spelt land variety ‘Oberkulmer’, was used. The previous studies indicated that Oberkulmer has larger but fewer grains, more spikes per plant and lower HI than Forno (Winzeler et al., 1994; Zanetti et al., 2001), and their F_1 hybrids exhibit a very high relative heterosis (Winzeler et al., 1994). Therefore, significant genetic variation in yield and yield components in this mapping population could be expected. This gave a chance to understand their genetic basis, and in turn, to exploit the favourable alleles from spelt for yield improvement in bread wheat. Genetic basis of yield and yield components was dissected by a QTL analysis. Furthermore, The QTL associated with grain threshability traits were also determined.

2.3 Materials and methods

2.3.1 Plant materials and field experiments

A total of 226 F_5 recombinant inbred lines (RILs) were produced from a cross between Swiss winter bread wheat (T. aestivum L. 'Forno') and Swiss winter spelt land variety (T. spelta L. 'Oberkulmer') (Messmer et al., 1999). Field experiments were carried out in two growing seasons: 2011–2012 (referred hereafter as 2012) and 2012–2013 (referred hereafter as 2013), at University of Nottingham Farm, Leicestershire, UK (52^o 50' N, 1^o 15' W, 50 m above sea level). Weather conditions during the two seasons are summarised in Fig. 2-1. The data of air temperature, rainfall and solar radiation were collected from the nearby meteorological station, and the historic station data from the Met Office (http://www.metoffice.gov.uk/) were compiled. The soil was a sandy loam (soil indices: N = 0, P = 4, K = 4, Mg = 4, pH = 7.6 in 2012; N = 0, P = 5, K = 4, Mg = 4, pH = 7.3 in 2013). An additional 140 (in 2012) and 160 (in 2013) kg N ha^{-1} in the form of ammonium nitrate prills were applied (three splits: early March, April and May). All the RILs, together with the parents, were arranged in a randomised complete block design with three replicates. The seeds were sown in 6 × 1.6 m plots on 19 October 2011 and in 12 × 1.6 m plots on 31 October 2012, with 250 seeds m^{-2}. A prophylactic programme of disease, weed and pest management was utilised to maintain undisturbed healthy crop growth. Nitrogen, potassium and phosphorus levels were maintained according to standard recommended agronomic practice. Phenotypic measurements such as grain threshability, machine-harvested grain yield, grains m^{-2} and thousand grain weight (TGW) were based on all 226 RILs. A subset including 72 RILs was selected in 2011−2012 season, with considerable differences in traits of interest, but similar flowering time (± 4 d in 2009−2010 and ± 1 d in 2010−2011) to minimise the confounding effect of different phasic development. This subset was enlarged to 110 RILs in 2012−2013 season. The remaining phenotypic measurements were carried out in the subsets.

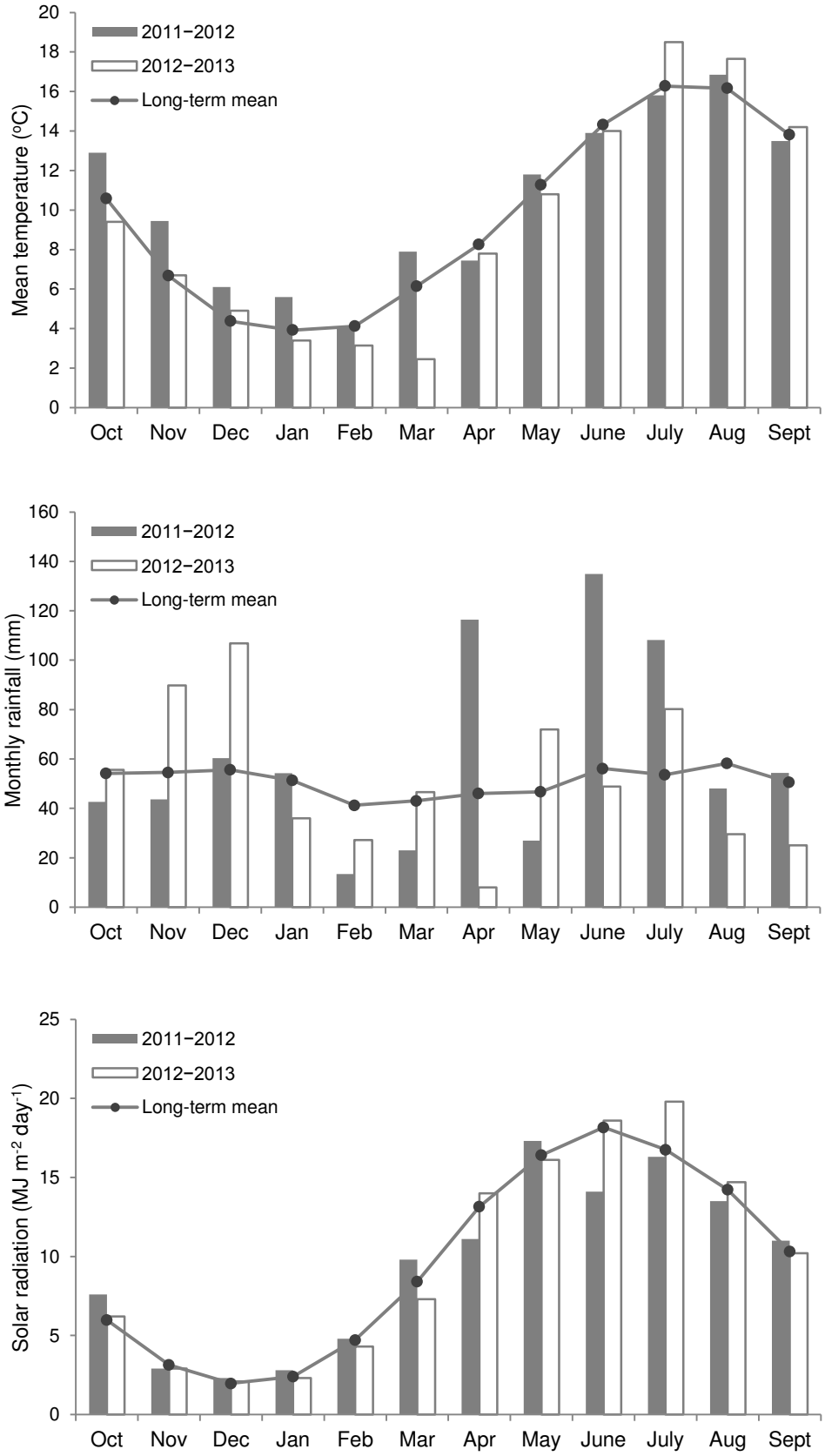

Fig. 2-1 Mean air temperature, rainfall and solar radiation at University of Nottingham Farm in 2011−2012 and 2012−2013 seasons. The long-term means of temperature (1959−2010), rainfall (1961−2010) and radiation (2000−2010) are also given.

2.3.2 Spike traits

Spike traits included grain threshability, glume tenacity, spike length and compactness. To measure percent threshability, 10 g grains were extracted randomly from the grain samples of each plot of 226 RILs after combining (2010, Sampo Rosenlew, Finland) at maturity. Both threshed and unthreshed grains of each sample were separated using a sieve, and counted by hand. Threshability was calculated as the percentage of completely threshed seeds from the total. Glume tenacity was assessed based on a scale of 1 (very soft glume) to 5 (very tenacious glume) in the subsets. This scale was developed by scoring the force necessary to detach or soften glumes at the base using forceps. Two spikelets in the middle of each of five spikes from each plot were tested. Spike length was measured on five spikes of main shoots in each plot, from the collars to tips of the spikes using a ruler, excluding the awns. The total spikelet number of each spike was counted. Spike compactness was then calculated by dividing the total spikelet number by spike length.

2.3.3 Yield and yield components

Yield and yield components (both numerical and physiological) were investigated at maturity. An area of 0.25 m^2 was sampled from each plot, and the total number of plants and fertile shoots (bearing spikes) was counted. Shoots (spikes) per plant and per m^2 were calculated by dividing the fertile shoot number by plant number, and by the fertile shoot number multiplying four, respectively. After cutting at ground level, a subsample of c. 70 g (with the fertile shoots counted) and 20 fertile shoots were obtained in 2012 and 2013, respectively. The spikes and stems of the subsamples were separated, dried in an oven at 85^{o}C for 48 h, and weighed. Dry weight per shoot was calculated by dividing the total dry weight of spikes and stems by shoot number, and then above-ground biomass m^{-2} was the dry weight per shoot multiplying shoots m^{-2}. The spikes were threshed by a thresher and completed by hand. Total grain dry weight was recorded, and grain weight per spike was calculated by dividing the total grain weight by shoot number. Grain yield m^{-2} was a consequence of grain weight per spike multiplying shoots m^{-2}, and subsequently converted into grain yield ha^{-1} (hand-harvested grain yield, HHY). Then, 250 grains were counted and weighed, and the average weight of individual grains was obtained. Grains per spike were calculated by dividing grain weight per spike by individual grain weight. Another five spikes were used to count the total spikelet number (and fertile and infertile spikelet number in

2013), and spikelets per spike (fertile and infertile spikelets per spike in 2013) were recorded. These spikes were also threshed, and the grains were counted to calculate the grains per spikelet. HI was the ratio of total grain to total shoot dry weight in the subsamples. After combining, the grain samples of 226 RILs were recorded for fresh weight and partly threshed; a subsample of 200 grains from each plot was then counted, oven-dried and weighed to calculate TGW. As most of the grain samples could not be threshed completely due to their low threshability, machine-harvested grain yield (MHY) was derived from the threshability analysis: MHY (t ha^{-1}) = (fresh weight of the total grain samples/10 g) * grain number in 10 g (the samples used for threshability analysis) * (TGW/1000) * 10^{-6}/ (harvested area in m^2 * 10^{-4}). Harvested area was calculated by measuring the actual plot length and width prior to combining. Grains m^{-2} were calculated as: grains m^{-2} = (fresh weight of the total grain samples/10 g) * grain number in 10 g/ harvested area.

2.3.4 Statistical analysis of phenotypic data

Genstat v17, GraphPad Prism v6.05 and Minitab v14 packages were used for statistical analysis for all phenotypic variables, including the use of ANOVA to test for the significance of genotypic effect, multiple comparisons (Fisher's unprotected LSD), regression analysis and Pearson correlations (the mean values across replicates used). Data were transformed by square root, logarithmic or arcsine methods to improve the normality of the trait distribution, if necessary. For each trait across years, linear mixed model analysis, using the method of residual maximum likelihood (REML), was performed to estimate the variance components, by considering environment (year) and replicate as fixed factors, and genotype and genotype-by-environment interaction as random factors. Broad sense heritability (H^2) of each trait was then estimated from the variance components using the following formula: $H^2 = \sigma_g^2/(\sigma_g^2 + \sigma_{ge}^2/n + \sigma_e^2/rn)$, where σ_g^2 is the genotypic variance, σ_{ge}^2 is the genotype-by-environment interaction variance, σ_e^2 is the error variance, n is the number of environments (years), and r is the number of replicates per environment.

2.3.5 QTL analysis

The genetic map of Forno × Oberkulmer is available in the GrainGenes database (http://wheat.pw.usda.gov/GG2/index.shtml). Linkage analysis was repeated with 182 polymorphic markers (RFLP and SSR) using the JoinMap v4 (Van Ooijen, 2006),

resulting in the same genetic map, with slightly different total coverage. This map included 230 segregating loci and 23 linkage groups, covering 2,469 cM (c. 2/3 of the whole genome of bread wheat and spelt) with an average marker density of 13.6 cM (Messmer et al., 1999). The MapQTL v6 software was used to carry out interval mapping to estimate the locations of significant QTL, logarithm of the odds (LOD) scores, additive effects and the percentage of phenotypic variation explained by individual QTL (R^2), based on the mean values over replicates of phenotypic data for each environment (Van Ooijen, 2009). The markers closest to the QTL peaks were selected as co-factors, and significant co-factors ($P < 0.02$) were used in the multiple-QTL model (MQM) mapping. A genome-wide significance threshold with a P-value of 0.05 was determined for each trait using a permutation test with 1,000 iterations. A QTL was declared present or significant when the LOD score was at or above the significance threshold in at least one year. Trait abbreviations and QTL designations were defined according to the Catalogue of Gene Symbols for Wheat (http://wheat.pw.usda.gov/GG2/Triticum/wgc/2008/); the 'Q' is followed by a trait designator, an institution designator (uon), and the suffixes consisting of the years in which a QTL was detected, and the parents providing the increasing alleles. The alleles from one of the parents, which increased the absolute values of the quantitative traits, were defined as increasing alleles. Accordingly, the other parent provided decreasing alleles, which relatively decreased the values of the same traits. The 1-LOD (drop-off from the QTL maximum LOD peaks) support intervals were used to estimate the map positions of significant QTL. The charts of linkage groups and locations of QTL were drawn using the MapChart v2.2 (Voorrips, 2002).

2.4 Results

2.4.1 Phenotypic analysis of spike traits, yield and yield components

Phenotypic differences in spike traits, yield and yield components between the spelt Oberkulmer and bread wheat Forno, and between the RILs, were found (Table 2-1 and Fig. 2-2). As expected, Oberkulmer had much lower threshability, tougher glumes, and longer but laxer spikes than Forno. Considerable genetic variation in spike traits was seen in the mapping population of Forno × Oberkulmer. Based on this variation, correlation analysis revealed that these traits were strongly associated with each other (Table 2-2). Glume tenacity was able to explain approximately 59% of the variation in threshability in both years (Fig. 2-3), indicating that more tenacious glumes were significantly associated with lower grain threshability. Spike compactness was mainly explained by the variation in spike length (79%) rather than spikelet number (Fig. 2-3 and Table 2-2). H^2 of the spike traits were high (0.82–0.95), indicating strong genetic control.

Yield and yield components were analysed through two approaches: numerical and physiological (Table 2-1). The spelt Oberkulmer had lower machine- and hand-harvested grain yield than the bread wheat Forno. Grain yield is a product of grain weight per spike and spikes per unit land area. Oberkulmer had lower grain weight per spike than Forno, but the difference was not significant. Oberkulmer also showed fewer spikes m^{-2}, particularly in 2012. In terms of other yield components, TGW was much higher in Oberkulmer in 2012, but lower in 2013, compared with Forno. Oberkulmer had fewer grains m^{-2} consistently across years. For grain number components, despite no significant differences in grains per spike, total spikelets per spike, grains per spikelet, Oberkulmer had fewer fertile spikelets and more infertile spikelets per spike than Forno, indicating its lower spikelet fertility. In addition, Oberkulmer tended to produce more fertile shoots per plant. Above-ground biomass m^{-2} was comparable between two parents, but Oberkulmer had higher dry weight per shoot, concurring with a lower HI. In the RILs, there were significant differences in all yield traits (Table 2-1). H^2 of hand-harvested yield, grain weight per spike, spikes per plant, above-ground biomass m^{-2} and HI were low, from 0.13 to 0.32, indicating large environmental effects.

Table 2-1 Descriptive statistics on spike traits, yield and yield components of the parents and recombinant inbred line (RIL) mapping population

Trait	Year	Parental lines			RILs			
		Forno	Oberkulmer	P-value	Mean (min; max)	P-value	S.E.D.	$H^{2\dagger}$
Threshability (%)	2012	98.1	25.5	< 0.01	52.7 (7.0; 99.5)	< 0.001	9.0	0.82
	2013	99.7	46.9	< 0.01	79.4 (27.1; 100.0)	< 0.001	5.8	
Glume tenacity (scores)	2012	1.1	3.5	< 0.01	3.3 (1.1; 5.0)	< 0.001	0.5	0.90
	2013	1.1	4.1	< 0.01	2.9 (1.0; 4.2)	< 0.001	0.4	
Spike length (cm)	2012	10.6	16.0	< 0.01	12.9 (9.1; 16.8)	< 0.001	0.7	0.92
	2013	9.7	18.1	< 0.01	13.3 (8.2; 19.7)	< 0.001	0.6	
Spike compactness (spikelets cm^{-1})	2012	2.1	1.3	< 0.01	1.7 (1.3; 2.6)	< 0.001	0.07	0.95
	2013	2.1	1.1	< 0.01	1.6 (1.1; 2.8)	< 0.001	0.06	
Machine-harvested grain yield (t ha^{-1})	2012	7.37	5.28	< 0.01	5.06 (2.62; 8.07)	< 0.001	0.58	0.60
	2013	9.56	5.60	< 0.01	6.48 (3.74; 10.39)	< 0.001	0.97	
Hand-harvested grain yield (t ha^{-1})	2012	5.15	3.42	< 0.05	4.13 (2.41; 6.17)	< 0.001	0.78	0.27
	2013	8.84	7.47	> 0.05	8.06 (5.34; 10.99)	< 0.01	1.22	
Grain weight per spike (g)	2012	1.48	1.38	> 0.05	1.46 (0.84; 1.96)	< 0.001	0.19	0.32
	2013	1.84	1.60	> 0.05	1.81 (1.21; 2.32)	< 0.001	0.15	
Thousand grain weight (g)	2012	33.9	47.3	< 0.01	40.7 (30.4; 50.5)	< 0.001	1.7	0.74
	2013	49.4	44.8	< 0.01	45.2 (33.9; 52.6)	< 0.001	1.3	
Grains m^{-2}	2012	20296	12393	< 0.01	12505 (5976; 21056)	< 0.001	1309	0.77
	2013	19367	12519	< 0.01	14389 (8476; 24864)	< 0.001	2086	
Grains per spike	2012	40	33	> 0.05	37 (24; 51)	< 0.001	4.6	0.78
	2013	38	36	> 0.05	40 (26; 54)	< 0.001	2.8	
Spikelets per spike	2012	22	21	> 0.05	22 (18; 25)	< 0.001	0.8	0.88
	2013	20	21	> 0.05	21 (19; 24)	< 0.001	0.6	
Fertile spikelets per spike	2013	19.5	17.3	< 0.05	19.1 (16.6; 22.4)	< 0.001	0.9	0.60
Infertile spikelets per spike	2013	0.9	3.5	< 0.01	2.0 (0.1; 4.2)	< 0.001	0.4	0.79
Grains per spikelet	2012	1.8	1.5	> 0.05	1.7 (1.1; 2.2)	< 0.001	0.2	0.75
	2013	1.9	1.8	> 0.05	1.9 (1.3; 2.5)	< 0.001	0.2	
Spikes m^{-2}	2012	726	472	< 0.01	544 (392; 848)	< 0.001	77	0.71
	2013	480	468	> 0.05	449 (300; 628)	< 0.001	54	
Spikes per plant	2012	2.6	2.9	> 0.05	2.5 (1.7; 3.3)	< 0.001	0.3	0.17
	2013	2.7	6.6	< 0.01	5.0 (2.5; 8.2)	< 0.001	0.8	
Above-ground biomass m^{-2} (g)	2012	1765	1443	> 0.05	1568 (1018; 1914)	< 0.05	182	0.28
	2013	1719	1914	> 0.05	1829 (1391; 2428)	< 0.001	249	
Dry weight per shoot (g)	2012	2.41	3.05	< 0.01	2.89 (1.94; 3.92)	< 0.001	0.20	0.69
	2013	3.58	4.09	< 0.05	4.11 (2.69; 5.21)	< 0.001	0.25	
Harvest index	2012	0.29	0.24	> 0.05	0.26 (0.16; 0.35)	< 0.001	0.03	0.13
	2013	0.51	0.39	< 0.01	0.44 (0.35; 0.49)	< 0.001	0.01	

† Broad sense heritability.

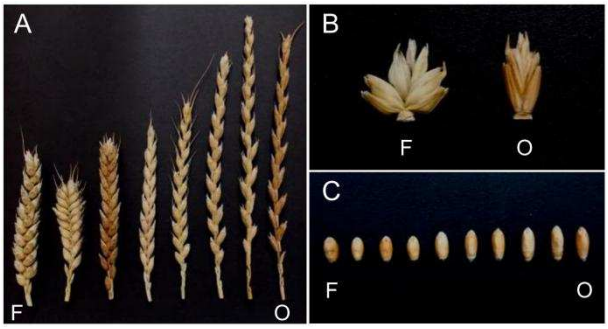

Fig. 2-2 Phenotypic variation in spike traits and grain size of the parents and mapping population. (A) Morphological variation in spike shapes (square or speltoid), length and compactness. (B) Spikelets of Forno and Oberkulmer showing the soft (Forno) and tenacious (Oberkulmer) glumes. (C) Grain size variation. F, bread wheat 'Forno'; O, spelt 'Oberkulmer'.

Correlation analysis showed that grain yield was positively associated with grain weight per spike, spikes m^{-2}, grains m^{-2}, biomass m^{-2} and HI (Table 2-2). Interestingly, TGW was negatively correlated with all the grain number components (grains m^{-2}, grains per spike, spikelets per spike, fertile spikelets per spike, grains per spikelet, and spikes m^{-2}, spikes per plant). For grain number components, grains m^{-2} were positively associated with grains per spike, spikes m^{-2}, fertile spikelets per spike and grains per spikelet. Grains per spike were positively correlated with the other grain number components within a plant, and exhibited a strong relationship with grains per spikelet, indicating the importance of floret fertility rather than spikelet number per spike.

Fig. 2-3 Relationships between spike traits in the Forno × Oberkulmer mapping population. The lower linear equation indicates the regression analysis in 2012, while the upper one indicates the regression analysis in 2013. In the graph of spike length and compactness, one common line could be fitted to explain both years.

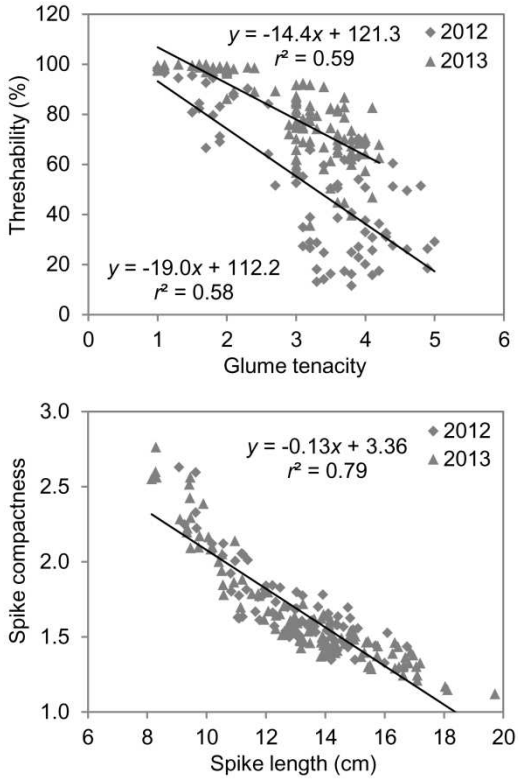

Table 2-2 Phenotypic correlation analysis of spike traits, yield and yield components in the Forno × Oberkulmer mapping population

Trait[†‡]	THR	GT	SL	SC	MHY	HHY	GWS	TGW	GPSM	GPS	SPS	FSS	ISS	GPST	SPSM	SPP	BPSM	DWS	HI
THR	1	-0.76**	-0.54**	0.60**	0.31**	0.35**	-0.17	-0.26**	0.40**	-0.04	0.16	–[§]	–	-0.19	0.22	0.10	0.04	-0.25*	0.37**
GT	-0.77**	1	0.49**	-0.65**	-0.38**	-0.17	0.21	0.31**	-0.50**	-0.01	-0.30**	–	–	0.20	-0.22	-0.06	0.09	0.34**	-0.25*
SL	-0.63**	0.71**	1	-0.82**	-0.16	-0.18	0.28*	0.21	-0.26*	0.23*	0.23*	–	–	0.18	-0.20	0.11	0.19	0.42**	-0.31**
SC	0.62**	-0.73**	-0.91**	1	0.12	0.09	-0.33**	-0.35**	0.29*	-0.06	0.34**	–	–	-0.31**	0.19	-0.04	-0.14	-0.37**	0.18
MHY	0.69**	-0.64**	-0.58**	0.55**	1	0.53**	0.34**	0.18	0.86**	0.14	-0.07	–	–	0.17	0.17	0.03	0.32**	0.11	0.35**
HHY	-0.02	0.11	0.13	-0.15	0.16	1	0.28*	0.34**	0.35**	-0.03	-0.20	–	–	0.06	0.16	0.12	0.46**	0.20	0.82**
GWS	-0.21*	0.38**	0.36**	-0.29**	-0.05	0.55**	1	0.47**	0.11	0.53**	-0.13	–	–	0.69**	-0.38**	-0.35**	0.18	0.67**	0.82**
TGW	0.15*	-0.13	-0.25**	0.13	0.18	-0.19*	0.14	1	-0.26*	-0.45**	-0.50**	–	–	-0.15	-0.45**	-0.45**	-0.02	0.55**	0.28*
GPSM	0.61**	-0.59**	-0.49**	0.50**	0.91**	0.22*	-0.10	-0.23*	1	0.31**	0.09	–	–	0.25*	0.43**	0.25*	0.30**	-0.20	0.18
GPS	-0.31**	0.40**	0.46**	-0.33**	-0.17	0.54**	0.78**	-0.50**	0.02	1	0.31**	–	–	0.83**	-0.03	0.19	0.17	0.42**	0.72**
SPS	-0.04	-0.02	0.17	0.19*	-0.07	-0.03	0.16	-0.38**	0.05	0.39**	1	–	–	-0.19	0.03	0.14	0.06	0.02	-0.24*
FSS	0.06	-0.10	-0.09	0.32**	0.14	0.05	0.17	-0.22*	0.21*	0.30**	0.74**	1	–	–	–	–	–	–	–
ISS	-0.14	0.11	0.37**	-0.15	-0.30**	-0.10	0.00	-0.24*	-0.21*	0.15	0.41**	-0.30**	1	–	–	–	–	–	–
GPST	-0.32**	0.44**	0.42**	-0.44**	-0.17	0.58**	0.77**	-0.37**	-0.02	0.90**	-0.03	-0.02	-0.02	1	-0.03	0.14	0.16	0.37**	0.79**
SPSM	0.18	-0.25**	-0.23*	0.14	0.23*	0.49**	-0.45**	-0.33**	0.36**	-0.23*	-0.21*	-0.14	-0.11	-0.17	1	0.67**	0.58**	-0.70**	-0.18
SPP	-0.46**	0.56**	0.56**	-0.54**	-0.53**	0.17	0.13	-0.32**	-0.41**	0.31**	0.00	-0.17	0.22*	0.34**	0.04	1	0.48**	-0.40**	-0.17
BPSM	-0.06	0.15	0.24*	-0.23*	-0.02	0.91**	0.43**	-0.17	0.04	0.43**	0.01	-0.01	0.03	0.44**	0.51**	0.26**	1	0.15	-0.11
DWS	-0.26**	0.43**	0.49**	-0.39**	-0.25**	0.36**	0.90**	0.20*	-0.32**	0.66**	0.23*	0.13	0.15	0.61**	-0.55**	0.22*	0.43**	1	0.14
HI	0.06	-0.04	-0.20*	0.14	0.41**	0.47**	0.40**	-0.09	0.44**	0.39**	-0.10	0.10	-0.29**	0.47**	0.10	-0.14	0.06	-0.04	1

*Significant at $P < 0.05$, ** significant at $P < 0.01$.

[†] Top right matrix: 2012 season; down left matrix: 2013 season.

[‡] Abbreviations for the traits: THR, threshability; GT, glume tenacity; SL, spike length; SC, spike compactness; MHY, machine-harvested grain yield; HHY, hand-harvested grain yield; GWS, grain weight per spike; TGW, thousand grain weight; GPSM, grains m^{-2}; GPS, grains per spike; SPS, spikelets per spike; FSS, fertile spikelets per spike; ISS, infertile spikelets per spike; GPST, grains per spikelet; SPSM, spikes m^{-2}; SPP, spikes per plant; BPSM, (above-ground) biomass m^{-2}; DWS, dry weight per shoot; HI, harvest index.

[§] Data absent.

Significant correlations between spike traits, and yield and yield components, were also found (Table 2-2). Grain threshability and spike compactness (the higher values seen in Forno) were positively correlated with grain yield, grains m^{-2} and HI, but negatively correlated with grain weight per spike, grains per spike and spikelet, spikes per plant and dry weight per shoot, with a few exceptions in either 2012 or 2013. In contrast, spike length and glume tenacity (the higher values seen in Oberkulmer) had the opposite relationships with these yield traits. It seems that the genetic factors distinguishing spelt from bread wheat by different spike features (threshability, glume tenacity, spike length and compactness), could also affect the yield and yield components.

2.4.2 QTL identification for the spike traits, yield and yield components

A total of 124 significant QTL for spike traits, yield and yield components, scattered across 19 different chromosomes (excluding only the 3D and 7A of wheat genome), were detected in the Forno × Oberkulmer mapping population over two years (Fig. 2-4, Tables 2-3 and 2-4).

2.4.2.1 QTL for spike traits

Thirty-seven significant QTL for spike traits were identified, with 12 QTL for threshability, five for glume tenacity, 12 for spike length and eight for spike compactness (Fig. 2-4, Tables 2-3 and 2-4). 76% of the QTL were from the A genome of wheat, 19% from the B genome and 5% from the D genome, indicating that the A genome was key to control spike traits, although it needs to be borne in mind that the D genome is classically poorly represented in genetic maps of wheat. These QTL had LOD scores ranging from 3.0 to 27.3, explaining 7.0–63.6% of the phenotypic variation. Across the whole genome, three QTL clusters for spike traits were found on chromosomes 3A, 4A and 5A. Many increasing alleles for threshability and spike compactness were coincident or linked, and had the same parents as conferrers, and so did those for glume tenacity and spike length, which explained the close, positive phenotypic correlations between threshability and spike compactness, and between glume tenacity and spike length (Fig. 2-4 and Table 2-2). The parents conferring the linked increasing alleles for threshability and spike compactness, however, were opposite to those conferring the increasing alleles for glume tenacity and spike length,

which supported the close but negative phenotypic relationships between threshability and glume tenacity, and between spike compactness and length (Fig. 2-3 and Fig. 2-4).

Oberkulmer and Forno both provided increasing alleles for spike traits (Fig. 2-4, Tables 2-3 and 2-4). Six alleles for low threshability (located on chromosomes 2A, 2B, 4A, and 5A), two for tenacious glumes (on 5A), three for long spikes (on 3B and 5A), and two for lax spikes (on 5A), were detected from the spelt Oberkulmer. As a bread wheat, Forno also had 24 alleles contributing to the characteristic speltoid spike phenotype. The QTL on 5AL (closest marker Xpsr918b-5A) had major effects on all spike traits, accounting for an average of 41.7% of the phenotypic variation for threshability over two years, 59.8% for glume tenacity, 40.1% for spike length and 46.6% for spike compactness. The marker Xpsr145-5A, which was also closely linked with these QTL above, is a flanking marker of the Q gene conferring the free-threshing habit (Muramatsu, 1963; Kato et al., 1998; Simonetti et al., 1999; Jantasuriyarat et al., 2004; Simons et al., 2006); thus, the QTL on 5AL in this study should correspond to the Q gene.

2.4.2.2 QTL for yield and yield components

A total of 87 significant QTL for yield and yield components were found, with five QTL for machine- and hand-harvested yield, three for grain weight per spike, 19 for TGW, 54 for grain number components, four for dry weight per shoot, and two for HI (Fig. 2-4, Tables 2-3 and 2-4). These QTL were located on 19 different chromosomes, individually explaining 6.5–26.7% of the phenotypic variation, indicating the complexity and polygenic nature of yield and yield components.

Among these QTL, 50 increasing alleles were identified from Oberkulmer, and 37 from Forno. Using the numerical approach, nine increasing alleles for TGW were detected from Oberkulmer; seven of them (78%) were coincident or linked with the increasing alleles for grain number components from Forno, and the remaining two alleles were independent. In addition, 31 increasing alleles for grain number components (excluding infertile spikelets per spike) were detected from Oberkulmer; 21 of them (68%) were coincident or linked with the increasing alleles for TGW from Forno, and the remaining 10 alleles were independent. Thus, 70% of the favourable alleles for TGW and grain number components in Oberkulmer were mapped to the

genomic regions where, in Forno counterparts, the favourable alleles for yield components were also mapped.

Considering all QTL from both parents, 40 (80%) QTL for grain number components were coincident or linked with those for TGW: 36 QTL with the opposite parents as increasing allele conferrers, and only four with the same parents as conferrers (Table 2-5). The remaining 10 QTL for grain number components were independent. In other words, the favourable alleles for grain number components were usually coincident or linked with unfavourable alleles for TGW in each of the parents, and vice versa. This is consistent with the negative relationships between grain number components and TGW. Within grain number components, the coincident QTL were often identified, with the increasing alleles usually conferred by the same parents, which explained the positive phenotypic correlations among them.

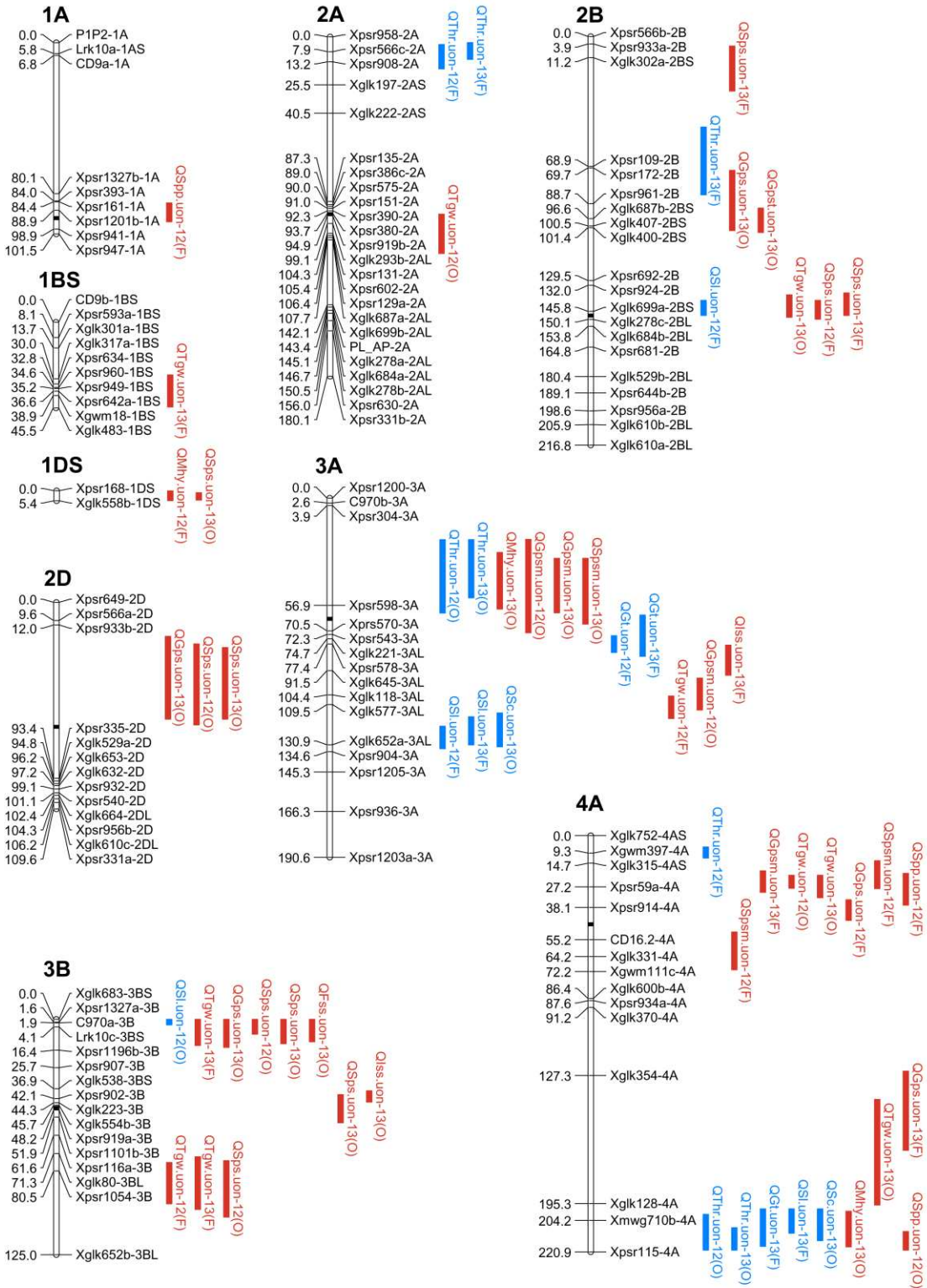

Fig. 2-4 (see the caption below)

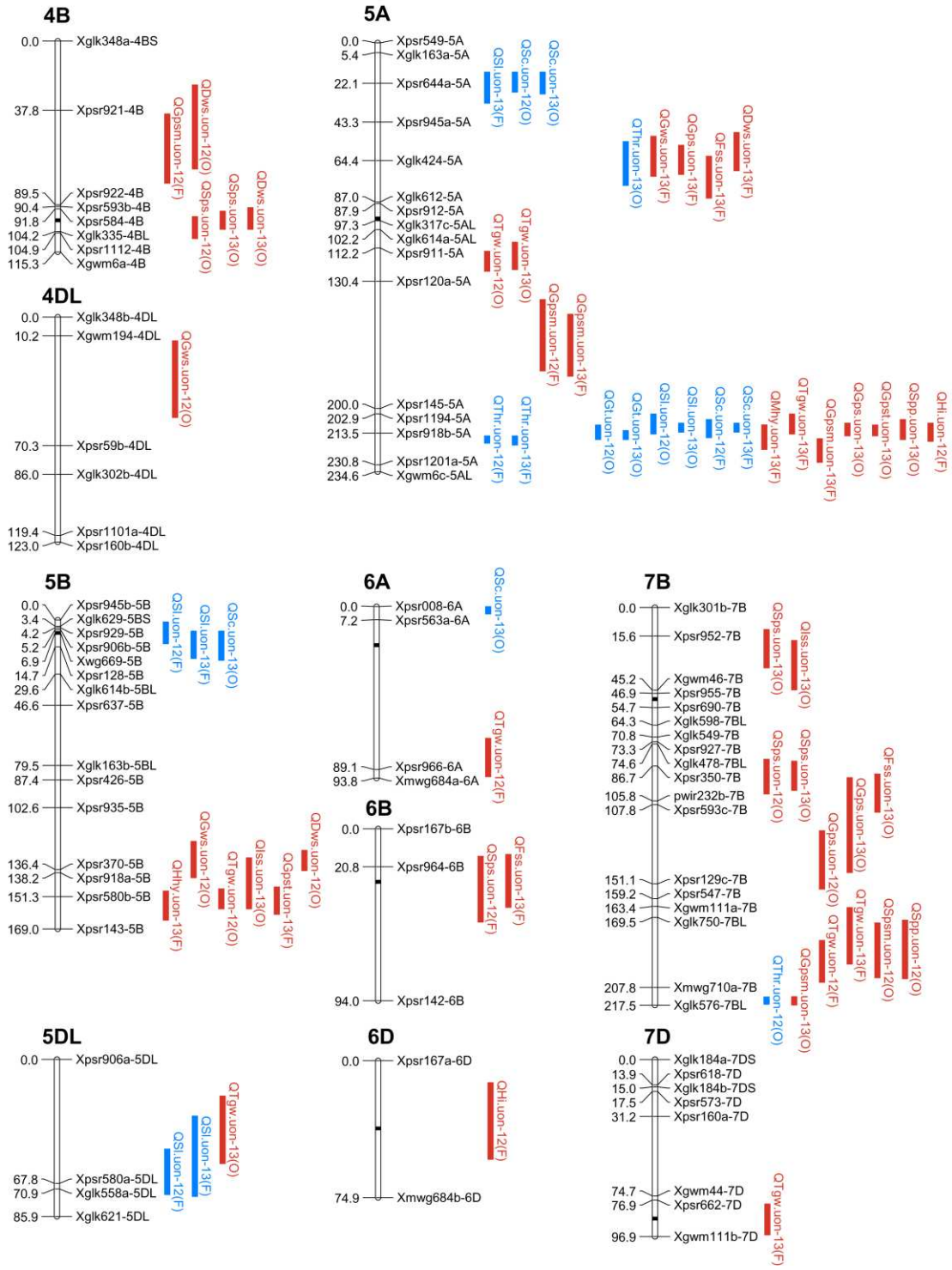

Fig. 2-4 (continued; see the caption below)

Fig. 2-4 Quantitative trait loci (QTL) associated with spike traits, yield and yield components in the Forno × Oberkulmer mapping population. The 1-LOD support intervals of significant QTL are indicated by blue (spike traits) and red (yield components) vertical bars. For locus symbols, the 'Q' is followed by the abbreviated names of quantitative traits and laboratory (uon). Abbreviations for the traits: Thr, threshability; Gt, glume tenacity; Sl, spike length; Sc, spike compactness; Mhy, machine-harvested yield; Hhy, hand-harvested yield; Gws, grain weight per spike; Tgw, thousand grain weight; Gpsm, grains m^{-2}; Gps, grains per spike; Sps, spikelets per spike; Fss, fertile spikelets per spike; Iss, infertile spikelets per spike; Gpst, grains per spikelet; Spsm, spikes m^{-2}; Spp, spikes per plant; Bpsm, biomass m^{-2}; Dws, dry weight per shoot; Hi, harvest index. The QTL detected in 2012 and 2013 are indicated by the suffixes 12 and 13, respectively. In the parentheses, the parents providing the increasing alleles (increasing the values of traits) are shown: F, Forno; O, Oberkulmer.

Table 2-3 Summary of the quantitative trait loci (QTL) detected in the Forno × Oberkulmer mapping population

Trait	QTL no.	Chromosome	LOD	$R^{2\dagger}$	Additive effect	Increasing allele no.	
						Forno	Oberkulmer
Spike traits							
Threshability (%)	12	2A, 2B, 3A, 4A, 5A, 7B	3.2–27.3	7.0–46.6	5.0–24.0	6	6
Glume tenacity (scores)	5	3A, 4A, 5A	3.1–24.2	12.2–63.6	0.3–1.0	3	2
Spike length (cm)	12	2B, 3A, 3B, 4A, 5A, 5B, 5DL	3.2–17.2	14.0–51.4	0.8–2.1	9	3
Spike compactness (spikelets cm^{-1})	8	3A, 4A, 5A, 5B, 6A	3.0–17.7	11.9–52.3	0.12–0.31	2	6
Yield traits							
Machine-harvested grain yield (t ha^{-1})	4	1DS, 3A, 4A, 5A	3.2–9.4	7.1–19.4	0.26–0.73	2	2
Hand-harvested grain yield (t ha^{-1})	1	5B	3.6	14.1	0.48	1	0
Grain weight per spike (g)	3	4DL, 5A, 5B	3.2–3.4	13.2–19.5	0.07–0.15	1	2
Thousand grain weight (g)	19	1BS, 2A, 2B, 3A, 3B, 4A, 5A, 5B, 5DL, 6A, 7B, 7D	2.9–11.0	6.5–22.3	0.94–2.24	10	9
Grains m^{-2}	9	3A, 4A, 4B, 5A, 7B	3.2–6.2	7.1–13.1	814–1920	5	4
Grains per spike	9	2B, 2D, 3B, 4A, 5A, 7B	3.1–5.1	12.0–20.5	2.2–6.0	3	6
Spikelets per spike	16	1DS, 2B, 2D, 3B, 4B, 6B, 7B	3.2–6.8	12.4–26.7	0.5–2.2	4	12
Fertile spikelets per spike	4	3B, 5A, 6B, 7B	3.4–4.0	13.2–15.4	0.5–0.7	2	2
Infertile spikelets per spike	4	3A, 3B, 5B, 7B	3.1–5.6	12.2–21.0	0.4–0.5	1	3
Grains per spikelet	3	2B, 5A, 5B	4.0–6.4	15.4–23.4	0.1	1	2
Spikes m^{-2}	4	3A, 4A, 7B	3.2–3.7	12.7–21.5	27–57	2	2
Spikes per plant	5	1A, 4A, 5A, 7B	3.1–6.3	18.6–23.1	0.2–0.8	2	3
Dry weight per shoot (g)	4	4B, 5A, 5B	3.0–4.2	11.9–24.4	0.17–0.31	1	3
Harvest index	2	5A, 6D	3.5–3.6	20.4–20.9	0.02–0.04	2	0
Total	124					57	67

† The proportion of phenotypic variation explained by individual QTL.

Table 2-4 Quantitative trait locus (QTL) identification in the Forno × Oberkulmer mapping population

Trait/Chromosome	Year	Position (cM)	LOD	$R^{2\dagger}$	Additive effect‡	Closest marker
Spike traits						
Threshability (%)						
2A	2013	7.9	4.5	9.8	5.0	Xpsr566c-2A
	2012	8.9	3.2	7.0	7.6	Xpsr566c-2A
2B	2013	75.7	4.4	9.4	6.2	Xpsr172-2B
3A	2012	35.9	4.5	9.9	-15.6	Xpsr598-3A
	2013	35.9	4.9	10.6	-9.4	Xpsr598-3A
4A	2012	9.3	4.6	10.0	9.4	Xgwm397-4A
	2012	212.2	3.7	8.2	-9.7	Xmwg710b-4A
	2013	214.2	5.1	10.9	-6.4	Xpsr115-4A
5A	2013	67.4	3.4	7.4	-5.5	Xglk424-5A
	2012	217.4	27.3	46.6	24.0	Xpsr918b-5A
	2013	218.4	20.0	36.7	12.4	Xpsr918b-5A
7B	2012	217.0	3.4	7.5	-7.8	Xglk576-7BL
Glume tenacity (scores)						
3A	2012	74.7	3.1	18.5	0.5	Xglk221-3AL
	2013	74.7	3.6	14.0	0.3	Xglk221-3AL
4A	2013	207.2	3.1	12.2	0.3	Xmwg710b-4A
5A	2012	211.9	12.5	55.9	-1.0	Xpsr918b-5A
	2013	215.4	24.2	63.6	-0.8	Xpsr918b-5A
Spike length (cm)						
2B	2012	145.8	3.4	20.1	0.8	Xglk699a-2BS
3A	2013	123.5	6.0	22.1	1.5	Xglk652a-3AL
	2012	130.9	4.0	23.1	0.9	Xglk652a-3AL
3B	2012	0.0	3.2	19.1	-0.8	Xglk683-3BS
4A	2013	204.2	3.8	14.7	1.0	Xmwg710b-4A
5A	2013	23.1	4.8	18.1	1.1	Xpsr644a-5A
	2012	208.9	5.2	28.8	-1.2	Xpsr918b-5A
	2013	209.9	17.2	51.4	-2.1	Xpsr918b-5A
5B	2012	8.9	3.4	19.8	1.0	Xwg669-5B
	2013	10.9	4.7	17.7	1.4	Xpsr128-5B
5DL	2012	68.8	4.5	25.7	1.0	Xpsr580a-5DL
	2013	70.8	3.6	14.0	1.1	Xglk558a-5DL
Spike compactness (spikelets cm^{-1})						
3A	2013	122.5	4.6	17.4	-0.20	Xglk652a-3AL
4A	2013	204.2	3.2	12.6	-0.13	Xmwg710b-4A
5A	2012	22.1	3.7	21.5	-0.12	Xpsr644a-5A
	2013	22.1	5.3	19.8	-0.16	Xpsr644a-5A
	2012	209.9	8.0	40.9	0.21	Xpsr918b-5A
	2013	210.9	17.7	52.3	0.31	Xpsr918b-5A
5B	2013	11.9	3.5	13.4	-0.18	Xpsr128-5B
6A	2013	0.0	3.0	11.9	-0.13	Xpsr008-6A

† The proportion of phenotypic variation explained by individual QTL.

‡ Positive additive effects indicate that the alleles from Forno increase the values of the traits, whereas negative additive effects indicate that the alleles from Oberkulmer increase the values of the traits.

Table 2-4 (continued)

Trait/Chromosome	Year	Position (cM)	LOD	R^2	Additive effect	Closest marker
Yield traits						
Machine-harvested grain yield (t ha^{-1})						
1DS	2012	2.0	3.2	7.1	0.26	Xpsr168-1DS
3A	2013	40.9	6.1	13.0	-0.73	Xpsr598-3A
4A	2013	210.2	3.9	8.5	-0.42	Xmwg710b-4A
5A	2013	218.4	9.4	19.4	0.68	Xpsr918b-5A
Hand-harvested grain yield (t ha^{-1})						
5B	2013	156.3	3.6	14.1	0.48	Xpsr580b-5B
Grain weight per spike (g)						
4DL	2012	36.2	3.2	18.7	-0.15	Xgwm194-4DL
5A	2013	63.3	3.4	13.2	0.10	Xglk424-5A
5B	2012	136.4	3.3	19.5	-0.07	Xpsr370-5B
Thousand grain weight (g)						
1BS	2013	42.9	4.8	10.3	1.17	Xglk483-1BS
2A	2012	105.4	4.6	10.0	-1.10	Xpsr602-2A
2B	2013	145.8	3.5	7.7	-0.94	Xglk699a-2BS
3A	2012	109.5	3.1	6.8	0.95	Xglk577-3AL
3B	2013	2.9	3.4	7.4	0.96	C970a-3B
	2013	79.3	5.0	10.8	1.20	Xpsr1054-3B
	2012	80.5	4.0	8.7	1.07	Xpsr1054-3B
4A	2012	23.7	11.0	22.3	-1.92	Xpsr59a-4A
	2013	25.7	6.5	13.8	-1.41	Xpsr59a-4A
	2013	161.3	2.9	6.5	-2.05	Xglk128-4A
5A	2013	114.1	3.2	7.1	-0.99	Xpsr911-5A
	2012	120.2	7.8	16.3	-1.71	Xpsr911-5A
	2013	208.9	4.3	9.3	1.26	Xpsr918b-5A
5B	2012	151.3	3.3	7.3	-0.94	Xpsr580b-5B
5DL	2013	37.0	4.3	9.2	-2.24	Xpsr580a-5DL
6A	2012	91.1	5.2	11.1	1.23	Xpsr966-6A
7B	2013	180.5	3.3	7.2	1.27	Xglk750-7BL
	2012	192.5	5.8	12.5	1.85	Xmwg710a-7B
7D	2013	87.8	4.1	8.9	1.23	Xgwm111b-7D
Grains m^{-2}						
3A	2012	37.9	4.1	9.0	-1202	Xpsr598-3A
	2012	106.4	5.0	11.0	-846	Xglk118-3AL
	2013	43.9	6.1	13.0	-1524	Xpsr598-3A
4A	2013	23.7	4.7	10.1	1018	Xpsr59a-4A
4B	2012	61.8	3.2	7.1	1185	Xpsr921-4B
5A	2012	163.4	4.1	9.1	1562	Xpsr120a-5A
	2013	166.4	4.5	9.8	1920	Xpsr145-5A
	2013	222.5	6.2	13.1	1263	Xpsr1201a-5A
7B	2013	217.4	3.9	8.6	-814	Xglk576-7BL

Table 2-4 (continued)

Trait/Chromosome	Year	Position (cM)	LOD	R^2	Additive effect	Closest marker
Grains per spike						
2B	2013	94.7	3.1	12.0	-2.2	Xglk687b-2BS
2D	2013	44.9	4.7	17.8	-6.0	Xpsr933b-2D
3B	2013	8.1	3.7	14.4	-2.7	Lrk10c-3BS
4A	2012	38.1	3.5	20.5	2.5	Xpsr914-4A
	2013	151.3	3.6	14.0	5.5	Xglk354-4A
5A	2013	64.4	4.5	17.3	2.9	Xglk424-5A
	2013	213.4	5.1	19.2	-2.9	Xpsr918b-5A
7B	2013	127.8	3.1	12.2	-3.4	Xpsr593c-7B
	2012	137.8	3.2	18.7	-3.6	Xpsr129c-7B
Spikelets per spike						
1DS	2013	5.4	3.2	12.5	-0.5	Xglk558b-1DS
2B	2013	9.9	3.2	12.4	0.5	Xglk302a-2BS
	2013	143.9	4.2	16.1	0.6	Xglk699a-2BS
	2012	146.8	3.3	19.2	0.8	Xglk699a-2BS
2D	2013	45.9	5.2	19.5	-1.4	Xpsr933b-2D
	2012	46.9	4.2	23.9	-2.2	Xpsr933b-2D
3B	2012	1.9	4.7	26.7	-1.0	C970a-3B
	2013	7.1	5.0	18.7	-0.7	Lrk10c-3BS
	2013	45.7	3.8	14.8	-0.5	Xglk554b-3B
	2012	90.5	3.5	20.8	-1.2	Xpsr1054-3B
4B	2013	97.8	5.4	20.2	-0.7	Xpsr584-4B
	2012	102.7	3.7	21.6	-0.9	Xglk335-4BL
6B	2012	20.7	3.5	20.7	0.8	Xpsr964-6B
7B	2013	21.6	3.8	14.6	-0.7	Xpsr952-7B
	2012	92.7	4.2	23.9	-1.1	Xpsr350-7B
	2013	93.7	6.8	24.9	-0.8	Xpsr350-7B
Fertile spikelets per spike						
3B	2013	1.6	3.4	13.2	-0.5	Xpsr1327a-3B
5A	2013	73.4	4.0	15.4	0.7	Xglk424-5A
6B	2013	20.7	3.4	13.3	0.5	Xpsr964-6B
7B	2013	99.7	3.7	14.4	-0.6	pwir232b-7B
Infertile spikelets per spike						
3A	2013	84.4	5.6	21.0	0.5	Xpsr578-3A
3B	2013	42.1	3.9	14.9	-0.4	Xpsr902-3B
5B	2013	146.2	3.2	12.4	-0.4	Xpsr580b-5B
7B	2013	29.6	3.1	12.2	-0.5	Xpsr952-7B
Grains per spikelet						
2B	2013	99.6	4.0	15.4	-0.1	Xglk407-2BS
5A	2013	213.4	6.4	23.4	-0.1	Xpsr918b-5A
5B	2013	155.2	5.2	19.6	0.1	Xpsr580b-5B
Spikes m^{-2}						
3A	2013	50.9	3.2	12.7	-27	Xpsr598-3A
4A	2012	20.7	3.7	21.4	45	Xglk315-4AS
	2012	60.2	3.6	21.0	42	Xglk331-4A
7B	2012	188.5	3.7	21.5	-57	Xglk750-7BL

Table 2-4 (continued)

Trait/Chromosome	Year	Position (cM)	LOD	R^2	Additive effect	Closest marker
Spikes per plant						
1A	2012	88.9	3.3	19.4	0.2	Xpsr1201b-1A
4A	2012	29.2	3.1	18.6	0.2	Xpsr59a-4A
	2012	219.2	3.6	20.9	-0.2	Xpsr115-4A
5A	2013	210.9	6.3	23.1	-0.8	Xpsr918b-5A
7B	2012	188.5	3.5	20.3	-0.2	Xmwg710a-7B
Dry weight per shoot (g)						
4B	2012	55.8	4.2	24.4	-0.31	Xpsr921-4B
	2013	95.8	3.0	11.9	-0.19	Xpsr584-4B
5A	2013	60.3	3.9	14.9	0.24	Xglk424-5A
5B	2012	136.4	3.9	22.8	-0.17	Xpsr370-5B
Harvest index						
5A	2012	213.4	3.5	20.4	0.02	Xpsr918b-5A
6D	2012	34.0	3.6	20.9	0.04	Xpsr167a-6D

Table 2-5 Allelic analysis of grain number components and thousand grain weight (TGW)

Grain number component	Total QTL no.	Linked with QTL for TGW, increasing alleles conferred by		Independent
		Same parents	Opposite parents	
Grains m^{-2}	9	1	7	1
Grains per spike	9	1	7	1
Spikelets per spike	16	0	10	6
Fertile spikelets per spike	4	0	3	1
Grains per spikelet	3	1	2	0
Spikes m^{-2}	4	0	4	0
Spikes per plant	5	1	3	1
Total	50	4	36	10
Proportion to the total	–	8%	72%	20%

2.4.3 QTL for yield and yield components independent of the non-free-threshing habit

As described above, six QTL for low threshability were mapped on chromosomes 2A, 2B, 4A, and 5A in spelt, while two for tenacious glumes mapped on chromosome 5A. In these genomic regions, only seven QTL for yield and yield components were detected, including two QTL for TGW, two for grains per spike, two for grains per spikelet, and one for spikes per plant (Fig. 2-4). The remaining 41 (85%) favourable QTL were independent of the non-free-threshing traits. At the locus of the major gene Q on chromosome 5AL (Xpsr918b-5A), the QTL for seven yield and yield components were coincident: the increasing alleles for grains per spike, grains per spikelet and spikes per plant were conferred by the spelt Oberkulmer (with the q allele), while the increasing alleles for machine-harvested yield, TGW, grains m^{-2} and HI conferred by the bread wheat Forno (with the Q allele) (Fig. 2-4). These coincidences supported the phenotypic relationships between spike traits, and yield and yield components (Table 2-2), and the hypothesis that the genetic factors distinguishing spelt from bread wheat by different spike features could also affect the yield and yield components.

2.5 Discussion

2.5.1 Usefulness of the spelt as a genetic resource for yield component improvement in bread wheat

In this study, the potential traits and genes of spelt were determined in order to improve yield and yield components of bread wheat. Phenotypic analysis showed that the spelt Oberkulmer produced much larger grains than bread wheat Forno in 2012, in line with the previous studies (Winzeler et al., 1994; Campbell, 1997; Zanetti et al., 2001; Konvalina et al., 2010). TGW of Forno was low in this year, and this was also seen in another bread wheat cultivar 'Duxford' grown together as a check (25.2 g, details not shown), likely due to the high rainfall and low level of solar radiation during grain filling (June and July). In contrast, the spelt Oberkulmer seemed to perform well under this condition. In 2013, however, Oberkulmer had slightly smaller grains than Forno, which may result from more grains per spike and more fertile tillers per plant established in this season. In terms of the physiological components of yield, spelt tended to have more above-ground biomass, but lower HI, as also reported in Koutroubas et al. (2012). High biomass is an especially valuable trait to raise yield potential of bread wheat, because HI is approaching the limit of approximately 0.64, and there has been no significant progress since the early 1990s (0.50−0.55) (Foulkes et al., 2011). The other potential traits are the long, lax spikes. The present study exhibited that spike length was positively correlated with grain weight per spike, grains per spike, and grains per spikelet, whereas spike compactness negatively correlated with these traits. Short, compact spikes were mainly associated with the reduced grain set of apical spikelets within spikes (data not shown). Thus, the phenotype of long and lax spikes in spelt may be used to increase spike fertility, and in turn sink size in bread wheat.

Genetic analysis showed that a total of 48 favourable alleles for yield and yield components were detected from spelt. In contrast, only 39 favourable alleles were found from bread wheat. The accumulative additive effects over all increasing alleles detected from Oberkulmer are: 1.15 t ha^{-1} for machine-harvested grain yield, 0.22 g for grain weight per spike, 13.3 g for TGW, 4 386 grains m^{-2}, 20.8 grains per spike, 11.7 spikelets per spike, 1.1 fertile spikelets per spike, 0.2 grains per spikelet, 84 spikes m^{-2}, 1.2 spikes per plant, and 0.67 g for dry weight per shoot. This indicates that spelt can be considered as an important gene source for yield and yield

component improvement in bread wheat. In addition, three and two alleles were identified from spelt for long and lax spikes, respectively; these genes could potentially be used to improve spike fertility indirectly.

2.5.2 Maintaining the free-threshing habit while utilising spelt as a gene source

Grain threshability is a key domestication trait, and modern bread wheat must be free-threshing for combining efficiency. Spelt is not typically free-threshing; the traits and genes of spelt for bread wheat improvement should be relatively independent of those for low threshability. To clarify this, a first step is to determine the gene locations for the non-free-threshing habit of spelt. In this study, six alleles associated with low threshability were identified from spelt, indicating polygenic control. Glume tenacity explained approximately 59% of the phenotypic variation in threshability, similar to the report of Jantasuriyarat et al. (2004). A major QTL for glume tenacity, accounting for 59.8% of the phenotypic variation, was mapped on chromosome 5AL, and stable across two years. The increasing allele was from spelt, coincident with the major allele for low threshability, which confirmed the role of tenacious glume as a component of threshability. A physical determinant of glume tenacity might be the size of glume bases attached on the rachises of spikes (Nalam et al., 2007).

Based on common marker analysis, it was found that the QTL on 5AL, which had major effects on threshability and glume tenacity, corresponded to the domestication gene Q in wheat (Kato et al., 1998; Simonetti et al., 1999). This gene also largely affected the other two spike traits: spike length and compactness. The Q allele from bread wheat Forno increased threshability (18.2%) and spike compactness (0.26 spikelets per cm) but decreased glume tenacity (a score of 0.9) and spike length (1.7 cm), whereas the q allele from the spelt Oberkulmer had the opposite effects. In another bread wheat × spelt mapping population, the major QTL controlling spike length and compactness were also mapped at the locus of Q gene (Manickavelu et al., 2011). This pleiotropy has been found in many previous studies (Muramatsu, 1963; Jantasuriyarat et al., 2004; Simons et al., 2006). To maintain the free-threshing habit of bread wheat, thus, the Q allele should be retained, whereas the q allele in spelt needs to be excluded.

QTL linkage analysis showed that only seven QTL for yield components (two QTL for TGW and five for grain number components) were coincident or linked with those

for low threshability and tenacious glumes in spelt. There were still 41 (85%) independent favourable QTL, which can be used easily for yield improvement of bread wheat. At the locus of the Q gene, seven QTL for yield and yield component traits (grain yield, TGW, grains m^{-2}, grains per spike, grains per spikelet, spikes per plant, and HI) were mapped. The increasing alleles for grains per spike, grains per spikelet and spikes per plant were from the spelt Oberkulmer, coincident with the q allele responsible for low threshability and tenacious glumes. The increasing alleles for grain yield, TGW, grains m^{-2} and HI were from the bread wheat Forno, coincident with the Q allele responsible for the free-threshing habit. This implies that the Q gene may also affect the yield and yield components in wheat, as a result of pleiotropic effects or tight gene linkage. Using single-chromosome (5A) recombinant lines, Kato et al. (2000) mapped the QTL for grain weight per spike and spikelets per spike at the locus q, and the QTL for 50-grain weight at the locus Q. In addition, more spikelets and grains per spike but slightly lower individual grain weight appeared when the allele Q is replaced with q (Zhang et al., 2011). The pleiotropic effects of the q allele or tight gene linkage in spelt would make it very difficult to use the three favourable alleles for grain number components (i.e. grains per spike, grains per spikelet and spikes per plant) for bread wheat improvement.

2.5.3 Transfer of the desirable traits and genes from spelt to bread wheat

Different genetic architectures of yield and yield components between spelt and bread wheat were found in this study. In F_1 hybrids, high heterosis effects on yield and yield components can be expected, as reported by Winzeler et al. (1994), due to the expressions of respective favourable genes. However, the present study revealed that 78% of the increasing alleles for TGW from Oberkulmer were mapped to the chromosomal regions where, in Forno, the increasing alleles for grain number components were mapped. Moreover, 68% of the increasing alleles for grain number components from Oberkulmer were mapped to the chromosomal regions where, in Forno, the increasing alleles for TGW were mapped. In other words, F_1 hybrids of bread wheat and spelt would have the increasing alleles for both TGW and grain number at the same or nearby positions of homologous chromosomes: one allele from bread wheat increasing TGW, the other from spelt increasing grain number, and vice versa. This would result in high heterosis effects in F_1 hybrids (Winzeler et al., 1994). On the other hand, it would be difficult to combine both favourable alleles on the

same chromosomes through crossover processes. Therefore, traditional hybridisation between bread wheat and spelt may not work for introgression of 70% of the favourable alleles from spelt to improve yield components of bread wheat; however, it would work for the remaining independent alleles. Additional strategies such as gene cloning and transferring are needed.

2.5.4 Trade-off between individual grain weight and grain number while transferring the traits and genes from spelt to bread wheat

Individual grain weight and grain number are two major components of yield, and it is expected that both components should be improved. However, a negative relationship between individual grain weight and grain number has been a barrier to yield progress (Slafer and Andrade, 1989, 1993; Miralles and Slafer, 1995). In this study, TGW was negatively associated with all the grain number components. Interestingly, 80% of QTL for grain number components were coincident or linked with those for TGW, and most of them had increasing alleles conferred by the opposite parents. That is, the favourable alleles for grain number were usually coincident or linked with the unfavourable alleles for TGW in each of the parents, and vice versa. This indicates that the negative relationship between individual grain weight and grain number, results not only from source size, but also the intrinsic genetic control.

In wheat breeding history, grain yield progress has been found to be highly associated with grain number (Sayre et al., 1997; Shearman et al., 2005; Peltonen-Sainio et al., 2007; Foulkes et al., 2011). One of the reasons is the responsiveness of grain number to high resource input during cultivation (Sadras, 2007). Artificial breeding selection pressure on grain number would have accumulated many favourable alleles for grain number, but likely lost favourable alleles for grain weight at the same time. As a result, there has been no systematic genetic gain for grain weight improvement over the last decades (Sayre et al., 1997; Shearman et al., 2005; Acreche et al., 2008), or even a decreasing trend (Waddington et al., 1986).

To boost both individual grain weight and grain number of bread wheat using the spelt as a gene source, there may be four options. First, if the genes controlling both components are independent or loosely linked in spelt, they can be easily combined to the same genetic background of bread wheat through genetic recombination. Second, if these genes for both traits are tightly linked, their linkages need to be broken

through a slow recombining process. To select the genotypes with broken gene linkage from offspring, molecular markers specific for each linked gene would help in a low-cost, efficient way. Third, if the genes show negative pleiotropic effects on both traits, the use of these genes should be minimised. When they have to be used, other independent genes should be added as complements. Fourth, source size should be enlarged to supply enough assimilates. Source limited plants usually show a negative relationship between grain number and individual grain weight, even if there is no pleiotropy or gene linkage.

In conclusion, this study revealed that spelt had a number of desirable traits for yield and yield component improvement of bread wheat, namely larger grains, more fertile tillers per plant, higher biomass, longer and laxer spikes. Many favourable alleles for yield and yield components were identified from spelt, and most of them were independent of those for the non-free-threshing habit. The results suggest that spelt is a valuable genetic resource to improve yield of bread wheat. To transfer these desirable genes from spelt to bread wheat, additional strategies rather than traditional hybridisation may be needed, because it is difficult to produce recombinant lines of bread wheat and spelt combining favourable alleles for both grain size and grain number. This study, therefore, would allow better use of spelt as a gene source to widen genetic diversity in bread wheat.

2.6 Acknowledgements

This work was supported by the grants from the China Scholarship Council and the University of Nottingham. We thank Beat Keller (Institute of Plant Biology, University of Zurich, Switzerland) for providing the mapping population and Monika Messmer (Research Institute of Organic Agriculture, Switzerland) for providing the molecular marker data. We also thank Chuong Nguyen, John Alcock, Matthew Tovey and Fiona Wilkinson (University of Nottingham) for their help with field trials and laboratory work.

2.7 References

Abdel-Aal ESM, Hucl P, Sosulski FW, Bhirud PR. 1997. Kernel, milling and baking properties of spring-type spelt and einkorn wheats. Journal of Cereal Science **26**, 363-370.

Acreche MM, Briceño-Félix G, Sánchez JAM, Slafer GA. 2008. Physiological bases of genetic gains in Mediterranean bread wheat yield in Spain. European Journal of Agronomy **28**, 162-170.

Aguilar V, Stamp P, Winzeler M, Winzeler H, Schachermayr G, Keller B, Zanetti S, Messmer MM. 2005. Inheritance of field resistance to Stagonospora nodorum leaf and glume blotch and correlations with other morphological traits in hexaploid wheat (Triticum aestivum L.). Theoretical and Applied Genetics **111**, 325-336.

An X, Li Q, Yan Y, Xiao Y, Hsam SLK, Zeller FJ. 2005. Genetic diversity of European spelt wheat (Triticum aestivum ssp. spelta L. em. Thell.) revealed by glutenin subunit variations at the Glu-1 and Glu-3 loci. Euphytica **146**, 193-201.

Bertin P, Gregoire D, Massart S, de Froidmont D. 2004. High level of genetic diversity among spelt germplasm revealed by microsatellite markers. Genome **47**, 1043-1052.

Braun HJ, Atlin G, Payne T. 2010. Multi-location testing as a tool to identify plant response to global climate change. In: Reynolds MP, ed. Climate Change and Crop Production. Surrey: CABI, 115-138.

Burgos MS, Messmer MM, Stamp P, Schmid JE. 2001a. Flooding tolerance of spelt (Triticum spelta L.) compared to wheat (Triticum aestivum L.) – A physiological and genetic approach. Euphytica **122**, 287-295.

Burgos S, Stamp P, Schmid JE. 2001b. Agronomic and physiological study of cold and flooding tolerance of spelt (Triticum spelta L.) and wheat (Triticum aestivum L.). Journal of Agronomy and Crop Science **187**, 195-202.

Caballero L, Martin LM, Alvarez JB. 2001. Allelic variation of the HMW glutenin subunits in Spanish accessions of spelt wheat (Triticum aestivum ssp. spelta L. em. Thell.). Theoretical and Applied Genetics **103**, 124-128.

Caballero L, Martin LM, Alvarez JB. 2004. Variation and genetic diversity for gliadins in Spanish spelt wheat accessions. Genetic Resources and Crop Evolution **51**, 679-686.

Campbell KG. 1997. Spelt: agronomy, genetics, and breeding. In: Janick J, ed. Plant breeding reviews, Vol. 15. USA: John Wiley & Sons, 187-213.

Dyck PL, Sykes EE. 1994. Genetics of leaf-rust resistance in three spelt wheats. Canadian Journal of Plant Science **74**, 231-233.

FAO. 2014. FAOSTAT. http://faostat.fao.org/.

Foulkes MJ, Slafer GA, Davies WJ, Berry PM, Sylvester-Bradley R, Martre P, Calderini DF, Griffiths S, Reynolds MP. 2011. Raising yield potential of wheat. III. Optimizing partitioning to grain while maintaining lodging resistance. Journal of Experimental Botany **62**, 469-486.

Gomez-Becerra HF, Erdem H, Yazici A, Tutus Y, Torun B, Ozturk L, Cakmak I. 2010. Grain concentrations of protein and mineral nutrients in a large collection of spelt wheat grown under different environments. Journal of Cereal Science **52**, 342-349.

Guzman C, Caballero L, Yamamori M, Alvarez JB. 2012. Molecular characterization of a new waxy allele with partial expression in spelt wheat. Planta **235**, 1331-1339.

Hou Y, Pu Z, Shang H, Li W. 2010. Analysis of agronomic traits of Triticum spelta L. germplasms. Southwest China Journal of Agricultural Sciences **23**, 315-321.

Jantasuriyarat C, Vales M, Watson C, Riera-Lizarazu O. 2004. Identification and mapping of genetic loci affecting the free-threshing habit and spike compactness in wheat (Triticum aestivum L.). Theoretical and Applied Genetics **108**, 261-273.

Kato K, Miura H, Akiyama M, Kuroshima M, Sawada S. 1998. RFLP mapping of the three major genes, Vrn1, Q and B1, on the long arm of chromosome 5A of wheat. Euphytica **101**, 91-95.

Kato K, Miura H, Sawada S. 2000. Mapping QTLs controlling grain yield and its components on chromosome 5A of wheat. Theoretical and Applied Genetics **101**, 1114-1121.

Konvalina P, Capouchova I, Stehno Z, Moudry J. 2010. Agronomic characteristics of the spring forms of the wheat landraces (einkorn, emmer, spelt, intermediate bread wheat) grown in organic farming. Journal of Agrobiology **27**, 9-17.

Koutroubas SD, Fotiadis S, Damalas CA. 2012. Biomass and nitrogen accumulation and translocation in spelt (Triticum spelta) grown in a Mediterranean area. Field Crops Research **127**, 1-8.

Manickavelu A, Kawaura K, Imamura H, Mori M, Ogihara Y. 2011. Molecular mapping of quantitative trait loci for domestication traits and β-glucan content in a wheat recombinant inbred line population. Euphytica **177**, 179-190.

Messmer MM, Keller M, Zanetti S, Keller B. 1999. Genetic linkage map of a wheat × spelt cross. Theoretical and Applied Genetics **98**, 1163-1170.

Miralles DJ, Slafer GA. 1995. Individual grain weight responses to genetic reduction in culm length in wheat as affected by source-sink manipulations. Field Crops Research **43**, 55-66.

Mohler V, Singh D, Singruen C, Park RF. 2012. Characterization and mapping of Lr65 in spelt wheat 'Altgold Rotkorn'. Plant Breeding **131**, 252-257.

Muramatsu M. 1963. Dosage effect of the spelta gene q of hexaploid wheat. Genetics **48**, 469-482.

Nalam VJ, Vales MI, Watson CJ, Johnson EB, Riera-Lizarazu O. 2007. Map-based analysis of genetic loci on chromosome 2D that affect glume tenacity and threshability, components of the free-threshing habit in common wheat (Triticum aestivum L.). Theoretical and Applied Genetics **116**, 135-145.

Peltonen-Sainio P, Kangas A, Salo Y, Jauhiainen L. 2007. Grain number dominates grain weight in temperate cereal yield determination: Evidence based on 30 years of multi-location trials. Field Crops Research **100**, 179-188.

Raman H, Rahman R, Luckett D, Raman R, Bekes F, Lang L, Bedo Z. 2009. Characterisation of genetic variation for aluminium resistance and polyphenol oxidase activity in genebank accessions of spelt wheat. Breeding Science **59**, 373-381.

Reynolds M, Bonnett D, Chapman SC, Furbank RT, Manès Y, Mather DE, Parry MAJ. 2011. Raising yield potential of wheat. I. Overview of a consortium approach and breeding strategies. Journal of Experimental Botany **62**, 439-452.

Ruibal-Mendieta NL, Delacroix DL, Meurens M. 2002. A comparative analysis of free, bound and total lipid content on spelt and winter wheat wholemeal. Journal of Cereal Science **35**, 337-342.

Ruibal-Mendieta NL, Delacroix DL, Mignolet E, et al. 2005. Spelt (Triticum aestivum ssp. spelta) as a source of breadmaking flours and bran naturally enriched in oleic acid and minerals but not phytic acid. Journal of Agricultural and Food Chemistry **53**, 2751-2759.

Sadras VO. 2007. Evolutionary aspects of the trade-off between seed size and number in crops. Field Crops Research **100**, 125-138.

Sayre KD, Rajaram S, Fischer RA. 1997. Yield potential progress in short bread wheats in northwest Mexico. Crop Science **37**, 36-42.

Schmid JE, Winzeler H. 1990. Genetic studies of crosses between common wheat (Triticum aestivum L.) and spelt (Triticum spelta L.). Journal of Genetics and Breeding **44**, 75-80.

Shearman VJ, Sylvester-Bradley R, Scott RK, Foulkes MJ. 2005. Physiological processes associated with wheat yield progress in the UK. Crop Science **45**, 175-185.

Simon MR, Khlestkina EK, Castillo NS, Boerner A. 2010. Mapping quantitative resistance to septoria tritici blotch in spelt wheat. European Journal of Plant Pathology **128**, 317-324.

Simonetti MC, Bellomo MP, Laghetti G, Perrino P, Simeone R, Blanco A. 1999. Quantitative trait loci influencing free-threshing habit in tetraploid wheats. Genetic Resources and Crop Evolution **46**, 267-271.

Simons KJ, Fellers JP, Trick HN, Zhang Z, Tai YS, Gill BS, Faris JD. 2006. Molecular characterization of the major wheat domestication gene Q. Genetics **172**, 547-555.

Slafer GA. 2007. Physiology of determination of major wheat yield components. In: Buck HT, Nisi JE, Salomón N, eds. Wheat production in stressed environments. The Netherlands: Springer, 557-565.

Slafer GA, Andrade FH. 1989. Genetic improvement in bread wheat (Triticum aestivum) yield in Argentina. Field Crops Research **21**, 289-296.

Slafer GA, Andrade FH. 1993. Physiological attributes related to the generation of grain yield in bread wheat cultivars released at different eras. Field Crops Research **31**, 351-367.

Stallknecht GF, Gilbertson KM, Ranney JE. 1996. Alternative wheat cereals as food grains: einkorn, emmer, spelt, kamut, and triticale. In: Janick J, ed. Progress in new crops. Alexandria, VA: ASHS Press, 156-170.

Sun Q, Wei Y, Ni Z, Xie C, Yang T. 2002. Microsatellite marker for yellow rust resistance gene Yr5 in wheat introgressed from spelt wheat. Plant Breeding **121**, 539-541.

Troccoli A, Codianni P. 2005. Appropriate seeding rate for einkorn, emmer, and spelt grown under rainfed condition in southern Italy. European Journal of Agronomy **22**, 293-300.

Van Ooijen JW. 2006. JoinMap® 4, software for the calculation of genetic linkage maps in experimental populations. The Netherlands: Kyazma BV.

Van Ooijen JW. 2009. MapQTL® 6, software for the mapping of quantitative traits loci in experimental populations of diploid species. The Netherlands: Kyazma BV.

Voorrips RE. 2002. MapChart: software for the graphical presentation of linkage maps and QTLs. Journal of Heredity **93**, 77-78.

Waddington SR, Ransom JK, Osmanzai M, Saunders DA. 1986. Improvement in the yield potential of bread wheat adapted to northwest Mexico. Crop Science **26**, 698-703.

Wang Y, Peng H, Liu G, Xie C, Ni Z, Yang T, Liu Z, Sun Q. 2010. Identification and molecular mapping of a leaf rust resistance gene in spelt wheat landrace Altgold. Euphytica **174**, 371-375.

Winzeler H, Schmid JE, Winzeler M. 1994. Analysis of the yield potential and yield components of F1 and F2 hybrids of crosses between wheat (Triticum aestivum L.) and spelt (Triticum spelta L.). Euphytica **74**, 211-218.

Zanetti S, Winzeler M, Feuillet C, Keller B, Messmer M. 2001. Genetic analysis of bread-making quality in wheat and spelt. Plant Breeding **120**, 13-19.

Zhang Z, Belcram H, Gornicki P, et al. 2011. Duplication and partitioning in evolution and function of homoeologous Q loci governing domestication characters in polyploid wheat. Proceedings of the National Academy of Sciences, USA **108**, 18737-18742.

Zhao FJ, Su YH, Dunham SJ, Rakszegi M, Bedo Z, McGrath SP, Shewry PR. 2009. Variation in mineral micronutrient concentrations in grain of wheat lines of diverse origin. Journal of Cereal Science **49**, 290-295.

Chapter 3

Optimising Tiller Production and Survival for Grain Yield Improvement in Wheat

3.1 Abstract

• Background and Aims Tiller production and survival determine final spike number, and play key roles in grain yield formation in wheat (Triticum aestivum). This study aimed to understand the genetic and physiological basis of tillering process, and its trade-offs with other yield components.

• Methods Dynamics of tillering and red:far red ratio (R:FR) at the base of canopy arising from neighbouring plants in a bread wheat (Triticum aestivum 'Forno') × spelt (Triticum spelta 'Oberkulmer') mapping population, were measured in the field in two growing seasons. Additional thinning and shading experiments were conducted in the field and glasshouse, respectively. Yield components were analysed for all experiments, followed by identification of quantitative trait loci (QTL) associated with each trait.

• Key Results Large genetic variation in tillering was observed, and more fertile shoots per plant were associated with more total shoots initiated, faster tillering rate, delayed tillering onset and cessation, and higher shoot survival. A total of 34 QTL for tillering traits were identified, and analysis of allelic effects confirmed the above associations. Low R:FR was associated with early tillering cessation, few total shoots, high infertile shoot number and shoot abortion, concurring with the thinning and shading experiments. These probably resulted from an assimilate shortage for tiller buds or developing tillers, due to early stem elongation and enhanced stem growth induced by low R:FR. More fertile tillers normally contributed to plant yield and grain number without reducing yield and grain set of individual shoots. However, there was a decrease in grain weight, partly because of smaller carpels and fewer stem water soluble carbohydrates at anthesis caused by pleiotropy or tight gene linkages.

• Conclusions Tillering is under control of both genetic factors and R:FR. Genetic variation in tillering and tolerance to low R:FR, can be used to optimise tillering patterns for yield improvement in wheat.

Key words: Carpel, grain number, grain weight, quantitative trait locus, red:far red ratio, spelt, stem water soluble carbohydrates, tillering, Triticum aestivum, Triticum spelta, wheat, yield.

3.2 Introduction

Tillering in wheat (Triticum aestivum) determines plant canopy size, photosynthetic area, and, more importantly, the number of spikes bearing grains at maturity (fertile shoots), which is a key component of yield. Wheat plants undergo several events to form final fertile shoots: axillary bud initiation, first bud outgrowth, tillering cessation, tiller abortion, and the development of surviving tillers. Tiller buds are initiated from the axillary meristems in the axils of developing leaves on the main shoots, and bud number is associated with total number of leaves (Baker and Gallagher, 1983; Longnecker et al., 1993). Early tillers can also be parent shoots producing secondary buds and tillers (Evers and Vos, 2013).

Outgrowth of the first tiller buds represents the onset of apparent tillering. In the field, this can occur from autumn to spring, depending on sowing date and temperature thereafter (Sylvester-Bradley et al., 2008). Tillering normally ceases just before stem elongation (Baker and Gallagher, 1983; Gomez-Macpherson et al., 1998; Sylvester-Bradley et al., 2008), and the remaining axillary buds become dormant. However, the dormancy is not definitive, and can be released in some cases like early lodging and damage to the apices of parent shoots (Rameau et al., 2015). The timing of tillering cessation and number of total tillers initiated are regulated by many genetic, physiological and environmental factors. A tiller inhibition gene (tin1), which has been mapped on chromosome 1AS (Richards, 1988; Spielmeyer and Richards, 2004), has been found to reduce tillering through the early cessation of axillary bud outgrowth (Duggan et al., 2002; Kebrom et al., 2012). This inhibition may result from the sugar deficit for lateral tiller buds due to precocious internode elongation (Kebrom et al., 2012), concurring with the report of Langer et al. (1973), who showed that bud growth is inhibited after reducing assimilate supply by partial defoliation and application of DCMU (3-(3,4-dichlorophenyl)-1,1-dimethylurea, decreasing leaf photosynthesis) on main shoots. In the same study, it was observed that kinetin (a type of cytokinin) contributes to bud elongation, and is able to relieve the inhibition caused by reduced assimilate availability. When the auxin transport is suppressed by TIBA (2,3,5-triiodobenzoic acid), the bud growth is enhanced. In terms of other plant hormones, applications of abscisic and gibberellic acids lead to repression of tiller bud growth (Cai et al., 2014). These indicate that the classical hormones have similar

effects on axillary bud outgrowth in wheat, as found in other plants (Rameau et al., 2015).

Environmental factors such as plant density, shade and nutrient supply, also affect tillering cessation. Higher plant population has been shown to be associated with earlier tillering cessation and fewer maximum tillers per plant (Evers et al., 2006; Sparkes et al., 2006). In dense communities, the red and blue wavelengths are absorbed by surrounding plants, and most of far red is reflected and transmitted, resulting in reduction in light intensity and quality (red:far red ratio, R:FR), or shade. With the expansion and closure of canopy, shade is more remarkable, in particular at the base of canopy where most tiller buds are located (Chelle et al., 2007). There is evidence that tiller bud outgrowth responds to light quality, and to a lesser extent, light intensity (Sparkes et al., 2006). Cessation of axillary bud outgrowth coincides with a relatively conservative R:FR of 0.20−0.40 (Evers et al., 2006; Sparkes et al., 2006; Dreccer et al., 2013). High R:FR delays tillering cessation, and increases total tiller number (Toyota et al., 2014). Treatment with far red light has the opposite effects, which can be reversed by adding red light, suggesting phytochrome perception (Kasperbauer and Karlen, 1986; Casal, 1988; Ugarte et al., 2010). Tillering (branching) response to low R:FR or shade has also been observed in ryegrass (Lolium multiflorum) (Casal et al., 1990), barley (Hordeum vulgare) (Davis and Simmons, 1994), sorghum (Sorghum bicolor) (Kebrom et al., 2006), soybean (Glycine max) (Kasperbauer, 1987), and Arabidopsis (Arabidopsis thaliana) (Reddy et al., 2013). Shade acts as a warning signal of impending competition from neighbouring plants, and the consequent reduction of shoot branching is able to enhance apical growth for more incident light, known as a part of the shade avoidance syndrome (Gommers et al., 2013; Rameau et al., 2015). In addition to light environment, wheat plants grown under nutrient deficiency (e.g. nitrogen, phosphorus and sulphur) produce fewer total tillers (Longnecker et al., 1993; Wang et al., 2010; Alzueta et al., 2012).

Tiller abortion ensues immediately after the arrest of tiller bud outgrowth. Of the total tillers initiated, 10−80% are destined to die, as affected by genotype, season, growing location, seeding rate and nutrient supply (Ishag and Taha, 1974; Hucl and Baker, 1989; Sharma, 1995; Berry et al., 2003). Tiller abortion usually takes place between the onset of stem elongation and anthesis, and those appearing last die first (Sylvester-Bradley et al., 2008). As there is a net loss of dry matter from non-surviving tillers,

they have been thought to be detrimental for yield potential, especially when a further increase in harvest index is required (Sharma, 1995; Berry et al., 2003; Foulkes et al., 2011). Therefore, tiller survival needs to be improved in future breeding, and a first step would be to clarify its genetic and physiological basis that still remains unknown to date. In contrast, fertile shoot or spike number at maturity has been widely investigated. Three genes, tin1 on chromosome 1AS (Richards, 1988; Duggan et al., 2005), tin2 on 2A (Peng et al., 1998), and tin3 on $3A^{m}L$ (Kuraparthy et al., 2007), have been identified to reduce final tiller number. This trait is often expressed quantitatively, and many quantitative trait loci (QTL) have been detected on at least 12 chromosomes (Kato et al., 2000; Deng et al., 2011; Naruoka et al., 2011; Jia et al., 2013; Zhang et al., 2013).

Despite the importance of tillering dynamics in terms of yield formation in wheat, knowledge of the genetic and environmental factors regulating this process is still scarce. The questions that need to be addressed include: (1) what are the genes or QTL controlling the timing and rate of tillering, tillering capacity, and the degree of tiller abortion and survival; (2) whether or not, and how the shade from neighbouring plants affects tillering dynamics, particularly tiller abortion; if so, what is the genetic basis of the shade kinetics arising from a genotype grown in the field; (3) whether or not more fertile tillers contribute to plant productivity, considering the possible negative effects on other yield components. In this study, we aimed to address these questions in a recombinant inbred line mapping population of bread wheat (Triticum aestivum 'Forno') × spelt (Triticum spelta 'Oberkulmer'). Dynamics of the tillering and R:FR were measured consecutively in the field in two seasons, and this was also done in the thinning study. In the third season, a shading experiment was carried out in the glasshouse to determine its effect on fertile tiller number. Yield components of each genotype in all seasons were then analysed. Subsequently, the QTL underlying these traits were identified.

3.3 Materials and methods

Details of plant materials, field conditions, statistical analysis of phenotypic data and QTL identification have been described previously in the section of **Materials and methods** of **Chapter 2**.

3.3.1 Tillering, R:FR and yield components in the field experiments

Ten central plants per plot were selected and labelled after emergence in 2012 and 2013. To create relatively uniform populations among plots, plant density was adjusted by removing extra surrounding plants. Once tillering was initiated, shoot number of each plant was counted every c. 100 degree days (^{o}Cd, base temperature 0^{o}C) until tillering cessation. Dying tillers, whose newest leaves started yellowing, were tagged using wires so that all shoots produced during tillering were taken into account. At the late stage of grain filling, the fertile shoots bearing spikes were counted. Immediately after each shoot count, R:FR at the base of each plant was measured using a two-channel radiometer (SKR 116, Skye Instruments, Llandrindod Wells, UK), following the method of Sparkes et al. (2006). Measurements were made under sunny days, with the sensor facing north against the stem bases, which allowed the light reflected and transmitted from the neighbouring plants to reach the sensor.

Data of shoots per plant and R:FR from each plot were then fitted over the accumulated thermal time from sowing using a logistic function (Fig. 3-1) (Sparkes et al., 2006).

$$S \text{ or } R = A + \frac{C}{1 + e^{-B(t - M)}}$$

where S is the shoots per plant, R is the R:FR, A is the lower asymptote, (A + C) is the upper asymptote, B is the doubled relative rate of tillering or R:FR reduction at the time M, M is the accumulated thermal time when tillering rate or R:FR decline rate is at maximum and when shoot number or R:FR reaches (A + 0.5C), and t is the accumulated thermal time after sowing. The parameters used to describe the kinetics of tillering and R:FR are: total shoots per plant (A + C), fertile shoots per plant (counted at late grain filling), shoot survival (fertile shoots divided by total shoots, %), infertile shoots per plant (the difference between total and fertile shoots), shoot abortion (infertile shoots divided by total shoots, %), tillering onset (t_{to}, when A + 0.1C is reached, t_{to} = M – 2.1972/B), tillering cessation (t_{tc}, when A + 0.9C is reached,

t_{tc} = M + 2.1972/B), tillering duration (t_{td}, $t_{td} = t_{tc} - t_{to}$), tillering rate (0.8C/t_{td}), the onset of R:FR reduction ($t_{R:FRor}$, when A + 0.9C is reached $t_{R:FRor}$ = M + 2.1972/B), the end of R:FR reduction ($t_{R:FRer}$, when A + 0.1C is reached $t_{R:FRer}$ = M − 2.1972/B), and stabilised R:FR (the lower asymptote A). In addition, R:FR at tillering onset and cessation were calculated.

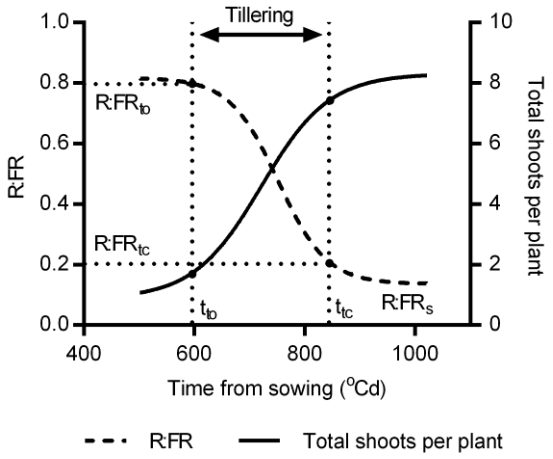

Fig. 3-1 Dynamics of tillering and red:far red ratio (R:FR) at the base of canopy in the mapping population of Forno and Oberkulmer. Data of shoot number per plant and R:FR from each plot were fitted over the accumulated thermal time from sowing using a logistic function. Definitions of the parameters: t_{to}, the time at tillering onset; t_{tc}, the time at tillering cessation; R:FR$_{to}$, R:FR at tillering onset; R:FR$_{tc}$, R:FR at tillering cessation; R:FR$_s$, stabilised R:FR. The base temperature 0^{o}C was used to calculate the accumulated thermal time from sowing.

Another key event during tillering is the onset of stem elongation (Growth Stage 31, GS31) (Zadoks et al., 1974). Five plants in central rows from each plot were split to observe the first internodes every four days. A line was judged to enter this stage when three or more main shoots had the first internodes longer than 1 cm. R:FR at GS31 was then calculated. In 2013, 15 RILs were selected randomly; five plants from each plot were measured for R:FR, counted for shoot number, and split for initial stem length (removing leaf sheaths and spikes) on 9 May (around GS31).

Thinning was carried out in five RILs in 2013. Plant density in these lines was reduced to 50% by removing every other plant after emergence. Ten central plants in the thinned area in each plot were selected, and another ten plants without thinning taken as control. Dynamics of the shoot number and R:FR of these plants were recorded for curve fitting, as described above.

Plant height, carpel size and stem water soluble carbohydrate (WSC) content at anthesis were analysed in both seasons. For each plot of the subsets, five (in 2012) and ten (in 2013) shoots with the first anthers on spikes just visible, were collected. Plant height was measured from the shoot bases to spike tips, excluding awns. Five spikes of each sample were used for carpel analysis. Two middle spikelets of each spike in 2012, and three spikelets (the third spikelets counted from the bases and tips, and the middle one between them on one side of a spike) in 2013, were dissected carefully. The carpels in the first three florets of a spikelet counting from the rachis were removed, oven-dried at 85^{o}C for 48 h, and weighed using an electronic balance (0.0001 g) (125A, Precisa, Dietikon, Switzerland). Average dry weight of individual carpels was then calculated. After removing leaves, all the stems (plus leaf sheaths) from the same shoots were collected, oven-dried immediately, weighed, and finely ground. Stem carbohydrates were extracted (80% ethanol and water), and WSC were measured using the anthrone method, following the protocols of van Herwaarden et al. (1998), and Yemm and Willis (1954). Average dry weight of stem WSC per shoot was then calculated.

At maturity, 5 and 20 spikes from each plot in 2012 and 2013, respectively, were collected and threshed by a thresher and then by hand. The grains were oven-dried at 85^{o}C for 48 h and weighed, and yield per shoot was calculated. Then, c. 200 grains were counted to calculate thousand grain weight (TGW) and grains per shoot. Yield and grains per plant were obtained by multiplying yield and grains per shoot by fertile shoot number, respectively.

3.3.2 Shading experiment in the glasshouse

A glasshouse experiment was conducted to test the effects of shade on tiller number and yield components in 2014. Green shade was achieved by using a green plastic filter (122 Fern Green; LEE Filters, Hampshire, UK) (Kegge et al., 2013). This green filter reduced photosynthetically active radiation (PAR, measured with a ceptometer: AccuPAR, Decagon Devices, Pullman, USA) to 220 µmol m^{-2} s^{-1} and R:FR (SKR 116, Skye Instruments, Llandrindod Wells, UK) to 0.2, compared with the control using clear filters (PAR = 680 µmol m^{-2} s^{-1} and R:FR = 1.0). The filters were fixed on four sides and top of a woody frame, but left a 15 cm gap at the top of each side for ventilation. Daily temperature inside the frames during treatment was recorded using a data logger (Tinytag Ultra 2, Gemini Data Loggers, West Sussex, UK), and the

average temperature between shading and control was the same (15.3 ^{o}C). The seeds of the subset (110 RILs) were sown on 17 Dec. 2013. The seedlings were vernalised at 6 ^{o}C for nine weeks, and then transplanted into 1 L pots (one plant per pot) filled with the loam-based compost (No. 3, John Innes, Norwich, UK). The RILs were arranged in a randomised complete block design with three replicates for both the shading and control. Frames were put on the plants from 27 Mar. (onset of tillering) to 2 May 2014. The plants were watered frequently, and individually fed with 40 kg N ha^{-1} at the beginning of stem elongation. At maturity, fertile shoots of each plant were counted, and all spikes were threshed. Total grains were oven-dried at 85^{o}C for 48 h, weighed and counted. Yield per plant, yield per shoot, grains per plant, grains per shoot, and TGW were then calculated.

3.4 Results

3.4.1 Phenotypic variation in tillering dynamics in the Forno × Oberkulmer mapping population

Tillering traits, including total shoots per plant, fertile and infertile shoots per plant, shoot survival and abortion, and tillering rate, were similar between the bread wheat Forno and spelt Oberkulmer in the field in 2012 (Fig. 3-2). However, Oberkulmer had many more total, fertile and infertile shoots per plant, higher shoot survival and tillering rate but lower shoot abortion than Forno in 2013. In the glasshouse experiment, fertile shoots per plant of Oberkulmer (5.3 shoots) was similar to that of Forno (5.0 shoots) under control condition, but Oberkulmer had 4.7 fertile shoots per plant under shading treatment, compared to Forno's 3.3. These indicate that spelt can produce equal or more shoots than bread wheat, depending on growth environments.

Large genetic variation in all tillering traits was found in the RILs in each year (Fig. 3-2). In addition to genotypes, years also affected tillering patterns: total shoots per plant (+38%), fertile shoots per plant (+60%), shoot survival (+9%), infertile shoots per plant (+16%) and tillering rate (+316%), were higher in 2013 than that in 2012 ($P < 0.01$); in contrast, shoot abortion decreased in 2013 (−9%, $P < 0.01$). Averaged across years, shoot survival was only 55% across the RILs in the field.

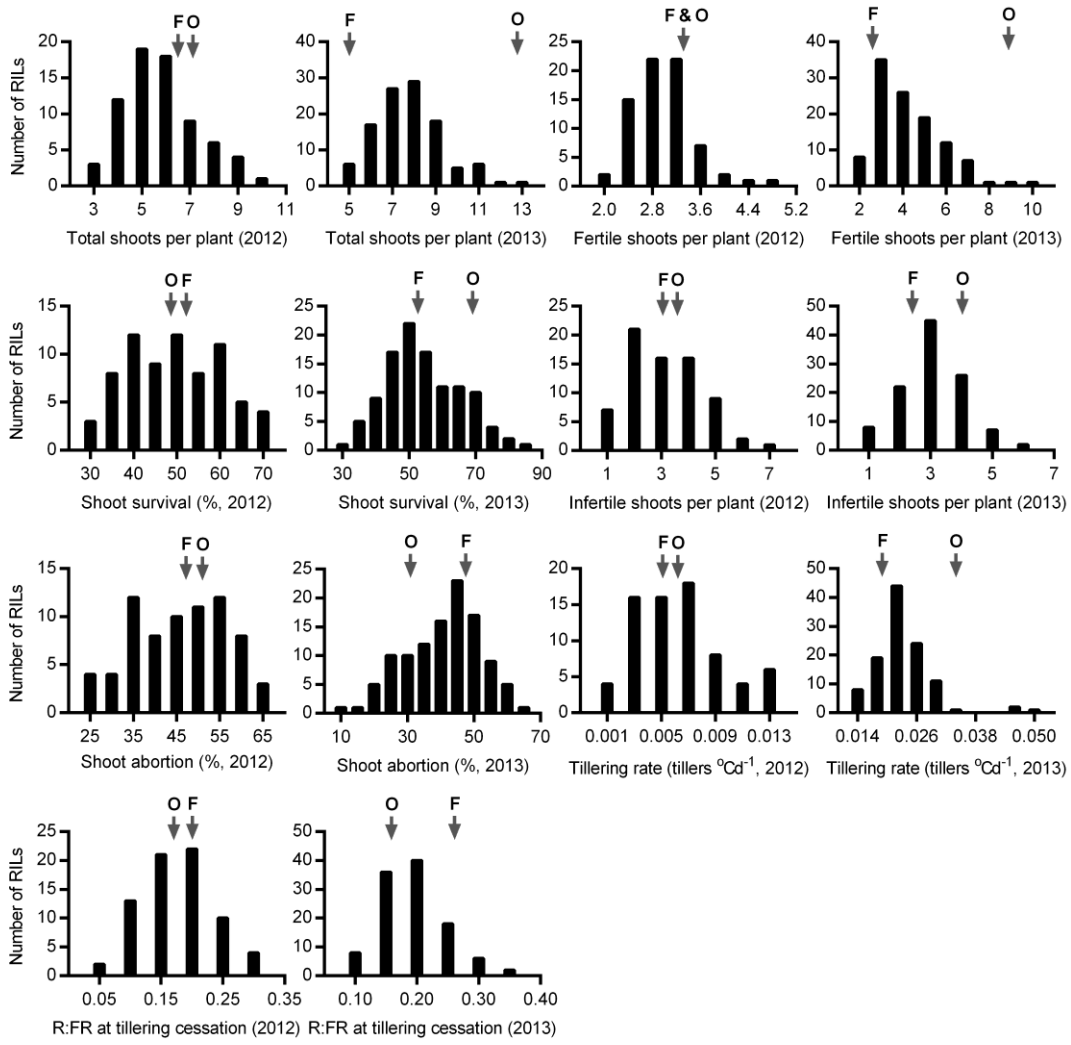

Fig. 3-2 Distributions of the recombinant inbred line (RIL) values for tillering and red:far red ratio (R:FR) at tillering cessation. Parental values are indicated with the arrows: F, Forno; O, Oberkulmer. Significant difference in each trait among the RILs was found ($P < 0.01$).

3.4.2 Phenotypic correlations between tillering traits

Total shoots per plant were positively associated with fertile and infertile shoots per plant (Table 3-1). However, the relationships between total shoots per plant, shoot survival and abortion differed across years: more total shoots were associated with lower shoot survival but with higher shoot abortion in 2012, and the opposite was true in 2013. Total shoots per plant were largely dependent on the tillering rate rather than its duration. There was no (in 2012) or weak (in 2013) negative relationship between fertile and infertile shoot number, indicating large independence. Both traits were positively associated with tillering rate. In addition, delayed onset and cessation of tillering appeared to be associated with more fertile shoots and higher shoot survival,

and with fewer infertile shoots and lower shoot abortion. Tillering onset showed a positive relationship with tillering rate, but a negative one with tillering duration, suggesting that the later tillering onset, the faster tillering rate, and the shorter tillering duration.

Table 3-1 Correlations between tillering traits in the mapping population of Forno and Oberkulmer

Tillering trait[a]	Total shoots per plant	Fertile shoots per plant	Shoot survival	Infertile shoots per plant	Shoot abortion	Tillering rate	Tillering onset	Tillering cessation	Tillering duration
Total shoots per plant	1	0.46**	-0.76**	0.94**	0.76**	0.90**	0.23*	-0.02	-0.21
Fertile shoots per plant	0.80**	1	0.19	0.14	-0.19	0.33**	0.36**	0.24*	-0.12
Shoot survival	0.31**	0.80**	1	-0.92**	-1.00**	-0.76**	0.00	0.21	0.16
Infertile shoots per plant	0.35**	-0.28**	-0.77**	1	0.92**	0.88**	0.12	-0.12	-0.19
Shoot abortion	-0.31**	-0.80**	-1.00**	0.77**	1	0.76**	0.00	-0.21	-0.16
Tillering rate	0.64**	0.50**	0.15	0.25**	-0.15	1	0.29*	-0.23*	-0.43**
Tillering onset	0.22*	0.40**	0.43**	-0.27**	-0.43**	0.43**	1	0.26*	-0.64**
Tillering cessation	0.48**	0.66**	0.61**	-0.26**	-0.61**	0.01	0.25**	1	0.57**
Tillering duration	0.26**	0.28**	0.21*	-0.02	-0.21*	-0.31**	-0.54**	0.69**	1

[a] Top right matrix: 2012 season; down left matrix: 2013 season.

* Significant at $P < 0.05$, ** significant at $P < 0.01$.

3.4.3 Identification of the QTL associated with tillering traits

A total of 34 QTL were identified for the tillering traits in the Forno × Oberkulmer mapping population, including one QTL for total shoots per plant, six for fertile shoots per plant, two for infertile shoots per plant, five for each of shoot survival and abortion, one for tillering rate, ten for tillering onset (containing nine for initial shoots per plant, which were recorded from the second tiller count at the beginning of tillering and used to measure tillering progress), and four for tillering cessation (Fig. 3-3 and Table 3-2). These QTL were scattered on ten chromosomes (1A, 2D, 3A, 3B, 4A, 4B, 5A, 5B, 7AL, and 7B), and most of them (76%) were located in the A genome. Phenotypic variation explained by individual QTL varied, ranging from 6.3−22.6%.

The QTL coincidences between tillering traits were mainly found on chromosomes 3A, 4A, and 5A (Fig. 3-3). For the QTL cluster on 3A, the alleles from the bread wheat Forno delayed tillering onset and cessation, and increased shoot survival. There were two regions of QTL coincidences on 4A: one was located on 4AS, where Forno conferred the alleles increasing fertile shoot number and shoot survival; the other was

located on the distal region of 4AL, where Oberkulmer conferred the alleles increasing initial and fertile shoot number. Likewise, there were also two regions of QTL coincidences on 5A: one was located on 5AS, where the alleles from Forno delayed tillering onset and cessation, increased shoot survival, and decreased infertile shoots; the other was located on 5AL, where the alleles from Oberkulmer delayed tillering onset and cessation, accelerated tillering rate, and increased total, fertile and infertile shoot number. However, one increasing and one decreasing alleles for shoot survival were also identified from Oberkulmer in this region; in other words, there were two closely linked alleles with the opposite effects on shoot survival, and their expressions depended on years.

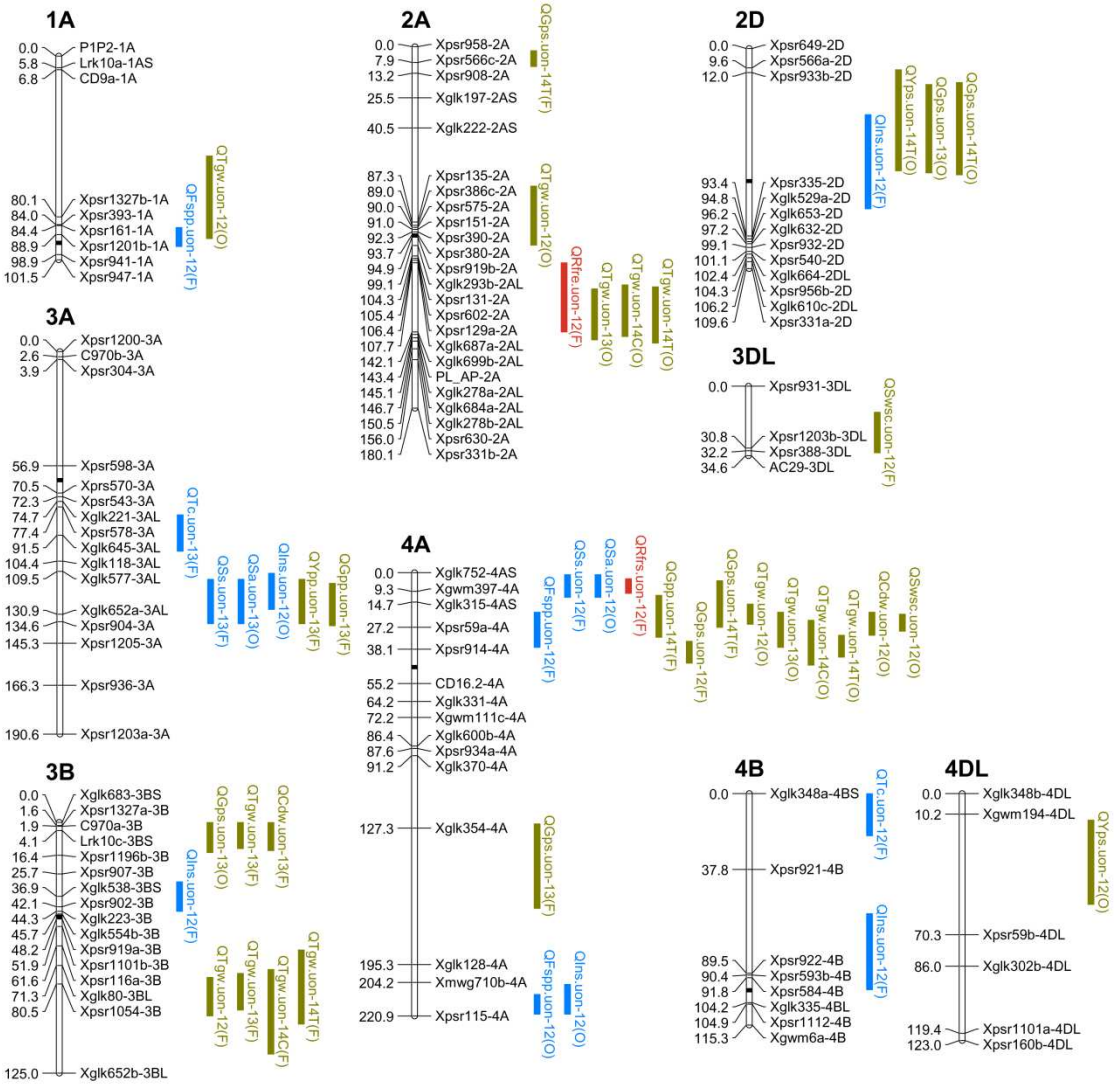

Fig. 3-3 Quantitative trait loci (QTL) for tillering, red:far red ratio (R:FR), and yield components in the mapping population of Forno and Oberkulmer. The 1-LOD support intervals of significant QTL are indicated by blue (tillering), red (R:FR) and green (yield components) vertical bars. For QTL symbols, the 'Q' is followed by the abbreviated names of quantitative traits and laboratory (uon). Abbreviations for the traits: Tspp, total shoots per plant; Fspp, fertile shoots per plant; Ss, shoot survival (%); Ispp, infertile shoots per plant; Sa, shoot abortion (%); Tr, tillering rate; Ins, initial shoots per plant; To, the time at tillering onset; Tc, the time at tillering cessation; Rfrto, R:FR at tillering onset; Rfr31, R:FR at GS31 (onset of stem elongation); Rfrs, stabilised R:FR; Rfre, the time at the end of R:FR reduction; Ypp, yield per plant; Yps, yield per shoot; Gpp, grains per plant; Gps, grains per shoot; Tgw, thousand grain weight; Cdw, carpel dry weight at anthesis; and Swsc, stem water soluble carbohydrate dry weight at anthesis. The QTL found in 2012 (field), 2013 (field), 2014 (glasshouse, control) and 2014 (glasshouse, shading treatment) are indicated by the suffixes 12, 13, 14C and 14T, respectively. In the parentheses, the parental lines providing the alleles increasing trait values are given: F, Forno; O, Oberkulmer.

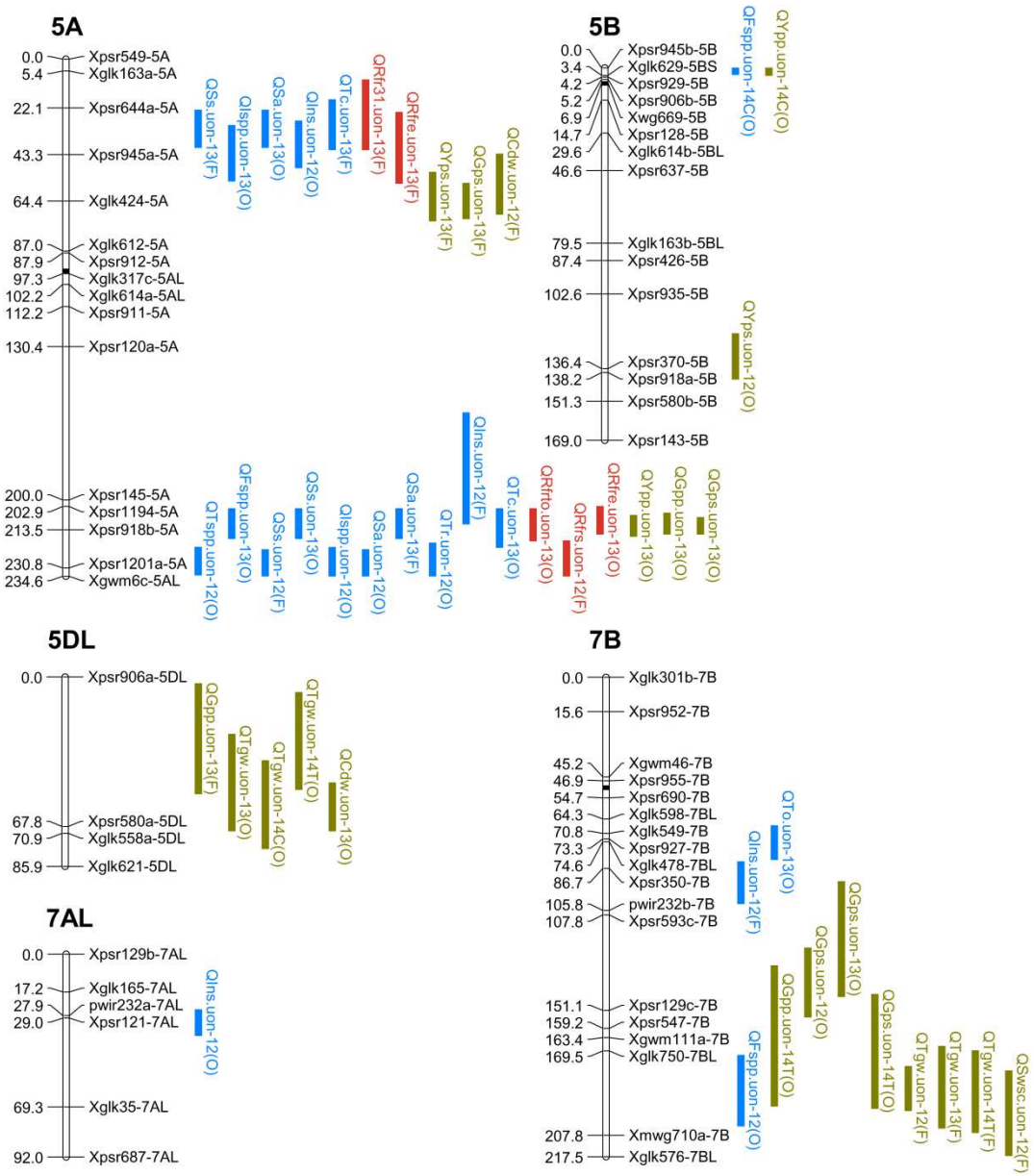

Fig. 3-3 (continued)

Table 3-2 Quantitative trait loci (QTL) for tillering, red:far red ratio (R:FR) and yield components in the Forno × Oberkulmer mapping population

Trait/Chromosome	Year[a]	Position (cM)	LOD	R^{2b}	Additive effect[c]	Closest marker
Tillering						
Total shoots per plant						
5A	2012	229.5	3.68	21.5	-0.7	Xpsr1201a-5A
Fertile shoots per plant						
1A	2012	88.9	3.28	19.4	0.2	Xpsr1201b-1A
4A	2012	30.2	3.13	18.6	0.2	Xpsr59a-4A
	2012	219.2	3.56	20.9	-0.2	Xpsr115-4A
5A	2013	209.9	5.85	21.7	-0.8	Xpsr918b-5A
5B	2014C	0.1	3.42	13.3	-0.4	Xpsr945b-5B
7B	2012	188.5	3.45	20.3	-0.2	Xmwg710a-7B
Shoot survival (%)						
3A	2013	124.5	3.28	12.8	5.1	Xglk652a-3AL
4A	2012	8.0	3.33	19.7	5.2	Xgwm397-4A
5A	2012	230.8	2.99	17.9	4.6	Xpsr1201a-5A
	2013	32.1	5.29	19.9	6.3	Xpsr644a-5A
	2013	209.9	6.12	22.6	-6.4	Xpsr918b-5A
Infertile shoots per plant						
5A	2012	231.8	3.62	21.2	-0.6	Xpsr1201a-5A
	2013	37.1	5.49	20.5	-0.5	Xpsr945a-5A
Shoot abortion (%)						
3A	2013	124.5	3.28	12.8	-5.1	Xglk652a-3AL
4A	2012	8.0	3.33	19.7	-5.2	Xgwm397-4A
5A	2012	230.8	2.99	17.9	-4.6	Xpsr1201a-5A
	2013	32.1	5.29	19.9	-6.3	Xpsr644a-5A
	2013	209.9	6.12	22.6	6.4	Xpsr918b-5A
Tillering rate (tillers $^{o}Cd^{-1}$)						
5A	2012	228.5	3.28	19.4	-0.0016	Xpsr1201a-5A
Initial shoots per plant						
2D	2012	55.9	3.53	7.8	0.3	Xpsr335-2D
3A	2012	119.5	4.78	10.4	-0.2	Xglk577-3AL
3B	2012	38.9	3.51	7.8	0.1	Xglk538-3BS
4A	2012	213.2	4.24	9.3	-0.2	Xpsr115-4A
4B	2012	91.8	3.54	7.8	0.1	Xpsr584-4B
5A	2012	35.1	5.88	12.7	-0.2	Xpsr945a-5A
	2012	205.9	4.59	10.0	0.2	Xpsr1194-5A
7AL	2012	27.9	3.18	7.1	-0.1	pwir232a-7AL
7B	2012	91.7	2.84	6.3	0.1	Xpsr350-7B
Time at tillering onset (^{o}Cd)						
7B	2013	75.6	3.24	12.7	-12	Xglk478-7BL
Time at tillering cessation (^{o}Cd)						
3A	2013	89.4	3.29	12.9	14	Xglk645-3AL
4B	2012	8.0	3.10	18.4	72	Xglk348a-4BS
5A	2013	30.1	3.35	13.1	15	Xpsr644a-5A
	2013	210.9	3.67	14.2	-15	Xpsr918b-5A

Table 3-2 (continued)

Trait/Chromosome	Year	Position (cM)	LOD	R^2	Additive effect	Closest marker
R:FR						
R:FR at tillering onset						
5A	2013	211.9	3.37	13.2	-0.02	Xpsr918b-5A
R:FR at GS31 (onset of stem elongation)						
5A	2013	31.1	3.59	13.9	0.02	Xpsr644a-5A
Stabilised R:FR						
4A	2012	9.3	3.13	18.6	0.01	Xgwm397-4A
5A	2012	225.5	4.46	25.5	0.02	Xpsr1201a-5A
Time at the end of R:FR reduction (^{o}Cd)						
2A	2012	125.7	2.59	15.7	91	Xglk699b-2AL
5A	2013	35.1	3.45	13.5	15	Xpsr945a-5A
	2013	208.9	4.73	17.9	-16	Xpsr918b-5A
Yield components						
Yield per plant (g)						
3A	2013	124.5	3.26	12.8	1.37	Xglk652a-3AL
5A	2013	211.9	6.94	25.2	-1.76	Xpsr918b-5A
5B	2014C	1.0	3.15	12.3	-0.80	Xpsr945b-5B
Yield per shoot (g)						
2D	2014T	40.9	3.60	14.0	-0.22	Xpsr933b-2D
4DL	2012	37.2	3.15	18.7	-0.15	Xgwm194-4DL
5A	2013	63.3	3.38	13.2	0.10	Xglk424-5A
5B	2012	136.4	3.30	19.5	-0.07	Xpsr370-5B
Grains per plant						
3A	2013	125.5	3.08	12.1	32	Xglk652a-3AL
4A	2014T	21.7	4.21	16.1	13	Xpsr59a-4A
5A	2013	209.9	7.74	27.7	-46	Xpsr918b-5A
5DL	2013	31.0	3.68	14.3	60	Xpsr906a-5DL
7B	2014T	156.1	4.24	16.3	-12	Xpsr547-7B
Grains per shoot						
2A	2014T	7.0	3.08	12.1	2	Xpsr566c-2A
2D	2013	45.9	4.69	17.8	-6	Xpsr933b-2D
	2014T	44.9	4.23	16.2	-5	Xpsr933b-2D
3B	2013	8.1	3.72	14.4	-3	Lrk10c-3BS
4A	2012	38.1	3.49	20.5	2	Xpsr914-4A
	2013	152.3	3.61	14.0	6	Xglk354-4A
	2014T	10.3	2.93	11.5	2	Xgwm397-4A
5A	2013	64.4	4.53	17.3	3	Xglk424-5A
	2013	213.5	5.10	19.2	-3	Xpsr918b-5A
7B	2012	138.8	3.15	18.7	-3	Xpsr129c-7B
	2013	128.8	3.09	12.1	-3	Xpsr593c-7B
	2014T	165.4	3.85	14.9	-2	Xgwm111a-7B

Table 3-2 (continued)

Trait/Chromosome	Year	Position (cM)	LOD	R^2	Additive effect	Closest marker
Thousand grain weight (g)						
1A	2012	80.1	3.57	20.9	-2.55	Xpsr1327b-1A
2A	2012	94.9	3.47	20.4	-2.50	Xpsr919b-2A
	2013	133.7	3.54	13.8	-2.00	Xglk699b-2AL
	2014C	133.7	2.98	11.7	-2.01	Xglk699b-2AL
	2014T	143.4	3.52	13.7	-1.60	PL_AP-2A
3B	2012	80.5	4.73	26.8	2.97	Xpsr1054-3B
	2013	2.9	3.44	13.4	1.60	C970a-3B
	2013	80.5	5.11	19.3	1.91	Xpsr1054-3B
	2014C	100.5	3.39	13.2	2.90	Xpsr1054-3B
	2014T	78.3	3.02	11.9	1.62	Xpsr1054-3B
4A	2012	20.7	7.17	37.6	-3.95	Xglk315-4AS
	2013	31.2	4.76	18.1	-2.09	Xpsr59a-4A
	2014C	32.2	4.10	15.8	-2.13	Xpsr59a-4A
	2014T	34.2	7.93	28.2	-2.61	Xpsr914-4A
5DL	2013	45.0	3.88	15.0	-3.17	Xpsr580a-5DL
	2014C	58.0	5.54	20.7	-3.05	Xpsr580a-5DL
	2014T	32.0	4.17	16.0	-3.62	Xpsr906a-5DL
7B	2012	187.5	5.97	32.5	4.64	Xglk750-7BL
	2013	187.5	3.24	12.7	2.24	Xglk750-7BL
	2014T	189.5	3.15	12.4	2.27	Xmwg710a-7B
Carpel dry weight at anthesis (mg)						
3B	2013	0.1	4.37	16.7	0.03	Xglk683-3BS
4A	2012	27.2	3.46	20.4	-0.06	Xpsr59a-4A
5A	2012	56.3	3.78	22.0	0.07	Xglk424-5A
5DL	2013	67.8	4.29	16.4	-0.03	Xpsr580a-5DL
Stem water soluble carbohydrate dry weight at anthesis (g)						
3DL	2012	23.0	3.49	20.5	0.069	Xpsr1203b-3DL
4A	2012	27.2	4.88	27.5	-0.069	Xpsr59a-4A
7B	2012	192.5	3.51	20.6	0.080	Xmwg710a-7B

[a] 2012 and 2013: field experiments; 2014: glasshouse experiment (C, control; T, shading treatment).

[b] The proportion of phenotypic variation explained by individual QTL.

[c] Positive additive effects indicate that the alleles from Forno increase the values of the traits, whereas negative additive effects indicate that the alleles from Oberkulmer increase the values of the traits.

3.4.4 Tillering dynamics as related to low R:FR

R:FR at the base of canopy in the field showed relationships with the tillering dynamics (Table 3-3). R:FR at tillering onset was positively associated with total and fertile shoot number, and shoot survival in 2013. Higher R:FR at that time was also associated with delayed tillering cessation across years. R:FR at tillering cessation and GS31, and stabilised R:FR, showed positive relationships with shoot survival, and negative relationships with infertile shoots per plant and shoot abortion, indicating that low R:FR established after tiller initiation promotes tiller death. R:FR at tillering cessation differed between the RILs, indicating the different responses of genotypes to low R:FR (Fig. 3-2). R:FR at tillering cessation was slightly higher in 2013 (0.21) than in 2012 (0.19) ($P < 0.05$).

As expected, thinning raised R:FR at tillering onset (+17%), leading to more total (+31%) and fertile (+47%) shoots per plant, higher shoot survival (+12%), and lower shoot abortion (−8%) (Fig. 3-4 and Table 3-4). A detailed analysis showed that thinning did not change the onset and rate of tillering, but delayed tillering cessation. These results are consistent with the above observations. There was no difference between thinned and control lines in R:FR at either tillering cessation or GS31, as well as stabilised R:FR.

R:FR around GS31 was measured in 15 RILs on a given day in 2013, and showed a positive relationship with fertile shoots per plant (Fig. 3-5). In addition, shading in the glasshouse also reduced fertile shoots per plant by 12% (Table 3-5).

Table 3-3 Correlations between tillering traits and red:far red ratio (R:FR) in the mapping population of Forno and Oberkulmer

Tillering trait	$R:FR_{to}$[a]		$R:FR_{tc}$		$R:FR_{31}$		$R:FR_{s}$		$R:FR_{or}$		$R:FR_{er}$	
	2012	2013	2012	2013	2012	2013	2012	2013	2012	2013	2012	2013
Total shoots per plant	0.12	0.33**	-0.55**	-0.34**	-0.59**	0.11	-0.59**	0.08	-0.22	0.03	0.06	0.31**
Fertile shoots per plant	-0.04	0.43**	-0.30**	-0.22*	-0.11	0.45**	-0.24*	0.30**	-0.12	-0.01	0.15	0.60**
Shoot survival	0.08	0.38**	0.40**	-0.05	0.59**	0.62**	0.50**	0.41**	0.16	-0.04	0.04	0.66**
Infertile shoots per plant	-0.10	-0.14	-0.50**	-0.21*	-0.62**	-0.52**	-0.56**	-0.33**	-0.19	0.06	0.01	-0.45**
Shoot abortion	-0.08	-0.38**	-0.40**	0.05	-0.59**	-0.62**	-0.50**	-0.41**	-0.16	0.04	-0.04	-0.66**
Tillering rate	-0.13	-0.18	-0.47**	0.12	-0.57**	0.03	-0.51**	0.06	-0.17	-0.03	0.03	0.18
Tillering onset	0.33**	0.10	-0.33**	0.02	0.18	0.25**	0.01	0.29**	0.09	0.04	0.21	0.37**
Tillering cessation	0.34**	0.44**	-0.30**	-0.61**	0.32**	0.49**	-0.04	0.30**	0.20	0.10	0.18	0.58**
Tillering duration	0.15	0.31**	-0.49**	-0.55**	0.10	0.24*	-0.04	0.04	0.08	0.06	-0.03	0.23*

[a] Abbreviations of the traits: $R:FR_{to}$, R:FR at tillering onset; $R:FR_{tc}$, R:FR at tillering cessation; $R:FR_{31}$, R:FR at GS31 (onset of stem elongation); $R:FR_{s}$, stabilised R:FR; $R:FR_{or}$, the time at the onset of R:FR reduction; $R:FR_{er}$, the time at the end of R:FR reduction.

* Significant at $P < 0.05$, ** significant at $P < 0.01$.

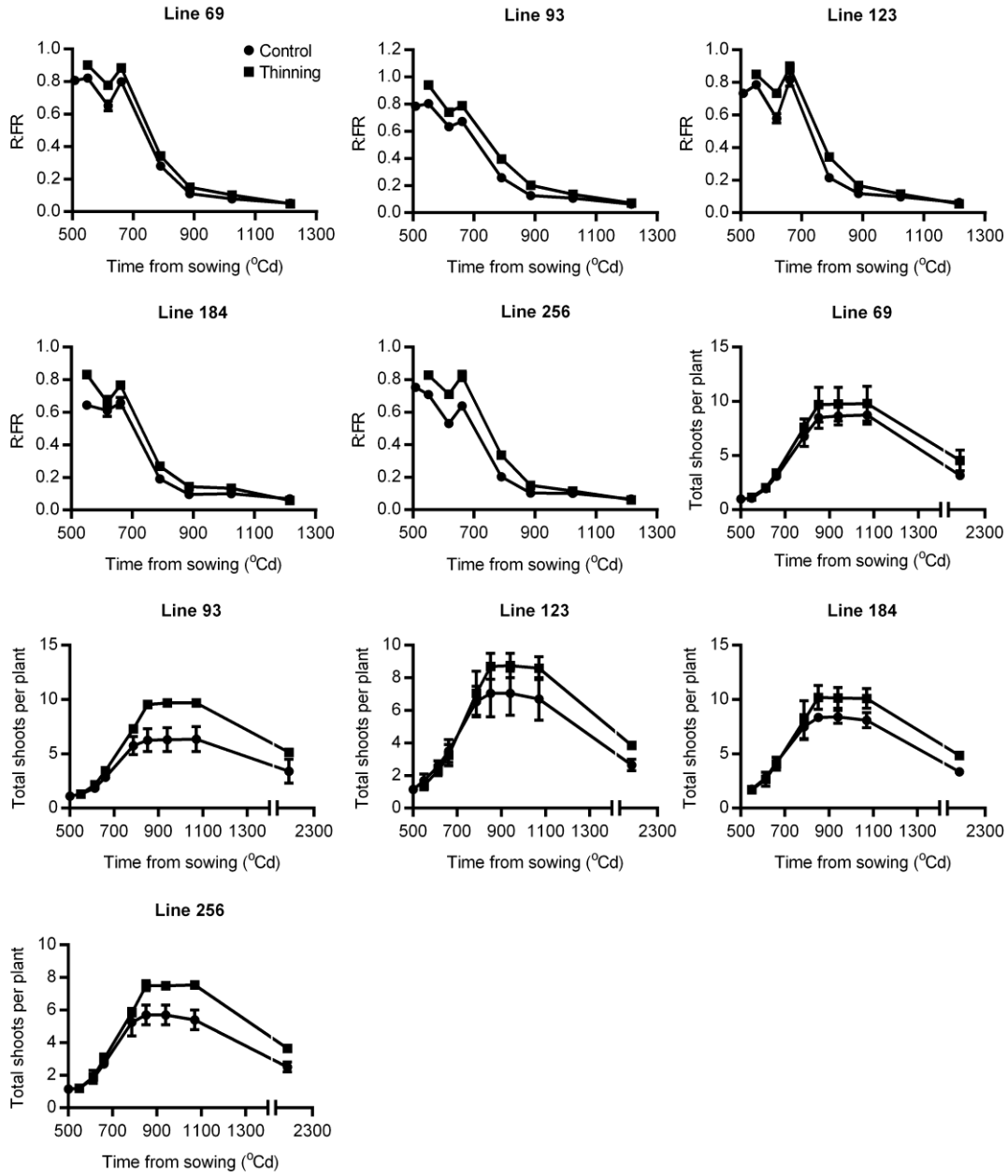

Fig. 3-4 Dynamics of tillering and red:far red ratio (R:FR) in the control (circles) and thinned (squares) lines. Values of shoot number per plant and R:FR at each time point are shown as mean ± standard error of the mean (bars). The last count, representing the fertile shoot number per plant, was taken at late grain filling. The base temperature 0°C was used to calculate the accumulated thermal time from sowing.

Table 3-4 Thinning effects on tillering and red:far red ratio (R:FR)

Trait	Mean across five lines (n = 3)		P-value (NS, not significant; *, P < 0.05; **, P < 0.01)			Thinning effect (%)
	Control	Thinning	Treatment	Line	Treatment × line	
Total shoots per plant	7.2	9.4	**	NS	NS	+ 31
Fertile shoots per plant	3.0	4.4	**	NS	NS	+ 47
Shoot survival (%)	42.2	47.1	*	*	NS	+ 12
Infertile shoots per plant	4.2	5.0	NS	*	NS	NS
Shoot abortion (%)	57.8	52.9	*	*	NS	− 8
Tillering rate (tillers $^{o}Cd^{-1}$)	0.024	0.027	NS	NS	NS	NS
Tillering onset (^{o}Cd)	580	590	NS	NS	NS	NS
Tillering cessation (^{o}Cd)	789	838	**	NS	NS	+ 6
Tillering duration (^{o}Cd)	210	248	NS	NS	NS	NS
R:FR at tillering onset	0.71	0.83	**	*	NS	+ 17
R:FR at tillering cessation	0.25	0.20	NS	NS	NS	NS
Onset of stem elongation (^{o}Cd, GS31)	882	930	**	**	NS	+ 5
R:FR at GS31	0.10	0.12	NS	NS	NS	NS
End of R:FR reduction (^{o}Cd)	832	854	**	**	*	+ 3
Stabilised R:FR	0.08	0.09	NS	NS	NS	NS

Table 3-5 Shading effects on fertile shoot number and other yield components

Trait	Mean across 112 lines (n = 3)		P-value (NS, not significant; *, P < 0.05; **, P < 0.01)			Shading effect (%)
	Control	Shading	Treatment	Line	Treatment × line	
Fertile shoots per plant	5.1	4.5	**	**	NS	− 12
Yield per plant (g)	7.60	5.23	**	**	NS	− 31
Yield per shoot (g)	1.47	1.21	**	**	NS	− 18
Grains per plant	162	111	**	**	NS	− 31
Grains per shoot	31	25	**	**	NS	− 19
Thousand grain weight (g)	47.4	47.8	NS	**	NS	NS

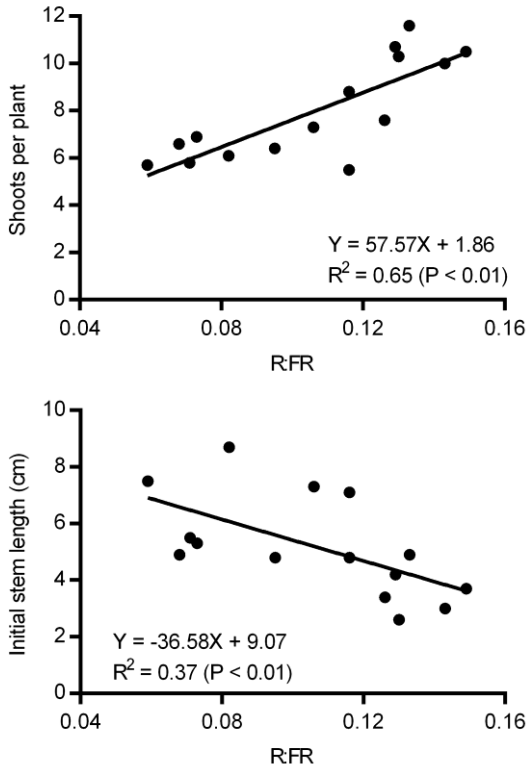

Fig 3-5 Relationships between red:far red ratio (R:FR), shoots per plant and initial stem length around the onset of stem elongation

Genetic analysis revealed a total of seven QTL for R:FR, including one QTL for each of R:FR at tillering onset and GS31 on chromosome 5A, two for stabilised R:FR on 4A and 5A, and three for the timing of R:FR reduction on 2A and 5A (Fig. 3-3 and Table 3-2). A QTL for stabilised R:FR was coincident with those for tillering traits on 4A; the increasing alleles from Forno raised stabilised R:FR, fertile shoot number and shoot survival. In addition, the QTL coincidences between R:FR and tillering occurred on chromosome 5A. Forno provided the alleles on 5AS increasing the R:FR at GS31, delaying tillering onset and cessation, increasing shoot survival, and decreasing infertile shoot number and shoot abortion. In contrast, Oberkulmer provided the alleles on 5AL increasing the R:FR at tillering onset, delaying tillering onset and cessation, and increasing total and fertile shoots per plant, as well as shoot survival. A QTL for stabilised R:FR was also coincident with the other QTL for shoot survival in this region, with the increasing alleles from Forno. These results support the phenotypic relationships between R:FR and tillering.

3.4.5 Responses of the onset of stem elongation and plant height to low R:FR

There were positive relationships between the R:FR just before GS31 and the accumulated thermal time for GS31 ($r = 0.40$, $P < 0.01$ in 2012; $r = 0.33$, $P < 0.01$ in 2013), indicating that the lower R:FR, the earlier onset of stem elongation. Consistent with this, R:FR around GS31 was negatively associated with the initial stem length at the same time (Fig. 3-5). In addition, the R:FR was increased by thinning, resulting in a delay of the onset of stem elongation (Table 3-4).

Plant height at anthesis was negatively associated with R:FR at tillering cessation ($r = -0.28$, $P < 0.05$ in 2012; $r = -0.20$, $P < 0.05$ in 2013), and with stabilised R:FR in 2012 ($r = -0.31$, $P < 0.01$).

3.4.6 Synchrony among tillering cessation, R:FR stabilisation and the onset of stem elongation

Tillering ceased at 1196 and 844 ^{o}Cd after sowing over all RILs in 2012 and 2013, respectively, coincident with R:FR stabilisation (1273 ^{o}Cd in 2012 and 862 ^{o}Cd in 2013) and GS31 (1214 ^{o}Cd in 2012 and 905 ^{o}Cd in 2013). This was also found in the thinning experiment, including both control and treatment (Table 3-4). The onset of stem elongation was slightly later than tillering cessation and R:FR stabilisation. However, taking account of the measurement of GS31 (the first internodes > 1 cm), the exact beginning of stem elongation might coincide with the other two events.

3.4.7 Relationships between tillering and yield components

Total shoots per plant contributed to yield and grain number per plant, and did not affect yield and grain number per shoot, and TGW (Table 3-6). Similarly, fertile shoots per plant and shoot survival in the field in 2012 and 2013, and fertile shoots per plant in the glasshouse in 2014 (both control and shading), were closely and positively associated with yield and grains per plant. More fertile shoots and higher shoot survival did not reduce yield per shoot, and even showed associations with slightly increased grains per shoot, despite an accompanying slight decline in TGW. One exception was the fertile shoots per plant in shading treatment, where more fertile shoots were associated with lower yield per shoot, which resulted mainly from reduced grains per shoot (Tables 3-5 and 3-6).

Table 3-6 Correlations between tillering traits and yield components in the mapping population of Forno and Oberkulmer

Tillering trait	Yield per plant		Yield per shoot		Grains per plant		Grains per shoot		Thousand grain weight	
Field	2012	2013	2012	2013	2012	2013	2012	2013	2012	2013
Total shoots per plant	0.31**	0.69**	-0.07	-0.12	0.26*	0.67**	-0.11	-0.01	0.01	-0.16
Fertile shoots per plant	0.70**	0.94**	-0.07	0.04	0.80**	0.93**	0.20	0.20*	-0.28*	-0.26**
Shoot survival	0.15	0.81**	0.04	0.17	0.27*	0.82**	0.26*	0.33**	-0.20	-0.27**
Infertile shoots per plant	0.09	-0.36**	-0.05	-0.25**	-0.01	-0.39**	-0.20	-0.33**	0.12	0.15
Shoot abortion	-0.15	-0.81**	-0.04	-0.17	-0.27*	-0.82**	-0.26*	-0.33**	0.20	0.27**
Tillering rate	0.25*	0.44**	-0.03	-0.06	0.20	0.41**	-0.07	-0.02	0.01	-0.05
Tillering onset	0.47**	0.37**	0.24*	-0.04	0.41**	0.40**	0.23*	0.12	0.05	-0.24**
Tillering cessation	0.31**	0.64**	0.19	0.08	0.21	0.64**	0.07	0.19*	0.16	-0.20*
Tillering duration	-0.15	0.28**	-0.05	0.10	-0.19	0.25**	-0.14	0.08	0.08	0.00
Glasshouse (2014)	Control	Shading	Control	Shading	Control	Shading	Control	Shading	Control	Shading
Fertile shoots per plant	0.71**	0.54**	0.11	-0.46**	0.76**	0.53**	0.22*	-0.40**	-0.16	-0.12

* Significant at P < 0.05, ** significant at P < 0.01.

Table 3-7 Correlations between carpel size and stem water soluble carbohydrates (WSC) at anthesis, thousand grain weight and fertile shoots per plant at maturity in the mapping population of Forno and Oberkulmer

Trait	Thousand grain weight		Fertile shoots per plant	
	2012	2013	2012	2013
Carpel dry weight	0.46**	0.34**	-0.31**	-0.19*
Stem WSC	0.55**	0.20*	-0.52**	-0.16

* Significant at P < 0.05, ** significant at P < 0.01.

To understand how more fertile shoots reduced TGW, the carpel size and stem WSC content at anthesis were analysed (Table 3-7). Both carpel size and stem WSC content were positively associated with TGW, confirming their roles in determining grain weight. Furthermore, they showed negative relationships with fertile shoots per plant, so more fertile shoots tended to produce smaller carpels and less stem WSC per shoot, and in turn smaller grains.

A total of 44 QTL for yield components were identified in the field and glasshouse experiments, including three QTL for yield per plant, four for yield per shoot, five for grains per plant, 12 for grains per shoot, and 20 for TGW (Fig. 3-3 and Table 3-2). These QTL were scattered on 11 chromosomes (1A, 2A, 2D, 3A, 3B, 4A, 4DL, 5A, 5B, 5DL, and 7B), individually explaining 11.5−37.6% of the phenotypic variation. The QTL for grains per shoot on 2D, 4A and 7B were stable across 2−3 environments, while those for TGW on 2A, 3B, 4A, 5DL and 7B were stable across 3−4 environments. In the glasshouse experiment, one QTL for yield per shoot, two for

grains per plant, four for grains per shoot, and one for TGW, were identified only under shading treatment, indicating that they may be involved in shade responses. In terms of carpel size and stem WSC content at anthesis, four and three QTL were detected, respectively, individually explaining 16.4−27.5% of the phenotypic variation (Fig. 3-3 and Table 3-2).

The QTL coincidences between tillering traits and yield components were found on seven chromosomes (1A, 2D, 3A, 4A, 5A, 5B, and 7B) (Fig. 3-3). One QTL for total shoots per plant was coincident with one for each of yield and grains per plant as well as grains per shoot on 5A, with their increasing alleles conferred by Oberkulmer. Likewise, eight QTL for fertile shoots per plant and shoot survival were coincident with those for yield and grains per plant, and grains per shoot on 3A, 4A, 5A, 5B and 7B; their increasing alleles were provided by the same parents. In contrast, four QTL for fertile shoots per plant and shoot survival were also coincident with eight QTL for TGW on 1A, 4A and 7B, but their increasing alleles were provided by the opposite parents, confirming the negative relationships between them. A further analysis showed that three QTL for carpel size and two for stem WSC content at anthesis were coincident with 11 QTL for TGW on 3B, 4A, 5DL and 7B, with the increasing alleles provided by the same parents; additionally, one QTL for carpel size and two for stem WSC content were coincident with two QTL for fertile shoots per plant on 4A and 7B, with the increasing alleles conferred by the opposite parents.

There was no QTL coincidence between total and fertile shoot number, and yield per shoot; only one QTL for shoot survival was coincident with one for yield per shoot on 5AS, with the increasing alleles conferred by Forno. These results agree with the physiological relationships between tillering and yield components.

3.5 Discussion

3.5.1 Large variation in tillering dynamics and its genetic control

Significant genetic variation in total shoots per plant (tillering capacity), fertile and infertile shoots per plant, shoot survival and abortion, tillering rate and tillering timing (onset, cessation and duration), was found in the mapping population of Forno × Oberkulmer. The variation in these tillering traits between genotypes has also been observed previously (Ishag and Taha, 1974; Hucl and Baker, 1989; Sharma, 1995; Berry et al., 2003; Dreccer et al., 2013). Thus, it is possible to optimise wheat tillering patterns by genetic selection. A major target of tillering optimisation is to increase fertile shoot number per plant. There is evidence that modern wheat is more sink limited during grain filling (Slafer and Savin, 1994; Borras et al., 2004), and sink size has to be enlarged by a further increase in grain number (Miralles and Slafer, 2007). Numerically, grain number per unit land area is a product of plant number per unit land area, fertile shoots (spikes) per plant, and grain number per shoot. As an important component of grain number, fertile shoots per plant were positively associated with total shoots per plant, tillering rate, and the time for tillering onset and cessation, indicating that genetic selection for delayed but fast tillering, and high tillering capacity, can result in more fertile shoots. The positive relationship between total and fertile shoots per plant was also reported by Sharma (1995) and Dreccer et al. (2013). An additional strategy to increase fertile shoot number is to improve tiller survival. The present study showed that only 55% of the total shoots initiated produced spikes, and there was large variation in shoot survival among the RILs (31−87%). This variation has been demonstrated in several studies, for example, 37−68% in Berry et al. (2003) and 70−93% in Sharma (1995), suggesting an opportunity to select genotypes with high shoot survival for more spikes. Likewise, only c. half of the florets initiated within spikelets set grains, and the remaining ones (mainly those at distal positions) are aborted just before anthesis (Kirby, 1988; González-Navarro et al., 2015). Floret fertility has been known to largely determine grains per shoot at maturity, the other key component of grain number per unit land area (González et al., 2011). It has been found that shoot and floret fertility respond to the availability of environmental resources such as nutrients and radiation (Ishag and Taha, 1974; Fischer and Stockman, 1980; Thorne and Wood, 1987; Alzueta et al.,

2012), indicating plasticity. This attribute of wheat plants may play a crucial role in accommodating various environments and forming yield (Sadras and Rebetzke, 2013).

Based on the genetic variation in tillering dynamics, the QTL for these traits were then identified, and reported here for the first time, except the trait of fertile shoots per plant, which has been widely studied (Kato et al., 2000; Deng et al., 2011; Naruoka et al., 2011; Jia et al., 2013; Zhang et al., 2013). Most QTL for tillering dynamics were located on chromosomes 3A, 4A, and 5A. The most important QTL cluster was detected on 5AL, where the alleles from the spelt Oberkulmer were associated with increased total, fertile and infertile shoot number, accelerated tillering rate, and delayed tillering onset and cessation. In a single-chromosome (spelt 5A) recombinant line mapping population, Kato et al. (2000) also mapped a QTL for fertile tiller number per plant at this location. Another QTL coincidence for fertile shoots per plant and shoot survival was found in the distal region of 4AS, where the QTL for tillers per plant was identified in a previous study (Jia et al., 2013). Two QTL for fertile shoots per plant were coincident with those for total shoots per plant, shoot survival, tillering rate, tillering onset and cessation, and their increasing alleles were conferred by the same parents. This is in line with the above conclusion that more fertile shoots per plant can be achieved by increasing tillering capacity and survival, accelerating tillering rate, and delaying tillering onset and cessation.

Initial shoots per plant, which were counted at the beginning of tillering on a given day, were used to quantify the difference in phenology among the RILs. The QTL coincidences between initial shoots per plant and other tillering traits were observed on chromosomes 3A, 4A, 5A and 7B, implying the genetic relationships between plant developmental progression and tillering. It has been found that tillering rate increases under the shorter photoperiods but decreases under the longer ones (Miralles and Richards, 2000). The present study revealed a QTL for initial shoots per plant on 2D, corresponding to the Ppd-D1 gene, indicating that photoperiod response gene likely regulates the timing of tillering (Borras-Gelonch et al., 2012). The photoperiod insensitive allele Ppd-D1 advances plant development (e.g. heading and anthesis), leading to reduced tillering (Dyck et al., 2004). The Ppd-B1 gene shows a similar pleiotropic effect on reduced tiller number, but this effect appears to be less pronounced than that of Ppd-D1 (Kamran et al., 2014). In addition to photoperiod, the plants responsive to vernalisation tend to produce fewer tillers at heading (Levy and

Peterson, 1972). A further analysis regarding the interactions between phenology and tillering, especially between stem elongation, tillering cessation and tiller death, is needed in future studies.

3.5.2 Low R:FR inhibits tiller production, and increases tiller abortion

Apart from the genetic control, tillering dynamics was also affected significantly by the shade generated from neighbouring plants. It seems that wheat plants can sense R:FR at early stage of tillering. Low R:FR at the beginning of tillering was associated with fewer total shoots per plant, as confirmed in the thinning experiment, indicating a inhibition of tiller production. Detailed analysis showed that low R:FR did not reduce tillering rate, but led to early tiller cessation. The same results have been observed with the treatments of low R:FR, far red light, shade or high plant density (Evers et al., 2006; Sparkes et al., 2006; Ugarte et al., 2010; Toyota et al., 2014). Threshold of the R:FR for tillering cessation in the field was on average 0.20, similar to that of the previous reports (0.20−0.40) (Evers et al., 2006; Sparkes et al., 2006; Dreccer et al., 2013). However, significant variation in this trait among the RILs (0.07−0.37) was also determined, suggesting genetic difference in the tolerance of tiller bud outgrowth to low R:FR. This difference has previously been reported between the tiller inhibition (tin1) lines and free-tillering lines. The tin1 lines become more sensitive to light quality (0.18−0.22), compared with the free-tillering lines (0.09−0.11) (Moeller et al., 2014). The tin1 gene appears to be involved in the perception of R:FR. This gene inhibits tiller bud outgrowth by limiting sugar supply due to precocious internode development (Kebrom et al., 2012). Early stem elongation can be induced by low R:FR, as shown in the present study. Therefore, it can be hypothesised that a low R:FR promotes the onset of stem elongation, leading to assimilate deprivation from growing tiller buds and, in turn, bud dormancy. The tin1 mutants respond to low R:FR earlier, and start stem elongation earlier, resulting in earlier cessation of axillary tiller bud outgrowth, fewer buds growing out, and hence fewer total tillers. Thus, R:FR may function as a direct signal inhibiting tillering by inducing stem elongation in the tin1 lines. This model can also be used to explain the coincidence between tillering cessation and the onset of stem elongation in the present and previous studies (Baker and Gallagher, 1983; Gomez-Macpherson et al., 1998; Sylvester-Bradley et al., 2008).

Low R:FR at the beginning of tillering was also associated with few fertile shoots and low shoot survival. Similarly, low R:FR established after tiller initiation was

associated with low shoot survival, more infertile shoots, and high shoot abortion. That is, light quality not only inhibits tiller bud outgrowth, but also promotes the abortion of young tillers initiated. The underlying mechanism is not clear to date. Tiller death normally starts from the onset of stem elongation, and ends around flowering (Sylvester-Bradley et al., 2008). During this period, stems and spikes are growing rapidly, suggesting source limitation (Gomez-Macpherson et al., 1998; González et al., 2011). More carbohydrates have to be diverted to these expanding sinks, leading to a shortage for developing young tillers and, in turn, tiller death (Gomez-Macpherson et al., 1998). Intra-plant competition for assimilates has been established even at the beginning of stem elongation, when tiller buds are deprived of sugars due to internode elongation, and then become dormant (Kebrom et al., 2012). On the other hand, a release in intra-plant competition by increasing resource availability like radiation improves tiller survival (Thorne and Wood, 1987). In this study, it was found that low R:FR was associated with early stem elongation and taller plants at anthesis. These responses have been well known as part of shade avoidance syndrome in many other species, involving in phytochrome perception (mainly PHYB) and hormonal regulation (Gommers et al., 2013; Rameau et al., 2015). Therefore, low R:FR may increase stem sink, and intensify intra-plant competition indirectly; as a result, tiller abortion is enhanced.

To improve tiller survival, the genotypes with either high tolerance to shade or well-established light environment can be selected. Genetic variation in shade tolerance has been determined in this study. For the latter, light quality under a canopy is a complex trait, depending on plant architecture, for example, leaf characteristics (number, size, thickness, insertion angle, shape and colour) and plant height. A few QTL for R:FR kinetics were identified in the field, and could be used in wheat breeding.

3.5.3 Increasing fertile shoot number while maintaining the other yield components

Fertile shoot number per plant largely contributed to plant productivity, confirming its role as a key yield determinant (Sharma, 1995; Kato et al., 2000). This resulted from an increase in grain number per plant, rather than individual grain weight, which showed a negative relationship with fertile shoot number. A close look revealed that more fertile shoots did not significantly reduce yield and grains per shoot, as seen in the previous studies (Kato et al., 2000; Jia et al., 2013); there was even a positive

relationship between fertile shoots per plant and grains per shoot. An exception was under the shade, where yield and grains per shoot decreased with increasing fertile shoot number. Sufficient radiation during tillering, therefore, is essential to reduce the competition among yield components.

In full sunlight, fertile shoots per plant were only negatively associated with individual grain weight, as supported by analyses of the QTL coincidences and allelic effects. Grains are filled after anthesis, but the preanthesis period also plays an important role in determining final grain weight. Grains develop from the carpels growing mainly between booting and anthesis, and carpel size at anthesis has been considered as an upper limit to grain weight (Calderini et al., 1999). Another preanthesis trait affecting grain weight is the stem WSC remobilised into grains during grain filling (van Herwaarden et al., 1998). Each of these two traits was positively associated with grain weight in this study, consistent with the results of QTL analysis, confirming their roles as grain weight determinants. Carpel growth and stem WSC accumulation concur with tiller death and final tiller formation before anthesis. More fertile shoots produced were associated with smaller carpels and less stem WSC. Genetic analysis showed the QTL coincidences between fertile shoots per plant, carpel size and stem WSC content on chromosomes 4A and 7B, indicating that the negative relationships between them at least partly result from the pleiotropic effects or tight gene linkages. To break the negative relationships, these genes may be excluded, and/or more independent ones have to be added; at the same time, leaf photosynthesis and soil nutrient supply during the preanthesis period should be improved to increase source availability.

In conclusion, this study describes the tillering dynamics in detail, and its genetic and environmental control in wheat. Large genetic variation in tillering traits was determined, and it is proposed that the genotypes with higher tillering capacity, faster tillering rate, delayed tillering onset and cessation, and higher tiller survival, can be selected to increase fertile shoot number. Based on this variation, the QTL for tillering traits were identified, and QTL coincidence analysis agrees with the above proposition for fertile shoot improvement. In addition to genetic factors, light quality (R:FR) had significant effects on tillering: low R:FR generated from neighbouring plants inhibited tiller production by accelerated tillering cessation, and promoted infertile tillers and tiller abortion, probably resulting from an assimilate shortage due to early stem

elongation and enhanced stem growth induced by low R:FR. A few QTL for R:FR kinetics in the field were also detected. After these processes, final shoot number was defined. More fertile shoots at maturity contributed to plant yield and grain number, without reducing single-shoot productivity and grain set. However, this was accompanied with a slight decrease in individual grain weight, partly as an outcome of reduced carpel size and stem WSC content at anthesis. Therefore, this study will improve our knowledge of the genetic and environmental determination of tillering process, and, in turn, grain yield formation in wheat.

3.6 Acknowledgements

We thank Beat Keller (University of Zurich, Switzerland) for providing the Forno × Oberkulmer mapping population, and Monika Messmer (Research Institute of Organic Agriculture, Switzerland) for providing the molecular marker data. We also thank John Alcock, Matthew Tovey and Mark Meacham for their help with field and glasshouse experiments. This work was supported by a joint grant from the China Scholarship Council and University of Nottingham.

3.7 References

Alzueta I, Abeledo LG, Mignone CM, Miralles DJ. 2012. Differences between wheat and barley in leaf and tillering coordination under contrasting nitrogen and sulfur conditions. European Journal of Agronomy **41**, 92-102.

Baker CK, Gallagher JN. 1983. The development of winter wheat in the field. 1. Relation between apical development and plant morphology within and between seasons. Journal of Agricultural Science **101**, 327-335.

Berry PM, Spink JH, Foulkes MJ, Wade A. 2003. Quantifying the contributions and losses of dry matter from non-surviving shoots in four cultivars of winter wheat. Field Crops Research **80**, 111-121.

Borras-Gelonch G, Rebetzke GJ, Richards RA, Romagosa I. 2012. Genetic control of duration of pre-anthesis phases in wheat (Triticum aestivum L.) and relationships to leaf appearance, tillering, and dry matter accumulation. Journal of Experimental Botany **63**, 69-89.

Borras L, Slafer GA, Otegui ME. 2004. Seed dry weight response to source-sink manipulations in wheat, maize and soybean: a quantitative reappraisal. Field Crops Research **86**, 131-146.

Cai T, Xu H, Peng D, et al. 2014. Exogenous hormonal application improves grain yield of wheat by optimizing tiller productivity. Field Crops Research **155**, 172-183.

Calderini DF, Abeledo LG, Savin R, Slafer GA. 1999. Effect of temperature and carpel size during pre-anthesis on potential grain weight in wheat. Journal of Agricultural Science **132**, 453-459.

Casal JJ. 1988. Light quality effects on the appearance of tillers of different order in wheat (Triticum aestivum). Annals of Applied Biology **112**, 167-173.

Casal JJ, Sanchez RA, Gibson D. 1990. The significance of changes in the red/far-red ratio, associated with either neighbour plants or twilight, for tillering in Lolium multiflorum Lam. New Phytologist **116**, 565-572.

Chelle M, Evers JB, Combes D, Varlet-Grancher C, Vos J, Andrieu B. 2007. Simulation of the three-dimensional distribution of the red:far-red ratio within crop canopies. New Phytologist **176**, 223-234.

Davis MH, Simmons SR. 1994. Tillering response of barley to shifts in light quality caused by neighboring plants. Crop Science **34**, 1604-1610.

Deng S, Wu X, Wu Y, et al. 2011. Characterization and precise mapping of a QTL increasing spike number with pleiotropic effects in wheat. Theoretical and Applied Genetics **122**, 281-289.

Dreccer MF, Chapman SC, Rattey AR, et al. 2013. Developmental and growth controls of tillering and water-soluble carbohydrate accumulation in contrasting wheat (Triticum aestivum L.) genotypes: can we dissect them? Journal of Experimental Botany **64**, 143-160.

Duggan BL, Richards RA, Tsuyuzaki H. 2002. Environmental effects on stunting and the expression of a tiller inhibition (tin) gene in wheat. Functional Plant Biology **29**, 45-53.

Duggan BL, Richards RA, Van Herwaarden AF, Fettell NA. 2005. Agronomic evaluation of a tiller inhibition gene (tin) in wheat. I. Effect on yield, yield components, and grain protein. Australian Journal of Agricultural Research **56**, 169-178.

Dyck JA, Matus-Cádiz MA, Hucl P, Talbert L, Hunt T, Dubuc JP, Nass H, Clayton G, Dobb J, Quick J. 2004. Agronomic performance of hard red spring wheat isolines sensitive and insensitive to photoperiod. Crop Science **44**, 1976-1981.

Evers JB, Vos J, Andrieu B, Struik PC. 2006. Cessation of tillering in spring wheat in relation to light interception and red:far-red ratio. Annals of Botany **97**, 649-658.

Evers JB, Vos J. 2013. Modeling branching in cereals. Frontiers in Plant Science **4**, 399.

Fischer RA, Stockman YM. 1980. Kernel number per spike in wheat (Triticum aestivum L.): responses to preanthesis shading. Functional Plant Biology **7**, 169-180.

Foulkes MJ, Slafer GA, Davies WJ, et al. 2011. Raising yield potential of wheat. III. Optimizing partitioning to grain while maintaining lodging resistance. Journal of Experimental Botany **62**, 469-486.

Gomez-Macpherson H, Richards RA, Masle J. 1998. Growth of near-isogenic wheat lines differing in development—plants in a simulated canopy. Annals of Botany **82**, 323-330.

Gommers CMM, Visser EJW, Onge KRS, Voesenek LACJ, Pierik R. 2013. Shade tolerance: when growing tall is not an option. Trends in Plant Science **18**, 65-71.

González-Navarro OE, Griffiths S, Molero G, Reynolds MP, Slafer GA. 2015. Dynamics of floret development determining differences in spike fertility in an elite population of wheat. Field Crops Research **172**, 21-31.

González FG, Miralles DJ, Slafer GA. 2011. Wheat floret survival as related to pre-anthesis spike growth. Journal of Experimental Botany **62**, 4889-4901.

Hucl P, Baker RJ. 1989. Tillering patterns of spring wheat genotypes grown in a semiarid environment. Canadian Journal of Plant Science **69**, 71-79.

Ishag HM, Taha MB. 1974. Production and survival of tillers of wheat and their contribution to yield. Journal of Agricultural Science **83**, 117-124.

Jia H, Wan H, Yang S, et al. 2013. Genetic dissection of yield-related traits in a recombinant inbred line population created using a key breeding parent in China's wheat breeding. Theoretical and Applied Genetics **126**, 2123-2139.

Kamran A, Iqbal M, Spaner D. 2014. Flowering time in wheat (Triticum aestivum L.): a key factor for global adaptability. Euphytica **197**, 1-26.

Kasperbauer MJ, Karlen DL. 1986. Light-mediated bioregulation of tillering and photosynthate partitioning in wheat. Physiologia Plantarum **66**, 159-163.

Kasperbauer MJ. 1987. Far-red light reflection from green leaves and effects on phytochrome-mediated assimilate partitioning under field conditions. Plant Physiology **85**, 350-354.

Kato K, Miura H, Sawada S. 2000. Mapping QTLs controlling grain yield and its components on chromosome 5A of wheat. Theoretical and Applied Genetics **101**, 1114-1121.

Kebrom TH, Burson BL, Finlayson SA. 2006. Phytochrome B represses Teosinte Branched1 expression and induces sorghum axillary bud outgrowth in response to light signals. Plant Physiology **140**, 1109-1117.

Kebrom TH, Chandler PM, Swain SM, King RW, Richards RA, Spielmeyer W. 2012. Inhibition of tiller bud outgrowth in the tin mutant of wheat is associated with precocious internode development. Plant Physiology **160**, 308-318.

Kegge W, Weldegergis BT, Soler R, et al. 2013. Canopy light cues affect emission of constitutive and methyl jasmonate-induced volatile organic compounds in Arabidopsis thaliana. New Phytologist **200**, 861-874.

Kirby EJM. 1988. Analysis of leaf, stem and ear growth in wheat from terminal spikelet stage to anthesis. Field Crops Research **18**, 127-140.

Kuraparthy V, Sood S, Dhaliwal H, Chhuneja P, Gill B. 2007. Identification and mapping of a tiller inhibition gene (tin3) in wheat. Theoretical and Applied Genetics **114**, 285-294.

Langer RHM, Prasad PC, Laude HM. 1973. Effects of kinetin on tiller bud elongation in wheat (Triticum aestivum L.). Annals of Botany **37**, 565-571.

Levy J, Peterson ML. 1972. Responses of spring wheats to vernalization and photoperiod. Crop Science **12**, 487-490.

Longnecker N, Kirby EJM, Robson A. 1993. Leaf emergence, tiller growth, and apical development of nitrogen-deficient spring wheat. Crop Science **33**, 154-160.

Miralles DJ, Richards RA. 2000. Responses of leaf and tiller emergence and primordium initiation in wheat and barley to interchanged photoperiod. Annals of Botany **85**, 655-663.

Miralles DJ, Slafer GA. 2007. Sink limitations to yield in wheat: how could it be reduced? Journal of Agricultural Science **145**, 139-149.

Moeller C, Evers JB, Rebetzke G. 2014. Canopy architectural and physiological characterization of near-isogenic wheat lines differing in the tiller inhibition gene tin. Frontiers in Plant Science **5**, 617.

Naruoka Y, Talbert LE, Lanning SP, Blake NK, Martin JM, Sherman JD. 2011. Identification of quantitative trait loci for productive tiller number and its relationship to agronomic traits in spring wheat. Theoretical and Applied Genetics **123**, 1043-1053.

Peng Z, Yen C, Yang J. 1998. Genetic control of oligo-culms in common wheat. Wheat Information Service **86**, 19-24.

Rameau C, Bertheloot J, Leduc N, Andrieu B, Foucher F, Sakr S. 2015. Multiple pathways regulate shoot branching. Frontiers in Plant Science **5**, 741.

Reddy SK, Holalu SV, Casal JJ, Finlayson SA. 2013. Abscisic acid regulates axillary bud outgrowth responses to the ratio of red to far-red light. Plant Physiology **163**, 1047-1058.

Richards RA. 1988. A tiller inhibitor gene in wheat and its effect on plant growth. Australian Journal of Agricultural Research **39**, 749-757.

Sadras VO, Rebetzke GJ. 2013. Plasticity of wheat grain yield is associated with plasticity of ear number. Crop and Pasture Science **64**, 234-243.

Sharma RC. 1995. Tiller mortality and its relationship to grain yield in spring wheat. Field Crops Research **41**, 55-60.

Slafer GA, Savin R. 1994. Source-sink relationships and grain mass at different positions within the spike in wheat. Field Crops Research **37**, 39-49.

Sparkes DL, Holme SJ, Gaju O. 2006. Does light quality initiate tiller death in wheat? European Journal of Agronomy **24**, 212-217.

Spielmeyer W, Richards RA. 2004. Comparative mapping of wheat chromosome 1AS which contains the tiller inhibition gene (tin) with rice chromosome 5S. Theoretical and Applied Genetics **109**, 1303-1310.

Sylvester-Bradley R, Berry P, Blake J, et al. 2008. The wheat growth guide. London: HGCA.

Thorne GN, Wood DW. 1987. Effects of radiation and temperature on tiller survival, grain number and grain yield in winter wheat. Annals of Botany **59**, 413-426.

Toyota M, Tatewaki N, Morokuma M, Kusutani A. 2014. Tillering responses to high red/far-red ratio of four Japanese wheat cultivars. Plant Production Science **17**, 124-130.

Ugarte CC, Trupkin SA, Ghiglione H, Slafer G, Casal JJ. 2010. Low red/far-red ratios delay spike and stem growth in wheat. Journal of Experimental Botany **61**, 3151-3162.

van Herwaarden AF, Angus JF, Richards RA, Farquhar GD. 1998. 'Haying-off', the negative grain yield response of dryland wheat to nitrogen fertiliser. II. Carbohydrate and protein dynamics. Australian Journal of Agricultural Research **49**, 1083-1093.

Wang L, Chen F, Zhang F, Mi G. 2010. Two strategies for achieving higher yield under phosphorus deficiency in winter wheat grown in field conditions. Field Crops Research **118**, 36-42.

Yemm EW, Willis AJ. 1954. The estimation of carbohydrates in plant extracts by anthrone. Biochemical Journal **57**, 508-514.

Zadoks JC, Chang TT, Konzak CF. 1974. A decimal code for the growth stages of cereals. Weed Research **14**, 415-421.

Zhang J, Wu J, Liu W, et al. 2013. Genetic mapping of a fertile tiller inhibition gene, ftin, in wheat. Molecular Breeding **31**, 441-449.

Chapter 4

Optimising Biomass Accumulation and Partitioning to Improve Yield and Yield Components in Wheat

4.1 Abstract

Wheat plants consist of leaves, stems, spikes and grains that are the organ harvestable for food production. This study aimed to understand the development of plant and plant organs, and their relationships with yield determination. In a mapping population of bread wheat (Triticum aestivum 'Forno') and its relative spelt (Triticum spelta 'Oberkulmer') contrasting for biomass, dry weight of plant and plant organs, biomass-related traits, yield and yield components, were analysed at GS39 (full flag leaf emergence), anthesis and maturity, followed by identification of quantitative trait loci (QTL). Plant and plant organ size and leaf area at GS39 and anthesis, and the crop growth rate between two stages, were positively associated with thousand grain weight, grains per spike, final above-ground biomass and yield per spike. Increasing biomass by removing other tillers at GS39 led to higher grain number and yield per spike. These results indicate the importance of the preanthesis plant and plant organ size for yield definition. The spikes grew mainly from GS39 to anthesis: the larger spikes at anthesis, the more grains per spike that could reduce sink limitation. Genetic analysis revealed 193 QTL associated with biomass accumulation and partitioning, and other biomass-related traits. Frequent QTL coincidences between these biomass and yield traits were observed, mainly on chromosomes 2B, 3A, 4A, 4B, 5A, 6A and 7B, indicating pleiotropy or tight gene linkages, consistent with their phenotypic associations. Significant genetic variation in biomass identified here, and the underlying QTL, are useful for the trait-based physiological and molecular breeding in wheat.

Keywords: Biomass accumulation; biomass partitioning; bread wheat; grain number; grain weight; harvest index; QTL; spelt; yield

4.2 Introduction

Wheat alone provides 19% of the calories and 20% of the proteins for human diets (Braun et al., 2010), and hence is a key contributor to global food security. A substantial increase in wheat production is required to keep pace with the burgeoning world population, being over 9 billion by 2050, as projected by the United Nations. However, the annual growth rates of wheat production and yield have slowed down, that is, only around 1.0% for both in last decades, less than that of demand (1.7%) (Ray et al., 2013; Reynolds et al., 2012; The Wheat Initiative, 2013). Future yield gain has also been challenged by global climate change, diminishing natural resources, rising prices for fertilisers and pesticides, and competition for arable land (Reynolds et al., 2012). From a prospective of breeding, wheat cultivars need to be improved for further genetic gain. Conventional breeding has been mainly based on grain yield per se, together with the resistance to lodging, and biotic and abiotic stresses. Such a strategy can be substantially enhanced by understanding the physiological and genetic basis of yield. Given its complexity, wheat grain yield can be dissected into relatively simpler traits: grain number and individual grain weight (numerical components), or biomass and harvest index (HI, biomass partitioning to grains) (physiological components). Traits influencing these components during plant growth and development have to be clarified so that the pathways of yield determination can be understood. The genetic basis of trait interactions must be identified to validate their relationships in terms of physiological processes. Favourable traits and their underlying genes will be assembled to form ideotypes for wheat breeding. This strategy, i.e. trait-based physiological and molecular breeding, is more fundamental for yield improvement, and the knowledge of trait interactions in yield formation pathways is more deliverable and able to accelerate breeding progress in new environments (Foulkes et al., 2011).

For numerical components, yield progress has been highly associated with an increase in grain number rather than individual grain weight (Sanchez-Garcia et al., 2013; Sayre et al., 1997; Shearman et al., 2005; Slafer and Andrade, 1993). In some regions, grain weight has also been improved and contributed most to yield gain, especially in recent decades (Sadras and Lawson, 2011; Wu et al., 2014). Grain number is mainly determined during the stem elongation phase, and the most critical period commences from penultimate leaf emergence until anthesis (González et al., 2011; Slafer and

Whitechurch, 2001). Floret initiation starts from the late stage of spikelet differentiation. Each spikelet produces up to ten florets, but fewer than five (mainly those closest to rachis) can set grains, and the remaining ones die just before anthesis (González-Navarro et al., 2015; Kirby, 1988). It seems that the proportion of fertile florets, rather than the total number of floret primordia, is the main cause to determine the final number of fertile florets at anthesis (Brooking and Kirby, 1981; González-Navarro et al., 2015). Distal floret death may result from autophagy that is triggered by sugar starvation during spike development (Ghiglione et al., 2008). Because of the coincidences of floret death and rapid growth of spikes and stems, much research has focused on the links among them in terms of resource allocations. There is a strong and positive relationship between spike dry weight (DW) at anthesis and floret survival (Fischer, 1985, 2011; González et al., 2011). As spike DW can be expressed as a function of spike growth duration (SGD), crop growth rate (CGR), and biomass partitioning to spikes (spike partitioning index, SPI), an increase in these traits during the critical period before anthesis would favour spike growth and in turn floret survival (Fischer, 2011; Garcia et al., 2014). On the other hand, biomass partitioning to stems should be decreased to minimise the competition between spikes and stems for assimilates (Kirby, 1988). By using the dwarfing genes (Rht) during the Green Revolution, plant height has been reduced, whereas SPI, spike DW, floret survival and grain number have been increased (Brooking and Kirby, 1981; Flintham et al., 1997; Youssefian et al., 1992).

Individual grain weight is largely determined during grain filling, but a short period before anthesis, while carpels are growing, is also important. It has been proposed that carpel size prior to anthesis may set an upper limit for grain development, as there is a strong and positive relationship between them (Calderini et al., 1999; Hasan et al., 2011). Carpel growth is responsive to preanthesis biomass accumulation and partitioning; for example, reduced plant height due to the use of dwarfing genes favours spike growth, allowing larger carpels at anthesis (Youssefian et al., 1992). Similarly, increasing assimilate availability through de-graining at heading leads to greater carpel size (Calderini and Reynolds, 2000). On the contrary, high temperature between heading and anthesis results in smaller carpels and in turn final grain weight (Calderini et al., 1999). After fertilisation, there is a lag phase, during which cell differentiation, division and expansion take place in grains. Endosperm cell number,

as affected by the assimilate availability during the first two weeks after anthesis, is a major factor influencing final grain weight (Brocklehurst, 1977). Rapid dry matter (e.g. starch and protein) accumulation is then initiated, followed by grain maturation and desiccation. During grain filling, the assimilates are supplied from the current photosynthesis and dry matter translocation of leaves, spikes and stems. The amount of newly synthetic biomass between anthesis and maturity depends on the timing of plant senescence, and delayed senescence is usually believed favourable (Gregersen et al., 2013). Preanthesis assimilates of the vegetative organs play an important role in grain filling as well, and include two types: non-structural and structural. Water soluble carbohydrates (WSC) in vegetative parts (mainly stems) are the major components of the non-structural form, and show positive associations with grain weight and yield (Foulkes et al., 2007; Rebetzke et al., 2008). It has been estimated that the contribution of total WSC to yield can be as high as 50%, depending on growing conditions (e.g. more significant in drought environment) (Rebetzke et al., 2008; van Herwaarden et al., 1998a). Structural carbohydrates in plant organs become available at late grain filling when terminal senescence and subsequent structural macromolecule degradation occur. These nutrients (particularly nitrogen) can be partly recycled and translocated to growing grains (Distelfeld et al., 2014).

Physiologically, yield is a product of plant biomass and HI. HI has been largely improved with the use of dwarfing genes, and closely associated with yield progress (Sadras and Lawson, 2011; Sanchez-Garcia et al., 2013; Sayre et al., 1997; Shearman et al., 2005). HI currently reaches c. 0.45−0.50 in spring wheat and 0.50−0.55 in winter wheat, approaching its theoretical maximum value (c. 0.64 in winter wheat) (Foulkes et al., 2011; Reynolds et al., 2012). To further increase HI, biomass partitioning to different plant organs needs to be optimised. Genetic variation in biomass partitioning has been observed in elite wheat lines, and this variation can be broadened by introducing desirable traits from wild species existing in Triticeae (Foulkes et al., 2011; Reynolds et al., 2012). Another potential strategy is to raise nutrient translocation efficiency from senescing organs to developing grains by modifying terminal senescence patterns (Wu et al., 2012). However, given no systematic progress in HI since the early 1990s, future yield gain will depend more on an increase in biomass (Fischer, 2011; Reynolds et al., 2012). Recent yield improvement has showed an association with increased biomass (Sadras and Lawson,

2011; Shearman et al., 2005). Biomass is a function of light interception (LI) and radiation use efficiency (RUE, biomass per unit of radiation intercepted) (Reynolds et al., 2012). LI can be improved by optimising canopy size (e.g. large leaves and spikes), architecture (e.g. erect leaves) and longevity (e.g. early vigour and late senescence), while increasing plant photosynthesis is required for higher RUE (Reynolds et al., 2012).

As stated above, the previous studies have been mainly focused on the relationships between floret fertility and the rapid growth of spikes and stems, and among grain filling, the preanthesis reserves in vegetative organs and postanthesis stay-green trait. The present work aimed to provide a comprehensive understanding of the physiological and genetic associations between the growth of plant and plant organs, particularly during the preanthesis period, and yield determination. Plant biomass accumulation and partitioning at key growth stages (GS), namely GS39 (full flag leaf emergence), anthesis and maturity, were analysed in a mapping population of bread wheat and spelt contrasting for biomass. The physiological traits of biomass associated with yield and yield components were then determined. Subsequently, the genetic dissection of biomass, biomass-related traits, yield and yield components, was carried out via a detailed quantitative trait locus (QTL) analysis.

4.3 Materials and methods

Details of plant materials, field conditions, statistical analysis of phenotypic data and QTL identification have been described previously in the section of **Materials and methods** of **Chapter 2**.

4.3.1 Biomass, leaf area, yield and yield components

Biomass and its partitioning to different plant organs were assessed at key growth stages (GS), namely GS39 (flag leaf ligule just visible), GS61 (anthesis), and GS92 (maturity) (Zadoks et al., 1974). In 2012, a central area of 0.5 × 0.5 m from each plot of the subsets was harvested at GS39. A sub-sample of c. 100 g was separated randomly after cutting at ground level, and the fertile shoots were counted. The shoots were then partitioned into leaves, and stems plus sheaths (referred hereafter as stems). Total leaf area was measured using an area meter (LI3100, LI-COR, USA). Each part was then dried in an oven at 85^{o}C for 48 h, and weighed. Biomass per shoot (excluding roots) and biomass partitioning to different plant organs (absolute weight and percentages) were calculated. Specific leaf area (SLA) was calculated as the leaf area divided by leaf DW. Meanwhile, five main shoots from each plot were also sampled exactly at GS39, by daily observation for the growth stages of individual RILs. The spikes were collected by dissecting stems, and then the DW of spikes and remaining shoots was recorded. At anthesis, five main shoots from each plot were harvested exactly at GS61 (the first anthers just visible), and partitioned into flag and remaining leaves, stems, and spikes. Leaf area was measured, and then each organ was oven-dried immediately at 85^{o}C for 48 h. SLA of flag and remaining leaves were calculated. To measure stem water soluble carbohydrate (WSC) content at anthesis, the dried stems were finely ground by a mill. Carbohydrates were extracted in 80% ethanol and water, following the method of van Herwaarden et al. (1998a). WSC content in the extracts was determined using the anthrone method of Yemm and Willis (1954). Stem WSC content per shoot was calculated, and structural stem DW was the difference between total stem and WSC weight. The ratio of spike to structural stem DW (spike:structural stem) was obtained. At maturity, a central area of 0.5 × 0.5 m from each plot was harvested. A sub-sample of c. 70 g was counted for fertile shoots, and partitioned into leaves, stems, and spikes. The DW of each organ was recorded after drying at 85^{o}C for 48 h. The spikes were then threshed, and the total grain and

chaff weight was obtained. Yield per spike was calculated as the total grain weight divided by shoot number. A sample of 250 grains was counted and weighed to calculate thousand grain weight (TGW). Grain number per spike was computed from yield per spike and TGW. HI was the total grain weight divided by total biomass. Spike fertility index (SFI) was calculated as the grains per spike divided by spike DW at anthesis. In 2013, 10, 10 and 20 main shoots were sampled exactly at GS39, anthesis, and maturity, respectively, and measurements on biomass, leaf area, and yield components followed the procedures used in 2012. In addition, stem WSC content at maturity in 2013 was also measured in ten genotypes contrasting for grain weight.

Based on the above data, accumulated dry matter (ADM) of the whole shoots from GS39 to anthesis and from anthesis to maturity was obtained. CGR was calculated from the ADM and accumulated thermal time (degree days, ^{o}Cd; base temperature 0 ^{o}C) during each period. To determine the initiation of spike growth, five main shoots from each plot were collected approximately at GS33 (the third node of stem detectable) in both years. The spikes were removed by opening the sheaths, oven-dried, and weighed. Spike growth rates (SGR) from GS33 to GS39, and from GS39 to anthesis, were calculated as the differences in spike DW divided by accumulated thermal time during each period.

Apparent dry matter translocation (DMT) of leaves and stem WSC to grains during grain filling was calculated as the differences in leaf DW and stem WSC content between anthesis and maturity, respectively (not considering the losses of respiration and translocation to other organs). This was not done for structural stems and spikes, as these organs continued to grow after anthesis. Dry matter translocation efficiency (DMTE) was calculated as the ratios of DMT to leaf DW and stem WSC at anthesis, while the contributions of DMT (CDMT) to grain yield were the ratios of DMT to yield per spike (Alvaro et al., 2008; Koutroubas et al., 2012).

4.3.2 De-tillering at GS39

To increase the resource availability from GS39 onwards, five well-established RILs were subject to de-tillering in 2013. Ten central plants in each plot were selected randomly, but c. 50 cm from each other. All tillers of these plants were removed in order to allow the remaining main shoots to grow under relatively saturated resource

supply. Ten main shoots from intact plants were used as control. De-tillering and control shoots were tagged, harvested and processed at maturity. TGW, grains per spike, biomass per shoot, HI and yield per spike were calculated.

4.3.3 De-graining at anthesis

The whole subset (110 RILs) was used for source-sink manipulation during grain filling in 2013. Five main spikes at GS61 were selected from each plot, and all spikelets along one side of each spike were trimmed, potentially doubling the source capacity for the remaining grains (Slafer and Savin, 1994). The trimmed spikes, together with five intact spikes as control, were collected, threshed, oven-dried, and weighed. Grain weight in trimmed and intact spikes was defined as potential (PGW) and actual grain weight (AGW), respectively (Fischer and Hillerislambers, 1978). The difference between PGW and AGW was considered as extra assimilate use. Ten grains from each of ten RILs contrasting for grain weight were measured for grain dimensions (length, width and height) using an electronic calliper (OD-15CP, Mitutoyo, UK). Grain volume was calculated using the formula: $V_g = (4/3)\pi abc$, where V_g = grain volume, $\pi = 3.1416$, a = 0.5 grain length, b = 0.5 grain width, and c = 0.5 grain height (Hasan et al., 2011). Grain density was calculated from grain weight and volume.

4.3.4 Leaf angle and plant height

Leaf angle and plant height were measured in the whole subsets in both seasons. Flag leaf angles relative to vertical axis (rather than to stems) were visually rated at the beginning of grain filling, using a scale of either 1 (erect leaves, 0–60^o), 2 (horizontal leaves, 60–120^o), or 3 (pendant leaves; 120–180^o) according to the appearance of most plants in a plot (Torres and Pietragalla, 2012). Five main shoots from each plot were measured from stem bases to spike tips (excluding awns) at maturity for plant height.

4.3.5 Grain weight and number within spikes

Distributions of grain weight and number within spikes were analysed in the whole subset in 2012. Five spikes from each plot were sampled at maturity, and the total spikelets of each spike were counted. The spikes were then divided equally into three parts: basal, central and apical. All spikelets from each part were dissected as Grain 1 (G1), Grain 2 (G2), and Grain 3 (G3), counting from the rachis. Grain 4 and more distal grains within spikelets were ignored because only a few RILs had them. Grains

at different positions were counted, oven-dried and weighed. TGW, grains per spikelet (for basal, central and apical spikelets) or per floret (for G1, G2 and G3), yield per spike, and yield partitioning (YP) were calculated for each position.

4.4 Results

4.4.1 Genetic variation in biomass and yield traits in the Forno × Oberkulmer mapping population

The accumulation, partitioning and translocation of plant biomass at key growth stages (GS39, anthesis and maturity), leaf area, plant height, yield and yield components were analysed for phenotypic variation (Supplementary Table S4-1). As expected, the spelt Oberkulmer usually accumulated more total biomass, and accordingly produced larger plant organs (leaves, stems and spikes) at each stage than bread wheat Forno, but showing lower HI and similar grain yield. Higher leaf area, lower SFI, taller plants and faster spike growth from GS39 to anthesis were also found in Oberkulmer. The RILs derived from Forno × Oberkulmer showed large variation and transgressive segregation in all traits (Supplementary Table S4-1). H^2 differed greatly among traits: TGW, grains per spike, spike DW at different stages (spike = chaff at maturity), spike:structural stem, total leaf and stem DW at maturity, and plant height, had relatively high H^2 (> 0.70), whereas the traits such as HI, yield per spike and CGR had low H^2 (< 0.40) (Supplementary Table S4-1).

4.4.2 Yield and yield components

Positive relationships between yield components (TGW, grains per spike, final biomass per shoot, and HI) and yield per spike were found in both years (Fig. 4-1). Grains per spike showed a stronger relationship with yield per spike than TGW in 2013, and there was a negative relationship between two numerical components ($r = -0.45$, $P < 0.01$ in 2012; $r = -0.50$, $P < 0.01$ in 2013). In contrast, final biomass and HI were both closely associated with yield (Fig. 4-1), and no significant relationship between two physiological components was observed.

4.4.3 Relationships of biomass and green area at GS39 with yield and yield components

At GS39, biomass per shoot was strongly associated with total leaf and stem DW, rather than spike DW (Supplementary Table S4-2), indicating that biomass accumulated at this stage was mainly used to grow leaves and stems. In addition, biomass per shoot showed no or weak relationships with the percentage leaf and stem DW, suggesting that more total biomass increased them proportionally. A negative relationship between biomass per shoot and percentage spike DW was observed, so

more total biomass could slightly reduce the proportion of spike DW. Among plant organs, leaf and stem DW were positively correlated, but their percentage partitioning negatively correlated. In contrast, spike DW and its percentage partitioning were weakly correlated with that of leaves and stems, indicating relatively independent growth at this stage. Total leaf area showed a close relationship with biomass per shoot at GS39 in both years (Fig. 4-2).

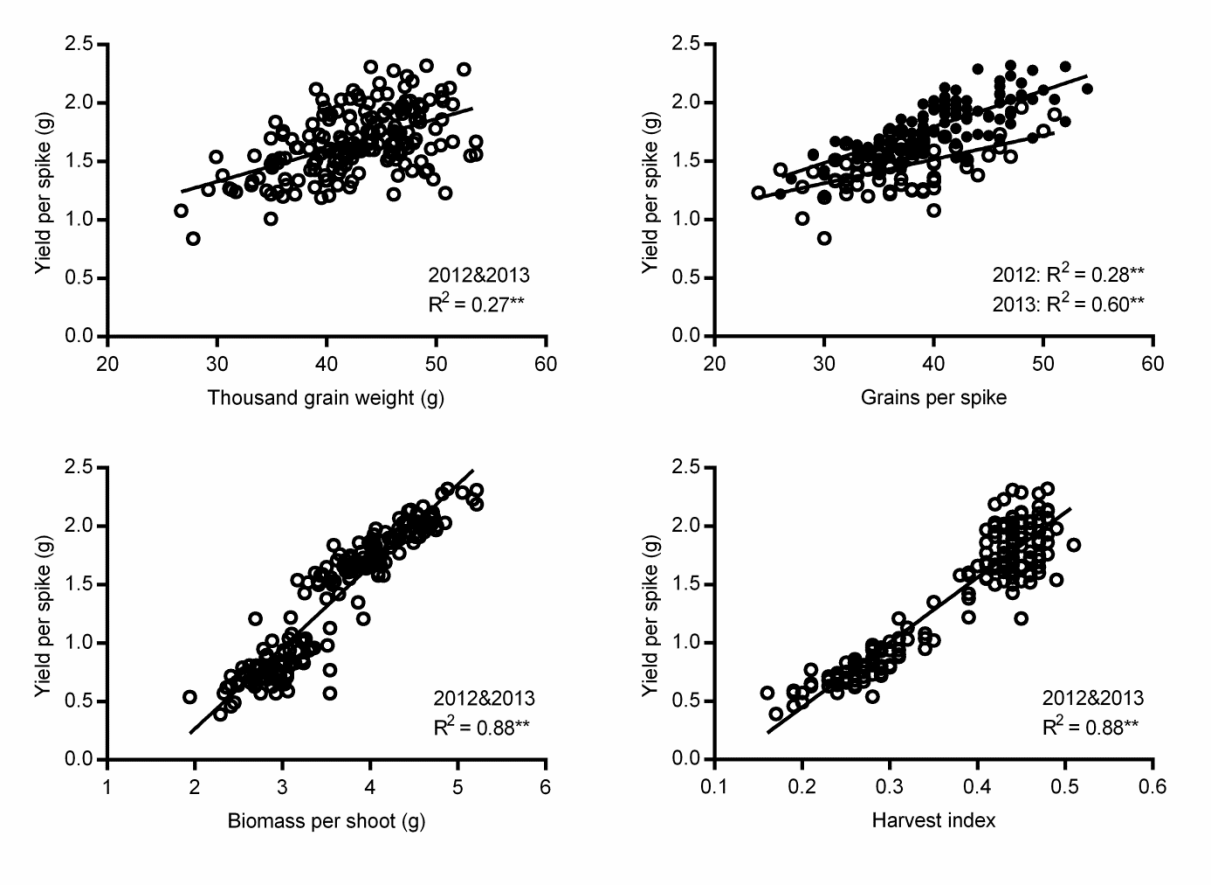

Fig. 4-1 Relationships between yield and yield components. Data in 2012 and 2013 are shown as open and closed circles, respectively. A common line is used to explain both years in the graphs indicated by 2012 & 2013. For regression analysis: * $P < 0.05$; ** $P < 0.01$.

Biomass accumulation and partitioning at GS39 were associated with yield and yield components (Table 4-1). Biomass per shoot showed positive relationships with TGW, grains per spike, final biomass, and in turn yield per spike. The effects of leaf DW on yield components depended on years: it contributed to TGW in 2012, but to grains per spike in 2013. However, more leaf DW was associated with higher final biomass and yield in both seasons. Stem DW consistently contributed to TGW, final biomass and yield. Spike size, on the other hand, appeared not to affect grains per spike and other

yield components. The percentage partitioning of biomass influenced yield components only in 2013: increased percentage leaf DW was associated with slightly lower TGW, more grains per spike, higher final biomass and yield, whereas the percentage stem and spike DW had the opposite effects. Leaf area at GS39 showed similar relationships with yield components as leaf DW did, but SLA had opposite effects (Table 4-2).

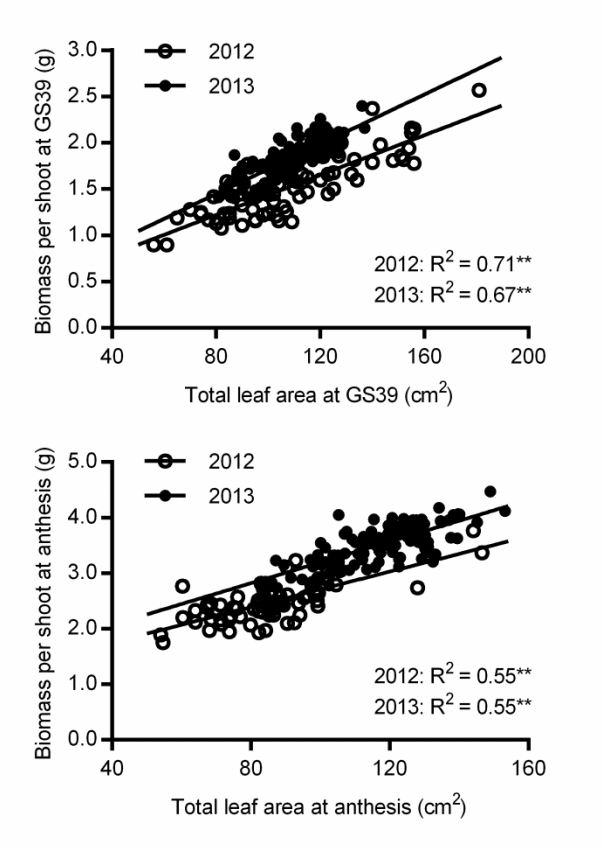

Fig. 4-2 Relationships between leaf area and biomass at GS39 (flag leaf ligule emergence) and anthesis. For regression analysis: * $P < 0.05$; ** $P < 0.01$ (n = 72 in 2012; n = 110 in 2013).

Table 4-1 Correlations between biomass at GS39 (flag leaf ligule emergence) and yield components

Biomass at GS39 (DW, dry weight)	Thousand grain weight		Grains per spike		Biomass per shoot at maturity		Harvest index		Yield per spike	
	2012	2013	2012	2013	2012	2013	2012	2013	2012	2013
Total leaf DW	0.38**	0.00	0.00	0.51**	0.50**	0.74**	-0.14	-0.17	0.25*	0.59**
Stem DW	0.43**	0.26**	0.11	0.17	0.52**	0.59**	0.06	-0.31**	0.35**	0.39**
Spike DW	0.13	0.28**	-0.03	-0.17	0.12	0.00	0.14	0.03	0.18	0.02
Biomass per shoot	0.43**	0.18	0.24*	0.33**	0.57**	0.70**	0.00	-0.27**	0.42**	0.51**
Total leaf DW (%)	0.05	-0.28**	0.22	0.52**	0.20	0.39**	-0.28*	0.08	0.19	0.38**
Stem DW (%)	0.03	0.27**	0.12	-0.48**	0.15	-0.33**	0.16	-0.11	0.20	-0.35**
Spike DW (%)	-0.06	0.17	-0.12	-0.38**	-0.17	-0.44**	0.04	0.19*	-0.06	-0.31**

* Significant at P < 0.05, ** significant at P < 0.01.

Table 4-2 Correlations between total leaf area at GS39 (flag leaf ligule emergence) and yield components

Yield trait	Total leaf area		Specific leaf area	
	2012	2013	2012	2013
Thousand grain weight	0.26*	0.10	-0.37**	0.15
Grains per spike	0.02	0.44**	0.00	-0.34**
Biomass per shoot	0.38**	0.67**	-0.44**	-0.43**
Harvest index	-0.19	-0.05	-0.11	0.25**
Yield per spike	0.20	0.59**	-0.31**	-0.28**

* Significant at P < 0.05, ** significant at P < 0.01.

4.4.4 Relationships of biomass and green area at anthesis with yield and yield components

At anthesis, biomass per shoot was closely correlated with the DW of each organ (Supplementary Table S4-3), but showed no or weak correlations with the percentage organ DW (Supplementary Table S4-4), indicating relatively proportional growth. Plant organ DW was positively correlated with each other (Supplementary Table S4-3). Remaining leaf DW was more closely correlated with stem WSC content than flag leaf DW. In terms of the percentage DW partitioning, there were no or positive relationships between leaves and spikes (Supplementary Table S4-4), but both were strongly and negatively correlated with total stems. It appeared that the percentage partitioning of flag leaves was negatively correlated with that of stem WSC, while the percentage partitioning of the remaining leaves and structural stems were negatively correlated. A strong negative relationship between the percentage partitioning of WSC and structural stems was found. Again, total leaf area and biomass per shoot at anthesis were positively associated in both years (Fig. 4-2).

Higher DW of the whole shoot and each organ was associated with increased TGW in 2012, grains per spike in 2013, final biomass and yield in both years, with the exceptions of stem WSC content and spike DW, which contributed to TGW and grains per spike consistently across years, respectively (Table 4-3). To avoid the effect of spikelet number difference on the relationship between spike DW and grains per spike, the spikelet DW and grains per spikelet were calculated, and still exhibited a positive relationship ($r = 0.35$, $P < 0.01$ in 2012; $r = 0.64$, $P < 0.01$ in 2013). Furthermore, SFI was also positively associated with grains per spike ($r = 0.57$, $P < 0.01$ in 2012; $r = 0.33$, $P < 0.01$ in 2013). Increased biomass (mainly structural stems) was associated with slightly reduced HI in 2013. Spike:structural stem showed positive relationships with grains per spike, HI and yield, but a negative relationship with TGW. For the percentage partitioning of biomass, the increased proportion of flag leaf DW was associated with increased grains per spike, final biomass, and yield in 2013 (Table 4-3). Percentage stem DW (mainly WSC) was positively associated with TGW, but negatively associated with grains per spike, whereas the opposite was true for percentage spike DW (SPI), resulting in increased or decreased yield, depending on years.

Flag leaf area was positively correlated with grains per spike, final biomass and yield in both years (Table 4-4). Remaining and total leaf area was positively correlated with TGW in 2012, grains per spike in 2013, final biomass and yield in both years.

Table 4-3 Correlations between biomass at anthesis and yield components

Biomass at anthesis (DW, dry weight)	Thousand grain weight		Grains per spike		Biomass per shoot at maturity		Harvest index		Yield per spike	
	2012	2013	2012	2013	2012	2013	2012	2013	2012	2013
Flag leaf DW	0.32**	-0.02	0.09	0.54**	0.35**	0.70**	0.02	-0.09	0.32**	0.60**
Remaining leaf DW	0.49**	0.07	0.18	0.40**	0.48**	0.68**	0.06	-0.20*	0.34**	0.53**
Total leaf DW	0.52**	0.04	0.18	0.49**	0.52**	0.75**	0.06	-0.17	0.39**	0.60**
Stem DW	0.53**	0.22*	0.2	0.16	0.61**	0.58**	0.08	-0.41**	0.40**	0.34**
Stem WSC[a]	0.55**	0.20*	0.17	-0.11	0.56**	0.12	0.21	-0.16	0.48**	0.04
Structural stem DW	0.39**	0.14	0.16	0.26**	0.49**	0.62**	-0.01	-0.39**	0.26*	0.38**
Spike DW	0.23*	-0.23*	0.32**	0.69**	0.51**	0.70**	-0.09	-0.05	0.32**	0.62**
Spike:structual stem	-0.22	-0.42**	0.25*	0.59**	-0.01	0.26**	-0.14	0.29**	-0.01	0.37**
Biomass per shoot	0.51**	0.09	0.21	0.39**	0.62**	0.72**	0.05	-0.32**	0.40**	0.51**
Flag leaf DW (%)	-0.11	-0.1	-0.05	0.49**	-0.18	0.49**	-0.02	0.11	-0.03	0.49**
Remaining leaf DW (%)	0.21	-0.03	-0.03	0.12	0.07	0.09	0.05	0.14	0.09	0.15
Total leaf DW (%)	0.13	-0.08	-0.06	0.37**	-0.04	0.34**	0.04	0.17	0.06	0.38**
Stem DW (%)	0.27*	0.37**	-0.16	-0.66**	0.19	-0.41**	0.18	-0.26**	0.09	-0.49**
Stem WSC (%)	0.43**	0.17	-0.01	-0.32**	0.37**	-0.24**	0.24*	-0.02	0.39**	-0.23*
Structural stem DW (%)	-0.23*	0.1	-0.09	-0.17	-0.22	-0.05	-0.12	-0.18	-0.24*	-0.14
Spike DW (%)	-0.50**	-0.47**	0.27*	0.67**	-0.21	0.33**	-0.28*	0.26**	-0.32**	0.42**

[a] WSC, water soluble carbohydrate.

* Significant at $P < 0.05$, ** significant at $P < 0.01$.

Table 4-4 Correlations between leaf area at anthesis and yield components

Yield trait	Leaf area						Specific leaf area					
	Flag leaf		Remaining leaf		Total leaf		Flag leaf		Remaining leaf		Total leaf	
	2012	2013	2012	2013	2012	2013	2012	2013	2012	2013	2012	2013
Thousand grain weight	0.20	-0.01	0.27*	0.01	0.25*	0.00	-0.28*	0.03	-0.19	-0.12	-0.24*	-0.09
Grains per spike	0.24*	0.51**	0.07	0.47**	0.10	0.53**	-0.11	-0.15	0.06	0.10	0.08	0.02
Biomass per shoot	0.25*	0.69**	0.42**	0.65**	0.41**	0.72**	-0.30**	-0.14	-0.06	-0.10	-0.12	-0.16
Harvest index	0.03	-0.08	0.05	-0.07	0.05	-0.08	0.04	-0.05	-0.31**	0.22*	-0.32**	0.19*
Yield per spike	0.32**	0.59**	0.27*	0.56**	0.27*	0.62**	-0.14	-0.13	-0.26*	0.02	-0.29*	-0.05

* Significant at P < 0.05, ** significant at P < 0.01.

Table 4-5 Correlations between biomass partitioning at maturity and yield components

Biomass at maturity (DW, dry weight)	Thousand grain weight		Grains per spike		Biomass per shoot		Harvest index		Yield per spike	
	2012	2013	2012	2013	2012	2013	2012	2013	2012	2013
Total leaf DW	0.48**	0.09	0.08	0.55**	0.71**	0.87**	0.03	-0.17	0.45**	0.71**
Stem DW	0.43**	0.32**	0.09	0.26**	0.82**	0.81**	-0.10	-0.50**	0.38**	0.52**
Chaff DW	0.10	0.04	0.37**	0.60**	0.56**	0.87**	-0.52**	-0.19*	0.37**	0.71**
Total leaf DW (%)	0.00	-0.09	-0.14	0.14	-0.16	0.26**	-0.10	-0.25**	-0.06	0.11
Stem DW (%)	-0.18	0.21*	-0.16	-0.63**	-0.13	-0.27**	-0.34**	-0.74**	-0.35**	-0.58**
Chaff DW (%)	-0.25*	-0.17	0.31**	0.35**	0.01	0.44**	-0.71**	-0.29**	-0.51**	0.27**

* Significant at P < 0.05, ** significant at P < 0.01.

4.4.5 Relationships of biomass partitioning at maturity with yield and yield components

More biomass per shoot at maturity was closely associated with higher DW of leaves, stems, grains and chaff (Supplementary Table S4-5). More total biomass did not affect the percentage partitioning of biomass to different organs in 2012, but was weakly associated with higher proportions of flag leaves and chaff, and with lower proportion of stems in 2013 (Supplementary Table S4-6). Positive relationships among plant organ DW were found (Supplementary Table S4-5). For the percentage partitioning of biomass, there were no (in 2012) or positive (in 2013) relationships between leaves and chaff, but both were negatively correlated with stems (Supplementary Table S4-6).

Turning to yield and yield components, the DW of leaves, stems and chaff was positively correlated with either TGW or grains per spike, resulting in higher yield (Table 4-5). Higher DW and percentage partitioning of stems and chaff were associated with reduced HI.

4.4.6 Crop growth dynamics

Dynamics of biomass accumulation and partitioning from GS39 to maturity were analysed (Fig. 4-3). Total biomass accumulation was rapid from GS39 to anthesis, but became slow thereafter. Only a slight increase in total leaf DW was found between GS39 and anthesis, during which stems grew fast; both decreased during grain filling. The percentage leaf DW decreased continuously, while that of stem DW levelled off at GS39 and then underwent a reduction after anthesis. Spikes were very small at GS33 (only 0.6% of spike DW at anthesis in 2012, and 0.7% in 2013) and GS39 (5.4% in 2012 and 6.0% in 2013), and then grew fast until anthesis. Among plant organs, only grain weight increased significantly after anthesis. Despite similar growth patterns, crops developed earlier in 2013 than in 2012.

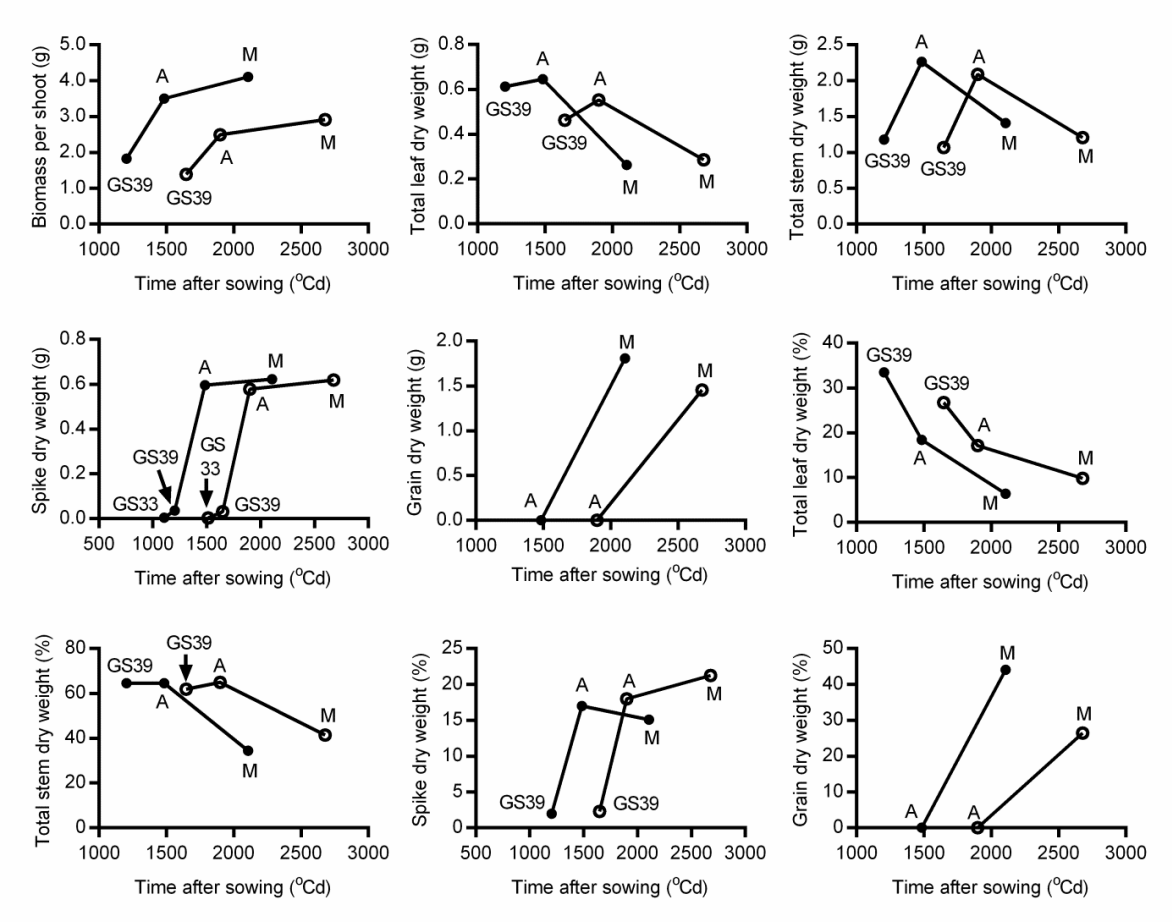

Fig. 4-3 Dynamics of biomass accumulation and partitioning. Data in 2012 and 2013 are shown as open and closed circles, respectively. GS33, the time when the third stem node is just detectable; GS39, the time when flag leaf ligule is just visible; A, anthesis; M, maturity. The base temperature 0°C was used to calculate the accumulated thermal time from sowing.

ADM and CGR during each phase were calculated (Supplementary Table S4-1). It was found that ADM and CGR from anthesis to maturity were only 32% and 12% of that from GS39 to anthesis, respectively. Correlation analysis showed that ADM and CGR between GS39 to anthesis were positively associated with spike DW at anthesis, TGW (only in 2012), grains per spike (only in 2013), final biomass and yield in both years (Table 4-6). Similarly, ADM and CGR during grain filling were positively associated with grains per spike in 2013, and with TGW, final biomass and yield in both years.

As the spikes grew mainly from GS39 to anthesis, only the SGR during this period was analysed (Supplementary Table S4-1). Spike DW at anthesis was strongly associated with SGR, rather than the duration from GS39 to anthesis (Table 4-6). SGR contributed to TGW in 2012, grains per spike in 2013, final biomass and yield in both years (Table 4-6).

Table 4-6 Correlations between crop and spike growth, and yield components

Crop and spike growth trait[a]	Spike dry weight (A)		Thousand grain weight		Grains per spike		Biomass per shoot (M)		Harvest index		Yield per spike	
	2012	2013	2012	2013	2012	2013	2012	2013	2012	2013	2012	2013
ADM (GS39−A)	0.74**	0.63**	0.38**	-0.02	0.10	0.29**	0.40**	0.46**	-0.01	-0.23*	0.28*	0.31**
CGR (GS39−A)	0.62**	0.44**	0.43**	0.09	-0.04	0.12	0.31**	0.31**	0.08	-0.21*	0.23*	0.19*
ADM (A−M)	0.12	0.13	0.31**	0.20*	0.13	0.49**	0.50**	0.63**	-0.08	0.29**	0.35**	0.71**
CGR (A−M)	0.07	0.06	0.30**	0.22*	0.10	0.45**	0.51**	0.60**	-0.04	0.29**	0.31**	0.69**
SGR (GS39−A)	0.87**	0.95**	0.34**	-0.19*	0.14	0.64**	0.43**	0.65**	0.02	0.00	0.30**	0.59**

[a] Abbreviations of the traits: ADM, accumulated dry matter; CGR, crop growth rate; SGR, spike growth rate; GS39, the time when flag leaf ligule is just visible; A, anthesis; M, maturity.
* Significant at $P < 0.05$, ** significant at $P < 0.01$.

4.4.7 Dry matter translocation (DMT) from the vegetative parts to grains

Given the inadequacy of ADM from anthesis to maturity for grain filling (only 34% and 35% of grain yield in 2012 and 2013, respectively), DMT, DMTE and CDMT of leaves and stem WSC were analysed (Supplementary Table S4-1). DMTE of flag, remaining and total leaves were 45%, 64%, and 53%, apparently contributing 4%, 17%, and 20% to grain yield, respectively. DMTE of stem WSC in ten RILs was, on average, 95% (90−98%), so presumably all WSC were translocated to grains in all RILs. CDMT of stem WSC were then calculated, and similar in both years (33%). In total, CDMT of leaves and stem WSC were 53%, so that the remaining part of yield (12%) could be contributed by the DMT of structural stems and spikes. Correlation analysis showed that the greater total leaf DW at anthesis the higher DMT ($r = 0.85$, $P < 0.01$ in 2012; $r = 0.91$, $P < 0.01$ in 2013), and the higher CDMT ($r = 0.58$, $P < 0.01$ in 2012; $r = 0.28$, $P < 0.01$ in 2013). A strong relationship between stem WSC at anthesis and its CDMT was also found ($r = 0.83$, $P < 0.01$ in 2012; $r = 0.82$, $P < 0.01$ in 2013).

4.4.8 Responses of yield and yield components to de-tillering at GS39

De-tillering at GS39 slightly reduced TGW, but increased grains per spike, biomass per shoot, and yield per spike (Table 4-7). No significant effect on HI was observed.

4.4.9 Responses of grain weight and dimensions to de-graining at anthesis

De-graining at anthesis only slightly increased TGW (7.8%) (Fig. 4-4 and Table 4-8). Grain morphological analysis showed that the treated RILs had higher grain width, height, and volume; however, this treatment did not affect grain length, and even reduced grain density, indicating that grain volume was more responsive to increased assimilate supply than grain weight. Furthermore, the RILs with smaller and more grains tended to increase TGW more than the others (Fig. 4-4).

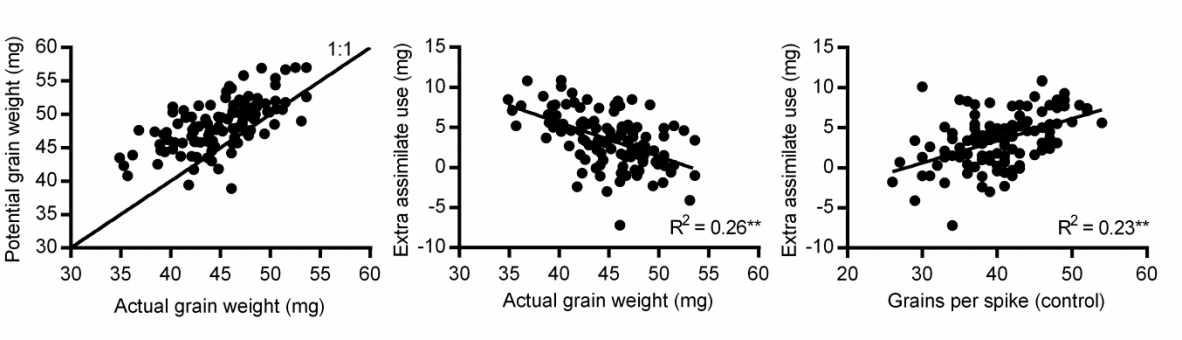

Fig. 4-4 Grain weight response to de-graining at anthesis. Actual grain weight, the grain weight of control spikes (intact); potential grain weight, the grain weight of trimmed spikes; extra assimilate use, the difference between potential and actual grain weight. For regression analysis: * P < 0.05; ** P < 0.01.

Table 4-7 Effects of de-tillering at GS39 (flag leaf ligule emergence) on yield and yield components

Yield trait	Mean across five lines		P-value (NS, not significant; *, P < 0.05; **, P < 0.01)			De-tillering effect (%)
	Control	De-tillering	Treatment	Line	Treatment × line	
Thousand grain weight (g)	44.2	41.3	**	**	NS	− 6.6
Grains per spike	39.9	46.9	**	**	NS	+ 17.5
Biomass per shoot (g)	3.83	4.28	**	**	NS	+ 11.7
Harvest index	0.46	0.44	NS	*	NS	NS
Yield per spike (g)	1.75	1.91	*	**	NS	+ 9.1

Table 4-8 Effects of de-graining at anthesis on thousand grain weight (TGW, 112 lines used) and grain dimensions (10 lines used)

Trait	Mean across the lines used		P-value (NS, not significant; *, P < 0.05; **, P < 0.01)			De-graining effect (%)
	Control	De-graining	Treatment	Line	Treatment × line	
TGW (g)	45.0	48.5	**	**	**	+ 7.8
Grain length (mm)	7.4	7.5	NS	**	*	NS
Grain width (mm)	3.2	3.5	**	**	*	+ 9.4
Grain height (mm)	2.8	3.0	**	**	NS	+ 7.1
Grain volume (mm^3)	35.8	41.1	**	**	NS	+ 14.8
Grain density ($g\ cm^{-3}$)	1.26	1.17	**	NS	NS	− 7.1

4.4.10 Relationships of leaf angle and plant height with yield and yield components

Flag leaf angle was positively correlated with final biomass per shoot in 2013 ($r = 0.30$, $P < 0.01$), and no significant relationship was found for the other yield traits. Plant height was weakly correlated with final biomass, and there were some RILs having short plants but relatively high biomass (Fig. 4-5). Plant height was not associated with the other yield traits except a negative relationship with HI in 2013 ($r = -0.60$, $P < 0.01$).

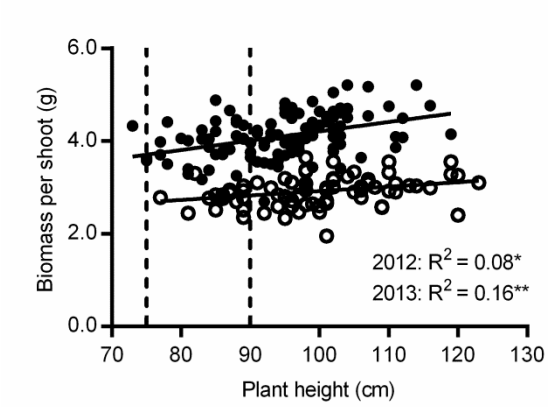

Fig. 4-5 Relationship between plant height and biomass at maturity. Data in 2012 and 2013 are shown as open and closed circles, respectively. Vertical dashed lines indicate the range of plant height of wheat cultivars currently used in the UK. For regression analysis: * $P < 0.05$; ** $P < 0.01$.

4.4.11 Relationships of biomass accumulation and partitioning with yield components within spikes

Grain weight, grain number and YP varied largely within spikes (Supplementary Table S4-1). Grains in apical spikelets and distal florets (G3) within spikelets were smaller than the others ($P < 0.01$). Grain number per spikelet was highest in central part, followed by apical and basal parts ($P < 0.01$). Within spikelets, the first and second florets had similar fertility, much higher than that of the third ones ($P < 0.01$). There were positive relationships among different positions for grain weight and for grain number (Supplementary Table S4-7). Central spikelets accounted for c. half of the grain yield per spike, and YP in basal and apical spikelets was similar. G1 and G2 within spikelets contributed equally to yield (a total of 91%), much higher than G3 ($P < 0.01$).

Effects of biomass accumulation and partitioning on grain weight and number varied among different positions within spikes (Supplementary Table S4-8). In general, biomass of total shoot, leaves and stems at each stage, ADM, CGR and SGR from GS39 to anthesis showed closer relationships with the TGW of apical spikelets and G2, than that at other positions. There were positive relationships between the percentage leaf DW (both at GS39 and anthesis) and grains per apical spikelet. Spike DW at anthesis was positively associated with the fertility of basal and central spikelets, G1 and G3. ADM, CGR and SGR between GS39 and anthesis were positively associated with grains per basal spikelet. Grain yield per spike showed closer relationships with the TGW of G2, and the fertility of basal spikelets, G1 and G3.

4.4.12 QTL for yield and yield components

A total of 36 significant QTL for yield and yield components were identified in two years, including 19 QTL for TGW, nine for grains per spike, four for final biomass, one for HI, and three for yield per spike (Fig. 4-6 and Table 4-9). These QTL were scattered on 15 chromosomes, and individually explained 6.5−24.4% of the phenotypic variation. One QTL for each of TGW and grains per spike, and two for final biomass were coincident with those for yield per spike, and their increasing alleles were conferred by the same parents, in line with the positive relationships between them. There was no QTL coincidence between final biomass and HI, whereas seven QTL for grains per spike were coincident with those for TGW, with increasing alleles conferred by the opposite parents, confirming their negative phenotypic relationship.

4.4.13 QTL for biomass and leaf area at different stages, and their coincidences with those for yield and yield components

For biomass accumulation and partitioning, 156 QTL were detected at GS39, anthesis and maturity, individually explaining 11.3−33.9% of the phenotypic variation (Fig. 4-6 and Table 4-9). Ten QTL for biomass per shoot across different stages were found on 4A, 4B, 5A, and 5B; nine of them were coincident with 37 QTL for the DW of leaves, stems and spikes, with all increasing alleles from the same parents, consistent with the strong positive relationships between total biomass and plant organs. Most QTL for the DW of leaves (flag and remaining leaves at anthesis and maturity), stems

(WSC and structural stems at anthesis), and spikes (spikelets at anthesis and chaff at maturity) were usually coincident, and their increasing alleles came from the same parents, explaining the positive relationships among them. Furthermore, most QTL for the percentage partitioning of biomass to different organs were also coincident, mainly on 1BS, 2B, 5A, and 7B; the increasing alleles for leaves and spikes were from the same parents (with the exceptions of some QTL for spike DW at GS39), which usually conferred the decreasing alleles for stems.

The QTL coincidences between biomass and yield traits were also observed (Fig. 4-6). Specifically, 48 QTL for biomass per shoot and plant organ DW at GS39 and anthesis were coincident with 14 QTL for TGW, nine for grains per spike, three for final biomass, one for HI, and two for yield; the increasing alleles were usually conferred by the same parents, except those located on 3B, 4A and 5A, where the negative QTL coincidences between TGW and grains per spike were present. There were five and two QTL detected for spike DW at anthesis and SFI, respectively, and all of them were coincident with those for grains per spike. Ten QTL for SPI were identified, and half of them coincident with grains per spike. The increasing alleles of these coincident QTL were conferred by the same parents, confirming the positive relationships between spike DW, SFI, SPI, and grains per spike. At maturity, 18 QTL for the DW of leaves, stems and chaff were also coincident with six QTL for TGW, four for grains per spike, and two for yield.

A total of 21 QTL for leaf area at GS39 and anthesis were found (Fig. 4-6 and Table 4-9). Of them, 19 QTL were coincident with those for the biomass of whole shoots and plant organs at GS39 and anthesis, while 17 were coincident with those for yield and yield components. The parents conferring increasing alleles for leaf area also provided the increasing alleles for biomass at different stages, either TGW or grains per spike (but not both), and yield, in line with their positive phenotypic relationships. In addition, six QTL for SLA were detected.

4.4.14 QTL for crop growth dynamics, and their coincidences with those for yield and yield components

One QTL for ADM from GS39 to anthesis was identified on 5B, coincident with those for biomass and leaf area at anthesis (Fig. 4-6 and Table 4-9). Five QTL for SGR were identified on 2B, 2D, 5A, and 7B, coincident with five QTL for spike DW at anthesis,

one for TGW, six for grains per spike, one for final biomass, one for HI, and one for yield (Fig. 4-6 and Table 4-9). The increasing alleles originated from the same parents, except those for TGW and HI on 5A.

4.4.15 QTL for dry matter translocation and potential grain weight, and their coincidences with those for yield and yield components

Fifteen QTL for DMT and CDMT of flag and remaining leaves were found on 3A, 4A, 5A, and 5B, coincident with 14 QTL for leaf DW at anthesis, and with nine for yield and yield components (Fig. 4-6 and Table 4-9). Only one QTL for CDMT of stem WSC was detected on 2B.

After de-graining at anthesis, one QTL for PGW was identified on 2A, coincident with one QTL for TGW (Fig. 4-6 and Table 4-9). Additionally, two QTL for extra assimilate use were found on 7B, coincident with two QTL for grains per spike (with the increasing alleles from Oberkulmer) and two for TGW (with the increasing alleles from Oberkulmer and Forno, respectively), confirming that the RILs with more and smaller grains were more responsive to increased assimilate availability.

4.4.16 QTL for leaf angle and plant height

One and two QTL for flag leaf angle and plant height were identified on 4A and 2A, respectively (Fig. 4-6 and Table 4-9), and no QTL coincidence with yield and yield components was found.

4.4.17 QTL for grain weight and number within spikes, and their coincidences with those for biomass traits

QTL for either grain weight or grain number differed at different positions within spikes (Fig. 4-6 and Table 4-9). For TGW, the QTL on 4A and 7B were shared by all spikelets (basal, central, and apical), G1, and G2. Chromosome 3B also harboured the QTL for these positions, except basal spikelets. Central spikelets shared the QTL on 2A with basal ones, and on 2A and the other region of 7B with G1. The QTL on 1A was specific for central spikelets, and the one on 5DL specific for G1. The QTL for TGW at different positions were coincident with those for the biomass of total shoot, leaves and stems at different stages on 1A, 4A and 7B. Fewer independent QTL for G2 were found, leading to closer relationships between the TGW at this position and biomass traits.

For grain number, one QTL for grains per central spikelet and three for grains per apical spikelet were identified, and all position-specific. QTL coincidences between the percentage leaf DW (both at GS39 and anthesis) and grains per apical spikelet were found on 5A.

Fig. 4-6 Quantitative trait loci (QTL) for biomass, biomass-related traits, yield and yield components in the Forno × Oberkulmer mapping population. The 1-LOD support intervals of significant QTL are indicated by the vertical colour bars: red (yield and yield components), grey (biomass traits at GS39, namely the time at flag leaf ligule emergence), green (biomass traits at anthesis), blue (biomass traits at maturity), and purple (other biomass-related traits). For the QTL symbol, a 'Q' is followed by the abbreviations of the quantitative trait and laboratory (uon). Abbreviations of the traits: Tgw, thousand grain weight (TGW); Gps, grains per spike; Bps, biomass per shoot; Hi, harvest index; Yps, yield per spike; Tlf, total leaf dry weight; Spe, spike dry weight; Ptlf, total leaf dry weight (%); Pstm, stem dry weight (%); Pspe, spike dry weight (%); Tla, total leaf area; Tsla, specific leaf area (SLA) of total leaf; Flf, flag leaf dry weight; Rlf, remaining leaf dry weight; Stm, stem dry weight; Wsc, stem water soluble carbohydrate (WSC) dry weight; Sstm, structural stem dry weight; Spt, spikelet dry weight; Sfi, spike fertility index; Sss, spike:structural stem; Pflf, flag leaf dry weight (%); Prlf, remaining leaf dry weight (%); Pwsc, stem WSC dry weight (%); Pss, structural stem dry weight (%); Fla, flag leaf area; Rla, remaining leaf area; Flae, flag leaf angle; Chf, chaff dry weight; Pchf, chaff dry weight (%); Pht, plant height; Admea, accumulated dry matter (GS39−Anthesis); Spe33, spike dry weight at GS33 (the time when the third stem node is just detectable); Sgr, spike growth rate; Fldmt, flag leaf dry matter translocation (DMT); Rldmt, remaining leaf DMT; Tldmt, total leaf DMT; Cfl, contribution of flag leaf DMT to yield; Cwsc, contribution of the WSC DMT to yield; Pgw, potential grain weight; Eau, extra assimilate use; Tgwb, TGW of basal spikelet; Tgwc, TGW of central spikelet; Tgwa, TGW of apical spikelet; Tgw1, TGW of Grain 1; Tgw2, TGW of Grain 2; Gpcs, grains per central spikelet; and Gpas, grains per apical spikelet. The suffix '12' or '13' indicates that the QTL was detected in 2012 or 2013. The parental lines providing increasing alleles (increasing the trait values) are given in the parentheses: F, Forno; O, Oberkulmer.

Fig. 4-6

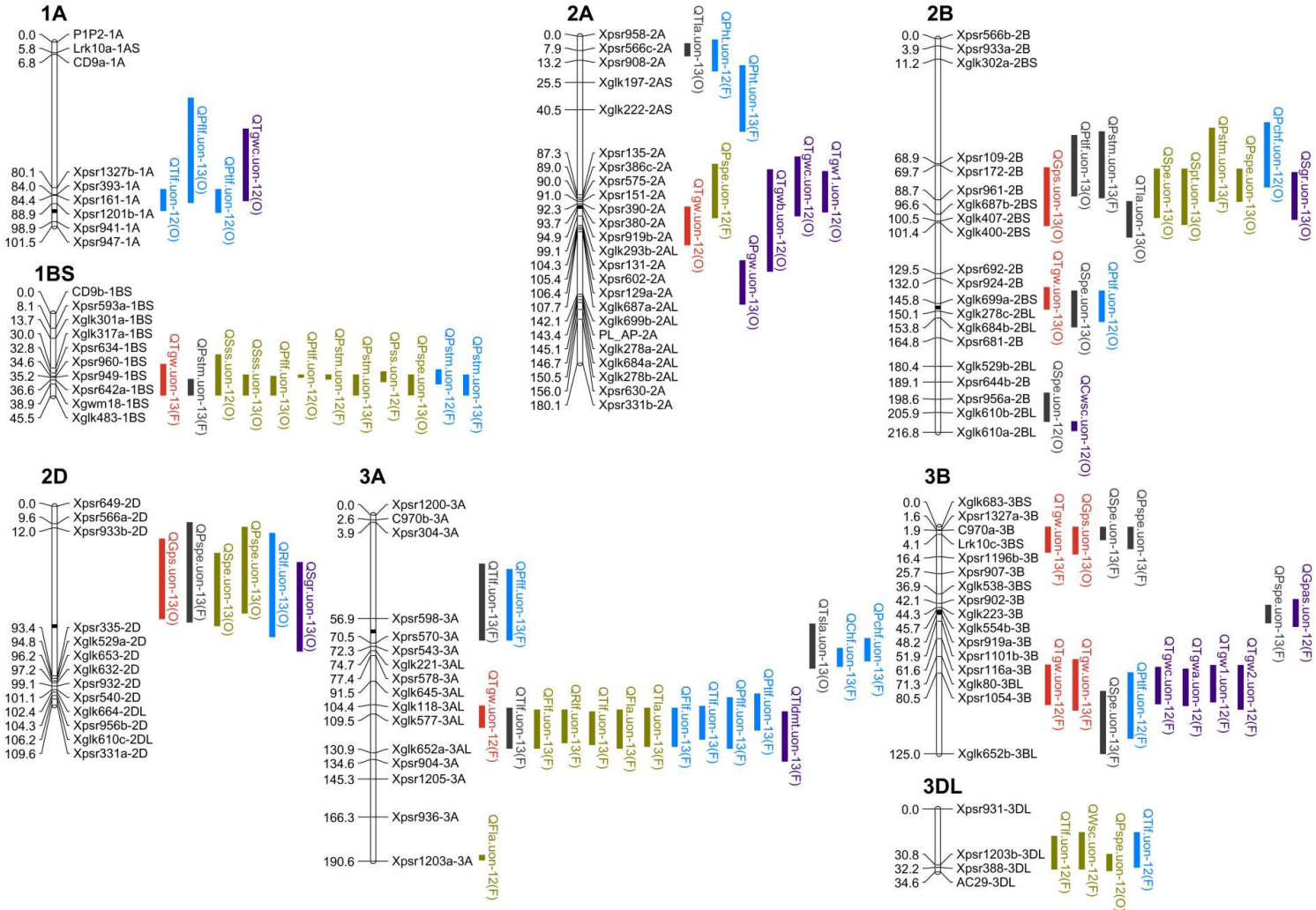
1A
0.0 P1P2-1A
5.8 Lrk10a-1AS
6.8 CD9a-1A
80.1 Xpsr1327b-1A
84.0 Xpsr393-1A
84.4 Xpsr161-1A
88.9 Xpsr1201b-1A
98.9 Xpsr941-1A
101.5 Xpsr947-1A
QTgwc.uon-12(O)
QPtff.uon-13(O)
QPtff.uon-12(O)
QTtff.uon-12(O)
1BS
0.0 CD9b-1BS
8.1 Xpsr593a-1BS
13.7 Xglk301a-1BS
30.0 Xglk317a-1BS
32.8 Xpsr634-1BS
34.6 Xpsr960-1BS
35.2 Xpsr949-1BS
36.6 Xpsr642a-1BS
38.9 Xgwm18-1BS
45.5 Xglk483-1BS
QTgw.uon-13(F)
QSss.uon-12(O)
QSss.uon-13(O)
QPtff.uon-13(O)
QPtff.uon-12(O)
QPstm.uon-12(F)
QPstm.uon-13(F)
QPss.uon-12(F)
QPspe.uon-13(O)
QPstm.uon-12(F)
QPstm.uon-13(F)
2A
0.0 Xpsr958-2A
7.9 Xpsr566c-2A
13.2 Xpsr908-2A
25.5 Xglk197-2AS
40.5 Xglk222-2AS
87.3 Xpsr135-2A
89.0 Xpsr386c-2A
90.0 Xpsr575-2A
91.0 Xpsr151-2A
92.3 Xpsr390-2A
93.7 Xpsr380-2A
94.9 Xpsr919b-2A
99.1 Xglk293b-2AL
104.3 Xpsr131-2A
105.4 Xpsr602-2A
106.4 Xpsr129a-2A
107.7 Xglk687a-2AL
142.1 Xglk699b-2AL
143.4 PL_AP-2A
145.1 Xglk278a-2AL
146.7 Xglk684a-2AL
150.5 Xglk278b-2AL
156.0 Xpsr630-2A
180.1 Xpsr331b-2A
QTgw.uon-12(F)
QTgw.uon-13(O)
QPspe.uon-12(F)
QTgw.uon-12(O)
QPht.uon-13(F)
QPht.uon-12(F)
QTla.uon-13(O)
QPgw.uon-13(O)
QTgwb.uon-12(O)
QTgwc.uon-12(O)
QTgw1.uon-12(O)
2B
0.0 Xpsr566b-2B
3.9 Xpsr933a-2B
11.2 Xglk302a-2BS
68.9 Xpsr109-2B
69.7 Xpsr172-2B
88.7 Xpsr961-2B
96.6 Xglk687b-2BS
100.5 Xglk407-2BS
101.4 Xglk400-2BS
129.5 Xpsr692-2B
132.0 Xpsr924-2B
145.8 Xglk699a-2BS
150.1 Xglk278c-2BL
153.8 Xglk684b-2BL
164.8 Xpsr681-2B
180.4 Xglk529b-2BL
189.1 Xpsr644b-2B
198.6 Xpsr956a-2B
205.9 Xglk610b-2BL
216.8 Xglk610a-2BL
QCwsc.uon-12(O)
QSpe.uon-12(O)
QSpe.uon-13(O)
QPtff.uon-12(O)
QTgw.uon-13(O)
QGps.uon-13(O)
QPtff.uon-13(O)
QPstm.uon-13(F)
QTla.uon-13(O)
QSpe.uon-13(O)
QSpt.uon-13(O)
QPstm.uon-13(F)
QPspe.uon-13(O)
QPcht.uon-12(O)
QSgr.uon-13(O)
2D
0.0 Xpsr649-2D
9.6 Xpsr566a-2D
12.0 Xpsr933b-2D
93.4 Xpsr335-2D
94.8 Xglk529a-2D
96.2 Xglk653-2D
97.2 Xglk632-2D
99.1 Xpsr932-2D
101.1 Xpsr540-2D
102.4 Xglk664-2DL
104.3 Xpsr956b-2D
106.2 Xglk610c-2DL
109.6 Xpsr331a-2D
QSgr.uon-13(O)
QRtf.uon-13(O)
QSpe.uon-13(O)
QPspe.uon-13(O)
QGps.uon-13(O)
QPspe.uon-13(F)
3A
0.0 Xpsr1200-3A
2.6 C970b-3A
3.9 Xpsr304-3A
56.9 Xpsr598-3A
70.5 Xprs570-3A
72.3 Xpsr543-3A
74.7 Xglk221-3AL
77.4 Xpsr578-3A
91.5 Xglk645-3AL
104.4 Xglk118-3AL
109.5 Xglk577-3AL
130.9 Xglk652a-3AL
134.6 Xpsr904-3A
145.3 Xpsr1205-3A
166.3 Xpsr936-3A
190.6 Xpsr1203a-3A
QFla.uon-12(F)
QTgw.uon-12(F)
QTtf.uon-13(F)
QPtff.uon-13(F)
QTtf.uon-13(F)
QFtf.uon-13(F)
QRtf.uon-13(F)
QTtf.uon-13(F)
QFla.uon-13(F)
QTla.uon-13(F)
QPtff.uon-13(F)
QPtff.uon-13(F)
QPtff.uon-13(F)
QTtf.uon-13(F)
QTtdmt.uon-13(F)
QTsla.uon-13(O)
QChf.uon-13(F)
QPchf.uon-13(F)
3B
0.0 Xglk683-3BS
1.6 Xpsr1327a-3B
1.9 C970a-3B
4.1 Lrk10c-3BS
16.4 Xpsr1196b-3B
25.7 Xpsr907-3B
36.9 Xglk538-3BS
42.1 Xpsr902-3B
44.3 Xglk223-3B
45.7 Xglk554b-3B
48.2 Xpsr919a-3B
51.9 Xpsr1101b-3B
61.6 Xpsr116a-3B
71.3 Xglk80-3BL
80.5 Xpsr1054-3B
125.0 Xglk652b-3BL
QPspe.uon-13(F)
QSpe.uon-13(F)
QTgw.uon-13(O)
QGps.uon-13(O)
QTgw.uon-13(F)
QTgw.uon-12(F)
QSpe.uon-13(F)
QPtff.uon-12(F)
QTgwc.uon-12(F)
QTgwa.uon-12(F)
QTgw1.uon-12(F)
QTgw2.uon-12(F)
QPspe.uon-13(F)
QGpas.uon-12(F)
3DL
0.0 Xpsr931-3DL
30.8 Xpsr1203b-3DL
32.2 Xpsr388-3DL
34.6 AC29-3DL
QTtf.uon-12(F)
QWsc.uon-12(O)
QPspe.uon-12(O)
QTtf.uon-12(F)

Fig. 4-6 (continued)

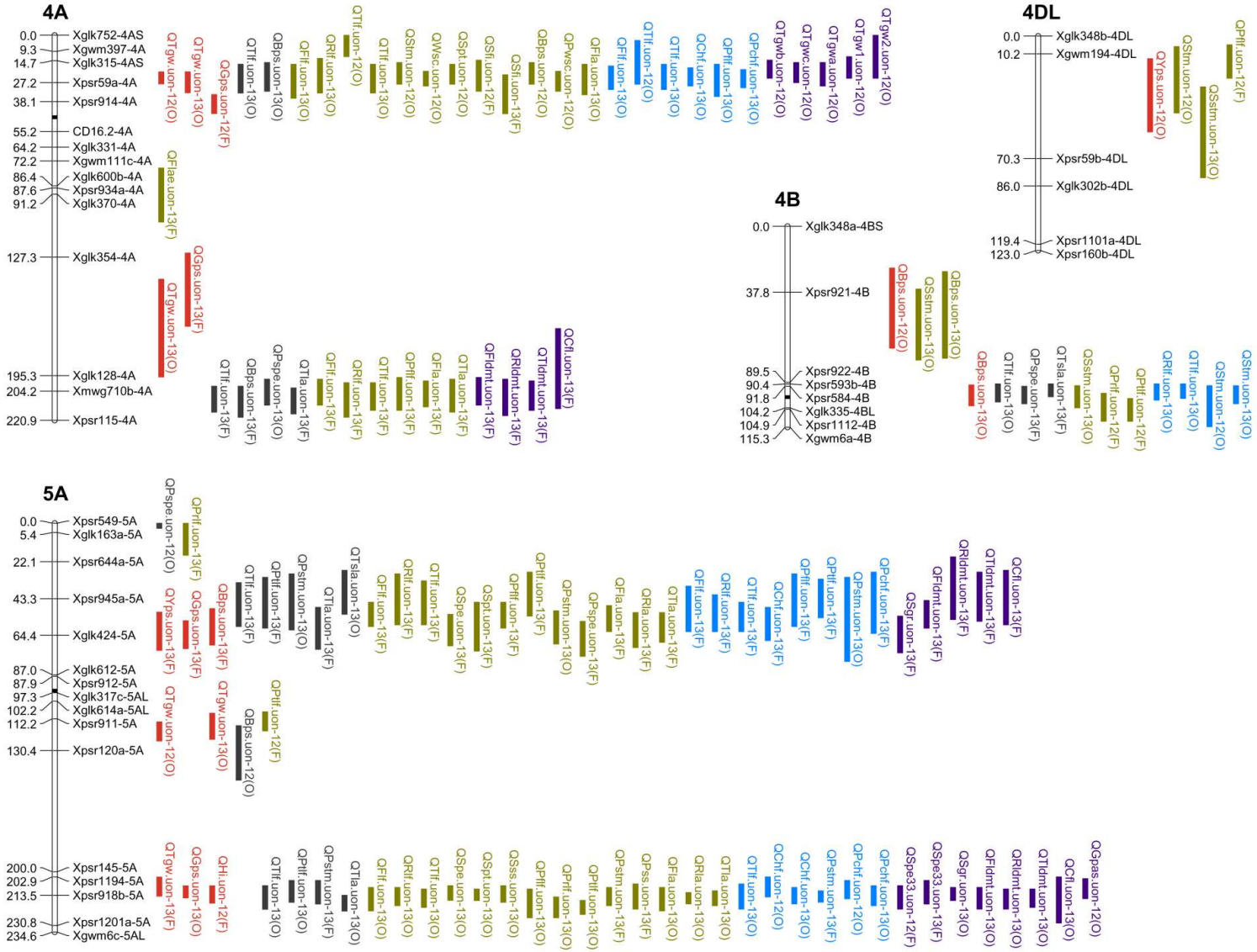

Fig. 4-6 (continued)

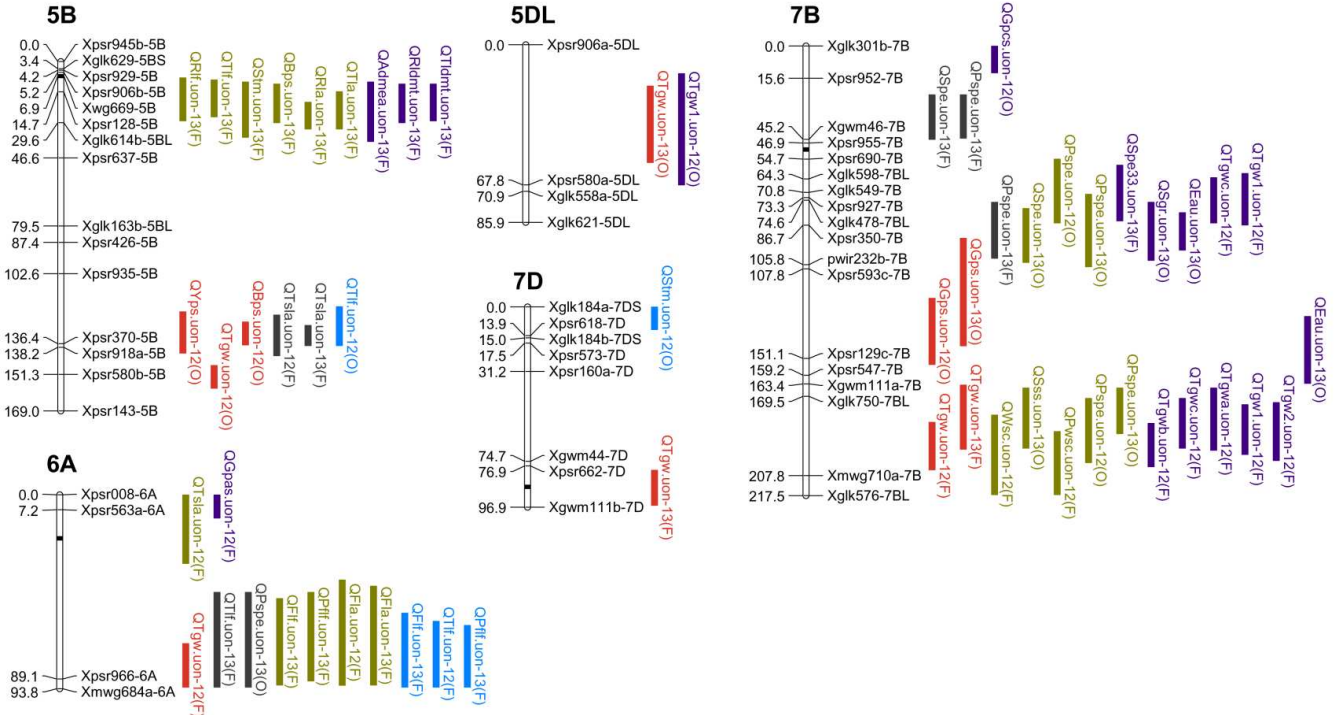

Table 4-9 Quantitative trait locus (QTL) identification for biomass, biomass-related traits, yield and yield traits in the Forno × Oberkulmer mapping population

Trait/Chromosome	Year	Position (cM)	LOD	R^{2a}	Additive effect[b]	Closest marker
Yield traits						
Thousand grain weight (TGW, g)						
1BS	2013	42.9	4.8	10.3	1.17	Xglk483-1BS
2A	2012	105.4	4.6	10.0	-1.10	Xpsr602-2A
2B	2013	145.8	3.5	7.7	-0.94	Xglk699a-2BS
3A	2012	109.5	3.1	6.8	0.95	Xglk577-3AL
3B	2012	80.5	4.0	8.7	1.07	Xpsr1054-3B
	2013	2.9	3.4	7.4	0.96	C970a-3B
	2013	79.3	5.0	10.8	1.20	Xpsr1054-3B
4A	2012	23.7	11.0	22.3	-1.92	Xpsr59a-4A
	2013	25.7	6.5	13.8	-1.41	Xpsr59a-4A
	2013	161.3	2.9	6.5	-2.05	Xglk128-4A
5A	2012	120.2	7.8	16.3	-1.71	Xpsr911-5A
	2013	114.1	3.2	7.1	-0.99	Xpsr911-5A
	2013	208.9	4.3	9.3	1.26	Xpsr918b-5A
5B	2012	151.3	3.3	7.3	-0.94	Xpsr580b-5B
5DL	2013	37.0	4.3	9.2	-2.24	Xpsr580a-5DL
6A	2012	91.1	5.2	11.1	1.23	Xpsr966-6A
7B	2012	192.5	5.8	12.5	1.85	Xmwg710a-7B
	2013	180.5	3.3	7.2	1.27	Xglk750-7BL
7D	2013	87.8	4.1	8.9	1.23	Xgwm111b-7D
Grains per spike						
2B	2013	94.7	3.1	12.0	-2.2	Xglk687b-2BS
2D	2013	44.9	4.7	17.8	-6.0	Xpsr933b-2D
3B	2013	8.1	3.7	14.4	-2.7	Lrk10c-3BS
4A	2012	38.1	3.5	20.5	2.5	Xpsr914-4A
	2013	151.3	3.6	14.0	5.5	Xglk354-4A
5A	2013	64.4	4.5	17.3	2.9	Xglk424-5A
	2013	213.4	5.1	19.2	-2.9	Xpsr918b-5A
7B	2012	137.8	3.2	18.7	-3.6	Xpsr129c-7B
	2013	127.8	3.1	12.2	-3.4	Xpsr593c-7B
Biomass per shoot (g)						
4B	2012	55.8	4.2	24.4	-0.31	Xpsr921-4B
	2013	95.8	3.0	11.9	-0.19	Xpsr584-4B
5A	2013	60.3	3.9	14.9	0.24	Xglk424-5A
5B	2012	136.4	3.9	22.8	-0.17	Xpsr370-5B
Harvest index						
5A	2012	213.4	3.5	20.4	0.02	Xpsr918b-5A
Yield per spike (g)						
4DL	2012	36.2	3.2	18.7	-0.15	Xgwm194-4DL
5A	2013	63.3	3.4	13.2	0.10	Xglk424-5A
5B	2012	136.4	3.3	19.5	-0.07	Xpsr370-5B

[a] The proportion of phenotypic variation explained by individual QTL.
[b] Positive additive effects indicate that the alleles from Forno increase the values of the traits, whereas negative additive effects indicate that the alleles from Oberkulmer increase the values of the traits.

Table 4-9 (continued)

Trait/Chromosome	Year	Position (cM)	LOD	R^2	Additive effect	Closest marker
At GS39 (flag leaf ligule emergence)						
Total leaf dry weight (g)						
3A	2013	43.9	3.0	11.9	0.05	Xpsr598-3A
	2013	117.5	3.1	12.2	0.04	Xglk577-3AL
4A	2013	23.7	3.9	15.0	-0.04	Xpsr59a-4A
	2013	208.2	4.6	17.5	0.04	Xmwg710b-4A
4B	2013	93.8	3.2	12.4	-0.04	Xpsr584-4B
5A	2013	52.3	6.8	24.8	0.06	Xpsr945a-5A
	2013	216.5	6.6	24.0	-0.06	Xpsr918b-5A
6A	2013	75.2	3.2	12.7	0.05	Xpsr966-6A
Spike dry weight (g)						
2B	2012	201.6	3.1	18.4	-0.0035	Xpsr956a-2B
	2013	147.8	3.3	12.7	-0.0025	Xglk699a-2BS
3B	2013	1.9	5.2	19.6	0.0031	C970a-3B
	2013	109.5	3.0	11.9	0.0042	Xglk652b-3BL
7B	2013	32.6	4.5	17.1	0.0040	Xgwm46-7B
Biomass per shoot (g)						
4A	2013	22.7	3.8	14.8	-0.10	Xpsr59a-4A
	2013	210.2	3.9	14.9	0.10	Xmwg710b-4A
5A	2012	123.2	3.6	21.1	-0.11	Xpsr120a-5A
Total leaf dry weight (%)						
2B	2013	76.7	3.7	14.4	-1.2	Xpsr172-2B
5A	2013	53.3	6.5	23.7	1.7	Xpsr945a-5A
	2013	209.9	6.9	24.9	-1.6	Xpsr918b-5A
Stem dry weight (%)						
1BS	2013	40.9	3.3	12.8	1.0	Xgwm18-1BS
2B	2013	77.7	3.6	14.1	1.2	Xpsr172-2B
5A	2013	53.3	5.7	21.1	-1.5	Xpsr945a-5A
	2013	209.9	6.4	23.5	1.4	Xpsr918b-5A
Spike dry weight (%)						
2D	2013	43.9	3.5	13.7	0.3	Xpsr933b-2D
3B	2013	1.9	4.5	17.2	0.2	C970a-3B
	2013	44.3	3.3	12.8	0.1	Xglk223-3B
4A	2013	203.3	3.5	13.5	-0.1	Xmwg710b-4A
4B	2013	96.8	5.8	21.6	0.2	Xpsr584-4B
5A	2012	0.1	3.1	18.2	-0.3	Xpsr549-5A
6A	2013	72.2	3.5	13.7	-0.2	Xpsr966-6A
7B	2013	32.6	5.1	19.0	0.2	Xgwm46-7B
	2013	81.6	3.8	14.7	0.2	Xpsr350-7B
Total leaf area (cm^2)						
2A	2013	7.9	3.3	12.8	-5	Xpsr566c-2A
2B	2013	95.7	3.2	12.6	-5	Xglk687b-2BS
4A	2013	210.2	5.8	21.4	7	Xmwg710b-4A
5A	2013	57.3	5.4	20.1	8	Xglk424-5A
	2013	218.5	8.5	29.8	-9	Xpsr918b-5A

Table 4-9 (continued)

Trait/Chromosome	Year	Position (cM)	LOD	R^2	Additive effect	Closest marker
Specific leaf area (SLA) of total leaf (cm^2 g^{-1})						
3A	2013	71.5	3.8	14.9	-6	Xpsr543-3A
4B	2013	91.8	4.4	16.7	6	Xpsr584-4B
5A	2013	38.1	3.3	13.0	-6	Xpsr945a-5A
5B	2012	136.4	3.7	21.5	8	Xpsr370-5B
	2013	136.4	3.1	12.0	5	Xpsr370-5B
At anthesis						
Flag leaf dry weight (g)						
3A	2013	118.5	3.7	14.3	0.02	Xglk577-3AL
4A	2013	23.7	3.7	14.3	-0.02	Xpsr59a-4A
	2013	202.3	4.8	18.4	0.02	Xmwg710b-4A
5A	2013	53.3	8.7	30.5	0.02	Xpsr945a-5A
	2013	216.4	5.4	20.2	-0.02	Xpsr918b-5A
6A	2013	71.2	4.6	17.6	0.03	Xpsr966-6A
Remaining leaf dry weight (g)						
3A	2013	116.5	3.7	14.2	0.03	Xglk577-3AL
4A	2013	23.7	2.9	11.5	-0.02	Xpsr59a-4A
	2013	210.2	3.6	14.1	0.02	Xmwg710b-4A
5A	2013	38.1	4.7	18.0	0.03	Xpsr945a-5A
	2013	214.4	6.8	24.8	-0.03	Xpsr918b-5A
5B	2013	18.7	3.3	13.0	0.03	Xpsr128-5B
Total leaf dry weight (g)						
3A	2013	117.5	4.3	16.5	0.04	Xglk577-3AL
3DL	2012	27.0	3.2	18.9	0.04	Xpsr1203b-3DL
4A	2012	4.0	3.6	21.1	-0.04	Xglk752-4AS
	2013	23.7	3.7	14.6	-0.04	Xpsr59a-4A
	2013	207.2	4.6	17.4	0.04	Xmwg710b-4A
5A	2013	51.3	6.8	24.9	0.05	Xpsr945a-5A
	2013	215.4	7.5	26.9	-0.05	Xpsr918b-5A
5B	2013	16.7	3.5	13.6	0.04	Xpsr128-5B
Stem dry weight (g)						
4A	2012	23.7	3.3	19.8	-0.15	Xpsr59a-4A
4DL	2012	26.2	3.2	18.7	-0.22	Xgwm194-4DL
5B	2013	21.7	3.2	12.4	0.11	Xpsr128-5B
Stem water soluble carbohydrate (WSC) dry weight (g)						
3DL	2012	23.0	3.5	20.5	0.07	Xpsr1203b-3DL
4A	2012	27.2	4.9	27.5	-0.07	Xpsr59a-4A
7B	2012	192.5	3.5	20.6	0.08	Xmwg710a-7B
Structural stem dry weight (g)						
4B	2013	59.8	3.3	13.0	-0.13	Xpsr921-4B
	2013	97.7	3.5	13.5	-0.08	Xpsr584-4B
4DL	2013	48.2	3.0	11.7	-0.12	Xpsr59b-4DL

Table 4-9 (continued)

Trait/Chromosome	Year	Position (cM)	LOD	R^2	Additive effect	Closest marker
Spike dry weight (g)						
2B	2013	82.7	3.2	12.5	-0.04	Xpsr961-2B
2D	2013	47.9	4.7	17.8	-0.09	Xpsr933b-2D
5A	2013	60.3	6.4	23.4	0.05	Xglk424-5A
	2013	213.4	5.0	19.0	-0.04	Xpsr918b-5A
7B	2013	95.7	4.2	16.1	-0.04	Xpsr350-7B
Spikelet dry weight (g)						
2B	2013	82.7	3.2	12.7	-0.002	Xpsr961-2B
4A	2012	24.7	3.6	21.2	-0.002	Xpsr59a-4A
5A	2013	57.3	3.8	14.7	0.002	Xglk424-5A
	2013	213.5	6.3	23.2	-0.002	Xpsr918b-5A
Spike fertility index (grains g^{-1})						
4A	2012	22.7	3.4	19.8	6	Xpsr59a-4A
	2013	31.2	3.2	12.5	3	Xpsr59a-4A
Spike:structural stem						
1BS	2012	33.8	3.1	18.7	-0.02	Xpsr960-1BS
	2013	40.9	2.9	11.4	-0.02	Xgwm18-1BS
5A	2013	213.5	5.3	19.7	-0.02	Xpsr918b-5A
7B	2013	179.5	3.2	12.5	-0.02	Xglk750-7BL
Biomass per shoot (g)						
4A	2012	23.7	3.3	19.3	-0.21	Xpsr59a-4A
4B	2013	59.8	3.2	12.7	-0.23	Xpsr921-4B
5B	2013	19.7	3.8	14.8	0.18	Xpsr128-5B
Flag leaf dry weight (%)						
1BS	2013	41.9	3.5	13.7	-0.3	Xgwm18-1BS
4A	2013	204.2	3.1	12.0	0.2	Xmwg710b-4A
4DL	2012	10.2	4.4	25.2	0.4	Xgwm194-4DL
5A	2013	53.3	7.4	26.6	0.5	Xpsr945a-5A
	2013	219.4	4.8	18.2	-0.4	Xpsr918b-5A
6A	2013	65.2	4.9	18.6	0.6	Xpsr966-6A
Remaining leaf dry weight (%)						
4B	2012	104.9	3.5	20.9	0.6	Xpsr1112-4B
5A	2013	2.0	3.7	14.3	0.3	Xpsr549-5A
	2013	220.4	5.8	21.6	-0.5	Xpsr918b-5A
Total leaf dry weight (%)						
1BS	2012	35.2	3.9	22.6	-0.7	Xpsr949-1BS
4B	2012	104.9	3.9	22.5	0.6	Xpsr1112-4B
5A	2012	112.2	2.8	16.7	0.6	Xpsr911-5A
	2013	35.1	6.5	23.8	0.7	Xpsr945a-5A
	2013	220.4	9.1	31.8	-0.9	Xpsr918b-5A
Stem dry weight (%)						
1BS	2012	35.2	4.5	25.6	1.0	Xpsr949-1BS
	2013	39.9	3.8	14.6	1.0	Xgwm18-1BS
2B	2013	78.7	3.2	12.4	1.1	Xpsr172-2B
5A	2013	58.3	6.9	25.2	-1.6	Xglk424-5A
	2013	213.4	6.9	25.0	1.3	Xpsr918b-5A

Table 4-9 (continued)

Trait/Chromosome	Year	Position (cM)	LOD	R^2	Additive effect	Closest marker
Stem WSC dry weight (%)						
4A	2012	27.2	3.3	19.8	-1.3	Xpsr59a-4A
7B	2012	215.8	3.2	18.8	1.2	Xglk576-7BL
Structural stem dry weight (%)						
1BS	2012	35.2	4.5	25.8	1.6	Xpsr949-1BS
5A	2013	214.4	4.3	16.4	1.4	Xpsr918b-5A
Spike dry weight (%)						
1BS	2013	38.9	3.0	11.8	-0.6	Xgwm18-1BS
2A	2012	94.9	3.4	20.1	0.6	Xpsr919b-2A
2B	2013	80.7	3.9	15.2	-0.8	Xpsr961-2B
2D	2013	36.9	3.3	13.0	-1.3	Xpsr933b-2D
3DL	2012	32.2	3.3	19.7	-0.6	Xpsr388-3DL
5A	2013	67.4	5.0	18.9	0.9	Xglk424-5A
7B	2012	71.8	3.3	19.4	-0.6	Xglk549-7B
	2012	186.5	3.5	20.8	-0.9	Xglk750-7BL
	2013	98.7	3.1	12.2	-0.7	pwir232b-7B
	2013	173.5	4.2	16.2	-0.8	Xglk750-7BL
Flag leaf area (cm^2)						
3A	2012	190.0	4.6	25.9	3	Xpsr1203a-3A
	2013	118.5	3.4	13.2	2	Xglk577-3AL
4A	2013	23.7	3.8	14.7	-2	Xpsr59a-4A
	2013	203.3	4.1	15.8	2	Xmwg710b-4A
5A	2013	55.3	7.6	27.2	3	Xglk424-5A
	2013	217.5	5.9	22.0	-3	Xpsr918b-5A
6A	2012	62.2	3.0	18.1	4	Xpsr966-6A
	2013	64.2	4.4	16.9	4	Xpsr966-6A
Remaining leaf area (cm^2)						
5A	2013	61.3	5.0	19.0	6	Xglk424-5A
	2013	214.4	8.4	29.7	-6	Xpsr918b-5A
5B	2013	29.6	3.8	14.7	4	Xglk614b-5BL
Total leaf area (cm^2)						
3A	2013	116.5	3.1	12.1	6	Xglk577-3AL
4A	2013	207.2	3.2	12.7	5	Xmwg710b-4A
5A	2013	58.3	6.9	25.4	9	Xglk424-5A
	2013	215.4	9.2	31.9	-9	Xpsr918b-5A
5B	2013	24.7	3.4	13.2	7	Xglk614b-5BL
SLA of total leaf ($cm^2\ g^{-1}$)						
6A	2012	5.0	3.3	19.5	10	Xpsr563a-6A
Flag leaf angle (scores)						
4A	2013	84.2	3.4	13.4	0.2	Xglk600b-4A

Table 4-9 (continued)

Trait/Chromosome	Year	Position (cM)	LOD	R^2	Additive effect	Closest marker
At maturity						
Flag leaf dry weight (g)						
3A	2013	117.5	3.5	13.7	0.01	Xglk577-3AL
4A	2013	22.7	5.1	19.2	-0.01	Xpsr59a-4A
5A	2013	54.3	5.8	21.5	0.01	Xglk424-5A
6A	2013	91.0	4.7	17.9	0.01	Xpsr966-6A
Remaining leaf dry weight (g)						
2D	2013	47.9	3.2	12.5	-0.02	Xpsr933b-2D
4B	2013	93.7	3.7	14.3	-0.01	Xpsr584-4B
5A	2013	54.3	5.4	20.1	0.01	Xglk424-5A
Total leaf dry weight (g)						
1A	2012	87.4	4.6	26.0	-0.02	Xpsr1201b-1A
3A	2013	113.5	3.4	13.1	0.02	Xglk577-3AL
3DL	2012	23.0	3.2	18.8	0.02	Xpsr1203b-3DL
4A	2012	21.7	3.8	22.0	-0.02	Xpsr59a-4A
	2013	22.7	4.1	15.7	-0.02	Xpsr59a-4A
4B	2013	92.8	3.5	13.7	-0.02	Xpsr584-4B
5A	2013	54.3	6.4	23.6	0.03	Xglk424-5A
	2013	213.4	3.2	12.5	-0.02	Xpsr918b-5A
5B	2012	129.6	3.7	21.5	-0.02	Xpsr370-5B
6A	2012	91.1	3.5	20.7	0.02	Xpsr966-6A
Stem dry weight (g)						
4B	2012	108.9	3.9	22.8	-0.09	Xpsr1112-4B
	2013	96.8	4.9	18.8	-0.09	Xpsr584-4B
7D	2012	4.0	3.8	21.9	-0.09	Xglk184a-7DS
Chaff dry weight (g)						
3A	2013	75.7	3.4	13.1	0.04	Xglk221-3AL
4A	2013	24.7	4.6	17.4	-0.05	Xpsr59a-4A
5A	2012	208.9	5.7	31.4	-0.09	Xpsr918b-5A
	2013	57.3	5.6	21.0	0.07	Xglk424-5A
	2013	213.4	5.4	20.3	-0.06	Xpsr918b-5A
Flag leaf dry weight (%)						
1A	2013	49.8	3.4	13.4	-0.3	Xpsr1327b-1A
3A	2013	49.9	3.1	12.0	0.2	Xpsr598-3A
	2013	118.5	3.6	13.9	0.2	Xglk577-3AL
4A	2013	23.7	3.9	15.2	-0.2	Xpsr59a-4A
5A	2013	37.1	4.8	18.1	0.2	Xpsr945a-5A
6A	2013	90.0	5.9	22.1	0.2	Xpsr966-6A
Total leaf dry weight (%)						
1A	2012	86.4	3.2	19.1	-0.5	Xpsr161-1A
2B	2012	146.8	3.4	20.3	-0.5	Xglk699a-2BS
3A	2013	105.3	3.6	14.2	0.2	Xglk118-3AL
3B	2012	100.5	3.1	18.7	0.8	Xpsr1054-3B
5A	2013	40.1	5.7	21.2	0.3	Xpsr945a-5A

Table 4-9 (continued)

Trait/Chromosome	Year	Position (cM)	LOD	R^2	Additive effect	Closest marker
Stem dry weight (%)						
1BS	2012	35.2	3.6	21.1	1.6	Xpsr949-1BS
	2013	39.9	3.4	13.3	1.1	Xgwm18-1BS
5A	2013	56.3	2.9	11.3	-1.2	Xglk424-5A
	2013	213.4	5.8	21.7	1.4	Xpsr918b-5A
Chaff dry weight (%)						
2B	2012	71.7	3.6	20.9	-2.1	Xpsr172-2B
3A	2013	75.7	5.7	21.2	0.8	Xglk221-3AL
4A	2013	25.7	4.3	16.4	-0.7	Xpsr59a-4A
5A	2012	209.9	6.3	33.9	-2.8	Xpsr918b-5A
	2013	53.3	4.0	15.4	0.8	Xpsr945a-5A
	2013	213.4	6.5	23.7	-0.9	Xpsr918b-5A
Plant height (cm)						
2A	2012	11.9	3.1	18.6	4.4	Xpsr908-2A
	2013	35.5	3.5	13.4	4.0	Xglk222-2AS
Crop and spike growth dynamics						
Accumulated dry matter (GS39−Anthesis, g)						
5B	2013	22.7	3.2	12.5	0.11	Xglk614b-5BL
Spike dry weight at GS33 (g) (the third stem node just detectable)						
5A	2012	216.5	6.7	35.7	0.0012	Xpsr918b-5A
	2013	209.9	6.0	22.2	0.0011	Xpsr918b-5A
7B	2013	78.6	3.8	14.7	0.0009	Xglk478-7BL
Spike growth rate (g $^{o}Cd^{-1}$)						
2B	2013	91.7	3.6	14.1	-0.0001	Xpsr961-2B
2D	2013	53.9	3.6	13.9	-0.0003	Xpsr335-2D
5A	2013	62.3	5.2	19.5	0.0001	Xglk424-5A
	2013	213.5	5.6	20.8	-0.0001	Xpsr918b-5A
7B	2013	92.7	3.2	12.4	-0.0001	Xpsr350-7B
Dry matter translocation (DMT)						
Flag leaf DMT (g)						
4A	2013	201.3	5.2	19.6	0.009	Xmwg710b-4A
5A	2013	53.3	6.7	24.4	0.012	Xpsr945a-5A
	2013	217.4	7.5	27.1	-0.012	Xpsr918b-5A
Remaining leaf DMT (g)						
4A	2013	209.2	3.6	14.0	0.018	Xmwg710b-4A
5A	2013	34.1	2.9	11.4	0.018	Xpsr945a-5A
	2013	216.4	6.5	23.8	-0.025	Xpsr918b-5A
5B	2013	20.7	4.4	16.7	0.023	Xpsr128-5B
Total leaf DMT (g)						
3A	2013	120.5	3.3	12.8	0.024	Xglk652a-3AL
4A	2013	208.2	5.2	19.6	0.026	Xmwg710b-4A
5A	2013	36.1	4.8	18.4	0.027	Xpsr945a-5A
	2013	216.4	8.6	30.2	-0.035	Xpsr918b-5A
5B	2013	19.7	4.6	17.6	0.029	Xpsr128-5B

Table 4-9 (continued)

Trait/Chromosome	Year	Position (cM)	LOD	R^2	Additive effect	Closest marker
Contribution of flag leaf DMT to yield (%)						
4A	2013	200.3	3.4	13.3	0.4	Xmwg710b-4A
5A	2013	39.1	3.2	12.4	0.4	Xpsr945a-5A
	2013	221.4	3.7	14.4	-0.4	Xpsr918b-5A
Contribution of WSC DMT to yield (%)						
2B	2012	216.0	3.5	20.8	-3.5	Xglk610a-2BL
De-graining treatment						
Potential grain weight (mg)						
2A	2013	143.4	3.3	12.7	-1.38	PL_AP-2A
Extra assimilate use (mg grain^{-1})						
7B	2013	88.7	3.2	12.5	-1.38	Xpsr350-7B
	2013	157.1	4.7	17.9	-1.59	Xpsr547-7B
Grain weight and number within spike						
TGW (basal spikelet) (g)						
2A	2012	94.9	3.1	18.5	-2.59	Xpsr919b-2A
4A	2012	19.7	6.9	36.6	-4.20	Xglk315-4AS
7B	2012	192.5	5.7	31.3	4.89	Xmwg710a-7B
TGW (central spikelet) (g)						
1A	2012	80.1	3.6	21.3	-2.81	Xpsr1327b-1A
2A	2012	94.9	3.8	22.0	-2.83	Xpsr919b-2A
3B	2012	80.5	5.0	27.8	3.31	Xpsr1054-3B
4A	2012	21.7	5.9	32.5	-4.03	Xpsr59a-4A
7B	2012	70.7	4.4	25.2	3.14	Xglk549-7B
	2012	184.5	5.3	29.5	4.72	Xglk750-7BL
TGW (apical spikelet) (g)						
3B	2012	80.5	5.0	28.0	3.17	Xpsr1054-3B
4A	2012	21.7	5.1	28.6	-3.61	Xpsr59a-4A
7B	2012	183.5	4.2	24.3	4.04	Xglk750-7BL
TGW (Grain 1) (g)						
2A	2012	94.9	3.4	20.1	-2.50	Xpsr919b-2A
3B	2012	80.5	3.6	21.1	2.66	Xpsr1054-3B
4A	2012	18.7	5.7	31.4	-3.54	Xglk315-4AS
5DL	2012	39.0	3.1	18.2	-4.93	Xpsr580a-5DL
7B	2012	70.7	3.0	17.9	2.44	Xglk549-7B
	2012	186.5	4.8	26.9	4.23	Xglk750-7BL
TGW (Grain 2) (g)						
3B	2012	85.5	4.9	27.7	3.85	Xpsr1054-3B
4A	2012	19.7	7.1	37.3	-4.19	Xglk315-4AS
7B	2012	188.5	4.0	23.1	4.22	Xglk750-7BL
Grains per central spikelet						
7B	2012	4.0	2.9	17.4	-0.12	Xglk301b-7B
Grains per apical spikelet						
3B	2012	45.7	2.9	17.6	0.12	Xglk554b-3B
5A	2012	211.9	3.8	22.1	-0.15	Xpsr918b-5A
6A	2012	0.1	3.3	19.6	0.12	Xpsr008-6A

4.5 Discussion

4.5.1 Optimising grain weight and number, final biomass and HI for yield improvement

Grain yield is a complex quantitative trait, and can be dissected into numerical (grain weight and number) and physiological (final biomass and HI) components to facilitate the understanding of its determination. There were positive relationships between four components and yield, as reported by previous studies (Bustos et al., 2013; Gonzalez et al., 2011; Sadras and Lawson, 2011; Sayre et al., 1997; Shearman et al., 2005). Among yield components, final biomass was not significantly associated with HI, so they may be improved in parallel (Garcia et al., 2013). Moreover, final biomass showed weak association with plant height, indicating that more biomass can be achieved in short plants, which is essential for lodging resistance. In contrast, TGW was consistently negatively associated with grains per spike, which has often been seen in wheat (Bustos et al., 2013; Garcia et al., 2013; Gonzalez et al., 2011; Sadras and Lawson, 2011).

Genetic analysis revealed many QTL for yield and yield components, and QTL coincidences between them were found, in line with the previous reports (Hai et al., 2008; Mason et al., 2013; McIntyre et al., 2010). This confirms that yield can be considered as a function of a few simpler traits. Negative QTL coincidences between TGW and grains per spike were detected on chromosomes 3B, 4A, 5A, and 7B, which provides the genetic evidence for their inverse relationship. The windows of determination of grain number and weight are overlapped in a short period immediately before anthesis when rapid spike growth, floret death and carpel growth take place. It was found that QTL for grains per spike and carpel size at anthesis were also negatively coincident on 3B, 4A and 5A in the same population (data not shown), indicating that more grains were associated with smaller carpels due to pleiotropy or tight gene linkages. Therefore, when more grains are defined, plants may slightly reduce the upper limit of individual grain size by limiting carpel growth, so that the newly established grains can be filled with extra assimilates after anthesis and become viable and relatively uniform. This mechanism would also protect maternal plants from being exhausted during grain filling, in particular under postanthesis stress environments. In fact, modern wheat plants could be more ‘optimistic’, as there are adequate assimilates available from current photosynthesis and preanthesis reserve

remobilisation during grain filling under favourable conditions as a consequence of breeding (Borras et al., 2004; Slafer and Savin, 1994). Thus, the over-protection system in modern wheat should be loosened somewhat by eliminating these genes under coincident QTL and combining more independent ones for each of grain weight and number.

4.5.2 Optimising biomass accumulation and partitioning for the improvement of yield and yield components

Benefiting from the large difference between the bread wheat Forno and spelt Oberkulmer in biomass, significant variation in biomass accumulation and its partitioning to different plant organs was observed, confirming the likelihood for modification (Foulkes et al., 2011). Total biomass and plant organ DW at GS39 and anthesis consistently contributed to grain yield, with an exception of spike DW at GS39. These results suggest the importance of the preanthesis plant growth: the larger plants, the higher grain yield. Biomass is an outcome of LI and RUE, so it is deduced that the traits influencing each or both of them may affect yield. For a single shoot, leaf area determines canopy size for LI. The present study revealed that leaf area was positively associated with the total biomass at each stage and with yield across years. The positive relationships between preanthesis RUE and biomass, and between preanthesis RUE and yield have been observed previously, and the recent genetic gain of yield has been associated with increased preanthesis RUE due to improved stomatal conductance and greener leaves (Sadras and Lawson, 2011; Shearman et al., 2005).

To understand how the preanthesis plant growth affected final yield, the relationships between biomass and yield components were analysed. In terms of the numerical components, the total biomass and plant organ DW at GS39 and anthesis contributed to either TGW (mainly that of apical spikelets and G2) or grain number, depending on years. Furthermore, larger plants at these stages were found in 2013 than in 2012, and accompanied with more and larger grains. These agree with the hypothesis that grain weight and number are adjusted to match the preanthesis plant growth status, which essentially depends on the availability of environmental resources (e.g. radiation and nutrients in soil) (Sadras and Denison, 2009; Sadras and Lawson, 2011). Grain number is more plastic and responsive to resource availability compared with grain weight (Sadras, 2007), benefiting from the over-production of floret primordia (González-Navarro et al., 2015; Kirby, 1988). More resources available during the

critical period when rapid spike growth and floret death occur, would lead to higher floret survival and, in turn, more grains. This is supported by the de-tillering at GS39 increasing resource availability, showing higher biomass and grain number (and yield). Likewise, reduced tillers by using the tin gene (Duggan et al., 2005; Gaju et al., 2014), lower plant density (Bustos et al., 2013), accelerated crop growth by increased RUE between stem elongation and anthesis (Sadras and Lawson, 2011), and nitrogen application (van Herwaarden et al., 1998b), also improve spike fertility. The responsiveness of grain number to resource availability may contribute to its increase during yield improvement when more fertilisers have been applied. While distal floret death takes place to define final grain number through sugar starvation, stem soluble carbohydrates are accumulating (Ghiglione et al., 2008; Sadras and Denison, 2009). In addition, the dry matter accumulated in other organs (leaves, structural stems and spikes) before anthesis can also be partly remobilised to grains during terminal senescence, accounting for up to 70% of yield in total (Alvaro et al., 2008; Koutroubas et al., 2012; van Herwaarden et al., 1998a). Hence, it seems that the preanthesis plant size determines the assimilate supply for growing grains in two ways: providing photosynthetic sites and dry matter translocation. By measuring preanthesis plant size, grain number is then derived, and the assimilates from the above routes should be enough to fill these grains under normal conditions, resulting in a narrow range of grain weight favouring maternal fitness (Sadras and Denison, 2009). This proposition is in line with the findings that the heritability of grain weight is relatively high in the present and other studies (McIntyre et al., 2010; Sadras, 2007).

Turning to the physiological components of yield, the preanthesis biomass of the whole shoots and plant organs was constantly positively associated with final biomass at maturity. In addition, fast CGR from GS39 to maturity, reflecting a combined outcome of LI and RUE, also favoured final biomass. CGR from GS39 to anthesis was c. eight times faster than that from anthesis to maturity across all the RILs over two years. However, CGR during grain filling was more closely associated with final biomass. There was a large genetic variation in CGR among the RILs: 0.0018−0.0108 g $^{o}Cd^{-1}$ from GS39 to anthesis, and 0−0.0021 g $^{o}Cd^{-1}$ from anthesis to maturity. Genetic selection for the genotypes with fast CGR would be useful to improve crop biomass. It has been reported that the greater CGR from heading to maturity in modern bread wheat cultivars contributes to grain yield progress (Karimi and Siddique,

1991). Therefore, CGR may be incorporated into wheat ideotypes in future breeding. As the H^2 of CGR were low (0.28−0.32), it needs to be borne in mind that the genotypes selected should be tested in multiple environments.

There are also opportunities to improve yield and yield components by modifying the proportions of biomass partitioning to different organs. In general, the percentage leaf DW at GS39 and anthesis could be increased, likely leading to more grains per spike (mainly for apical spikelets) and higher yield. The net effects of the percentage DW of total stems (and WSC at anthesis) and spikes at these stages on yield were either positive or negative over years, because of their respective opposite influences on grain weight and number. The percentage DW of structural stems at anthesis, stems and chaff at maturity showed negative effects on HI and yield, so their proportions could be minimised, in agreement with the earlier opinions (Foulkes et al., 2011; Reynolds et al., 2012). When attempting to reduce the proportion of structural stems, care must be taken to maintain plant lodging resistance.

Genetic basis of the preanthesis biomass accumulation and partitioning, as related to yield and yield components, has rarely been reported. Liang et al. (2010) identified 18 QTL for the DW of leaves, stems and the whole shoots at jointing and anthesis stages. The QTL coincidences between these traits have been located on 1D, 3B and 5D, but yield data has been absent. Stem WSC content at anthesis has received wide interest, and a large number of QTL have been identified, many of which are coincident with those for yield and yield components (McIntyre et al., 2010; Rebetzke et al., 2008). Flag leaf DW at anthesis has been reported to be positively associated with yield per spike; however, there is no coincident QTL between them (Su et al., 2006). The present study detected numerous QTL for biomass and its partitioning to leaves, stems (WSC and structural stems) and spikes at GS39 and anthesis; most QTL for the DW of whole shoots and different plant organs across two stages were coincident, especially on 1BS, 3A, 4A, 4B, and 5A, indicating pleiotropy or tight gene linkages. Additionally, there were positive QTL coincidences between biomass accumulation and partitioning, and yield and yield components, in line with the above conclusion that the preanthesis plant growth contributes to yield and yield components. Due to the negative QTL coincidences between TGW and grains per spike, however, larger plants were associated with larger but fewer grains on 3B and 4AS, and with smaller but more grains on 4AL and 5AL. In 2013, more biomass and associated QTL were

found, accompanying with the appearance of more coincident QTL for grains per spike, confirming that grain number responds to the preanthesis biomass accumulation.

4.5.3 Increasing potential grain weight (PGW) and grain number to reduce sink limitation

There is evidence that grains grow under saturated assimilate supply during the postanthesis period (sink limited) (Borras et al., 2004; Miralles and Slafer, 2007; Slafer and Savin, 1994), concurring with the present study that showed only a slight increase in grain weight in response to de-graining at anthesis. Genetic analysis identified one QTL for PGW on 2A, coincident with those for TGW (mean of all RILs and that of basal and central spikelets, and G1). In addition, QTL for carpel size at anthesis and grain volume at maturity were also detected at this location, and all the favourable alleles were conferred by the spelt Oberkulmer (data not shown). This confirms that carpel size is the upper limit of PGW (Calderini et al., 1999; Hasan et al., 2011). However, given the large responsiveness to the increased assimilate availability after de-graining, grain volume appears not to function as a physical constraint but an outcome reflecting assimilate status. To overcome sink limitation, therefore, a potential strategy is to improve carpel growth prior to anthesis and in turn PGW.

Different genotypes responded differently to de-graining; that is, the lines with more grains had a larger gap between actual and potential grain weight (more source limited), and a larger increase when the assimilates became sufficient. It has been found that most modern wheat cultivars show higher source limitation than old ones, with increasing grain number (Acreche and Slafer, 2009; Fischer and Hillerislambers, 1978). Thus, a further reduction in sink limitation is likely achieved through a continuous increase in spike fertility (Miralles and Slafer, 2007). As discussed above, grain number responded to the preanthesis biomass accumulation and partitioning. Grains per spike was positively associated with spike DW, SPI and SFI, consistent with the earlier reports (Bustos et al., 2013; Fischer, 2011; Garcia et al., 2014; González et al., 2011; Zhang et al., 2012). Their relationships were further supported by the positive QTL coincidences. Rapid spike growth occurred mainly between GS39 and anthesis; spike DW at anthesis was determined by SGR (neither SGD nor initial growth at GS33 and GS39), and essentially depended on ADM and CGR during this

period. Thus, increasing biomass accumulation at that time would improve grain number, as confirmed by de-tillering at GS39.

In conclusion, there was a large genetic variation in biomass accumulation and its partitioning to plant organs at different developmental stages, which could allow wheat plants to be redesigned for grain yield improvement. This work emphasises that the biomass accumulation and partitioning during the preanthesis period, especially between GS39 and anthesis, are key for yield determination: the larger plants, the higher yield and yield components. Therefore, the preanthesis plant growth should be incorporated into the ideotypes in future wheat breeding. Further improvement of the plant growth prior to anthesis may be involved in understanding the physiological (e.g. canopy architecture and photosynthetic capacity) and genetic (e.g. the genes within the QTL identified in this study) basis of biomass production. In addition, the relative species of bread wheat such as spelt can be used to introduce desirable biomass traits and genes. Subsequently, crop management should also be optimised to ensure sufficient resource supply and undisturbed plant growth, for example, adjusting sowing date for early canopy size and longer preanthesis growth duration, applying fertilisers for saturated nutrient availability, and protecting crop from biotic and abiotic stresses.

4.6 Acknowledgements

This study was financially supported by the China Scholarship Council (CSC) and University of Nottingham. We thank Beat Keller (University of Zurich, Switzerland) for providing the plant materials used in this work, and Monika Messmer (Research Institute of Organic Agriculture, Switzerland) for providing the molecular marker data. We are also grateful to Chuong Nguyen, John Alcock and Matthew Tovey (University of Nottingham) for their help with the field experiments and sample processing.

4.7 References

Acreche MM, Slafer GA. 2009. Grain weight, radiation interception and use efficiency as affected by sink-strength in Mediterranean wheats released from 1940 to 2005. Field Crops Research **110**, 98-105.

Alvaro F, Isidro J, Villegas D, Garcia del Moral LF, Royo C. 2008. Breeding effects on grain filling, biomass partitioning, and remobilization in Mediterranean durum wheat. Agronomy Journal **100**, 361-370.

Borras L, Slafer GA, Otegui ME. 2004. Seed dry weight response to source-sink manipulations in wheat, maize and soybean: a quantitative reappraisal. Field Crops Research **86**, 131-146.

Braun HJ, Atlin G, Payne T. 2010. Multi-location testing as a tool to identify plant response to global climate change. In: Reynolds MP, ed. Climate Change and Crop Production. Surrey: CABI, 115-138.

Brocklehurst PA. 1977. Factors controlling grain weight in wheat. Nature **266**, 348-349.

Brooking IR, Kirby EJM. 1981. Interrelationships between stem and ear development in winter wheat: the effects of a Norin 10 dwarfing gene, Gai/Rht_2. Journal of Agricultural Science **97**, 373-381.

Bustos DV, Hasan AK, Reynolds MP, Calderini DF. 2013. Combining high grain number and weight through a DH-population to improve grain yield potential of wheat in high-yielding environments. Field Crops Research **145**, 106-115.

Calderini DF, Abeledo LG, Savin R, Slafer GA. 1999. Effect of temperature and carpel size during pre-anthesis on potential grain weight in wheat. Journal of Agricultural Science **132**, 453-459.

Calderini DF, Reynolds MP. 2000. Changes in grain weight as a consequence of de-graining treatments at pre- and post-anthesis in synthetic hexaploid lines of wheat (Triticum durum × T. tauschii). Australian Journal of Plant Physiology **27**, 183-191.

Distelfeld A, Avni R, Fischer AM. 2014. Senescence, nutrient remobilization, and yield in wheat and barley. Journal of Experimental Botany **65**, 3783-3798.

Duggan BL, Richards RA, van Herwaarden AF, Fettell NA. 2005. Agronomic evaluation of a tiller inhibition gene (tin) in wheat. I. Effect on yield, yield components, and grain protein. Australian Journal of Agricultural Research **56**, 169-178.

Fischer RA. 1985. Number of kernels in wheat crops and the influence of solar radiation and temperature. Journal of Agricultural Science **105**, 447-461.

Fischer RA. 2011. Wheat physiology: a review of recent developments. Crop and Pasture Science **62**, 95-114.

Fischer RA, Hillerislambers D. 1978. Effect of environment and cultivar on source limitation to grain weight in wheat. Australian Journal of Agricultural Research **29**, 443-458.

Flintham JE, Borner A, Worland AJ, Gale MD. 1997. Optimizing wheat grain yield: effects of Rht (gibberellin-insensitive) dwarfing genes. Journal of Agricultural Science **128**, 11-25.

Foulkes MJ, Slafer GA, Davies WJ, Berry PM, Sylvester-Bradley R, Martre P, Calderini DF, Griffiths S, Reynolds MP. 2011. Raising yield potential of wheat. III. Optimizing partitioning to grain while maintaining lodging resistance. Journal of Experimental Botany **62**, 469-486.

Foulkes MJ, Sylvester-Bradley R, Weightman R, Snape JW. 2007. Identifying physiological traits associated with improved drought resistance in winter wheat. Field Crops Research **103**, 11-24.

Gaju O, Reynolds MP, Sparkes DL, Mayes S, Ribas-Vargas G, Crossa J, Foulkes MJ. 2014. Relationships between physiological traits, grain number and yield potential in a wheat DH population of large spike phenotype. Field Crops Research **164**, 126-135.

Garcia GA, Hasan AK, Puhl LE, Reynolds MP, Calderini DF, Miralles DJ. 2013. Grain yield potential strategies in an elite wheat double-haploid population grown in contrasting environments. Crop Science **53**, 2577-2587.

Garcia GA, Serrago RA, Gonzalez FG, Slafer GA, Reynolds MP, Miralles DJ. 2014. Wheat grain number: Identification of favourable physiological traits in an elite doubled-haploid population. Field Crops Research **168**, 126-134.

Ghiglione HO, Gonzalez FG, Serrago R, Maldonado SB, Chilcott C, Cura JA, Miralles DJ, Zhu T, Casal JJ. 2008. Autophagy regulated by day length determines the number of fertile florets in wheat. Plant Journal **55**, 1010-1024.

González-Navarro OE, Griffiths S, Molero G, Reynolds MP, Slafer GA. 2015. Dynamics of floret development determining differences in spike fertility in an elite population of wheat. Field Crops Research **172**, 21-31.

González FG, Miralles DJ, Slafer GA. 2011. Wheat floret survival as related to pre-anthesis spike growth. Journal of Experimental Botany **62**, 4889-4901.

Gonzalez FG, Terrile II, Falcon MO. 2011. Spike fertility and duration of stem elongation as promising traits to improve potential grain number (and yield): variation in modern Argentinean wheats. Crop Science **51**, 1693-1702.

Gregersen PL, Culetic A, Boschian L, Krupinska K. 2013. Plant senescence and crop productivity. Plant Molecular Biology **82**, 603-622.

Hai L, Guo H, Wagner C, Xiao S, Friedt W. 2008. Genomic regions for yield and yield parameters in Chinese winter wheat (Triticum aestivum L.) genotypes tested under varying environments correspond to QTL in widely different wheat materials. Plant Science **175**, 226-232.

Hasan AK, Herrera J, Lizana C, Calderini DF. 2011. Carpel weight, grain length and stabilized grain water content are physiological drivers of grain weight determination of wheat. Field Crops Research **123**, 241-247.

Karimi MM, Siddique KHM. 1991. Crop growth and relative growth rates of old and modern wheat cultivars. Australian Journal of Agricultural Research **42**, 13-20.

Kirby EJM. 1988. Analysis of leaf, stem and ear growth in wheat from terminal spikelet stage to anthesis. Field Crops Research **18**, 127-140.

Koutroubas SD, Fotiadis S, Damalas CA. 2012. Biomass and nitrogen accumulation and translocation in spelt (Triticum spelta) grown in a Mediterranean area. Field Crops Research **127**, 1-8.

Liang Y, Zhang K, Zhao L, Liu B, Meng Q, Tian J, Zhao S. 2010. Identification of chromosome regions conferring dry matter accumulation and photosynthesis in wheat (Triticum aestivum L.). Euphytica **171**, 145-156.

Mason RE, Hays DB, Mondal S, Ibrahim AMH, Basnet BR. 2013. QTL for yield, yield components and canopy temperature depression in wheat under late sown field conditions. Euphytica **194**, 243-259.

McIntyre CL, Mathews KL, Rattey A, Chapman SC, Drenth J, Ghaderi M, Reynolds M, Shorter R. 2010. Molecular detection of genomic regions associated with grain yield and yield-related components in an elite bread wheat cross evaluated under irrigated and rainfed conditions. Theoretical and Applied Genetics **120**, 527-541.

Miralles DJ, Slafer GA. 2007. Sink limitations to yield in wheat: how could it be reduced? Journal of Agricultural Science **145**, 139-149.

Ray DK, Mueller ND, West PC, Foley JA. 2013. Yield trends are insufficient to double global crop production by 2050. PLoS ONE **8**, e66428.

Rebetzke GJ, van Herwaarden AF, Jenkins C, Weiss M, Lewis D, Ruuska S, Tabe L, Fettell NA, Richards RA. 2008. Quantitative trait loci for water-soluble carbohydrates and associations with agronomic traits in wheat. Australian Journal of Agricultural Research **59**, 891-905.

Reynolds M, Foulkes J, Furbank R, Griffiths S, King J, Murchie E, Parry M, Slafer G. 2012. Achieving yield gains in wheat. Plant Cell and Environment **35**, 1799-1823.

Sadras VO. 2007. Evolutionary aspects of the trade-off between seed size and number in crops. Field Crops Research **100**, 125-138.

Sadras VO, Denison RF. 2009. Do plant parts compete for resources? An evolutionary viewpoint. New Phytologist **183**, 565-574.

Sadras VO, Lawson C. 2011. Genetic gain in yield and associated changes in phenotype, trait plasticity and competitive ability of South Australian wheat varieties released between 1958 and 2007. Crop and Pasture Science **62**, 533-549.

Sanchez-Garcia M, Royo C, Aparicio N, Martin-Sanchez JA, Alvaro F. 2013. Genetic improvement of bread wheat yield and associated traits in Spain during the 20th century. Journal of Agricultural Science **151**, 105-118.

Sayre KD, Rajaram S, Fischer RA. 1997. Yield potential progress in short bread wheats in northwest Mexico. Crop Science **37**, 36-42.

Shearman VJ, Sylvester-Bradley R, Scott RK, Foulkes MJ. 2005. Physiological processes associated with wheat yield progress in the UK. Crop Science **45**, 175-185.

Slafer GA, Andrade FH. 1993. Physiological attributes related to the generation of grain yield in bread wheat cultivars released at different eras. Field Crops Research **31**, 351-367.

Slafer GA, Savin R. 1994. Source-sink relationships and grain mass at different positions within the spike in wheat. Field Crops Research **37**, 39-49.

Slafer GA, Whitechurch EM. 2001. Manipulating wheat development to improve adaptation. In: Reynolds MP, Ortiz-Monasterio JI, McNab A, eds. Application of Physiology in Wheat Breeding. Mexico: CIMMYT, 160-170.

Su JY, Tong YP, Liu QY, Li B, Jing RL, Li JY, Li ZS. 2006. Mapping quantitative trait loci for post-anthesis dry matter accumulation in wheat. Journal of Integrative Plant Biology **48**, 938-944.

The Wheat Initiative. 2013. An International Vision for Wheat Improvement. Paris, France.

Torres A, Pietragalla J. 2012. Crop morphological traits. In: Pask AJD, Pietragalla J, Mullan DM, Reynolds MP, eds. Physiological Breeding II: A Field Guide to Wheat Phenotyping. Mexico: CIMMYT, 106-112.

van Herwaarden AF, Angus JF, Richards RA, Farquhar GD. 1998a. 'Haying-off', the negative grain yield response of dryland wheat to nitrogen fertiliser. II. Carbohydrate and protein dynamics. Australian Journal of Agricultural Research **49**, 1083-1093.

van Herwaarden AF, Farquhar GD, Angus JF, Richards RA, Howe GN. 1998b. 'Haying-off', the negative grain yield response of dryland wheat to nitrogen fertiliser. I. Biomass, grain yield, and water use. Australian Journal of Agricultural Research **49**, 1067-1081.

Wu W, Li C, Ma B, Shah F, Liu Y, Liao Y. 2014. Genetic progress in wheat yield and associated traits in China since 1945 and future prospects. Euphytica **196**, 155-168.

Wu XY, Kuai BK, Jia JZ, Jing HC. 2012. Regulation of leaf senescence and crop genetic improvement. Journal of Integrative Plant Biology **54**, 936-952.

Yemm EW, Willis AJ. 1954. The estimation of carbohydrates in plant extracts by anthrone. Biochemical Journal **57**, 508-514.

Youssefian S, Kirby EJM, Gale MD. 1992. Pleiotropic effects of the GA-insensitive Rht dwarfing genes in wheat. 2. Effects on leaf, stem, ear and floret growth. Field Crops Research **28**, 191-210.

Zadoks JC, Chang TT, Konzak CF. 1974. A decimal code for the growth stages of cereals. Weed Research **14**, 415-421.

Zhang H, Turner NC, Poole ML. 2012. Increasing the harvest index of wheat in the high rainfall zones of southern Australia. Field Crops Research **129**, 111-123.

4.8 Supplementary information

List of Supplementary files

Supplementary Table S4-1 Descriptive statistics on biomass, biomass-related traits, yield and yield components of the parents and recombinant inbred lines (RILs)

Supplementary Table S4-2 Correlations among plant organs at GS39 (flag leaf ligule emergence)

Supplementary Table S4-3 Correlations among plant organs at anthesis (dry weight)

Supplementary Table S4-4 Correlations among plant organs at anthesis (dry weight proportion, %)

Supplementary Table S4-5 Correlations among plant organs at maturity (dry weight)

Supplementary Table S4-6 Correlations among plant organs at maturity (dry weight proportion, %)

Supplementary Table S4-7 Correlations of grain number and grain weight among different positions within spikes in 2012

Supplementary Table S4-8 Significant correlations between biomass at different growth stages and yield components within spikes

Supplementary Table S4-1 Descriptive statistics on biomass, biomass-related traits, yield and yield components of the parents and recombinant inbred lines (RILs)

Trait[a]	Year	Parental lines			RILs			H^{2d}
		Forno	Oberkulmer	P-value	Mean (min; max)	P-value	S.E.D[c]	
Yield traits								
TGW (g)	2012	33.9	47.3	< 0.01	40.7 (30.4; 50.5)	< 0.001	1.7	0.74
	2013	49.4	44.8	< 0.01	45.2 (33.9; 52.6)	< 0.001	1.3	
Grains per spike	2012	40	33	> 0.05	37 (24; 51)	< 0.001	4.6	0.78
	2013	38	36	> 0.05	40 (26; 54)	< 0.001	2.8	
Biomass per shoot (g)	2012	2.41	3.05	< 0.01	2.89 (1.94; 3.92)	< 0.001	0.20	0.69
	2013	3.58	4.09	< 0.05	4.11 (2.69; 5.21)	< 0.001	0.25	
Harvest index	2012	0.29	0.24	> 0.05	0.26 (0.16; 0.35)	< 0.001	0.03	0.13
	2013	0.51	0.39	< 0.01	0.44 (0.35; 0.49)	< 0.001	0.01	
Yield per spike (g)	2012[b]	1.48	1.38	> 0.05	1.46 (0.84; 1.96)	< 0.001	0.19	0.32
	2013	1.84	1.60	> 0.05	1.81 (1.21; 2.32)	< 0.001	0.15	
At GS39 (flag leaf ligule emergence)								
Total leaf DW (g)	2012	0.41	0.69	< 0.05	0.46 (0.22; 0.77)	< 0.01	0.11	0.46
	2013	0.46	0.69	< 0.01	0.61 (0.42; 0.85)	< 0.001	0.04	
Stem DW (g)	2012	1.05	1.47	> 0.05	1.06 (0.66; 1.80)	< 0.01	0.25	0.58
	2013	0.91	1.36	< 0.01	1.18 (0.86; 1.52)	< 0.001	0.10	
Spike DW (g)	2012	0.023	0.045	< 0.01	0.031 (0.015; 0.047)	< 0.001	0.005	0.84
	2013	0.029	0.045	< 0.01	0.036 (0.022; 0.057)	< 0.001	0.003	
Biomass per shoot (g)	2012[b]	1.20	1.35	> 0.05	1.39 (1.04; 1.83)	< 0.001	0.16	0.58
	2013	1.40	2.10	< 0.01	1.83 (1.41; 2.40)	< 0.001	0.13	
Total leaf DW (%)	2012	24.5	29.0	> 0.05	26.7 (20.1; 35.2)	< 0.001	2.8	0.58
	2013	33.1	32.9	> 0.05	33.5 (27.5; 39.4)	< 0.001	1.2	
Stem DW (%)	2012	63.5	60.3	> 0.05	61.9 (47.4; 69.4)	< 0.001	4.4	0.58
	2013	64.8	64.9	> 0.05	64.6 (59.2; 70.1)	< 0.001	1.1	
Spike DW (%)	2012	1.9	3.3	< 0.01	2.3 (1.1; 4.2)	< 0.001	0.3	0.80
	2013	2.1	2.2	> 0.05	2.0 (1.1; 2.8)	< 0.001	0.2	
Total leaf area (cm^2)	2012	102	156	> 0.05	108 (56; 181)	< 0.05	28	0.31
	2013	87	119	< 0.01	108 (81; 137)	< 0.001	8	
SLA of total leaf ($cm^2\ g^{-1}$)	2012	245	225	> 0.05	235 (184; 280)	< 0.05	18	0.58
	2013	189	172	> 0.05	178 (136; 210)	< 0.001	9	
At anthesis								
Flag leaf DW (g)	2012	0.19	0.16	> 0.05	0.18 (0.11; 0.26)	< 0.01	0.03	0.73
	2013	0.11	0.18	< 0.01	0.17 (0.10; 0.24)	< 0.001	0.01	
Remaining leaf DW (g)	2012	0.30	0.47	< 0.01	0.37 (0.17; 0.46)	< 0.001	0.05	0.63
	2013	0.42	0.51	< 0.01	0.48 (0.36; 0.65)	< 0.001	0.03	
Total leaf DW (g)	2012	0.49	0.63	< 0.05	0.55 (0.28; 0.70)	< 0.001	0.07	0.71
	2013	0.53	0.69	< 0.01	0.65 (0.46; 0.86)	< 0.001	0.04	
Stem DW (g)	2012	1.76	2.40	< 0.01	2.09 (0.96; 2.60)	< 0.001	0.19	0.58
	2013	1.89	2.42	< 0.01	2.26 (1.82; 2.82)	< 0.001	0.14	
Stem WSC (g)	2012	0.46	0.68	< 0.05	0.46 (0.16; 0.74)	< 0.001	0.10	0.51
	2013	0.54	0.57	> 0.05	0.59 (0.30; 0.85)	< 0.001	0.11	

Supplementary Table S4-1 (continued)

Trait	Year	Parental lines			RILs			H^2
		Forno	Oberkulmer	P-value	Mean (min; max)	P-value	S.E.D.	
Structural stem DW (g)	2012	1.30	1.72	< 0.05	1.63 (0.80; 2.10)	< 0.001	0.17	0.62
	2013	1.35	1.86	< 0.01	1.67 (1.26; 2.14)	< 0.001	0.13	
Spike DW (g)	2012	0.46	0.68	< 0.01	0.58 (0.33; 0.78)	< 0.001	0.07	0.77
	2013	0.45	0.70	< 0.01	0.60 (0.40; 0.81)	< 0.001	0.03	
Spikelet DW (g)	2012	0.020	0.032	< 0.01	0.027 (0.017; 0.037)	< 0.001	0.003	0.76
	2013	0.022	0.034	< 0.01	0.028 (0.019; 0.041)	< 0.001	0.002	
Spike fertility index (grains g^{-1})	2012	88	49	< 0.01	65 (39; 91)	< 0.001	10	0.69
	2013	85	52	< 0.01	68 (50; 93)	< 0.001	6	
Biomass per shoot (g)	2012	2.70	3.72	< 0.01	3.22 (1.57; 4.03)	< 0.001	0.32	0.62
	2013	2.87	3.81	< 0.01	3.51 (2.74; 4.47)	< 0.001	0.19	
Flag leaf DW (%)	2012	7.0	4.4	< 0.01	5.7 (4.1; 9.1)	< 0.05	0.9	0.43
	2013	3.9	4.8	< 0.05	4.7 (3.2; 6.2)	< 0.001	0.34	
Remaining leaf DW (%)	2012	10.9	12.7	> 0.05	11.4 (6.9; 13.9)	< 0.001	0.9	0.66
	2013	14.6	13.4	< 0.05	13.7 (11.6; 16.0)	< 0.001	0.5	
Total leaf DW (%)	2012	17.9	17.1	> 0.05	17.1 (12.0; 20.9)	< 0.001	1.2	0.69
	2013	18.6	18.1	> 0.05	18.4 (15.7; 21.5)	< 0.001	0.6	
Stem DW (%)	2012	65.1	64.7	> 0.05	64.9 (59.9; 70.1)	< 0.001	1.5	0.74
	2013	65.9	63.5	< 0.05	64.6 (58.1; 69.8)	< 0.001	0.8	
Stem WSC (%)	2012	17.2	18.3	> 0.05	14.3 (8.8; 20.1)	< 0.01	2.8	0.43
	2013	18.7	14.9	> 0.05	16.9 (8.9; 24.0)	< 0.001	2.9	
Structural stem DW (%)	2012	47.9	46.4	> 0.05	50.6 (43.5; 56.9)	< 0.01	3.0	0.43
	2013	47.2	48.7	> 0.05	47.7 (40.1; 56.2)	< 0.001	2.8	
Spike DW (%)	2012	17.0	18.2	> 0.05	18.0 (15.1; 21.1)	< 0.001	0.9	0.80
	2013	15.5	18.3	< 0.01	17.0 (12.7; 21.9)	< 0.001	0.5	
Spike:structual stem	2012	0.36	0.39	> 0.05	0.36 (0.28; 0.46)	< 0.001	0.03	0.76
	2013	0.33	0.38	> 0.05	0.36 (0.26; 0.50)	< 0.001	0.03	
Flag leaf area (cm^2)	2012	32.5	27.4	> 0.05	30.1 (18.2; 42.2)	< 0.001	4.2	0.61
	2013	15.6	28.4	< 0.01	25.2 (14.7; 36.3)	< 0.001	1.8	
Remaining leaf area (cm^2)	2012	36.2	62.3	< 0.05	61.5 (35.1; 107.3)	< 0.001	11.1	0.46
	2013	83.9	99.7	< 0.05	91.3 (67.4; 118.4)	< 0.001	6.9	
Total leaf area (cm^2)	2012	54.0	83.9	< 0.05	86.6 (54.6; 146.6)	< 0.001	13.2	0.53
	2013	99.5	128.1	< 0.01	116.5 (84.2; 153.2)	< 0.001	7.6	
SLA of flag leaf (cm^2 g^{-1})	2012	172	167	> 0.05	167 (116; 192)	< 0.001	9.3	0.46
	2013	138.0	156.6	< 0.01	151.7 (134.6; 167.7)	< 0.001	6.4	
SLA of remaining leaf (cm^2 g^{-1})	2012	233	245	> 0.05	249 (200; 515)	< 0.001	26	0.51
	2013	200	196	> 0.05	191 (161; 231)	< 0.001	10	
SLA of total leaf (cm^2 g^{-1})	2012	206	221	> 0.05	223 (180; 295)	< 0.001	19	0.56
	2013	187	185	> 0.05	181 (157; 211)	< 0.001	8	
Flag leaf angle (scores)	2012	2.0	3.0	< 0.01	2.0 (1.0; 3.0)	< 0.001	0.3	0.61
	2013	2.0	3.0	< 0.01	2.5 (1.0; 3.0)	< 0.001	0.3	

Supplementary Table S4-1 (continued)

Trait	Year	Parental lines			RILs			H^2
		Forno	Oberkulmer	P-value	Mean (min; max)	P-value	S.E.D.	
At maturity								
Flag leaf DW (g)	2013	0.07	0.09	> 0.05	0.09 (0.05; 0.14)	< 0.001	0.01	0.83
Remaining leaf DW (g)	2013	0.14	0.19	< 0.01	0.17 (0.12; 0.24)	< 0.001	0.02	0.55
Total leaf DW (g)	2012	0.25	0.29	> 0.05	0.29 (0.19; 0.38)	< 0.001	0.03	0.75
	2013	0.21	0.27	< 0.05	0.26 (0.17; 0.37)	< 0.001	0.02	
Stem DW (g)	2012	1.00	1.27	< 0.01	1.21 (0.89; 1.63)	< 0.001	0.10	0.73
	2013	1.09	1.53	< 0.01	1.41 (0.99; 1.83)	< 0.001	0.11	
Chaff DW (g)	2012	0.44	0.75	< 0.01	0.62 (0.32; 1.00)	< 0.001	0.08	0.80
	2013	0.44	0.69	< 0.01	0.62 (0.26; 0.86)	< 0.001	0.06	
Flag leaf DW (%)	2013	2.1	2.1	> 0.05	2.2 (1.5; 3.0)	< 0.001	0.2	0.64
Remaining leaf DW (%)	2013	3.9	4.5	< 0.05	4.2 (3.4; 5.0)	< 0.001	0.3	0.44
Total leaf DW (%)	2012	10.4	9.4	> 0.05	9.8 (7.4; 12.3)	< 0.001	0.9	0.58
	2013	5.9	6.6	> 0.05	6.4 (5.2; 7.9)	< 0.001	0.4	
Stem DW (%)	2012	41.2	41.3	> 0.05	41.5 (35.2; 50.9)	< 0.001	3.0	0.65
	2013	30.5	37.3	< 0.01	34.5 (29.7; 43.8)	< 0.001	1.1	
Chaff DW (%)	2012	18.1	24.8	< 0.01	21.2 (13.7; 31.3)	< 0.001	2.4	0.55
	2013	12.2	17.0	< 0.01	15.1 (7.9; 18.5)	< 0.001	1.0	
Plant height (cm)	2012	81	111	< 0.01	100 (77; 123)	< 0.001	6	0.81
	2013	75	111	< 0.01	95 (73; 119)	< 0.001	4	
Crop and spike growth								
ADM (GS39−Anthesis) (g)	2012	1.50	2.37	< 0.05	1.83 (0.45; 2.59)	< 0.001	0.37	0.33
	2013	1.48	1.71	> 0.05	1.68 (1.04; 2.36)	< 0.001	0.23	
CGR (GS39−Anthesis) ($g\ ^oCd^{-1}$)	2012	0.0055	0.0097	< 0.05	0.0073 (0.0018; 0.0108)	< 0.001	0.0017	0.28
	2013	0.0055	0.0061	> 0.05	0.0060 (0.0036; 0.0078)	< 0.001	0.0009	
ADM (Anthesis−Maturity) (g)	2012	0.55	0.52	> 0.05	0.50 (0.00; 1.17)	< 0.001	0.22	0.37
	2013	0.71	0.28	> 0.05	0.64 (0.00; 1.41)	< 0.001	0.30	
CGR (Anthesis−Maturity) ($g\ ^oCd^{-1}$)	2012	0.0007	0.0007	> 0.05	0.0006 (0.0000; 0.0017)	< 0.001	0.0003	0.32
	2013	0.0011	0.0004	> 0.05	0.0010 (0.0000; 0.0021)	< 0.05	0.0005	
Spike DW at GS33 (g)	2012	0.0053	0.0029	< 0.05	0.0035 (0.0011; 0.0083)	< 0.001	0.0011	0.77
	2013	0.0077	0.0026	< 0.05	0.0041 (0.0012; 0.0111)	< 0.001	0.0018	
Spike growth rate ($g\ ^oCd^{-1}$)	2012	0.0016	0.0026	< 0.01	0.0022 (0.0012; 0.0029)	< 0.001	0.0003	0.60
	2013	0.0016	0.0023	< 0.01	0.0020 (0.0014; 0.0026)	< 0.001	0.0001	

Supplementary Table S4-1 (continued)

Trait	Year	Parental lines			RILs			H^2
		Forno	Oberkulmer	P-value	Mean (min; max)	P-value	S.E.D.	
Dry matter translocation (DMT)								
Flag leaf DMT (g)	2013	0.04	0.10	< 0.01	0.08 (0.04; 0.12)	< 0.001	0.01	0.52
Remaining leaf DMT (g)	2013	0.28	0.32	> 0.05	0.31 (0.22; 0.44)	< 0.001	0.04	0.45
Total leaf DMT (g)	2012	0.23	0.35	> 0.05	0.26 (0.09; 0.46)	< 0.001	0.06	0.35
	2013	0.32	0.42	< 0.05	0.38 (0.26; 0.52)	< 0.001	0.04	
Flag leaf DMTE (%)	2013	34.7	52.5	< 0.01	45.1 (28.7; 59.5)	< 0.001	5.6	0.16
Remaining leaf DMTE (%)	2013	67.1	63.6	> 0.05	64.0 (53.2; 74.3)	< 0.001	4.1	0.16
Total leaf DMTE (%)	2012	47.6	53.5	> 0.05	47.0 (30.5; 70.6)	< 0.05	7.5	0.27
	2013	60.2	60.7	> 0.05	59.3 (49.0; 71.2)	< 0.001	3.8	
CDMT of flag leaf (%)	2013	2.1	6.0	< 0.01	4.2 (1.8; 6.5)	< 0.001	0.9	0.33
CDMT of remaining leaf (%)	2013	15.3	20.5	< 0.05	17.3 (11.4; 28.7)	< 0.001	2.5	0.38
CDMT of total leaf (%)	2012	16.8	26.4	< 0.05	18.8 (8.8; 38.2)	< 0.001	4.4	0.36
	2013	17.5	26.4	< 0.01	21.5 (14.3; 34.8)	< 0.001	3.2	
CDMT of stem WSC (%)	2012	30.3	49.3	< 0.01	32.2 (16.4; 47.0)	< 0.001	6.9	0.48
	2013	29.2	35.6	> 0.05	33.5 (16.1; 69.5)	< 0.001	7.1	
De-graining treatment								
Potential grain weight (mg)	2013	50.0	47.3	> 0.05	48.5 (38.9; 57.0)	< 0.001	2.1	0.73
Extra assimilate use (mg grain^{-1})	2013	1.5	3.4	> 0.05	3.5 (-7.2; 10.9)	< 0.001	2.5	0.55
Yield components within spike								
TGW (basal spikelet, g)	2012	37.6	38.2	> 0.05	40.1 (27.1; 51.9)	< 0.001	4.0	0.59
TGW (central spikelet, g)	2012	37.6	39.7	> 0.05	40.6 (28.5; 52.9)	< 0.001	3.7	0.65
TGW (apical spikelet, g)	2012	27.3	42.6	< 0.01	35.6 (22.1; 48.9)	< 0.001	3.8	0.63
TGW (G1, g)	2012	39.3	42.2	> 0.05	40.0 (28.5; 52.9)	< 0.001	2.9	0.74
TGW (G2, g)	2012	36.1	45.2	< 0.01	42.4 (27.9; 52.4)	< 0.001	3.3	0.70
TGW (G3, g)	2012	28.8	23.4	> 0.05	32.1 (0.0; 46.6)	< 0.001	4.2	0.63
Grains per basal spikelet	2012	1.2	0.9	> 0.05	1.2 (0.4; 1.9)	< 0.001	0.2	0.37
Grains per central spikelet	2012	2.4	2.1	> 0.05	2.2 (1.6; 2.9)	< 0.001	0.2	0.39
Grains per apical spikelet	2012	1.7	1.5	> 0.05	1.7 (1.0; 2.1)	< 0.001	0.2	0.59
Grains per floret (G1)	2012	0.79	0.75	> 0.05	0.76 (0.53; 0.88)	< 0.001	0.06	0.45
Grains per floret (G2)	2012	0.76	0.68	> 0.05	0.73 (0.52; 0.87)	< 0.001	0.06	0.47
Grains per floret (G3)	2012	0.22	0.08	> 0.05	0.19 (0.0; 0.51)	< 0.001	0.09	0.43
YP (basal spikelet, %)	2012	25.7	15.3	< 0.05	23.3 (12.0; 32.9)	< 0.001	4.8	0.34
YP (central spikelet, %)	2012	50.3	52.2	> 0.05	48.3 (40.8; 59.0)	< 0.001	3.7	0.22
YP (apical spikelet, %)	2012	24.0	32.4	< 0.05	28.4 (18.3; 35.8)	< 0.001	4.0	0.30
YP (G1, %)	2012	47.1	49.6	> 0.05	45.3 (34.2; 54.5)	< 0.001	3.7	0.52
YP (G2, %)	2012	41.8	47.6	< 0.05	45.7 (39.8; 53.3)	< 0.001	2.4	0.26
YP (G3, %)	2012	9.8	2.8	> 0.05	8.9 (0.0; 23.5)	< 0.001	4.7	0.45

[a] Abbreviations of the traits: TGW, thousand grain weight; DW, dry weight; SLA, specific leaf area; WSC, water soluble carbohydrate; ADM, accumulated dry matter; CGR, crop growth rate; GS33, the time when the third stem node is just detectable. DMTE, dry matter translocation efficiency; CDMT, contribution of dry matter translocation to yield; G1−G3, Grain 1 to Grain 3 within spikelets counting from the rachis; YP, yield partitioning within spikes.

[b] Data derived from five main shoots.

[c] S.E.D., standard error of the difference of means.

[d] H^2, broad sense heritability.

Supplementary Table S4-2 Correlations among plant organs at GS39 (flag leaf ligule emergence)

Biomass trait[a]	Total leaf DW	Stem DW	Spike DW	Biomass per shoot	Total leaf DW (%)	Stem DW (%)	Spike DW (%)
Total leaf DW[b]	1	0.81**	0.24*	0.91**	0.56**	-0.08	-0.03
Stem DW	0.68**	1	0.24*	0.98**	0.05	0.39**	-0.05
Spike DW	0.03	0.22*	1	0.25*	0.05	-0.05	0.83**
Biomass per shoot	0.87**	0.95**	0.18	1	0.22	0.26*	-0.30**
Total leaf DW (%)	0.64**	-0.12	-0.22*	0.19*	1	-0.37**	0.01
Stem DW (%)	-0.59**	0.18	0.11	-0.13	-0.99**	1	-0.06
Spike DW (%)	-0.50**	-0.36**	0.80**	-0.43**	-0.34**	0.20*	1

[a] Shaded matrix: 2012 season; unshaded matrix: 2013 season.
[b] DW, dry weight.
* Significant at P < 0.05, ** significant at P < 0.01.

Supplementary Table S4-3 Correlations among plant organs at anthesis (dry weight)

Biomass trait[a]	Flag leaf	Remaining leaf	Total leaf	Stem	Stem WSC	Structural stem	Spike	Biomass per shoot
Flag leaf	1	0.34**	0.64**	0.46**	0.32**	0.42**	0.48**	0.53**
Remaining leaf	0.70**	1	0.94**	0.71**	0.57**	0.61**	0.62**	0.79**
Total leaf	0.87**	0.96**	1	0.75**	0.59**	0.65**	0.69**	0.84**
Stem	0.48**	0.70**	0.67**	1	0.70**	0.92**	0.75**	0.98**
Stem WSC[b]	0.04	0.36**	0.26**	0.55**	1	0.36**	0.53**	0.70**
Structural stem	0.56**	0.60**	0.63**	0.83**	0.00	1	0.68**	0.89**
Spike	0.76**	0.67**	0.76**	0.54**	0.09	0.60**	1	0.84**
Biomass per shoot	0.71**	0.84**	0.86**	0.94**	0.44**	0.83**	0.78**	1

[a] Shaded matrix: 2012 season; unshaded matrix: 2013 season.
[b] WSC, water soluble carbohydrate.
* Significant at P < 0.05, ** significant at P < 0.01.

Supplementary Table S4-4 Correlations among plant organs at anthesis (dry weight proportion, %)

Biomass trait[a]	Biomass per shoot	Flag leaf	Remaining leaf	Total leaf	Stem	Stem WSC	Structural stem	Spike
Biomass per shoot	1	-0.32**	0.11	-0.09	0.26*	0.32**	-0.13	-0.27*
Flag leaf	0.31**	1	-0.16	0.45**	-0.44**	-0.17	-0.12	0.15
Remaining leaf	-0.06	0.23*	1	0.81**	-0.49**	0.05	-0.35**	-0.13
Total leaf	0.13	0.74**	0.82**	1	-0.70**	-0.06	-0.39**	-0.03
Stem	-0.18	-0.76**	-0.47**	-0.76**	1	0.23*	0.42**	-0.69**
Stem WSC[b]	-0.03	-0.43**	-0.04	-0.27**	0.45**	1	-0.78**	-0.26*
Structural stem	-0.11	-0.12	-0.32**	-0.29**	0.29**	-0.72**	1	-0.20
Spike	0.17	0.53**	0.06	0.35**	-0.87**	-0.45**	-0.20*	1

[a] Shaded matrix: 2012 season; unshaded matrix: 2013 season.
[b] WSC, water soluble carbohydrate.
* Significant at P < 0.05, ** significant at P < 0.01.

Supplementary Table S4-5 Correlations among plant organs at maturity (dry weight)

Biomass trait[a]	Flag leaf	Remaining leaf	Total leaf	Stem	Grain	Chaff	Biomass per shoot
Flag leaf	1	–[b]	–	–	–	–	–
Remaining leaf	0.72**	1	–	–	–	–	–
Total leaf	0.91**	0.93**	1	0.44**	0.43**	0.48**	0.72**
Stem	0.57**	0.70**	0.69**	1	0.38**	0.32**	0.83**
Grain	0.65**	0.66**	0.71**	0.52**	1	0.37**	0.66**
Chaff	0.78**	0.76**	0.83**	0.62**	0.71**	1	0.56**
Biomass per shoot	0.78**	0.83**	0.87**	0.81**	0.90**	0.87**	1

[a] Shaded matrix: 2012 season; unshaded matrix: 2013 season.
[b] Data absent.
* Significant at P < 0.05, ** significant at P < 0.01.

Supplementary Table S4-6 Correlations among plant organs at maturity (dry weight proportion, %)

Biomass trait[a]	Biomass per shoot	Flag leaf	Remaining leaf	Total leaf	Stem	Grain	Chaff
Biomass per shoot	1	–[b]	–	-0.15	-0.13	0.13	0.00
Flag leaf	0.40**	1	–	–	–	–	–
Remaining leaf	0.03	0.22*	1	–	–	–	–
Total leaf	0.26**	0.78**	0.78**	1	-0.42**	-0.09	0.16
Stem	-0.27**	-0.31**	0.06	-0.17	1	-0.35**	-0.36**
Grain	-0.04	-0.12	-0.31**	-0.26**	-0.74**	1	-0.71**
Chaff	0.44**	0.45**	0.15	0.37**	-0.40**	-0.29**	1

[a] Shaded matrix: 2012 season; unshaded matrix: 2013 season.
[b] Data absent.
* Significant at P < 0.05, ** significant at P < 0.01.

Supplementary Table S4-7 Correlations of grain number and grain weight among different positions within spikes in 2012

	Basal spikelet	Central spikelet		Grain 1	Grain 2
Grain number					
Central spikelet	0.53**		Grain 2	0.58**	
Apical spikelet	0.33**	0.63**	Grain 3	0.40**	0.53**
Grain weight					
Central spikelet	0.80**		Grain 2	0.84**	
Apical spikelet	0.72**	0.80**	Grain 3	0.41**	0.53**

* Significant at P < 0.05, ** significant at P < 0.01.

Supplementary Table S4-8 Significant correlations between biomass at different growth stages and yield components within spikes

Biomass trait[a]	Thousand grain weight						Grain number					
	Basal	Central	Apical	Grain 1	Grain 2	Grain 3	Basal	Central	Apical	Grain 1	Grain 2	Grain 3
At GS39												
Total leaf DW	0.26*	0.23*	0.36**	0.21	0.35**	0.13	0.00	-0.03	0.04	0.13	-0.09	0.00
Stem DW	0.31**	0.30**	0.41**	0.34**	0.37**	0.08	-0.03	-0.07	-0.12	0.00	-0.20	-0.01
Biomass per shoot	0.21	0.17	0.30**	0.21	0.32**	0.02	-0.03	0.18	0.03	0.06	-0.15	0.18
Total leaf DW (%)	-0.02	-0.01	0.00	-0.13	0.08	0.19	0.13	0.12	0.30**	0.25*	0.16	0.15
At anthesis												
Flag leaf DW	0.24*	0.26*	0.21	0.17	0.33**	0.21	0.12	0.20	0.11	0.10	-0.03	0.27*
Remaining leaf DW	0.29*	0.28*	0.30**	0.19	0.36**	0.25*	0.22	0.08	0.13	0.28*	0.07	0.14
Total leaf DW	0.33**	0.32**	0.32**	0.23	0.42**	0.29*	0.22	0.14	0.14	0.26*	0.04	0.21
Stem DW	0.32**	0.28*	0.42**	0.30*	0.40**	0.16	0.17	0.07	-0.07	0.17	-0.11	0.11
Stem WSC	0.34**	0.38**	0.50**	0.37**	0.49**	0.28*	0.22	0.19	0.01	0.20	-0.04	0.22
Structural stem DW	0.24*	0.17	0.27*	0.18	0.25*	0.06	0.10	-0.02	-0.09	0.11	-0.12	0.03
Spike DW	0.07	0.00	0.10	-0.08	0.12	0.11	0.24*	0.27*	0.1	0.24*	0.11	0.25*
Biomass per shoot	0.30**	0.26*	0.37**	0.23*	0.38**	0.19	0.20	0.12	0.00	0.22	-0.05	0.17
Total leaf DW (%)	0.11	0.15	-0.02	0.02	0.15	0.21	0.05	0.06	0.25*	0.11	0.13	0.12
Stem DW (%)	0.23*	0.25*	0.37**	0.41**	0.23*	-0.02	-0.05	-0.21	-0.29*	-0.05	-0.27*	-0.19
Stem WSC (%)	0.28*	0.35**	0.45**	0.37**	0.42**	0.24*	0.15	0.16	0.03	0.15	-0.04	0.17
Structural stem DW (%)	-0.12	-0.17	-0.18	-0.09	-0.25*	-0.24*	-0.17	-0.29*	-0.21	-0.18	-0.14	-0.28*
Spike DW (%)	-0.42**	-0.50**	-0.49**	-0.58**	-0.47**	-0.18	0.02	0.24*	0.15	-0.03	0.25*	0.14
At maturity												
Total leaf DW	0.36**	0.35**	0.42**	0.29*	0.46**	0.25*	0.10	0.20	0.09	0.16	-0.08	0.20
Stem DW	0.32**	0.28*	0.35**	0.32**	0.37**	0.10	-0.07	0.07	0.01	0.01	-0.23*	0.09
Grain DW	0.40**	0.48**	0.40**	0.39**	0.60**	0.45**	0.64**	0.55**	0.44**	0.65**	0.39**	0.61**
Chaff DW	0.00	-0.04	0.06	-0.19	0.14	0.12	0.24*	0.31**	0.37**	0.36**	0.23*	0.32**
Biomass per shoot	0.42**	0.40**	0.46**	0.38**	0.54**	0.24*	0.12	0.24*	0.13	0.21	-0.11	0.28*
Stem DW (%)	-0.11	-0.15	-0.13	-0.04	-0.22	-0.18	-0.30**	-0.25*	-0.20	-0.32**	-0.21	-0.25*
Grain DW (%)	0.34**	0.38**	0.30**	0.48**	0.33**	0.13	0.06	0.01	-0.21	-0.05	-0.17	0.02
Chaff DW (%)	-0.27*	-0.29*	-0.22	-0.46**	-0.18	0.00	0.19	0.19	0.38**	0.32**	0.35**	0.19
ADM (GS39−Anthesis)	0.23	0.21	0.26*	0.15	0.26*	0.21	0.25*	0.04	-0.02	0.22	0.03	0.09
CGR (GS39−Anthesis)	0.29*	0.32**	0.33**	0.26*	0.34**	0.28*	0.26*	-0.04	-0.06	0.18	0.01	0.04
Spike growth rate	0.21	0.18	0.22	0.10	0.27*	0.25*	0.27*	0.14	0.02	0.22	0.07	0.18

[a] Abbreviations of the traits: DW, dry weight; WSC, water soluble carbohydrate; ADM, accumulated dry matter; CGR, crop growth rate; GS39, the time when flag leaf ligule is just visible.
* Significant at $P < 0.05$, ** significant at $P < 0.01$.

Chapter 5

Early Anthesis and Delayed but Fast Leaf Senescence Contribute to Individual Grain Dry Matter and Water Accumulation in Wheat

5.1 Abstract

The physiological process of how anthesis time and leaf senescence patterns affect wheat yield still remains unclear. In this study, a mapping population of bread wheat (Triticum aestivum L.) and spelt (Triticum spelta L.) contrasting for phasic development and leaf senescence kinetics was used to understand the physiological and genetic relationships among anthesis time, leaf senescence, grain filling processes, and individual grain weight (a major yield determinant after anthesis). Earlier anthesis and delayed leaf senescence were associated with larger grains. Furthermore, early anthesis and delayed but fast leaf senescence promoted grain filling rate (but shortening its duration), grain water absorption rate and maximum grain water content, while grain dry matter and water accumulation displayed strong relationships with grain weight. Frequent quantitative trait locus coincidences between these traits were observed on chromosomes 2A, 3B, 4A, 4DL, 5A, 5B, 5DL and 7B. Analysis of allelic effects confirmed the above physiological relationships. Therefore, anthesis time and leaf senescence affect grain weight at least partly through their effects on grain dry matter and water accumulation, resulting from pleiotropy or tight gene linkages. Slightly early anthesis, and delayed but fast leaf senescence, can be used to maximise grain weight and yield potential in wheat.

Keywords: Anthesis; grain filling; grain water; grain weight; leaf senescence; quantitative trait locus; spelt; wheat

5.2 Introduction

Anthesis, or flowering, in plants is a process of fertilising and setting seeds or fruits, and marks a shift from vegetative to reproductive growth. In wheat, anthesis is a key event during plant life cycle, as it defines the beginning of grain growth and yield formation. Anthesis date in wheat is flexible, which allows it to be cultivated in diverse environments in the world, from South America and southern Oceania to North America and northern Europe and Asia, and from sea level to c. 3000 m (Slafer and Whitechurch, 2001). For a given genotype, however, an appropriate anthesis date is needed to match its regional environment for adaption. In addition, fine-tuning of this time is also important to maximise grain yield. It has been found that the growth period immediately before anthesis, during which floret death occurs, coinciding with rapid spike growth, determines floret fertility and in turn grain number at maturity (Fischer, 1985; Slafer and Rawson, 1994; González et al., 2011). This critical period also overlaps with the ovary development in florets, and consequently affects individual grain weight (Calderini et al., 1999). Immediately after fertilisation, endosperm cell division and enlargement take place (Briarty et al., 1979; Shewry et al., 2012), which largely determine final grain weight (Brocklehurst, 1977; Lizana et al., 2010). Therefore, optimising the timing of anthesis can contribute to grain yield potential. On the other hand, wheat production is highly sensitive to environmental changes during the period at and around anthesis. Drought and high temperature during this time, for example, reduce yield (8–30%) and yield components (grain number and size) (Lizana and Calderini, 2013; Semenov et al., 2014). These effects can be true in global warming scenarios, where an increase in frequency of heat stress around anthesis has been predicted in Europe (Semenov et al., 2014). A potential strategy to adapt wheat for climate change is earlier anthesis, by escaping excessive temperature and drought through rapid development. Earliness may also work for wheat growing areas with terminal drought (Izanloo et al., 2008; Lopes and Reynolds, 2011), and with short growing seasons (Iqbal et al., 2007). Under normal field conditions, shortening the duration from sowing to anthesis may reduce plant biomass, but this can be compensated by increased harvest index; as a result, high or comparable grain yield are produced, depending on their genetic combinations and environments (Foulkes et al., 2004; Iqbal et al., 2007; Addisu et al., 2010; McIntyre et al., 2010).

In terms of genetic systems controlling anthesis time, there are mainly three groups of genes: vernalisation genes (Vrn), photoperiod sensitivity genes (Ppd), and earliness per se genes (Eps). Vrn1 encodes a MADS box transcription factor homologous to the AP1 of Arabidopsis thaliana (Alonso-Blanco et al., 2009), controls vernalisation response and promotes anthesis. Vrn2 encodes a putative transcription factor with a CCT domain, and represses Vrn1 through Vrn3 that encodes a long-distance flowering signal. Vrn1 in turn represses Vrn2, forming a feedback regulatory loop among Vrn genes (Alonso-Blanco et al., 2009; Brown et al., 2013). Ppd1 encoding a pseudoresponse regulator responds to long photoperiod, and promotes Vrn2 and Vrn3 (Brown et al., 2013). These sensitivity genes for vernalisation and photoperiod coordinately regulate each phase from sowing to anthesis. In contrast, Eps affects developmental rate independently of environmental signals, and many quantitative trait loci (QTL) have been determined (Snape et al., 2001).

From anthesis onwards, grain growth commences, coinciding with leaf senescence. Leaves are the major sites for current photosynthesis, which, together with the preanthesis reserves, supplies assimilates for grain filling. Leaf senescence kinetics during grain filling can be divided into two phases: full functionality and rapid senescence (Wu et al., 2012). Delayed onset of senescence with longer functional photosynthesis (stay-green) produces more assimilates for developing grains, and thus has potential to maximise grain yield. In fact, higher crop productivity has been well documented to be associated with delayed senescence, for example, in wheat (Verma et al., 2004; Christopher et al., 2008; Bogard et al., 2011; Gaju et al., 2011; Derkx et al., 2012), and other crops as reviewed by Gregersen et al. (2013). Stay-green phenotype is more advantageous when wheat plants grow under stressed conditions during the postanthesis period such as high temperature, drought, elevated ozone, nutrient deficits (e.g. nitrogen) and disease infections, where grain yield is more prone to be source-limited (Gelang et al., 2000; Joshi et al., 2007; Christopher et al., 2008; Gaju et al., 2011). A few exceptions of stay-green trait with decreased yield performance have also been observed (Sykorova et al., 2008; Naruoka et al., 2012; Kipp et al., 2014); thus, yield gain from stay-green may depend on genotypic and environmental effects. Rapid senescence is the final stage of leaf life cycle. Senesing leaves at this stage display yellowing and loss of photosynthetic capacity, proceeding from lamina tips to the bases close to stems. This process has been considered as a

form of programmed cell death (Gan and Amasino, 1997), and plays an important role in nutrient recycling. During senescence, chloroplasts are broken down; chlorophyll, proteins (e.g. Rubisco), membrane lipids and other macromolecules are then degraded, so that the resultant nutrients can be transported into growing grains. In particular, the remobilisation of nitrogen in forms of glutamate, aspartate, threonine, serine and glutamine from senesing leaves greatly contributes to grain protein concentration at maturity (Distelfeld et al., 2014; Gaju et al., 2014). It has been demonstrated that the functional Gpc-1 (NAM-1) genes confer wheat cultivars or lines earlier senescence, efficient nutrient remobilisation from leaves, and in turn higher grain protein and micronutrient (iron and zinc) contents; however, they reduce grain yield under some environments (Uauy et al., 2006; Distelfeld et al., 2014). Delayed leaf senescence favours grain yield improvement, but not nutrient use efficiency, a dilemma of senescence in wheat breeding (Gregersen et al., 2008). Therefore, optimising leaf senescence kinetics is needed to make better use of current photosynthetic capacity and degraded nutrients.

Grain yield is a complex trait, influenced by genetic and environmental factors. To understand the physiology of yield, grain yield is usually divided into two components: grain number and individual grain weight. Grain number is mainly determined by floret fertility within spikes before anthesis, whereas grain weight depends on the ovary growth prior to anthesis and grain filling thereafter. During the postanthesis period, yield potential is thus determined by individual grain development. Although many studies have demonstrated the direct phenotypic relationships between anthesis dates, leaf senescence and yield, the physiological processes and genetic basis underlying these relationships remain unknown. The present study aimed to understand how anthesis time and leaf senescence affected individual grain development during the postanthesis period in detail. A mapping population of bread wheat and spelt with contrasting phasic development and leaf senescence kinetics was used, and then the variation in anthesis time, the onset and progression of leaf senescence, grain dry matter accumulation, grain water uptake and loss, and final grain weight, was quantified. Physiological and genetic relationships between these processes were established, resulting in a trait interaction model, which can be used to build a wheat ideotype with appropriate anthesis and leaf senescence patterns for breeding.

5.3 Materials and methods

Details of plant materials, field conditions, statistical analysis of phenotypic data and QTL identification have been described previously in the section of **Materials and methods** of **Chapter 2**.

5.3.1 Anthesis dates

A spike was judged as flowering when the first anthers were exserted from the middle spikelets. Anthesis date of a plot was recorded when 50% of the spikes started flowering. Evaluation was carried out every day until all plots finished flowering. Calendar dates of anthesis were then converted into accumulated thermal time (degree days, ^{o}Cd). Temperature data was obtained from the nearby meteorological station. Daily thermal time was calculated as the average of maximum and minimum air temperature (or the base temperature 0^{o}C, whichever was higher).

5.3.2 Leaf senescence

Leaf senescence was assessed based on flag leaves, using two approaches: green area (GA) loss and chlorophyll (chl) loss, at a 5-day interval from anthesis onwards in both seasons. GA of the flag leaves in a plot was rated visually using a scale from 10 (0% yellowing) to 0 (100% yellowing) (Pask and Pietragalla, 2012). Meanwhile, the chl concentrations of flag leaves were non-destructively measured using a chlorophyll meter (SPAD 502, Minolta, USA). For each plot, measurements were taken on five healthy, clean leaves, three points along each leaf (one third, half and two thirds, avoiding the midrib and major veins). The average of 15 readings was recorded, and expressed as chlorophyll concentration index (CCI; ranging from 0 to 99.9).

Data of GA and chl loss of flag leaves were then fitted over the accumulated thermal time after anthesis using the Gompertz growth curve (Fig. 5-1) (Gooding et al., 2000).

$$G = A + C\mathrm{e}^{-\mathrm{e}^{-B(t-M)}}$$

where G is the visual scores or SPAD readings; A and (A + C) are the lower and upper asymptotes, respectively; B is the relative senescence rate at the time M; M is the accumulated thermal time when senescence rate is at maximum and when visual scores or SPAD readings decline to (A + 0.37C); and t is the accumulated thermal time after anthesis.

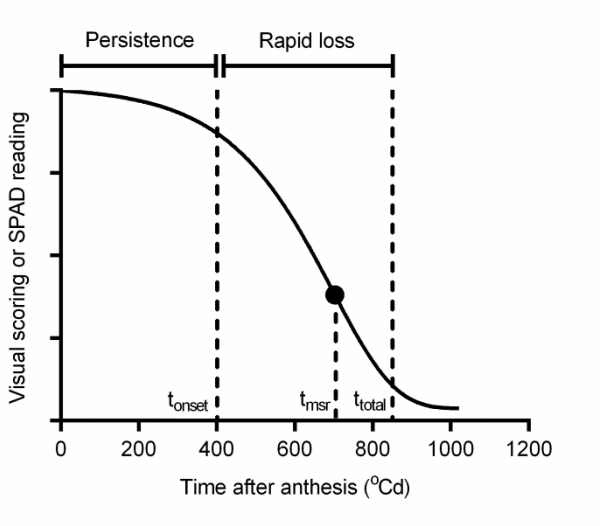

Fig. 5-1 Gompertz growth curve fitting for flag leaf senescence. Total duration of flag leaves (t_{total}) is defined as the period from anthesis to the time when 90% of the green area (visual scoring) or chlorophyll (SPAD reading) has been lost (90% senescence). t_{total} is then divided into two phases: persistence and rapid loss. Duration of leaf persistence (t_{onset}) is from anthesis to the time at 10% senescence, while the duration of leaf rapid loss is from t_{onset} to t_{total}. The closed circle on the curve indicates the maximum senescence rate (msr). The base temperature 0°C was used to calculate the accumulated thermal time from anthesis.

Total duration of flag leaves (t_{total}; GA_{tot} or Chl_{tot}) was defined as the period from anthesis to the time at 90% senescence. t_{total} consisted of two components: persistence phase (GA_{per} or Chl_{per}), from anthesis to t_{onset} (the onset of senescence, 10% senescence), and rapid loss phase (GA_{loss} or Chl_{loss}), from t_{onset} to t_{total} (Fig. 5-1). When t = M, maximum senescence rate (MSR), i.e. maximum GA loss rate (Max GALR) or maximum chl loss rate (Max CLR), was reached, and calculated as MSR = BC/e (e = 2.718). Area under the Gompertz curve from anthesis to t_{total} was also calculated as a measure of total flag leaf greenness of a genotype, and termed accumulated GA (GA_{accum}) or chl content (Chl_{accum}). In addition, maximum chl concentration (Max chl) was derived from the upper asymptote of the curve (A + C).

5.3.3 Grain dry matter and water accumulation

From anthesis onwards, young grains were sampled every five days to quantify the dynamics of grain dry matter and water accumulation. Five main spikes at anthesis and maturity, and two spikes during grain filling, were collected; two middle spikelets of each spike in 2012, and three spikelets of one side of each spike in 2013 (the third one from the base, the third one from the tip and the middle one between the two spikelets), were dissected for grains using forceps. All grains were then weighed for

fresh weight, and dried in an oven at 85^{o}C for 48 h, and weighed again for dry weight. Water content of individual grains was calculated as the difference between fresh and dry weight.

Data of grain dry weight was then fitted over the accumulated thermal time after anthesis using the logistic growth curve (Zahedi and Jenner, 2003; Wang et al., 2009).

$$W_{\mathrm{d}} = A + \frac{C}{1 + \mathrm{e}^{-B(t-M)}}$$

where W_d is the dry weight of individual grains, A is the lower asymptote, (A + C) is the upper asymptote (i.e. final grain weight), B is the doubled relative growth rate at the time M, M is the accumulated thermal time when grain filling rate (GFR) is at maximum and when grains grow at (A + 0.5C), and t is the accumulated thermal time after anthesis.

Grain filling (GF) duration (GFD) was defined as the period from anthesis to the time when grain weight reached (A + 0.99C), and calculated as: GFD = M + 4.5951/B. This duration was then divided equally into three phases: initial, rapid and late, which correspond to the timing of endosperm cell division and enlargement, rapid grain filling, and maturation, respectively (Shewry et al., 2012). Average GFR of each phase and across all three phases were calculated. Onset of GF (OGF), when grain weight reached (A + 0.05C), was calculated as: OGF = M – 2.9444/B. At the time M (t_{max}), maximum GFR (MGFR) was derived from MGFR = BC/4.

Water content of individual grains was fitted over the accumulated thermal time after anthesis using a cubic function.

$$W_{\mathrm{W}} = b_3 t^3 + b_2 t^2 + b_1 t + a$$

where W_w is the grain water content, t is the accumulated thermal time after anthesis, b_3, b_2, b_1 and a are coefficients.

When $dW_w/dt = 0$, $W_w = W_{max}$ (maximum water content, MWC), $t = t_{mwc}$ (the time at maximum water content),

$$W_{\max} = b_3 t_{\mathrm{mwc}}^3 + b_2 t_{\mathrm{mwc}}^2 + b_1 t_{\mathrm{mwc}} + a$$

$$t_{\mathrm{mwc}} = \frac{-b_2 - \sqrt{b_2^2 - 3b_1 b_3}}{3b_3}$$

Average water absorption rate (WAR) of grains from anthesis to t_{mwc}, and water loss rate (WLR) from t_{mwc} to the time for last measurement, were also calculated.

5.3.4 Grain weight at maturity

All the plots of 226 RILs and parents were combined at maturity using a harvester (2010, Sampo Rosenlew, Finland). Grain samples were threshed by a thresher again and completed by hand, because of low threshability derived from spelt. For each plot, 200 grains were dried in an oven at 85^{o}C for 48 h to calculate thousand grain weight (TGW).

5.4 Results

5.4.1 Large phenotypic variation between the parents and between the RILs in anthesis dates, flag leaf senescence, grain filling traits, and grain weight

Anthesis was later in spelt Oberkulmer than in bread wheat Forno over years (Supplementary Table S5-1). Compared with Forno, Oberkulmer had shorter persistence phases of flag leaves (GA_{per} and Chl_{per}), longer phases of rapid GA and chl loss (GA_{loss} and Chl_{loss}), and longer total duration of senescence (GA_{tot} and Chl_{tot}) (Fig. 5-2 and Supplementary Table S5-1); that is, Oberkulmer started rapid senescence earlier but finished later. This is consistent using two evaluation approaches (visual scoring and SPAD) in both years. Accordingly, maximum senescence rate (Max GALR and Max CLR) was lower in Oberkulmer than in Forno. GA_{accum} was higher in Oberkulmer; however, Chl_{accum} was comparable in both parents. In addition, significant differences between the parental lines in grain filling traits and grain weight were found, indicating great genetic distance between two species. As expected, the contrasting parents resulted in large variation of RILs in all traits observed (Supplementary Table S5-1), which enabled further physiological and genetic analyses. H^2 varied among different traits: relatively higher in anthesis dates, Chl_{per}, rapid and average GFR, MWC, WAR, and TGW ($H^2 > 0.70$), but lower in Chl_{loss}, initial and late GFR, the onset and duration of GF, and t_{mwc} ($H^2 < 0.40$), suggesting different genetic and environmental control (Supplementary Table S5-1).

5.4.2 Significant physiological relationships between anthesis dates and flag leaf senescence

Earlier anthesis was associated with longer GA_{per} and Chl_{per} (delayed onset of senescence), shorter GA_{loss} and Chl_{loss}, and faster Max GALR and Max CLR (Table 5-1). In 2012, anthesis date was negatively associated with GA_{accum} and Chl_{accum}, but not in 2013. A positive relationship between anthesis dates and Max chl was found.

5.4.3 Anthesis dates and flag leaf senescence showed relationships with final grain weight

Correlation analysis revealed a negative relationship between anthesis dates and grain weight (Table 5-2), indicating that earlier anthesis contributed to larger grains. Longer GA_{per} and Chl_{per}, rather than GA_{loss} and Chl_{loss}, were significantly associated with larger grains. In 2012, final grain weight was negatively associated with Chl_{loss}, but

positively associated with Max CLR. GA_{accum} and Chl_{accum} showed positive associations with final grain weight in both years.

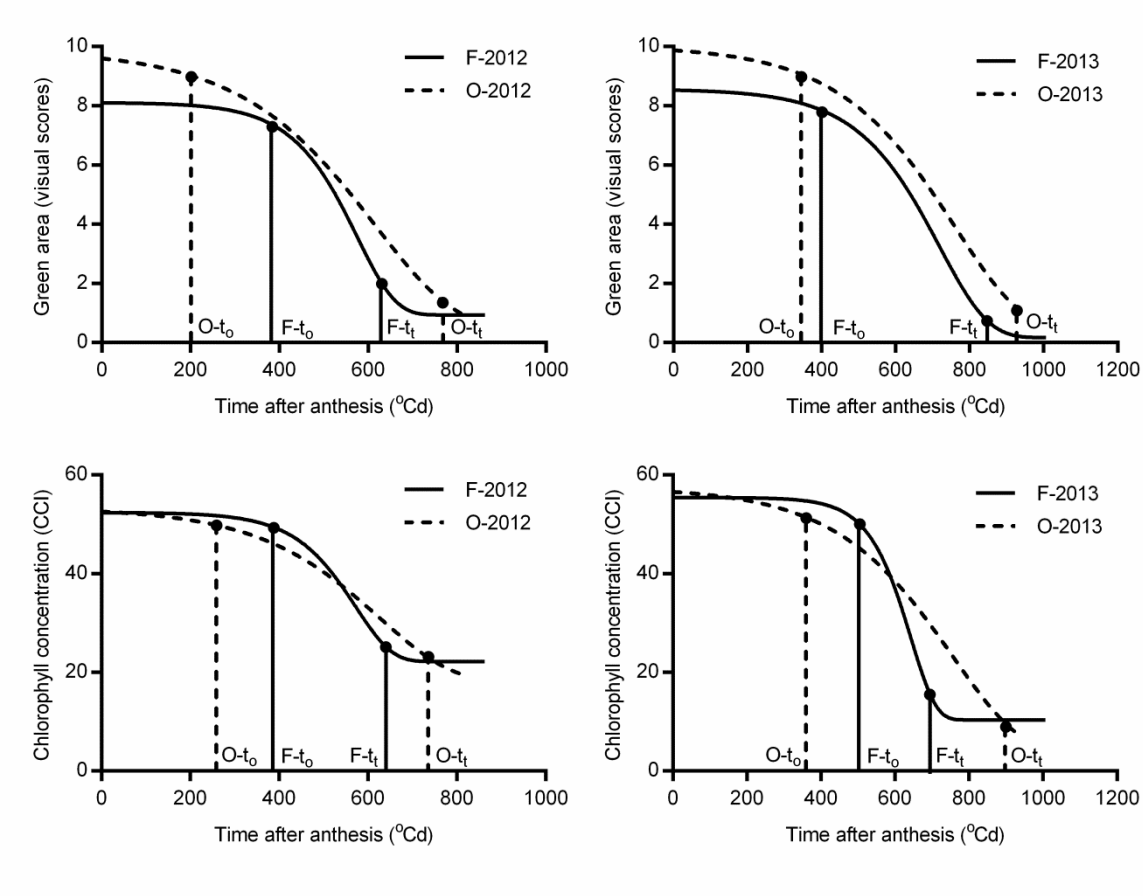

Fig. 5-2 Flag leaf senescence of bread wheat Forno and spelt Oberkulmer. Data of the green area and chlorophyll loss of flag leaves are fitted over the accumulated thermal time after anthesis in 2012 and 2013, using the Gompertz growth curve. Abbreviations: F, Forno; O, Oberkulmer; t_o (t_{onset}), onset of leaf senescence; and t_t (t_{total}), total duration of flag leaves. The base temperature 0°C was used to calculate the accumulated thermal time from anthesis.

Table 5-1 Phenotypic correlations between anthesis dates and flag leaf senescence

Trait[a]	Anthesis date		Trait	Anthesis date	
	2012	2013		2012	2013
GA_{per}	-0.40**[b]	-0.41**	Chl_{per}	-0.57**	-0.16
GA_{loss}	0.14	0.43**	Chl_{loss}	0.41**	0.26**
GA_{tot}	-0.18	0.29**	Chl_{tot}	-0.29*	0.23*
Max GALR	-0.25*	-0.39**	Max chl	0.17	0.35**
GA_{accum}	-0.51**	-0.04	Max CLR	-0.34**	-0.10
			Chl_{accum}	-0.55**	0.19*

[a] Trait abbreviations: GA_{per}, duration of green area persistence; GA_{loss}, duration of rapid green area loss; GA_{tot}, total duration of green area persistence and loss; Max GALR, maximum green area loss rate; GA_{accum}, accumulated green area; Chl_{per}, duration of chlorophyll persistence; Chl_{loss}, duration of rapid chlorophyll loss; Chl_{tot}, total duration of chlorophyll persistence and loss; Max chl, maximum chlorophyll content; Max CLR, maximum chlorophyll loss rate; and Chl_{accum}, accumulated chlorophyll content.
[b] * Significant at $P < 0.05$, ** significant at $P < 0.01$.

Table 5-2 Phenotypic correlations between anthesis dates, flag leaf senescence, and final grain weight

Trait[a]	Grain weight		Trait	Grain weight	
	2012	2013		2012	2013
Anthesis	-0.25*[b]	-0.32**	Chl_{per}	0.49**	0.21*
GA_{per}	0.33**	0.26**	Chl_{loss}	-0.44**	-0.08
GA_{loss}	0.02	-0.09	Chl_{tot}	0.10	0.03
GA_{tot}	0.32**	0.09	Max chl	0.03	0.12
Max GALR	0.08	0.00	Max CLR	0.39**	0.10
GA_{accum}	0.45**	0.37**	Chl_{accum}	0.34**	0.25**

[a] Trait abbreviations defined as in Table 5-1.
[b] * Significant at $P < 0.05$, ** significant at $P < 0.01$.

5.4.4 Anthesis dates showed relationships with grain dry matter and water accumulation

To understand how anthesis dates affected final grain weight, the relationships between anthesis dates and grain filling processes were analysed (Table 5-3). As a result, anthesis dates were negatively associated with GFR (initial, rapid, late, average, and maximum), and with MWC and WAR, indicating that earlier anthesis contributed to grain dry matter and water accumulation. In 2013, there were positive relationships between anthesis dates, GF duration, t_{max} and t_{mwc}, indicating earlier anthesis accelerated the progress of grain filling and shortened its duration.

Table 5-3 Phenotypic correlations between anthesis dates and grain filling traits

Grain filling[a]	Anthesis date		Grain filling	Anthesis date	
	2012	2013		2012	2013
Initial GFR	-0.16	0.00	GF duration	-0.05	0.35**
Rapid GFR	-0.18	-0.49**[b]	t_{max}	-0.09	0.21*
Late GFR	-0.16	-0.40**	MWC	-0.36**	-0.53**
Average GFR	-0.20	-0.50**	WAR	-0.41**	-0.60**
Max GFR	-0.18	-0.49**	WLR	0.22	-0.02
Onset of GF	-0.07	-0.19*	t_{mwc}	0.13	0.39**

[a] Trait abbreviations: GFR, grain filling rate; GF, grain filling; t_{max}, the time at maximum grain filling rate; MWC, maximum water content of grains; WAR, water absorption rate of grains; WLR, water loss rate of grains; and t_{mwc}, the time at maximum water content.

[b] * Significant at $P < 0.05$, ** significant at $P < 0.01$.

5.4.5 Flag leaf senescence showed relationships with grain dry matter and water accumulation

To understand how flag leaf senescence affected final grain weight, the relationships between flag leaf senescence and grain filling processes were analysed (Tables 5-4 and 5-5). It was found that GA_{per} and Chl_{per} were positively associated with GFR (rapid, late, average, and maximum), and with MWC and WAR, indicating that longer persistence of flag leaves (delayed onset of senescence) was associated with increased grain dry matter and water accumulation. Additionally, GA_{loss} and Chl_{loss} showed negative relationships with GFR and grain water accumulation, but the opposite was true for Max GALR and Max CLR, suggesting that shorter duration and accordingly faster rate of rapid senescence led to more effective dry matter synthesis and water uptake of grains. Meanwhile, shorter duration and faster rate of rapid senescence accelerated the progress of grain filling (t_{max} and t_{mwc}) and shortened its duration mainly in 2013. Max chl did not affect grain filling traits except WLR, which was positively associated with Max chl. GA_{accum} and Chl_{accum} showed positive associations with GFR and grain water accumulation in 2012, but did not in 2013.

Table 5-4 Phenotypic correlations between green area loss of flag leaves and grain filling traits

Grain filling[a]	GA_{per}		GA_{loss}		GA_{tot}		Max GALR		GA_{accum}	
	2012	2013	2012	2013	2012	2013	2012	2013	2012	2013
Initial GFR	0.06	0.01	-0.10	0.04	-0.07	0.07	0.23*	-0.14	0.06	0.14
Rapid GFR	0.34**[b]	0.34**	-0.02	-0.34**	0.28*	-0.21*	0.07	0.33**	0.46**	0.06
Late GFR	0.35**	0.30**	-0.02	-0.34**	0.27*	-0.25**	0.05	0.36**	0.44**	-0.06
Average GFR	0.34**	0.36**	-0.04	-0.36**	0.25*	-0.22*	0.12	0.31**	0.45**	0.07
Max GFR	0.35**	0.35**	-0.03	-0.37**	0.27*	-0.24**	0.08	0.36**	0.46**	0.01
Onset of GF	0.27*	0.09	0.12	-0.10	0.38**	-0.08	-0.16	0.19*	0.41**	0.00
GF duration	-0.09	-0.24**	0.08	0.41**	0.02	0.40**	-0.07	-0.40**	-0.10	0.28**
t_{max}	0.07	-0.18	0.15	0.35**	0.24*	0.38**	-0.17	-0.27**	0.13	0.31**
MWC	0.35**	0.31**	-0.04	-0.27**	0.26*	-0.13	0.13	0.19*	0.50**	0.20*
WAR	0.27*	0.36**	-0.16	-0.40**	0.04	-0.30**	0.27*	0.31**	0.34**	0.02
WLR	0.21	0.06	0.06	0.07	0.26*	0.15	-0.07	-0.09	0.27*	0.29**
t_{mwc}	0.15	-0.23*	0.22	0.45**	0.41**	0.48**	-0.27*	-0.37**	0.28*	0.38**

[a] Trait abbreviations: GFR, grain filling rate; GF, grain filling; t_{max}, the time at maximum grain filling rate; MWC, maximum water content of grains; WAR, water absorption rate of grains; WLR, water loss rate of grains; t_{mwc}, the time at maximum water content; GA_{per}, duration of green area persistence; GA_{loss}, duration of rapid green area loss; GA_{tot}, total duration of green area persistence and loss; Max GALR, maximum green area loss rate; and GA_{accum}, accumulated green area.
[b] * Significant at $P < 0.05$, ** significant at $P < 0.01$.

Table 5-5 Phenotypic correlations between chlorophyll degradation of flag leaves and grain filling traits

Grain filling[a]	Chl_{per}		Chl_{loss}		Chl_{tot}		Max chl		Max CLR		Chl_{accum}	
	2012	2013	2012	2013	2012	2013	2012	2013	2012	2013	2012	2013
Initial GFR	0.12	0.06	-0.21	-0.06	-0.14	-0.03	-0.18	0.17	0.24*	0.02	-0.10	0.15
Rapid GFR	0.45**[b]	0.18	-0.37**	-0.25**	0.15	-0.21*	0.05	-0.08	0.32**	0.24**	0.36**	-0.02
Late GFR	0.42**	0.13	-0.33**	-0.22*	0.17	-0.19*	0.11	-0.12	0.26*	0.22*	0.40**	-0.12
Average GFR	0.45**	0.20*	-0.39**	-0.29**	0.12	-0.23*	0.02	-0.03	0.35**	0.27**	0.33**	0.00
Max GFR	0.45**	0.18	-0.37**	-0.26**	0.15	-0.22*	0.07	-0.09	0.32**	0.26**	0.37**	-0.06
Onset of GF	0.34**	0.00	-0.18	0.02	0.27*	0.03	0.17	-0.16	0.13	0.02	0.43**	-0.08
GF duration	-0.06	-0.12	0.08	0.36**	0.04	0.38**	0.10	0.22*	-0.02	-0.30**	0.02	0.28**
t_{max}	0.13	-0.13	-0.02	0.42**	0.20	0.45**	0.21	0.10	0.05	-0.31**	0.27*	0.23*
MWC	0.54**	0.18	-0.48**	-0.19*	0.12	-0.13	0.04	0.08	0.43**	0.15	0.41**	0.11
WAR	0.45**	0.17	-0.49**	-0.31**	-0.04	-0.29**	-0.06	0.00	0.44**	0.23*	0.25*	-0.06
WLR	0.22	0.08	-0.19	0.04	0.06	0.10	0.27*	0.24**	0.19	0.01	0.20	0.29**
t_{mwc}	0.14	-0.10	0.02	0.44**	0.28*	0.50**	0.22	0.13	0.00	-0.30**	0.29*	0.36**

[a] Trait abbreviations: GFR, grain filling rate; GF, grain filling; t_{max}, the time at maximum grain filling rate; MWC, maximum water content of grains; WAR, water absorption rate of grains; WLR, water loss rate of grains; t_{mwc}, the time at maximum water content; Chl_{per}, duration of chlorophyll persistence; Chl_{loss}, duration of rapid chlorophyll loss; Chl_{tot}, total duration of chlorophyll persistence and loss; Max chl, maximum chlorophyll content; Max CLR, maximum chlorophyll loss rate; and Chl_{accum}, accumulated chlorophyll content.
[b] * Significant at $P < 0.05$, ** significant at $P < 0.01$.

5.4.6 Close relationships between grain filling processes and final grain weight

Grain weight at maturity was closely associated with GFR (initial, rapid, late, average, and maximum), rather than GF duration (Table 5-6), indicating the importance of dry matter synthesis efficiency. Similarly, there were strong relationships between final grain weight and grain water accumulation (MWC, WAR, and WLR) across years. Furthermore, correlation analysis also revealed a strong relationship between MWC and average GFR ($r = 0.91$, $P < 0.01$ in 2012; $r = 0.88$, $P < 0.01$ in 2013).

Table 5-6 Phenotypic correlations between grain filling traits and final grain weight

Grain filling[a]	Grain weight		Grain filling	Grain weight	
	2012	2013		2012	2013
Initial GFR	0.53**[b]	0.44**	GF duration	0.18	0.11
Rapid GFR	0.77**	0.63**	t_{max}	0.42**	0.08
Late GFR	0.64**	0.32**	MWC	0.84**	0.83**
Average GFR	0.83**	0.76**	WAR	0.60**	0.66**
Max GFR	0.76**	0.58**	WLR	0.68**	0.75**
Onset of GF	0.40**	-0.03	t_{mwc}	0.47**	0.11

[a] Trait abbreviations: GFR, grain filling rate; GF, grain filling; t_{max}, the time at maximum grain filling rate; MWC, maximum water content of grains; WAR, water absorption rate of grains; WLR, water loss rate of grains; and t_{mwc}, the time at maximum water content.

[b] * Significant at $P < 0.05$, ** significant at $P < 0.01$.

5.4.7 QTL coincidences explained the relationships between anthesis dates, flag leaf senescence, grain filling traits, and grain weight

A total of 118 significant QTL were identified in the mapping population of Forno × Oberkulmer in two years, including six QTL for anthesis dates, 24 for flag leaf senescence, 69 for grain filling traits, and 19 for grain weight (Fig. 5-3 and Table 5-7). These QTL individually explained 6.5−37.0% of the phenotypic variation, and were located on 17 chromosomes.

QTL coincidences among anthesis dates, flag leaf senescence, grain filling traits, and grain weight occurred (Fig. 5-3). Four QTL for anthesis dates were coincident with those for Chl_{per}, Max CLR, average GFR, MWC, WAR, and grain weight on chromosomes 4DL, 5A, and 7B (Fig. 5-3 and Table 5-8). In addition, a QTL for anthesis dates was also linked with two QTL for grain weight on the other region of 5A. These coincident or linked QTL had increasing alleles conferred by the opposite parents (either Forno or Oberkulmer), indicating that earlier anthesis (decreasing alleles) contributed to Chl_{per}, Max CLR, average GFR, MWC, WAR, and grain weight, due to pleiotropy or tight gene linkages. In contrast, three QTL for anthesis dates were

coincident with two QTL for Chl_{loss}, with the increasing alleles from the same parents, explaining their positive physiological relationship.

Three of four QTL for GA_{per} were coincident with six QTL for rapid GFR, two for late GFR, six for average GFR, four for max GFR, six for MWC, three for WAR, four for WLR, and five for grain weight on chromosomes 2A, 4A, and 7B; their increasing alleles originated from the same parents (Fig. 5-3 and Table 5-9), consistent with the positive relationships between them. Similarly, Chl_{per} had two QTL coincident with GFR (rapid, late, average, and max), grain water accumulation (MWC, WAR, and WLR), and final grain weight on chromosomes 4A (all increasing alleles derived from Oberkulmer) and 5A (increasing alleles from Forno) (Fig. 5-3 and Table 5-10). Additionally, another QTL for Chl_{per} was linked with one QTL for grain weight, and one for MWC on 2B, and Oberkulmer conferred their increasing alleles. On the other hand, Chl_{loss} showed QTL coincidences with GFR, grain water accumulation, and grain weight on 4A and 7B, but had increasing alleles conferred by the opposite parents (Fig. 5-3 and Table 5-11). Six QTL were identified for Max CLR, and five of them coincident with GFR, grain water accumulation, and final grain weight on 3A, 4A and 7B, with the increasing alleles from the same parents except those on 3A (Fig. 5-3 and Table 5-12). These QTL coincidences confirmed the physiological relationships between flag leaf senescence, and grain filling processes, and grain weight at maturity.

A total of 27 (84% of the total) QTL for GFR and 27 (82%) for grain water uptake and loss coincided with those for grain weight, and all the increasing alleles were conferred by the same parents (Fig. 5-3), explaining the close relationships between grain filling processes and final grain weight. Most of the QTL for average GFR (83% of the total) and for MWC (87%) were coincident, confirming their strong physiological relationship.

Taken together, earlier anthesis was associated with delayed onset of flag leaf senescence, shorter duration and faster rate of rapid senescence, which led to faster grain dry matter accumulation, faster grain water absorption, and higher maximum grain water content; as a consequence, larger grains were produced (Fig. 5-4). This physiological model is consistent with the genetic analysis showing a high level of QTL coincidences, suggesting pleiotropy or tight linkages of functionally related genes.

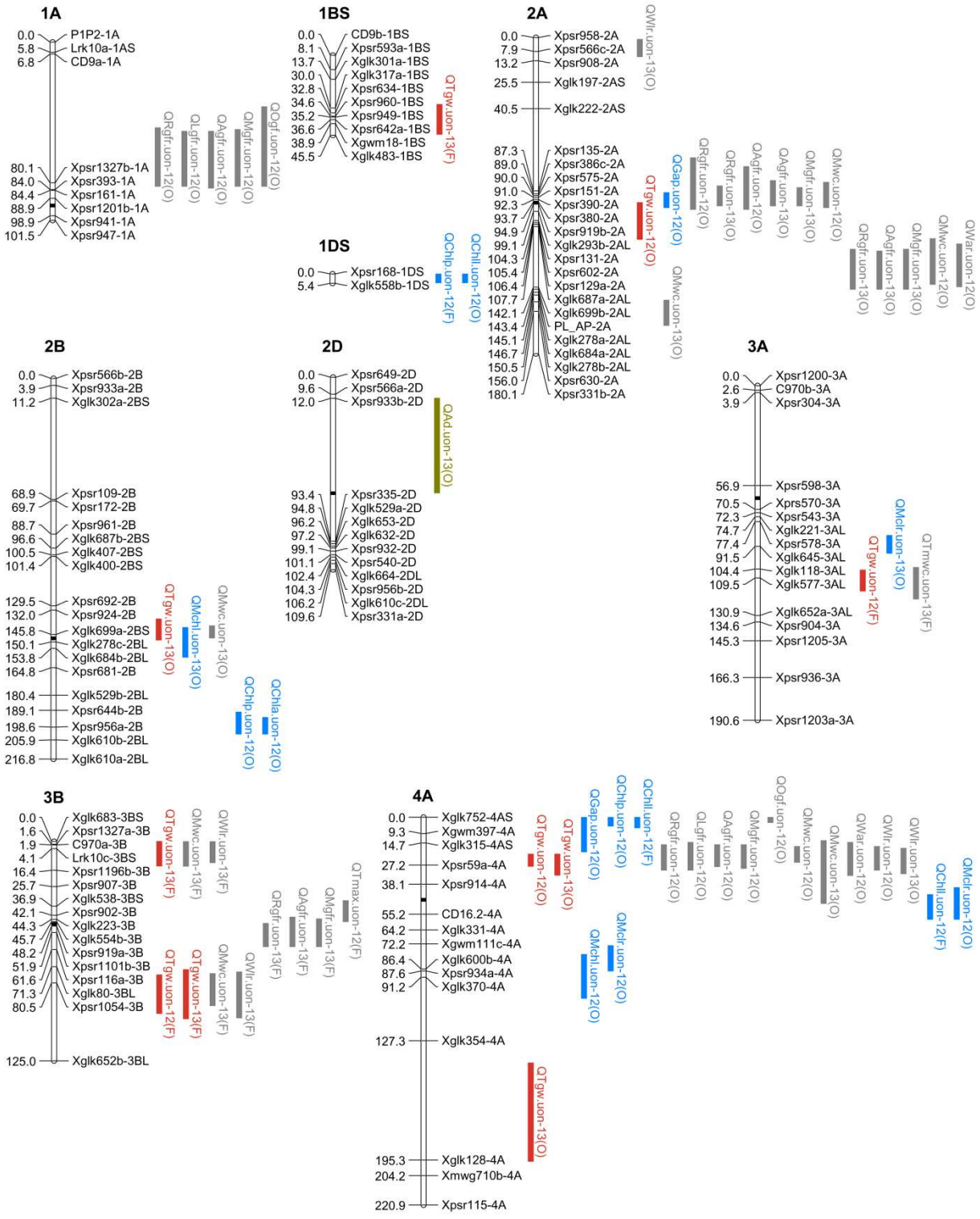

Fig. 5-3 (see the caption below)

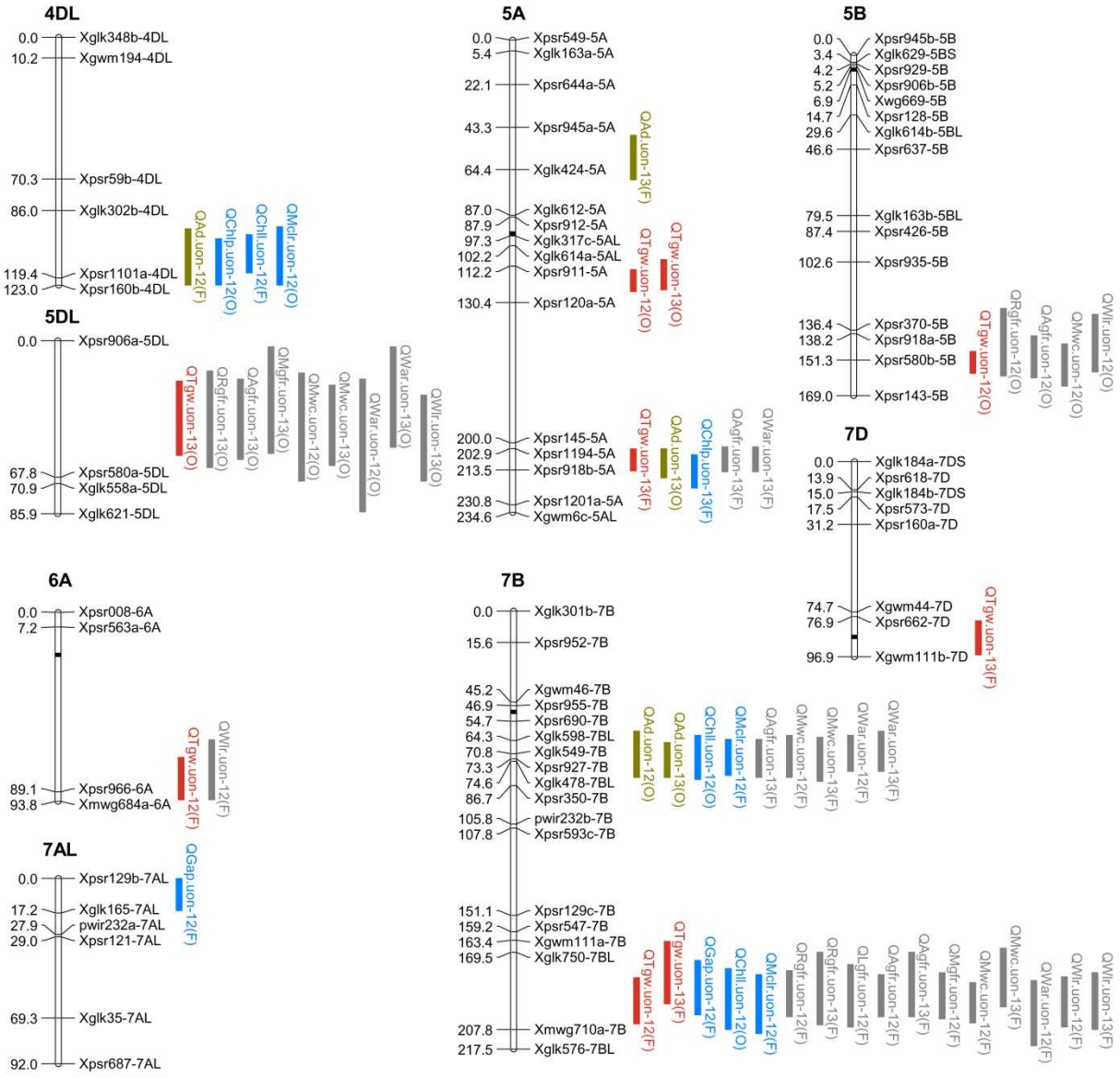

Fig. 5-3 QTL identification for anthesis dates, flag leaf senescence, grain filling traits, and final grain weight. The 1-LOD support intervals of significant QTL are indicated by red (grain weight), green (anthesis dates), blue (flag leaf senescence), and grey (grain filling traits) vertical bars. A QTL symbol includes a letter 'Q', trait abbreviation, laboratory name (uon), a suffix 12 or 13 indicating 2012 or 2013 in which the QTL was detected, and the parents in parentheses conferring the increasing alleles (increasing the values of the traits): F, bread wheat Forno; O, spelt Oberkulmer. Trait abbreviations: Tgw, thousand grain weight; Ad, anthesis date; Gap, duration of green area persistence; Chlp, duration of chlorophyll persistence; Chll, duration of rapid chlorophyll loss; Mchl, maximum chlorophyll content; Mclr, maximum chlorophyll loss rate; Chla, accumulated chlorophyll content; Rgfr, rapid grain filling rate; Lgfr, late grain filling rate; Agfr, average grain filling rate; Mgfr, maximum grain filling rate; Ogf, onset of grain filling; Tmax, the time at maximum grain filling rate; Mwc, maximum water content of grains; War, water absorption rate of grains; Wlr, water loss rate of grains; and Tmwc, the time at maximum water content.

Table 5-7 QTL identification for anthesis dates, flag leaf senescence, grain filling traits, and grain weight in the mapping population of bread wheat × spelt

Trait[a]/Chromosome	Year	Position (cM)	LOD	R^{2b}	Additive effect[c]	Closest marker
Anthesis date (^{o}Cd)						
2D	2013	45.9	3.7	14.3	-24.3	Xpsr933b-2D
4DL	2012	107.0	3.1	18.4	15.1	Xpsr1101a-4DL
5A	2013	58.3	3.8	14.8	13.3	Xglk424-5A
	2013	209.9	3.9	15.1	-12.0	Xpsr918b-5A
7B	2012	77.6	4.9	27.9	-15.8	Xglk478-7BL
	2013	77.6	4.5	17.1	-12.9	Xglk478-7BL
Flag leaf senescence						
GA_{per} (^{o}Cd)						
2A	2012	94.9	4.1	23.9	-40.0	Xpsr919b-2A
4A	2012	1.0	5.2	29.0	-47.3	Xglk752-4AS
7AL	2012	4.0	3.2	19.3	43.5	Xpsr129b-7AL
7B	2012	187.5	4.3	24.5	59.7	Xglk750-7BL
Chl_{per} (^{o}Cd)						
1DS	2012	1.0	3.3	19.3	58.7	Xpsr168-1DS
2B	2012	196.1	3.0	18.2	-57.7	Xpsr956a-2B
4A	2012	0.1	3.4	20.1	-61.1	Xglk752-4AS
4DL	2012	108.0	4.9	27.5	-92.1	Xpsr1101a-4DL
5A	2013	213.4	3.2	12.5	16.5	Xpsr918b-5A
Chl_{loss} (^{o}Cd)						
1DS	2012	0.1	3.2	19.1	-56.0	Xpsr168-1DS
4A	2012	0.1	3.4	20.3	60.0	Xglk752-4AS
	2012	51.1	4.6	26.0	72.4	CD16.2-4A
4DL	2012	106.0	5.1	28.6	94.6	Xpsr1101a-4DL
7B	2012	70.7	3.1	18.7	-56.9	Xglk549-7B
	2012	191.5	3.8	22.1	-87.4	Xmwg710a-7B
Max chl (CCI)						
2B	2013	147.8	3.7	14.4	-0.89	Xglk699a-2BS
4A	2012	88.6	5.1	28.4	-1.1	Xpsr934a-4A
Max CLR (CCI $^{o}Cd^{-1}$)						
3A	2013	91.5	3.2	12.7	-0.054	Xglk645-3AL
4A	2012	50.1	3.5	20.5	-0.018	CD16.2-4A
	2012	80.2	4.0	23.2	-0.019	Xglk600b-4A
4DL	2012	106.0	3.1	18.4	-0.021	Xpsr1101a-4DL
7B	2012	70.7	3.7	21.7	0.0166	Xglk549-7B
	2012	194.5	3.5	20.4	0.0220	Xmwg710a-7B
Chl_{accum} (CCI)						
2B	2012	198.6	3.2	18.9	-1155	Xpsr956a-2B

[a] Trait abbreviations: GA_{per}, duration of green area persistence; Chl_{per}, duration of chlorophyll persistence; Chl_{loss}, duration of rapid chlorophyll loss; Max chl, maximum chlorophyll content; Max CLR, maximum chlorophyll loss rate; Chl_{accum}, accumulated chlorophyll content; GFR, grain filling rate; GF, grain filling; t_{max}, the time at maximum grain filling rate; MWC, maximum water content of grains; WAR, water absorption rate of grains; WLR, water loss rate of grains; t_{mwc}, the time at maximum water content; TGW, thousand grain weight; CCI, chlorophyll concentration index.

[b] R^2: the proportion of phenotypic variation explained by individual QTL.

[c] Positive additive effects indicate that the alleles from Forno increase the values of the traits, whereas negative additive effects indicate that the alleles from Oberkulmer increase the values of the traits.

Table 5-7 (continued)

Trait/Chromosome	Year	Position (cM)	LOD	R^2	Additive effect	Closest marker
Grain filling traits						
Rapid GFR (mg $^oCd^{-1}$)						
1A	2012	80.1	3.9	22.9	-0.0076	Xpsr1327b-1A
2A	2012	94.9	3.1	18.3	-0.0067	Xpsr919b-2A
	2013	90.9	3.6	13.9	-0.0051	Xpsr151-2A
	2013	132.6	4.2	16.2	-0.0074	Xglk699b-2AL
3B	2013	54.9	4.4	16.7	0.0063	Xpsr1101b-3B
4A	2012	21.7	4.9	27.8	-0.0097	Xpsr59a-4A
5B	2012	147.2	3.1	18.2	-0.0073	Xpsr580b-5B
5DL	2013	38.0	3.6	14.0	-0.0109	Xpsr580a-5DL
7B	2012	190.5	5.0	28.0	0.0123	Xmwg710a-7B
	2013	188.5	3.1	12.3	0.0073	Xglk750-7BL
Late GFR (mg $^oCd^{-1}$)						
1A	2012	80.1	4.0	23.3	-0.0023	Xpsr1327b-1A
4A	2012	21.7	3.9	22.4	-0.0027	Xpsr59a-4A
7B	2012	190.5	3.6	21.1	0.0033	Xmwg710a-7B
Average GFR (mg $^oCd^{-1}$)						
1A	2012	80.1	3.5	20.5	-0.0033	Xpsr1327b-1A
2A	2012	94.9	3.6	21.2	-0.0033	Xpsr919b-2A
	2013	90.9	4.2	16.1	-0.0024	Xpsr151-2A
	2013	132.6	4.5	17.2	-0.0034	Xglk699b-2AL
3B	2013	53.9	3.8	14.9	0.0026	Xpsr1101b-3B
4A	2012	21.7	5.9	32.6	-0.0048	Xpsr59a-4A
5A	2013	206.9	3.2	12.6	0.0025	Xpsr1194-5A
5B	2012	149.2	3.2	19.0	-0.0033	Xpsr580b-5B
5DL	2013	38.0	4.5	17.2	-0.0054	Xpsr580a-5DL
7B	2012	190.5	5.6	30.9	0.0059	Xmwg710a-7B
	2013	76.6	3.6	13.9	0.0026	Xglk478-7BL
	2013	186.5	3.5	13.5	0.0034	Xglk750-7BL
Max GFR (mg $^oCd^{-1}$)						
1A	2012	80.1	3.9	22.6	-0.0089	Xpsr1327b-1A
2A	2013	90.9	3.5	13.5	-0.0066	Xpsr151-2A
	2013	133.6	3.6	14.1	-0.0089	Xglk699b-2AL
3B	2013	54.9	4.1	15.7	0.0080	Xpsr1101b-3B
4A	2012	21.7	5.1	28.7	-0.0116	Xpsr59a-4A
5DL	2013	34.0	3.3	13.0	-0.0140	Xpsr580a-5DL
7B	2012	190.5	4.8	27.4	0.0143	Xmwg710a-7B
Onset of GF (^oCd)						
1A	2012	60.8	3.3	19.5	-20	Xpsr1327b-1A
4A	2012	0.1	3.6	21.0	-12	Xglk752-4AS
t_{max} (^oCd)						
3B	2012	40.9	3.1	18.5	12.8	Xpsr902-3B

Table 5-7 (continued)

Trait/Chromosome	Year	Position (cM)	LOD	R^2	Additive effect	Closest marker
MWC (mg)						
2A	2012	94.9	3.3	19.4	-2.49	Xpsr919b-2A
	2012	126.6	3.4	20.1	-3.75	Xglk699b-2AL
	2013	155.5	3.5	13.8	-2.04	Xpsr630-2A
2B	2013	145.8	3.2	12.6	-1.88	Xglk699a-2BS
3B	2013	8.1	4.3	16.6	2.54	Lrk10c-3BS
	2013	80.5	3.7	14.4	2.12	Xpsr1054-3B
4A	2012	21.7	7.0	37.0	-4.03	Xpsr59a-4A
	2013	22.7	3.4	13.4	-2.35	Xpsr59a-4A
5B	2012	156.2	3.2	18.9	-2.87	Xpsr580b-5B
5DL	2012	39.0	3.1	18.5	-5.05	Xpsr580a-5DL
	2013	40.0	4.7	17.8	-4.69	Xpsr580a-5DL
7B	2012	68.3	3.3	19.3	2.62	Xglk549-7B
	2012	193.5	6.1	33.2	4.68	Xmwg710a-7B
	2013	78.6	4.5	17.3	2.65	Xglk478-7BL
	2013	184.5	4.1	15.9	3.14	Xglk750-7BL
WAR (mg $^{o}Cd^{-1}$)						
2A	2012	128.6	3.9	22.5	-0.0079	Xglk699b-2AL
4A	2012	21.7	3.9	22.8	-0.0064	Xpsr59a-4A
5A	2013	206.9	3.3	13.0	0.0053	Xpsr1194-5A
5DL	2012	42.0	3.0	18.1	-0.0098	Xpsr580a-5DL
	2013	33.0	3.6	14.0	-0.0102	Xpsr906a-5DL
7B	2012	69.3	3.2	19.2	0.0052	Xglk549-7B
	2012	195.5	4.7	26.5	0.0082	Xmwg710a-7B
	2013	66.3	4.9	18.7	0.0059	Xglk598-7BL
WLR (mg $^{o}Cd^{-1}$)						
2A	2013	6.0	4.3	16.7	-0.0035	Xpsr566c-2A
3B	2013	5.1	3.9	15.1	0.0035	Lrk10c-3BS
	2013	80.5	3.1	12.2	0.0031	Xpsr1054-3B
4A	2012	21.7	6.1	33.1	-0.0088	Xpsr59a-4A
	2013	22.7	7.9	28.3	-0.0053	Xpsr59a-4A
5B	2012	146.2	3.1	18.4	-0.0062	Xpsr580b-5B
5DL	2013	48.0	3.6	14.2	-0.0059	Xpsr580a-5DL
6A	2012	89.0	4.2	24.1	0.0064	Xpsr966-6A
7B	2012	192.5	4.6	26.3	0.0098	Xmwg710a-7B
	2013	192.5	4.4	17.0	0.0051	Xmwg710a-7B
t_{mwc} (^{o}Cd)						
3A	2013	110.5	3.4	13.2	13.2	Xglk577-3AL

Table 5-7 (continued)

Trait/Chromosome	Year	Position (cM)	LOD	R^2	Additive effect	Closest marker
TGW (g)						
1BS	2013	42.9	4.8	10.3	1.17	Xglk483-1BS
2A	2012	105.4	4.6	10.0	-1.10	Xpsr602-2A
2B	2013	145.8	3.5	7.7	-0.94	Xglk699a-2BS
3A	2012	109.5	3.1	6.8	0.95	Xglk577-3AL
3B	2012	80.5	4.0	8.7	1.07	Xpsr1054-3B
	2013	2.9	3.4	7.4	0.96	C970a-3B
	2013	79.3	5.0	10.8	1.20	Xpsr1054-3B
4A	2012	23.7	11.0	22.3	-1.92	Xpsr59a-4A
	2013	25.7	6.5	13.8	-1.41	Xpsr59a-4A
	2013	161.3	2.9	6.5	-2.05	Xglk128-4A
5A	2012	120.2	7.8	16.3	-1.71	Xpsr911-5A
	2013	114.1	3.2	7.1	-0.99	Xpsr911-5A
	2013	208.9	4.3	9.3	1.26	Xpsr918b-5A
5B	2012	151.3	3.3	7.3	-0.94	Xpsr580b-5B
5DL	2013	37.0	4.3	9.2	-2.24	Xpsr580a-5DL
6A	2012	91.1	5.2	11.1	1.23	Xpsr966-6A
7B	2012	192.5	5.8	12.5	1.85	Xmwg710a-7B
	2013	180.5	3.3	7.2	1.27	Xglk750-7BL
7D	2013	87.8	4.1	8.9	1.23	Xgwm111b-7D

Table 5-8 QTL coincidences between anthesis dates and flag leaf senescence, grain filling traits, and grain weight

Trait[a]	No. of QTL coincident with those for anthesis dates				
	2D (1)[b]	4DL (1)	5A.1[c] (1)	5A.2 (1)	7B (2)
Chl_{per}		1[#d]		1[#]	
Chl_{loss}		1			1
Max CLR		1[#]			1[#]
Average GFR				1[#]	1[#]
MWC					2[#]
WAR				1[#]	2[#]
Grain weight				1[#]	

[a] Trait abbreviations: Chl_{per}, duration of chlorophyll persistence; Chl_{loss}, duration of rapid chlorophyll loss; Max CLR, maximum chlorophyll loss rate; GFR, grain filling rate; MWC, maximum water content of grains; and WAR, water absorption rate of grains.
[b] Number in the parentheses indicates the QTL number located in this chromosomal region.
[c] Serial number following the chromosome name indicates multiple QTL regions on the same chromosome.
[d #] Increasing alleles conferred by the opposite parents.

Table 5-9 QTL coincidences between duration of green area persistence (GA_{per}) and grain filling traits, and grain weight

Trait[a]	No. of QTL coincident with those for GA_{per}			
	2A (1)[b]	4A (1)	7AL (1)	7B (1)
Rapid GFR	3	1		2
Late GFR		1		1
Average GFR	3	1		2
Max GFR	2	1		1
Onset of GF		1		
MWC	2	2		2
WAR	1	1		1
WLR		2		2
Grain weight	1	2		2

[a] Trait abbreviations: GFR, grain filling rate; GF, grain filling; MWC, maximum water content of grains; WAR, water absorption rate of grains; and WLR, water loss rate of grains.
[b] Number in the parentheses indicates the QTL number located in this chromosomal region.

Table 5-10 QTL coincidences between duration of chlorophyll persistence (Chl_{per}) and grain filling traits, and grain weight

Trait[a]	No. of QTL coincident with those for Chl_{per}				
	1DS (1)[b]	2B (1)	4A (1)	4DL (1)	5A (1)
Rapid GFR			1		
Late GFR			1		
Average GFR			1		1
Max GFR			1		
Onset of GF			1		
MWC			2		
WAR			1		1
WLR			2		
Grain weight			2		1

[a] Trait abbreviations: GFR, grain filling rate; GF, grain filling; MWC, maximum water content of grains; WAR, water absorption rate of grains; and WLR, water loss rate of grains.
[b] Number in the parentheses indicates the QTL number located in this chromosomal region.

Table 5-11 QTL coincidences between duration of rapid chlorophyll loss (Chl_{loss}) and grain filling traits, and grain weight

Trait[a]	No. of QTL coincident with those for Chl_{loss}				
	1DS (1)[b]	4A (2)	4DL (1)	7B.1[c] (1)	7B.2 (1)
Rapid GFR		1[#d]			2[#]
Late GFR		1[#]			1[#]
Average GFR		1[#]		1[#]	2[#]
Max GFR		1[#]			1[#]
Onset of GF		1[#]			
MWC		2[#]		2[#]	2[#]
WAR		1[#]		2[#]	1[#]
WLR		2[#]			2[#]
Grain weight		2[#]			2[#]

[a] Trait abbreviations: GFR, grain filling rate; GF, grain filling; MWC, maximum water content of grains; WAR, water absorption rate of grains; and WLR, water loss rate of grains.
[b] Number in the parentheses indicates the QTL number located in this chromosomal region.
[c] Serial number following the chromosome name indicates multiple QTL regions on the same chromosome.
[d #] Increasing alleles conferred by the opposite parents.

Table 5-12 QTL coincidences between maximum chlorophyll loss rate (Max CLR) and grain filling traits, and grain weight

Trait[a]	No. of QTL coincident with those for Max CLR				
	3A (1)[b]	4A (2)	4DL (1)	7B.1[c] (1)	7B.2 (1)
Rapid GFR		1			2
Late GFR		1			1
Average GFR		1		1	2
Max GFR		1			1
Onset of GF		1			
MWC		2		2	2
WAR		1		2	1
WLR		2			2
t_{mwc}	1[#d]				
Grain weight	1[#]	2			2

[a] Trait abbreviations: GFR, grain filling rate; GF, grain filling; MWC, maximum water content of grains; WAR, water absorption rate of grains; WLR, water loss rate of grains; and t_{mwc}, the time at maximum water content.
[b] Number in the parentheses indicates the QTL number located in this chromosomal region.
[c] Serial number following the chromosome name indicates multiple QTL regions on the same chromosome.
[d #] Increasing alleles conferred by the opposite parents.

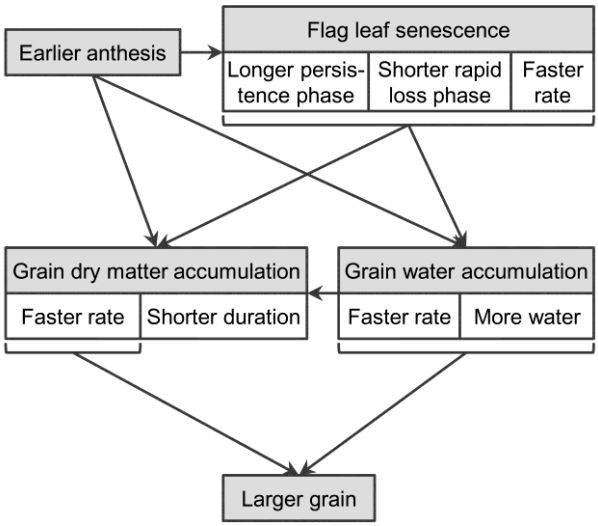

Fig. 5-4 A model showing the relationships between anthesis dates, flag leaf senescence, grain filling, and final grain weight. Earlier anthesis is associated with delayed onset of flag leaf senescence (longer persistence phase), shorter duration and faster rate of rapid senescence, which leads to faster grain dry matter accumulation, greater grain water absorption rate and more maximum grain water, consequently resulting in larger grains.

5.5 Discussion

5.5.1 Interactions between anthesis time and leaf senescence

In this study, anthesis time was negatively associated with GA_{per}, Chl_{per}, Max GALR, and Max CLR, but positively associated with GA_{loss} and Chl_{loss}, indicating that earlier anthesis contributed to longer persistence phase of flag leaves, faster rate and shorter duration of rapid senescence. In contrast, no consistent associations across years were found between anthesis time and total green leaf duration after anthesis, suggesting that it is worth partitioning the total duration into two phases different in functions. The negative relationship between anthesis time and the onset of leaf senescence is in line with the previous studies in wheat (Verma et al., 2004; Bogard et al., 2011; Kipp et al., 2014). There is also a negative association between heading time and green leaf duration calculated from heading (Naruoka et al., 2012). Bogard et al. (2011) reported that earlier anthesis is associated with longer duration of rapid senescence in the most of environments, inconsistent with the present study; however, a positive relationship between two traits was also observed under a few conditions, indicating that this relationship is likely dependent on growing environments.

QTL analysis showed that four QTL for anthesis dates were coincident with four QTL for Chl_{per} and Max CLR on chromosomes 4DL, 5A and 7B, with the increasing alleles conferred by the opposite parents, indicating negative pleiotropic effects or tight linkages of the genes regulating early anthesis, delayed senescence and fast senescing rate, or vice versa. Three QTL for anthesis dates also coincided with those for Chl_{loss} on 4DL and 7B, with the increasing alleles originating from the same parents. These QTL coincidences confirmed the physiological relationships between anthesis time and leaf senescence. It has been found that a photoperiod-response gene Ppd-D1 has pleiotropic effects; the Ppd-D1 allele (insensitivity to photoperiod) not only advances anthesis (c. 10 days), but also confers greater maintenance of green area after anthesis (Foulkes et al., 2004). Negative pleiotropic effects of Ppd-D1 on anthesis dates and the onset of leaf senescence have been validated in a recent report (Bogard et al., 2011). This gene is located on the short arm of 2D (Snape et al., 2001; Hanocq et al., 2004), corresponding to a QTL (QAd.uon-13) for anthesis dates in the present study. Furthermore, Bogard et al. (2011) also reported the QTL coincidences between anthesis dates and the onset of leaf senescence on 2A, showing negative pleiotropic effects or gene linkages; an exception has been determined on 7D, where the

coincident QTL contribute to early anthesis, early onset of leaf senescence, and longer duration of rapid senescence. In this study, four QTL for anthesis dates were detected on 5A and 7B, consistent with the previous observation in the same population grown in Switzerland (Keller et al., 1999), suggesting stability. Of these QTL, the one coincident with the onset of leaf senescence on 5AL corresponds to a previous QTL for ear emergence time based on common marker analysis (Kato et al., 1999; Simonetti et al., 1999). This QTL is approximately 40 cM distal to Vrn-A1, a predominant gene controlling vernalisation response in wheat; however, two genes have comparable effects on ear emergence time (c. 4 days) (Kato et al., 1999). In diploid wheat Triticum monococcum, similarly, there is a second vernalisation gene Vrn-A^m2, which is 50 cM distal to Vrn-A^m1 on $5A^m$L (Dubcovsky et al., 1998). Thus the QTL in the present study could be Vrn-A2 in hexaploid wheat. The Vrn-2 series have been predicted existing distally on the long arms of 4B, 4D and 5A (because of the 4A/5A translocation) (Snape et al., 2001). Intriguingly, a QTL for anthesis time was mapped on the distal region of 4DL, and could be the Vrn-D2 in hexaploid wheat. This QTL also showed coincidences with those for leaf senescence. Another independent QTL on 5A for anthesis time was located on the short arm, and the allele from bread wheat Forno delayed anthesis. Therefore, chromosome 5A should carry three genes governing anthesis time. On 7B, the coincident QTL for anthesis dates, and the duration and rate of rapid senescence, were identified, but whether or not they are related to Vrn-B3 gene is unknown (Yan et al., 2006). Taken together, leaf senescence in wheat is partially dependent on anthesis system. Interactions between them have also been found in other plants such as Arabidopsis (Wingler, 2011) and barley (Lacerenza et al., 2010).

5.5.2 Early anthesis, and delayed but fast leaf senescence contribute to grain weight through grain filling processes

As modern wheat cultivars have high grain set after anthesis (> 90%), individual grain development largely determines final yield thereafter (Slafer and Whitechurch, 2001; González et al., 2011). Grain growth occurs mainly during the grain filling period, and the main events are the accumulation of grain dry matter and water. In this study, a strong relationship between average grain filling rate, rather than grain filling duration, and final grain weight was observed in both years, indicating that the synthetic rate of dry matter is more important than its duration, consistent with several earlier reports

(Zahedi and Jenner, 2003; Wang et al., 2009). Across the whole grain filling process, the rapid grain filling phase appeared to be more critical than the initial and late ones. Likewise, there was a strong relationship between maximum grain water content and grain weight across two years, as reported previously (Lizana et al., 2010; Hasan et al., 2011), indicating the importance of grain water accumulation. In addition, grain water absorption and loss rates also showed close relationships with final grain weight. Water in grains may function as a driver of grain morphological enlargement, and provide material and suitable medium for the biochemical synthesis of storage products. The latter roles can be supported by the strong and positive relationship between maximum grain water content and grain filling rate. Genetic analysis revealed that most QTL for grain filling rates, grain water uptake and loss, and grain weight, were coincident, with the favourable alleles conferred by the same parents, confirming their close physiological relationships. Therefore, grain filling rates and grain water content are major contributors to individual grain weight, and any factors affecting grain weight likely function through their effects on grain dry matter and water accumulation.

Earlier anthesis and delayed leaf senescence were found to contribute to larger grains at maturity. Many reports have demonstrated the phenotypic relationships between anthesis time, leaf senescence, and yield; however, only a few have presented their associations with individual grain weight, a major determinant of yield after anthesis (Gooding et al., 2000; McIntyre et al., 2010; Naruoka et al., 2012). In 2012, there was a significant association between leaf senescence rate and final grain weight, as suggested in durum wheat by Hafsi et al. (2000). A detailed analysis showed that anthesis time and leaf senescence affected grain weight through grain filling processes, as expected. Specifically, early anthesis, delayed but short and fast leaf senescence tended to increase grain filling rates, grain water absorption rate and in turn maximum grain water content, but shorten the progression of grain dry matter and water accumulation. The latter observation does not follow the traditional notion that extending stay-green could increase grain filling duration. In fact, as discussed above, grain filling rate is more important than its duration for grain weight, and more responsive to the increased assimilate availability through stay-green. This responsiveness has also been seen under the stressed conditions such as heat, drought and elevated CO_2 that lead to faster but shorter grain filling (Li et al., 2001; Zahedi

and Jenner, 2003; Yang et al., 2004). Relationships between anthesis time, leaf senescence, grain filling rates, grain water uptake and loss, and final grain weight, are consistent with the genetic analysis showing considerable QTL coincidences between them. Thus, these processes may be coordinately regulated by the pleiotropic effects or close linkages of functionally related genes. Potential genes may include Vrn and Ppd responsible for flowering time. Among different vernalisation gene combinations, the genotypes with one or more dominant alleles display early flowering and higher individual grain weight than the combination of vrn-A1vrn-B1vrn-D1 (Zhang et al., 2014).

It has been demonstrated that wheat grains are growing under relatively adequate assimilate supply during grain filling, namely sink limitation (Slafer and Savin, 1994; Borras et al., 2004; Miralles and Slafer, 2007). This is also true in the Forno × Oberkulmer mapping population, where individual grain weight across all RILs was increased only by 7.8% after removing half of the spikelets at anthesis (details can be found in **Chapter 4**). Relative sink limitation is able to partially explain why there are significant but weak relationships between leaf persistence duration and individual grain weight. In spite of the overall sink limitation, it seems that there is a significant variation at different positions within spikes. Distal grains within spikelets are more responsive to an increase in assimilate availability by de-graining than the basal ones, indicating grains are more source limited from the basal to distal florets (details can be found in **Chapter 6**). Therefore, improved stay-green and source strength may be still important to enhance the growth of distal grains. In addition, modern bread wheat cultivars develop more grains than old ones, and the sink limitation has been released to some extent (Acreche and Slafer, 2009; Fischer and Hillerislambers, 1978). This requires stay-green phenotype to maximise grain yield in future breeding.

5.5.3 Early anthesis, and delayed but fast leaf senescence as the ideotypes for wheat breeding

This study demonstrated that earlier anthesis increased final grain weight through promoting grain filling rates and grain water accumulation. Thus, accelerating anthesis to some extent seems to be important for grain yield improvement under the rainfed conditions. With the predicted climate change and consequently more frequent heat stress at meiosis and anthesis, when wheat yield is most sensitive, early anthesis can confer summer drought escape (Semenov et al., 2014). An appropriate anthesis time is

likely achieved by adjusting the major genes responding to vernalisation and photoperiod. Examination of the isogenic lines has showed that the photoperiod insensitive allele Ppd-D1 reduces anthesis time by 6–14 days, increases spikelet fertility, and produces larger grains and higher yield, depending on growing environments and summer conditions (Snape et al., 2001). Genotypes combining one or more dominant alleles of Vrn genes tend to flower early with high grain weight and yield (Iqbal et al., 2007; Kamran et al., 2014; Zhang et al., 2014). In wheat breeding programmes, selection for early anthesis should be efficient, as this trait has high heritability (Keller et al., 1999; McIntyre et al., 2010). While designing wheat for local climatic conditions, care must be taken not to shorten the critical period for grain number generation, namely from the emergence of penultimate leaf to anthesis, during which the rapid growth of spikes occurs (González et al., 2011). Meanwhile, sowing time should be adjusted so that early genotypes are able to avoid frost damage in spring (Foulkes et al., 2004).

Turning to leaf senescence patterns, regardless of the assessment methods (visual scoring or SPAD), the parental line Forno exhibited delayed, shorter but faster leaf senescence than Oberkulmer across years. Forno is a modern bread wheat, and its phenotype of leaf senescence favours grain dry matter and water accumulation, contributing to larger grains. In contrast, spelt was a major ancient grain but currently has been cultivated as a minor crop; as a spelt, Oberkulmer did not show the favourable kinetics of leaf senescence. This may reflect the efforts and benefits of modern breeding in bread wheat.

Recently, a dilemma of leaf senescence has been proposed to describe that delayed senescence is associated with higher yield potential, but with lower nutrient use efficiency (Gregersen et al., 2008). To overcome this dilemma, Wu et al. (2012) suggested an ideotype of leaf senescence: delaying the onset, but speeding the rate, of senescence. Delayed senescence can extend the phase of functional photosynthesis so that more assimilates would be produced for grain filling. Once terminal leaf senescence is initiated, faster rate would improve the efficiency of nutrient remobilisation, leading to higher harvest index (the ratio of grain weight to total plant biomass). In the present study, the results concur with this model. Indeed, delayed leaf senescence increased grain filling rates (but not its duration), grain water absorption rate and maximum grain water content, resulting in larger grains. Although delayed

onset of leaf senescence reduced the duration of rapid senescence phase, the senescence rate was accelerated largely. Fast senescence allows the rapid degradation of macromolecules and subsequent remobilisation of these nutrients to grains. As a result, leaf senescence rate was positively associated with grain filling rates. On the other hand, longer senesing duration was associated with slower grain filling. This type of stay-green has also been found in tobacco P_{SAG12}:IPT transformants, which display a dramatic delay of senescence, followed by a sudden death, resulting in significant increases in biomass (40%) and seed yield (52%) (Gregersen et al., 2013). Therefore, delayed, shorter but faster leaf senescence would lead to better utilisation of current photosynthesis and structural nutrients. This ideotype can be used to maximise yield potential in wheat breeding.

In conclusion, this work describes the relationships between anthesis time, leaf senescence and grain weight, and the underlying physiological and genetic mechanisms using a mapping population of bread wheat and spelt with contrasting phasic development and leaf senescence kinetics. Earlier anthesis, and delayed, shorter but faster leaf senescence were associated with larger grains at maturity. This resulted from increased grain filling rates (but not its duration) and grain water accumulation, two major processes driving final grain weight. Genetic analysis revealed frequent QTL coincidences between these traits, indicating pleiotropic effects or tight gene linkages, which confirmed their physiological relationships. Therefore, slightly early anthesis, and delayed but fast leaf senescence are desirable traits to improve grain weight and, in turn, yield potential in wheat.

5.6 Acknowledgements

This work was supported by the grants from the China Scholarship Council and University of Nottingham. We thank Beat Keller (University of Zurich, Switzerland) for providing the mapping population, and Monika Messmer (Research Institute of Organic Agriculture, Switzerland) for providing the molecular marker data. We also thank John Alcock, Matthew Tovey and Fiona Wilkinson (University of Nottingham) for their help with field trials and laboratory work.

5.7 References

Acreche MM, Slafer GA. 2009. Grain weight, radiation interception and use efficiency as affected by sink-strength in Mediterranean wheats released from 1940 to 2005. Field Crops Research **110**, 98-105.

Addisu M, Snape JW, Simmonds JR, Gooding MJ. 2010. Effects of reduced height (Rht) and photoperiod insensitivity (Ppd) alleles on yield of wheat in contrasting production systems. Euphytica **172**, 169-181.

Alonso-Blanco C, Aarts MGM, Bentsink L, Keurentjes JJB, Reymond M, Vreugdenhil D, Koornneef M. 2009. What has natural variation taught us about plant development, physiology, and adaptation? Plant Cell **21**, 1877-1896.

Bogard M, Jourdan M, Allard V, et al. 2011. Anthesis date mainly explained correlations between post-anthesis leaf senescence, grain yield, and grain protein concentration in a winter wheat population segregating for flowering time QTLs. Journal of Experimental Botany **62**, 3621-3636.

Borras L, Slafer GA, Otegui ME. 2004. Seed dry weight response to source-sink manipulations in wheat, maize and soybean: a quantitative reappraisal. Field Crops Research **86**, 131-146.

Briarty LG, Hughes CE, Evers AD. 1979. The developing endosperm of wheat - a stereological analysis. Annals of Botany **44**, 641-658.

Brocklehurst PA. 1977. Factors controlling grain weight in wheat. Nature **266**, 348-349.

Brown HE, Jamieson PD, Brooking IR, Moot DJ, Huth NI. 2013. Integration of molecular and physiological models to explain time of anthesis in wheat. Annals of Botany **112**, 1683-1703.

Calderini DF, Abeledo LG, Savin R, Slafer GA. 1999. Effect of temperature and carpel size during pre-anthesis on potential grain weight in wheat. Journal of Agricultural Science **132**, 453-459.

Christopher JT, Manschadi AM, Hammer GL, Borrell AK. 2008. Developmental and physiological traits associated with high yield and stay-green phenotype in wheat. Australian Journal of Agricultural Research **59**, 354-364.

Derkx AP, Orford S, Griffiths S, Foulkes MJ, Hawkesford MJ. 2012. Identification of differentially senescing mutants of wheat and impacts on yield, biomass and nitrogen partitioning. Journal of Integrative Plant Biology **54**, 555-566.

Distelfeld A, Avni R, Fischer AM. 2014. Senescence, nutrient remobilization, and yield in wheat and barley. Journal of Experimental Botany **65**, 3783-3798.

Dubcovsky J, Lijavetzky D, Appendino L, Tranquilli G. 1998. Comparative RFLP mapping of Triticum monococcum genes controlling vernalization requirement. Theoretical and Applied Genetics **97**, 968-975.

Fischer RA. 1985. Number of kernels in wheat crops and the influence of solar radiation and temperature. Journal of Agricultural Science **105**, 447-461.

Fischer RA, Hillerislambers D. 1978. Effect of environment and cultivar on source limitation to grain weight in wheat. Australian Journal of Agricultural Research **29**, 443-458.

Foulkes MJ, Sylvester-Bradley R, Worland AJ, Snape JW. 2004. Effects of a photoperiod-response gene Ppd-D1 on yield potential and drought resistance in UK winter wheat. Euphytica **135**, 63-73.

Gaju O, Allard V, Martre P, Le Gouis J, Moreau D, Bogard M, Hubbart S, Foulkes MJ. 2014. Nitrogen partitioning and remobilization in relation to leaf senescence, grain yield and grain nitrogen concentration in wheat cultivars. Field Crops Research **155**, 213-223.

Gaju O, Allard V, Martre P, et al. 2011. Identification of traits to improve the nitrogen-use efficiency of wheat genotypes. Field Crops Research **123**, 139-152.

Gan S, Amasino RM. 1997. Making sense of senescence (molecular genetic regulation and manipulation of leaf senescence). Plant Physiology **113**, 313-319.

Gelang J, Pleijel H, Sild E, Danielsson H, Younis S, Sellden G. 2000. Rate and duration of grain filling in relation to flag leaf senescence and grain yield in spring wheat (Triticum aestivum) exposed to different concentrations of ozone. Physiologia Plantarum **110**, 366-375.

González FG, Miralles DJ, Slafer GA. 2011. Wheat floret survival as related to pre-anthesis spike growth. Journal of Experimental Botany **62**, 4889-4901.

Gooding MJ, Dimmock J, France J, Jones SA. 2000. Green leaf area decline of wheat flag leaves: the influence of fungicides and relationships with mean grain weight and grain yield. Annals of Applied Biology **136**, 77-84.

Gregersen PL, Culetic A, Boschian L, Krupinska K. 2013. Plant senescence and crop productivity. Plant Molecular Biology **82**, 603-622.

Gregersen PL, Holm PB, Krupinska K. 2008. Leaf senescence and nutrient remobilisation in barley and wheat. Plant Biology **10**, 37-49.

Hafsi M, Mechmeche W, Bouamama L, Djekoune A, Zaharieva M, Monneveux P. 2000. Flag leaf senescence, as evaluated by numerical image analysis, and its relationship with yield under drought in durum wheat. Journal of Agronomy and Crop Science **185**, 275-280.

Hanocq E, Niarquin M, Heumez E, Rousset M, Le Gouis J. 2004. Detection and mapping of QTL for earliness components in a bread wheat recombinant inbred lines population. Theoretical and Applied Genetics **110**, 106-115.

Hasan AK, Herrera J, Lizana C, Calderini DF. 2011. Carpel weight, grain length and stabilized grain water content are physiological drivers of grain weight determination of wheat. Field Crops Research **123**, 241-247.

Iqbal M, Navabi A, Yang RC, Salmon DF, Spaner D. 2007. The effect of vernalization genes on earliness and related agronomic traits of spring wheat in northern growing regions. Crop Science **47**, 1031-1039.

Izanloo A, Condon AG, Langridge P, Tester M, Schnurbusch T. 2008. Different mechanisms of adaptation to cyclic water stress in two South Australian bread wheat cultivars. Journal of Experimental Botany **59**, 3327-3346.

Joshi AK, Kumari M, Singh VP, Reddy CM, Kumar S, Rane J, Chand R. 2007. Stay green trait: variation, inheritance and its association with spot blotch resistance in spring wheat (Triticum aestivum L.). Euphytica **153**, 59-71.

Kamran A, Iqbal M, Spaner D. 2014. Flowering time in wheat (Triticum aestivum L.): a key factor for global adaptability. Euphytica **197**, 1-26.

Kato K, Miura H, Sawada S. 1999. QTL mapping of genes controlling ear emergence time and plant height on chromosome 5A of wheat. Theoretical and Applied Genetics **98**, 472-477.

Keller M, Karutz C, Schmid JE, Stamp P, Winzeler M, Keller B, Messmer MM. 1999. Quantitative trait loci for lodging resistance in a segregating wheat × spelt population. Theoretical and Applied Genetics **98**, 1171-1182.

Kipp S, Mistele B, Schmidhalter U. 2014. Identification of stay-green and early senescence phenotypes in high-yielding winter wheat, and their relationship to grain yield and grain protein concentration using high-throughput phenotyping techniques. Functional Plant Biology **41**, 227-235.

Lacerenza JA, Parrott DL, Fischer AM. 2010. A major grain protein content locus on barley (Hordeum vulgare L.) chromosome 6 influences flowering time and sequential leaf senescence. Journal of Experimental Botany **61**, 3137-3149.

Li AG, Hou YS, Trent A. 2001. Effects of elevated atmospheric CO_2 and drought stress on individual grain filling rates and durations of the main stem in spring wheat. Agricultural and Forest Meteorology **106**, 289-301.

Lizana XC, Calderini DF. 2013. Yield and grain quality of wheat in response to increased temperatures at key periods for grain number and grain weight determination: considerations for the climatic change scenarios of Chile. Journal of Agricultural Science **151**, 209-221.

Lizana XC, Riegel R, Gomez LD, Herrera J, Isla A, McQueen-Mason SJ, Calderini DF. 2010. Expansins expression is associated with grain size dynamics in wheat (Triticum aestivum L.). Journal of Experimental Botany **61**, 1147-1157.

Lopes MS, Reynolds MP. 2011. Drought adaptive traits and wide adaptation in elite lines derived from resynthesized hexaploid wheat. Crop Science **51**, 1617-1626.

McIntyre CL, Mathews KL, Rattey A, Chapman SC, Drenth J, Ghaderi M, Reynolds M, Shorter R. 2010. Molecular detection of genomic regions associated with grain yield and yield-related components in an elite bread wheat cross evaluated under irrigated and rainfed conditions. Theoretical and Applied Genetics **120**, 527-541.

Miralles DJ, Slafer GA. 2007. Sink limitations to yield in wheat: how could it be reduced? Journal of Agricultural Science **145**, 139-149.

Naruoka Y, Sherman JD, Lanning SP, Blake NK, Martin JM, Talbert LE. 2012. Genetic analysis of green leaf duration in spring wheat. Crop Science **52**, 99-109.

Pask A, Pietragalla J. 2012. Leaf area, green crop area and senescence. In: Pask AJD, Pietragalla J, Mullan DM, Reynolds MP, eds. Physiological Breeding II: A Field Guide to Wheat Phenotyping. Mexico: CIMMYT, 58-62.

Semenov MA, Stratonovitch P, Alghabari F, Gooding MJ. 2014. Adapting wheat in Europe for climate change. Journal of Cereal Science **59**, 245-256.

Shewry PR, Mitchell RAC, Tosi P, Wan Y, Underwood C, Lovegrove A, Freeman J, Toole GA, Mills ENC, Ward JL. 2012. An integrated study of grain development of wheat (cv. Hereward). Journal of Cereal Science **56**, 21-30.

Simonetti MC, Bellomo MP, Laghetti G, Perrino P, Simeone R, Blanco A. 1999. Quantitative trait loci influencing free-threshing habit in tetraploid wheats. Genetic Resources and Crop Evolution **46**, 267-271.

Slafer GA, Rawson HM. 1994. Sensitivity of wheat phasic development to major environmental factors: a re-examination of some assumptions made by physiologists and modellers. Functional Plant Biology **21**, 393-426.

Slafer GA, Savin R. 1994. Source-sink relationships and grain mass at different positions within the spike in wheat. Field Crops Research **37**, 39-49.

Slafer GA, Whitechurch EM. 2001. Manipulating wheat development to improve adaptation. In: Reynolds MP, Ortiz-Monasterio JI, McNab A, eds. Application of Physiology in Wheat Breeding. Mexico: CIMMYT, 160-170.

Snape JW, Butterworth K, Whitechurch E, Worland AJ. 2001. Waiting for fine times: genetics of flowering time in wheat. Euphytica **119**, 185-190.

Sykorova B, Kuresova G, Daskalova S, Trckova M, Hoyerova K, Raimanova I, Motyka V, Travnickova A, Elliott MC, Kaminek M. 2008. Senescence-induced ectopic expression of the A. tumefaciens ipt gene in wheat delays leaf senescence, increases cytokinin content, nitrate influx, and nitrate reductase activity, but does not affect grain yield. Journal of Experimental Botany **59**, 377-387.

Uauy C, Distelfeld A, Fahima T, Blechl A, Dubcovsky J. 2006. A NAC gene regulating senescence improves grain protein, zinc, and iron content in wheat. Science **314**, 1298-1301.

Verma V, Foulkes MJ, Worland AJ, Sylvester-Bradley R, Caligari PDS, Snape JW. 2004. Mapping quantitative trait loci for flag leaf senescence as a yield

determinant in winter wheat under optimal and drought-stressed environments. Euphytica **135**, 255-263.

Wang RX, Hai L, Zhang XY, You GX, Yan CS, Xiao SH. 2009. QTL mapping for grain filling rate and yield-related traits in RILs of the Chinese winter wheat population Heshangmai X Yu8679. Theoretical and Applied Genetics **118**, 313-325.

Wingler A. 2011. Interactions between flowering and senescence regulation and the influence of low temperature in Arabidopsis and crop plants. Annals of Applied Biology **159**, 320-338.

Wu XY, Kuai BK, Jia JZ, Jing HC. 2012. Regulation of leaf senescence and crop genetic improvement. Journal of Integrative Plant Biology **54**, 936-952.

Yan L, Fu D, Li C, Blechl A, Tranquilli G, Bonafede M, Sanchez A, Valarik M, Yasuda S, Dubcovsky J. 2006. The wheat and barley vernalization gene VRN3 is an orthologue of FT. Proceedings of the National Academy of Sciences of the United States of America **103**, 19581-19586.

Yang JC, Zhang JH, Wang ZQ, Xu GW, Zhu QS. 2004. Activities of key enzymes in sucrose-to-starch conversion in wheat grains subjected to water deficit during grain filling. Plant Physiology **135**, 1621-1629.

Zahedi M, Jenner CF. 2003. Analysis of effects in wheat of high temperature on grain filling attributes estimated from mathematical models of grain filling. Journal of Agricultural Science **141**, 203-212.

Zhang J, Dell B, Biddulph B, Khan N, Xu Y, Luo H, Appels R. 2014. Vernalization gene combination to maximize grain yield in bread wheat (Triticum aestivum L.) in diverse environments. Euphytica **198**, 439-454.

5.8 Supplementary information

List of Supplementary files

Supplementary Table S5-1 Descriptive statistics on anthesis dates, flag leaf senescence, grain filling traits, and grain weight in the recombinant inbred line (RIL) mapping population of bread wheat × spelt

Supplementary Table S5-1 Descriptive statistics on anthesis dates, flag leaf senescence, grain filling traits, and grain weight in the recombinant inbred line (RIL) mapping population of bread wheat × spelt

Trait[a]	Year	Parental lines			RILs			
		Forno	Oberkulmer	P-value	Mean (min; max)	P-value	S.E.D.[c]	H^{2d}
Anthesis date (^{o}Cd)	2012	1876	1916	< 0.01	1900 (1840; 1944)	< 0.001	9	0.87
	2013	1442	1509	< 0.01	1485 (1434; 1547)	< 0.001	9	
GA_{per} (^{o}Cd)	2012	384	204	< 0.01	280 (97; 469)	< 0.001	54	0.54
	2013	402	343	> 0.05	378 (82; 604)	< 0.001	57	
GA_{loss} (^{o}Cd)	2012	244	562	< 0.01	368 (161; 664)	< 0.001	97	0.67
	2013	445	588	< 0.05	345 (104; 688)	< 0.001	70	
GA_{tot} (^{o}Cd)	2012	628	766	< 0.05	648 (498; 935)	< 0.001	57	0.46
	2013	847	930	< 0.05	723 (573; 944)	< 0.001	41	
Max GALR (scores $^{o}Cd^{-1}$)	2012	0.033	0.019	< 0.05	0.028 (0.018; 0.047)	< 0.001	0.006	0.47
	2013	0.023	0.019	> 0.05	0.038 (0.017; 0.091)	< 0.001	0.014	
GA_{accum} (scores)	2012	4527	5259	< 0.01	4755 (3170; 6226)	< 0.001	203	0.41
	2013	5549	6615	< 0.01	5624 (4507; 6690)	< 0.001	269	
Chl_{per} (^{o}Cd)	2012	388	260	< 0.05	294 (0; 516)	< 0.001	55	0.73
	2013	509	365	< 0.01	435 (317; 548)	< 0.001	46	
Chl_{loss} (^{o}Cd)	2012	252	476	< 0.01	360 (165; 711)	< 0.001	62	0.34
	2013	176	532	< 0.01	190 (73; 504)	< 0.001	61	
Chl_{tot} (^{o}Cd)	2012	640	736	< 0.05	655 (530; 847)	< 0.001	45	0.43
	2013	684	897	< 0.01	626 (509; 868)	< 0.001	46	
Max chl (CCI[b])	2012	53.4	53.8	> 0.05	53.6 (49.0; 59.2)	< 0.001	1.3	0.62
	2013	50.6	54.1	< 0.05	53.6 (47.8; 58.4)	< 0.001	1.6	
Max CLR (CCI $^{o}Cd^{-1}$)	2012	0.136	0.087	< 0.05	0.106 (0.052; 0.200)	< 0.001	0.020	0.59
	2013	0.302	0.111	> 0.05	0.343 (0.107; 0.796)	< 0.001	0.111	
Chl_{accum} (CCI)	2012	35080	33699	> 0.05	34039 (27523; 40247)	< 0.001	1146	0.46
	2013	39091	38091	> 0.05	33886 (28622; 39978)	< 0.001	1461	
Initial GFR (mg $^{o}Cd^{-1}$)	2012	0.039	0.037	> 0.05	0.037 (0.022; 0.049)	< 0.01	0.005	0.23
	2013	0.041	0.021	< 0.05	0.034 (0.012; 0.052)	< 0.001	0.008	
Rapid GFR (mg $^{o}Cd^{-1}$)	2012	0.083	0.111	< 0.05	0.091 (0.059; 0.125)	< 0.001	0.011	0.71
	2013	0.121	0.107	> 0.05	0.111 (0.078; 0.143)	< 0.001	0.011	
Late GFR (mg $^{o}Cd^{-1}$)	2012	0.019	0.027	< 0.05	0.022 (0.013; 0.035)	< 0.001	0.004	0.36
	2013	0.029	0.031	> 0.05	0.029 (0.017; 0.061)	< 0.001	0.006	
Average GFR (mg $^{o}Cd^{-1}$)	2012	0.047	0.059	< 0.01	0.050 (0.033; 0.065)	< 0.001	0.004	0.82
	2013	0.064	0.053	< 0.01	0.058 (0.043; 0.072)	< 0.001	0.004	
Max GFR (mg $^{o}Cd^{-1}$)	2012	0.100	0.132	< 0.05	0.109 (0.070; 0.150)	< 0.001	0.014	0.67
	2013	0.143	0.131	> 0.05	0.133 (0.094; 0.198)	< 0.001	0.015	
Onset of GF (^{o}Cd)	2012	78	132	< 0.05	105 (56; 167)	< 0.01	26	0.31
	2013	117	189	< 0.05	129 (41; 233)	< 0.001	35	
GF duration (^{o}Cd)	2012	860	868	> 0.05	902 (730; 1099)	< 0.05	79	0.23
	2013	843	874	> 0.05	842 (714; 1033)	< 0.001	70	
t_{max} (^{o}Cd)	2012	383	420	> 0.05	417 (353; 489)	< 0.01	27	0.44
	2013	401	457	< 0.01	407 (360; 486)	< 0.001	19	

Supplementary Table S5-1 (continued)

Trait	Year	Parental lines			RILs			
		Forno	Oberkulmer	P-value	Mean (min; max)	P-value	S.E.D.	H^2
MWC (mg)	2012	33.6	42.3	< 0.01	36.7 (24.3; 49.8)	< 0.001	2.1	0.89
	2013	46.2	34.1	< 0.01	38.6 (27.3; 52.1)	< 0.001	2.1	
WAR (mg $^{o}Cd^{-1}$)	2012	0.076	0.070	> 0.05	0.072 (0.049; 0.101)	< 0.001	0.006	0.83
	2013	0.095	0.059	< 0.01	0.079 (0.049; 0.114)	< 0.001	0.006	
WLR (mg $^{o}Cd^{-1}$)	2012	0.051	0.110	< 0.01	0.069 (0.041; 0.098)	< 0.001	0.009	0.69
	2013	0.070	0.062	> 0.05	0.059 (0.041; 0.075)	< 0.001	0.004	
t_{mwc} (^{o}Cd)	2012	441	605	< 0.01	512 (442; 588)	< 0.001	38	0.38
	2013	485	578	< 0.01	491 (422; 617)	< 0.001	24	
TGW (g)	2012	33.9	47.3	< 0.01	40.7 (30.4; 50.5)	< 0.001	1.7	0.74
	2013	49.4	44.8	< 0.01	45.2 (33.9; 52.6)	< 0.001	1.3	

[a] Trait abbreviations: GA_{per}, duration of green area persistence; GA_{loss}, duration of rapid green area loss; GA_{tot}, total duration of green area persistence and loss; Max GALR, maximum green area loss rate; GA_{accum}, accumulated green area; Chl_{per}, duration of chlorophyll persistence; Chl_{loss}, duration of rapid chlorophyll loss; Chl_{tot}, total duration of chlorophyll persistence and loss; Max chl, maximum chlorophyll content; Max CLR, maximum chlorophyll loss rate; Chl_{accum}, accumulated chlorophyll content; GFR, grain filling rate; GF, grain filling; t_{max}, the time at maximum grain filling rate; MWC, maximum water content of grains; WAR, water absorption rate of grains; WLR, water loss rate of grains; t_{mwc}, the time at maximum water content; and TGW, thousand grain weight.

[b] CCI: chlorophyll concentration index.

[c] S.E.D.: standard error of the difference.

[d] H^2: broad sense heritability.

Chapter 6

Carpel Size, Individual Grain Dry Matter and Water Accumulation, and Grain Morphology, as Related to Individual Grain Weight in Wheat

6.1 Abstract

Grain weight is a major yield component in wheat. To provide a comprehensive understanding of grain weight determination, the carpel size at anthesis, grain dry matter accumulation, grain water uptake and loss, grain morphological expansion and final grain weight at different positions within spikelets, were investigated in a recombinant inbred line mapping population of bread wheat (Triticum aestivum L.) × spelt (Triticum spelta L.). Carpel size, grain dry matter and water accumulation, and grain dimensions, interacted strongly with each other. Furthermore, larger carpels, faster grain filling rate, earlier and longer grain filling, more grain water, faster grain water absorption and loss rates, and larger grain dimensions, were associated with higher grain weight. Frequent quantitative trait locus (QTL) coincidences between these traits were observed, particularly those on chromosomes 2A, 3B, 4A, 5A, 5DL and 7B, each of which harboured 16−49 QTL associated with more than 12 traits. Analysis of the allelic effects of coincident QTL confirmed their physiological relationships, indicating that the complex but orderly grain filling processes result mainly from pleiotropy or the tight linkages of functionally related genes. After grain filling, distal grains within spikelets were smaller than basal ones, primarily due to later grain filling and slower initial grain filling rate, followed by synchronous maturation among different grains. Distal grain weight was improved by increased assimilate availability from anthesis. These findings provide deeper insight into grain weight determination in wheat, and the high level of QTL coincidences should allow simultaneous improvement of multiple grain filling traits in breeding.

Keywords: Carpel, distal grain, grain filling, grain morphology, grain water, grain weight, QTL, spelt, wheat.

6.2 Introduction

Grain weight is a major yield determinant in wheat, and therefore a key breeding target to boost yield for global food security. In addition, larger grains are also preferred for their better milling performance and end-use quality (Gegas et al., 2010). Grain weight is mainly determined through the grain filling between anthesis and maturity, during which there are three physiological processes occurring simultaneously: grain dry matter accumulation, grain water accumulation and subsequent desiccation, and grain morphological expansion.

Grain dry matter accumulation is a process of deposition of starch (c. 60–70% of the mature grain weight), proteins (8–15%) and other nutrients (e.g. minerals, vitamins, and fibres) (Shewry, 2009). The assimilates for grain filling originate primarily from current photosynthesis and the remobilisation of soluble reserves accumulated in the vegetative organs before anthesis. Senescing organs can also supply some assimilates by transporting the nutrients from the structural macromolecule degradation into developing grains at the late stage of plant growth (Distelfeld et al., 2014). There is ample evidence that combined current photosynthetic capacity and reserve remobilisation are in excess of the demand of the growing grains; that is, grains are mainly sink limited after anthesis (Slafer and Savin, 1994; Borras et al., 2004; Miralles and Slafer, 2007). During the postanthesis period, therefore, the factors limiting synthesis and deposition of storage products within grains need to be determined. Grain filling can be divided into two components: rate and duration. Grain filling rate follows a slow-fast-slow pattern (Shewry et al., 2012), reflecting the biochemical reaction efficiency for starch and protein synthesis (Shewry et al., 2009). In contrast, its duration reflects the timing of the grain filling progress. The rate and duration of grain filling both contribute to final grain weight; however, there is occasionally a negative relationship between these two components (Charmet et al., 2005; Wang et al., 2009; Gonzalez et al., 2014). Despite the importance of grain dry matter accumulation, only a few studies have been conducted to determine its genetic basis, including gene expression analysis (Laudencia-Chingcuanco et al., 2007; Gillies et al., 2012), and QTL identification (Charmet et al., 2005; Wang et al., 2009).

The dynamics of grain water accumulation appears to be ‘bell’ shaped: water is absorbed rapidly until a plateau is reached, and then lost quickly during grain desiccation (Barlow et al., 1980; Lizana et al., 2010). Water is essential to transport

photoassimilates and other nutrients into developing grains. It also provides a suitable environment for metabolic processes, and directly takes part in the synthesis of storage products. A strong association between maximum grain water content and final grain weight has been found in wheat (Lizana et al., 2010; Hasan et al., 2011; Gonzalez et al., 2014), and in other crops such as maize (Zea mays L.) (Borras et al., 2003; Sala et al., 2007), and sunflower (Helianthus annuus L.) (Rondanini et al., 2009). However, little is known regarding the genetic determination of grain water dynamics.

Grain morphology changes along with dry matter and water accumulation. Immediately after fertilisation, grain length, width, height (thickness) and thus volume increase rapidly. The first dimension reaching its maximum value is grain length (c. 15 days after anthesis), followed by grain width, height and volume (c. 28 days) (Lizana et al., 2010; Hasan et al., 2011), corresponding to the period of endosperm cell enlargement (Briarty et al., 1979). Expansins, a type of protein inducing cell wall extension, have been found to be associated with grain size dynamics (Lizana et al., 2010). Grain dimensions then decrease slightly, and reach final size at maturity (Millet and Pinthus, 1984; Lizana et al., 2010). Final grain length, width, height and volume are closely associated with grain weight (Millet and Pinthus, 1984; Breseghello and Sorrells, 2007; Gegas et al., 2010; Lizana et al., 2010; Hasan et al., 2011), and many QTL for these traits have been identified (Breseghello and Sorrells, 2007; Gegas et al., 2010; Williams et al., 2013).

There is a great variation in final grain weight within spikes for a given genotype. A spike of wheat comprises c. 16−25 spikelets, and each spikelet sets c. 0−5 grains, depending on genotype, environment and spikelet position within spike. The second grain (G2) from the rachis is usually largest, followed by the first (G1), third (G3), and more distal ones if present (Calderini and Reynolds, 2000; Calderini and Ortiz-Monasterio, 2003; Hasan et al., 2011). The average grain weight across different positions within spikelets would be increased by c. 15% (estimated from numerous previous studies), if all other grains reach the grain weight of G2. For this to be realised, the distal grains (G3 and farther), therefore, need to be enlarged. It has been observed that the distal florets produce smaller carpels at anthesis (Singh and Jenner, 1982; Calderini et al., 1999). During grain filling, distal grains show a slower rate and shorter effective duration of grain filling (Simmons and Crookston, 1979; Millet and

Pinthus, 1984), lower grain water content and smaller grain dimensions (Lizana et al., 2010; Hasan et al., 2011), probably as a consequence of having fewer endosperm cells (Singh and Jenner, 1982; Gao et al., 1992).

How grain weight is determined throughout the grain filling has only been partially elucidated in wheat. Earlier studies usually focus on part of the grain filling processes through experiments evaluating a few contrasting genotypes. In this study, a large number of genotypes from a bread wheat × spelt mapping population were used, and a wide range of key traits (carpel size at anthesis, grain dry matter accumulation, grain water uptake and loss, grain morphological expansion, and final grain weight) were analysed to provide a comprehensive understanding of grain weight determination. Subsequently, the genetic loci underlying these traits were identified. To understand the grain weight variation within spikelets, the physiological and genetic differences in grain filling patterns between distal and basal grains were then evaluated in detail.

6.3 Materials and methods

Details of plant materials, field conditions, statistical analysis of phenotypic data and QTL identification have been described previously in the section of **Materials and methods** of **Chapter 2**.

6.3.1 Carpel dissection at anthesis

The carpel is the unfertilised female organ, containing ovary, style and feathery stigma (Fig. 6-1A). Five main spikes from each plot of the subsets were sampled once the first anthers in the middle spikes were just visible. Two middle spikelets of each spike in 2012 and three spikelets of one side of each spike (the third one counting from spike base, the third one from spike tip, and the middle one between them) in 2013 were collected. Carpels from the first, second and third florets within spikelets counting from the rachis, namely Carpel 1 (C1), Carpel 2 (C2) and Carpel 3 (C3), were removed carefully using forceps. The fourth and more distal florets were discarded as they finally became infertile in the most RILs. C1, C2 and C3 were pooled, respectively, and dried in an oven at 85^{o}C for 48 h. Carpel dry weight was recorded using an electronic balance (± 0.0001 g) (125A, Precisa, Switzerland).

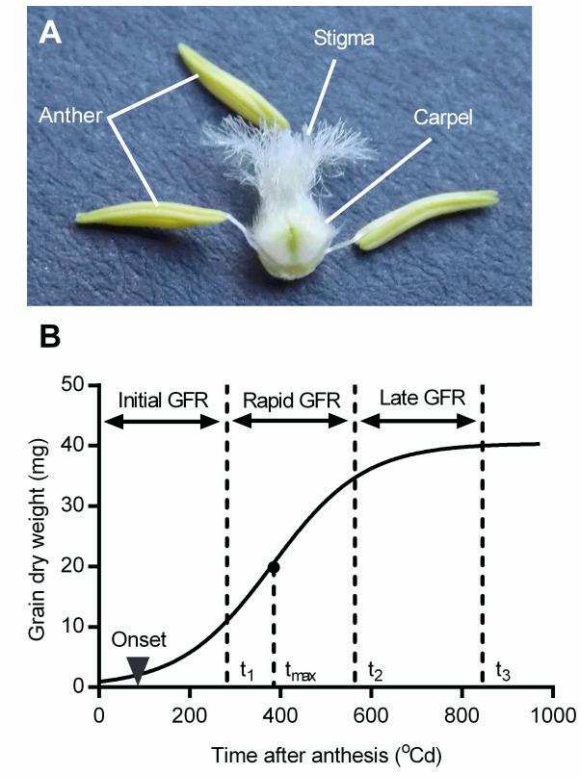

Fig. 6-1 Carpel from wheat floret (A) and the schematic diagram of grain dry matter accumulation over the accumulated thermal time from anthesis (base temperature 0 ^{o}C) (B). Data of grain dry weight was fitted to a logistic growth curve over time after anthesis. Total grain filling duration (t_3) was divided equally into three phases: initial (anthesis to t_1), rapid (t_1 to t_2), and late (t_2 to t_3). Average grain filling rate (GFR) during each phase was calculated, and termed initial, rapid and late GFR. Onset of grain filling and maximum grain filling rate are indicated by a triangle and closed circle (at the time t_{max}), respectively.

6.3.2 Grain dry matter and water accumulation

From anthesis onwards, the dynamics of grain dry matter and water accumulation were investigated until maturity. Two representative spikes (but five spikes at anthesis and maturity) from each plot were collected every five days. Spikelet sampling and dissecting followed the same procedure as that for carpel analysis. Grains from the first, second and third florets within spikelets counting from the rachis, were named Grain 1 (G1), Grain 2 (G2) and Grain 3 (G3), respectively. G1, G2 and G3 were weighed immediately for fresh weight and again after drying at 85^{o}C for 48 h, and grain water content was calculated as the difference between them.

For each of G1, G2 and G3, a logistic growth curve was fitted to the grain dry weight data (Fig. 6-1B) (Zahedi and Jenner, 2003; Wang et al., 2009).

$$W_{\mathrm{d}} = A + \frac{C}{1 + \mathrm{e}^{-B(t-M)}}$$

where W_d is the individual grain dry weight, A is the lower asymptote, (A + C) is the upper asymptote (final grain weight), B is the doubled relative growth rate at the time M, M is the time when the absolute grain filling rate is at maximum, and when grains grow to (A + 0.5C), and t is the accumulated thermal time after anthesis in degree days (^{o}Cd; degree days after anthesis, DAA).

Grain filling duration (t_3) was calculated from anthesis to the time when grains had grown to (A + 0.99C) (t_3 = M + 4.5951/B). This period was then divided equally into three phases, corresponding to the time courses of endosperm cell division and grain expansion, rapid grain filling, and maturation, respectively (Shewry et al., 2012). The grain filling rates during each phase and across the whole grain filling period were calculated, and termed initial, rapid, late and average grain filling rates. Onset of grain filling (t_{onset}) was calculated when grains had grown to (A + 0.05C) (t_{onset} = M – 2.9444/B). At the time M (t_{max}), maximum grain filling rate (MGFR) was reached (MGFR = BC/4).

For the water content of G1, G2 and G3, a cubic function was fitted.

$$W_{\mathrm{W}} = b_3 t^3 + b_2 t^2 + b_1 t + a$$

where W_w is the individual grain water content, t is the accumulated thermal time after anthesis, b_3, b_2, b_1 and a are coefficients.

When $dW_w/dt = 0$, $W_w = W_{max}$ (maximum water content, MWC), $t = t_{mwc}$ (the time at maximum water content),

$$W_{\max} = b_3 t_{\mathrm{mwc}}^3 + b_2 t_{\mathrm{mwc}}^2 + b_1 t_{\mathrm{mwc}} + a$$

$$t_{\mathrm{mwc}} = \frac{-b_2 - \sqrt{b_2^2 - 3b_1 b_3}}{3b_3}$$

Average water absorption rate and water loss rate (desiccation) of grains were also calculated as the slopes of linear functions from anthesis to t_{mwc}, and from t_{mwc} to the time for last measurement, respectively.

6.3.3 Grain dimensions

Ten genotypes differing in grain weight were selected to observe the dynamics of grain expansion in 2013. Grain samples were the same as those used for grain dry matter and water analysis. After dissection, grain length, width and height (thickness, grain crease downward) of G1, G2 and G3 were measured immediately using an electronic calliper (OD-15CP, Mitutoyo, UK).

At maturity, grain dimensions across G1, G2 and G3 were evaluated in the subset and 226 RILs in 2012 and 2013, respectively. In 2012, nine representative grains from each plot were measured for grain length, width and height using an electronic calliper (OD-15CP, Mitutoyo, UK). In 2013, digital image analysis for grain dimensions was used (Breseghello and Sorrells, 2007). Twenty grains from each plot were spread onto a scanner bed (Officejet 4500, HP, USA). For each sample, two images, one with grain crease downward and the other with lateral side downward, were taken at a resolution of 200 ppi. With the software ImageJ (National Institutes of Health, USA, http://rsbweb.nih.gov/ij/), the images were segmented into intact grains and background using the 'Color Threshold' feature, and grain dimensions were measured using the 'Analyze Particles' feature by fitting the best ellipses. Major and minor axes of the best fitting ellipses corresponded to grain length and width (the first image) or grain length and height (the second image), respectively.

Grain volume was calculated by considering grain as an ellipsoid and applying the geometric formula: $V_g = (4/3)\pi abc$, where V_g is the grain volume, $\pi = 3.1416$, a = 0.5 grain length, b = 0.5 grain width, and c = 0.5 grain height (Breseghello and Sorrells, 2007; Hasan et al., 2011). In addition, the ratios of grain length to width (L/W) and of

grain length to height (L/H) were calculated as grain shape parameters (Breseghello and Sorrells, 2007; Gegas et al., 2010).

6.3.4 Timing of rapid flag leaf senescence

Ten genotypes, as described previously, were used to determine the timing of rapid flag leaf senescence. In 2012, a scale of 10 (fully green) to 0 (fully senesced) was used for visual assessment based on the whole canopy. Assessment started from anthesis at a 5-day interval until maturity. In 2013, flag leaves from the same shoots used for grain dimension analysis were collected at a 5-day interval. Green and yellow parts of each leaf were separated, and both measured for area using an area meter (LI3100, LI-COR, USA). The percentage of green area was used to quantify the senescence progress.

A Gompertz descending curve was then fitted to the data of visual scoring and percent green area (Gooding et al., 2000).

$$G = A + C\mathrm{e}^{-\mathrm{e}^{-B(t-M)}}$$

where G is the visual scores or percent green area, A is the lower asymptote (fully senesced), (A + C) is the upper asymptote (the initial values), B is the relative senescence rate at the time M, M is the time when maximum senescence rate (msr) is reached (t_{msr}), and t is the accumulated thermal time after anthesis.

6.3.5 De-graining at anthesis

A de-graining experiment was conducted in the bread wheat parent Forno and another bread wheat cultivar T. aestivum L. 'Duxford' in 2013. Five main spikes from a plot were selected at anthesis, and all the spikelets along one side of each spike removed (virtually doubling the assimilate availability for the remaining grains), while five intact spikes were used as control. G1, G2 and G3 from the de-graining and control spikes were recorded for dry weight at maturity.

6.4 Results

6.4.1 Carpel size, grain dry matter and water accumulation, and grain dimensions, are associated with final grain weight

Large differences between the parents and between the RILs in final grain weight and grain filling traits were found (Supplementary Table S6-1), hence allowing further physiological and genetic analysis. H^2 of grain weight, average grain filling rate, grain water accumulation, and grain dimensions (except grain width) across different grain positions, were relatively high (0.68−0.81) (Supplementary Table S6-1), indicating strong genetic control.

Regression analysis showed that the carpel size at anthesis was positively associated with grain weight at maturity in both years (Fig. 6-2). Initial, rapid and maximum grain filling rates were also positively associated with final grain weight, and there was a close relationship between average grain filling rate and final grain weight. In contrast, grain filling duration and t_{max} were positively but weakly associated with grain weight. The onset of grain filling, however, was negatively associated with grain weight, indicating the importance of earlier grain filling. In addition, grain water accumulation showed close relationships with final grain weight consistently across years, especially the maximum grain water content (Fig. 6-2).

Grain dimensions expanded rapidly after anthesis (Supplementary Fig. S6-1), and grain length reached maximum first (410 DAA), followed by grain width, height and volume (530 DAA). Grain length, width, height and volume then decreased during the desiccation phase, by 6%, 16%, 13%, and 30%, respectively. Maximum and final grain dimensions were positively associated with grain weight, in particular maximum grain height and volume (Fig. 6-3). Slimmer grains (L/W) appeared to be associated with slightly heavier grains.

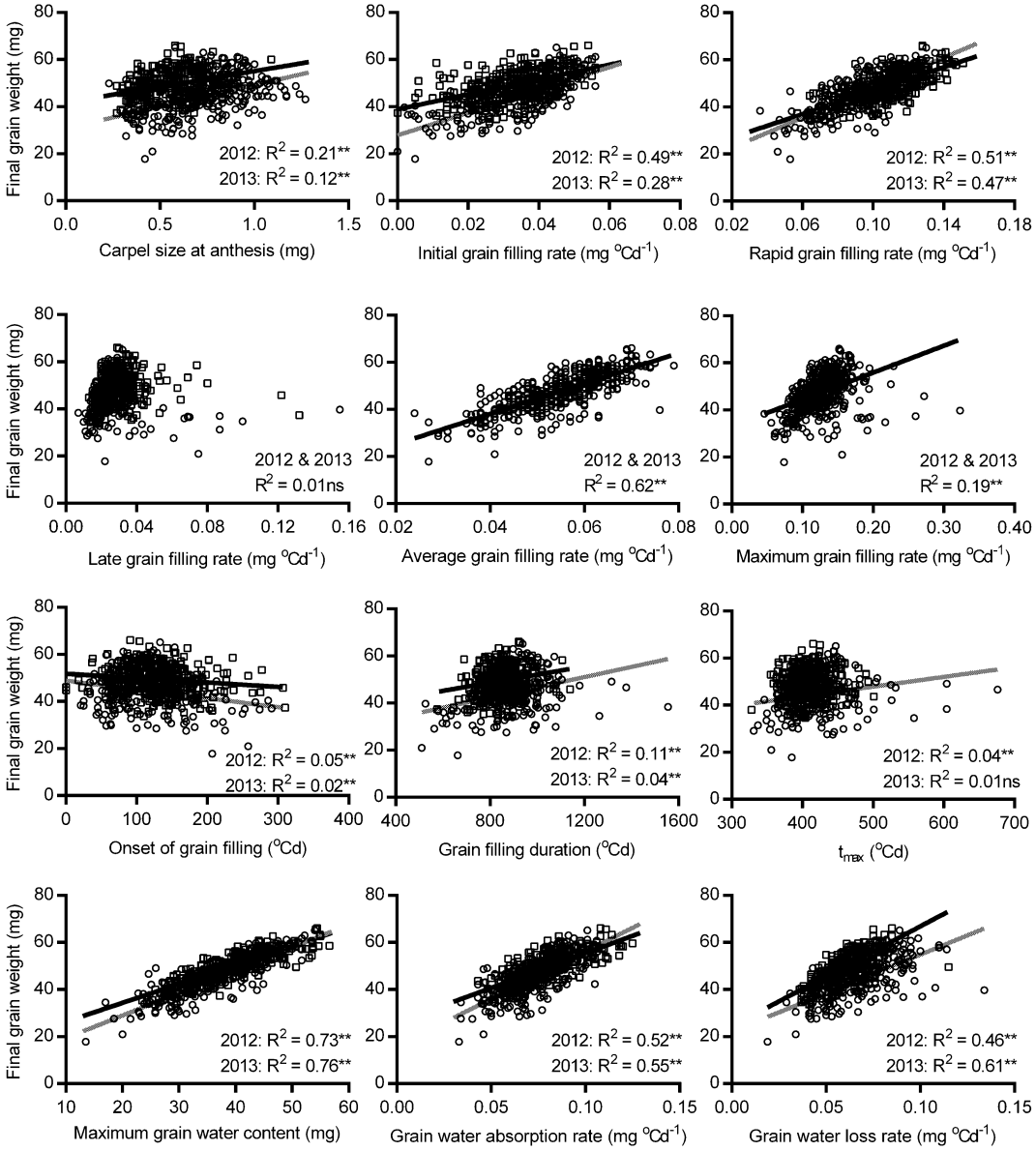

Fig. 6-2 Relationships between carpel size at anthesis, grain dry matter and water accumulation, and final grain weight. Data in 2012 and 2013 are indicated by the circles (grey regression lines) and squares (black regression lines), respectively. Significance levels for regression analysis: ns, not significant; * $P < 0.05$; ** $P < 0.01$. A common line is used to explain both years in the graphs indicated by '2012 & 2013'. Trait abbreviation: t_{max}, the time at maximum grain filling rate.

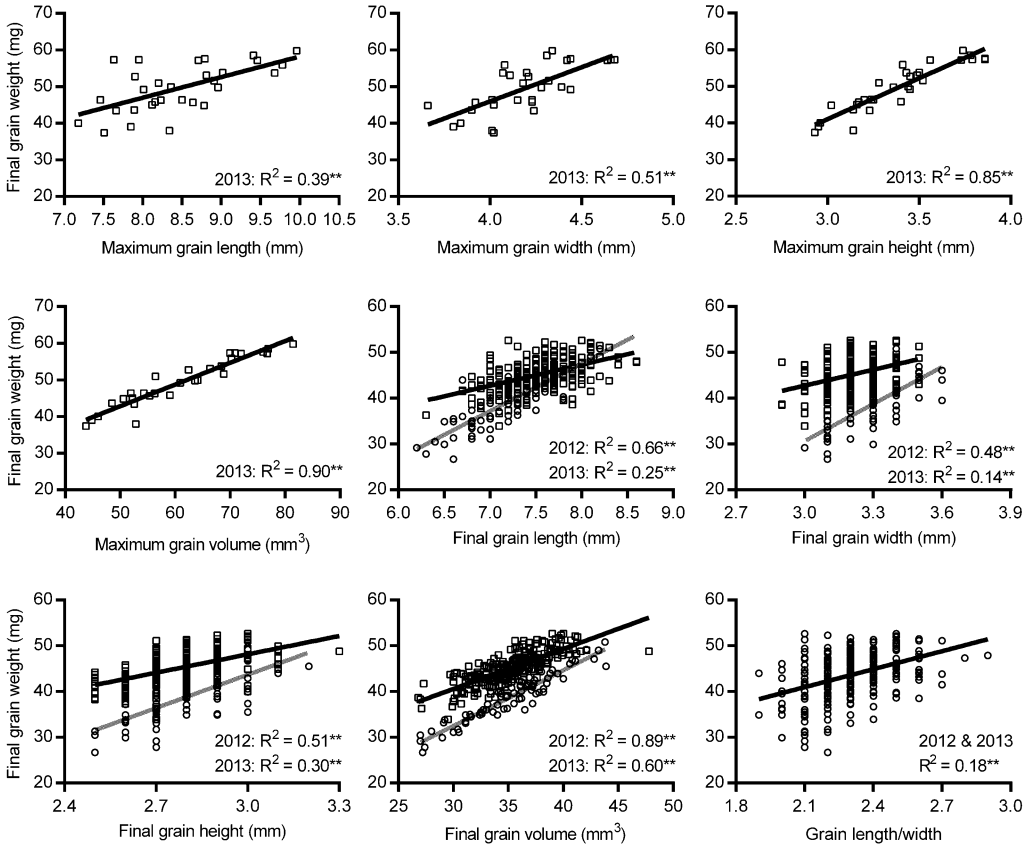

Fig. 6-3 Relationships between grain dimensions and final grain weight. Data in 2012 and 2013 are indicated by the circles (grey regression lines) and squares (black regression lines), respectively. Significance levels for regression analysis: * $P < 0.05$; ** $P < 0.01$. A common line is used to explain both years in the graph indicated by '2012 & 2013'.

6.4.2 Carpel size, grain dry matter and water accumulation, and grain dimensions interact with each other

Larger carpels at anthesis greatly contributed to higher initial rate, and to a lesser extent, rapid rate of grain filling; however, carpel size was negatively correlated with late grain filling rate (Table 6-1). Grain filling progress was also affected by carpel size: the larger carpels, the earlier grain filling and t_{max}, and the slightly longer grain filling duration. In addition, carpel size was positively associated with maximum grain water content, grain water absorption and loss rates (Table 6-1).

There were close relationships between grain water and dry matter accumulation (Table 6-2). Maximum grain water content, and grain water absorption and loss rates, strongly contributed to grain filling rates, especially the rapid one. Faster grain water absorption rate was associated with earlier grain filling and t_{max}. Additionally, grain water accumulation strongly contributed to maximum and final grain dimensions, in particular grain height and volume (Table 6-2).

Maximum and final grain dimensions were strongly correlated ($r = 0.83-0.92$, $P < 0.01$). Both showed similar positive relationships with grain filling rates (Tables 6-3 and 6-4).

Table 6-1 Phenotypic correlations between carpel size at anthesis, and grain dry matter and water accumulation

Grain filling trait[a]	Carpel size at anthesis	
	2012	2013
Initial grain filling rate	0.73**	0.51**
Rapid grain filling rate	0.21**	0.14**
Late grain filling rate	-0.31**	-0.26**
Average grain filling rate	0.28**	0.20**
Maximum grain filling rate	-0.10	-0.07
Onset of grain filling	-0.59**	-0.41**
Grain filling duration	0.16*	0.11*
t_{max}	-0.25**	-0.32**
Maximum grain water content	0.44**	0.33**
Water absorption rate	0.49**	0.39**
Water loss rate	0.28**	0.16**
t_{mwc}	-0.14*	-0.24**

[a] Trait abbreviations: t_{max}, the time at maximum grain filling rate; t_{mwc}, the time at maximum grain water content.

* $P < 0.05$, ** $P < 0.01$.

Table 6-2 Phenotypic correlations of grain water accumulation with grain dry matter accumulation and grain dimensions

Grain filling and dimension[a]	Maximum grain water content		Water absorption rate		Water loss rate		t_{mwc}	
	2012	2013	2012	2013	2012	2013	2012	2013
Initial grain filling rate	0.58**	0.44**	0.67**	0.50**	0.25**	0.26**	-0.26**	-0.30**
Rapid grain filling rate	0.84**	0.77**	0.69**	0.71**	0.75**	0.66**	0.28**	-0.04
Late grain filling rate	0.09	0.21**	-0.04	0.15**	0.33**	0.22**	0.34**	0.13*
Average grain filling rate	0.89**	0.87**	0.76**	0.82**	0.82**	0.72**	0.27**	-0.10
Maximum grain filling rate	0.51**	0.58**	0.34**	0.51**	0.64**	0.52**	0.39**	0.05
Onset of grain filling	-0.13	-0.07	-0.34**	-0.19**	0.21**	0.08	0.55**	0.37**
Grain filling duration	-0.09	-0.10	-0.08	-0.21**	-0.20**	0.02	0.00	0.31**
t_{max}	-0.19**	-0.19**	-0.34**	-0.44**	-0.07	0.12*	0.42**	0.75**
Maximum grain length	–[b]	0.65**	–	0.57**	–	0.75**	–	0.09
Maximum grain width	–	0.78**	–	0.78**	–	0.52**	–	-0.36*
Maximum grain height	–	0.91**	–	0.86**	–	0.78**	–	-0.19
Maximum grain volume	–	0.95**	–	0.89**	–	0.85**	–	-0.15
Final grain length	0.65**	0.45*	0.52**	0.34	0.60**	0.54**	0.27*	0.25
Final grain width	0.40**	0.57**	0.21	0.58**	0.33**	0.29	0.39**	-0.33
Final grain height	0.69**	0.84**	0.59**	0.78**	0.47**	0.75**	0.20	-0.14
Final grain volume	0.76**	0.84**	0.59**	0.77**	0.60**	0.75**	0.34**	-0.07
Grain length/width	0.37**	0.09	0.38**	-0.01	0.36**	0.31	-0.02	0.39*
Grain length/height	-0.02	-0.28	-0.05	-0.34	0.13	-0.12	0.08	0.36*

[a] Trait abbreviations: t_{max}, the time at maximum grain filling rate; t_{mwc}, the time at maximum grain water content.

[b] Data absent.

* P < 0.05, ** P < 0.01.

Table 6-3 Phenotypic correlations between maximum grain dimensions and grain dry weight accumulation

Grain filling trait	Maximum grain length	Maximum grain width	Maximum grain height	Maximum grain volume
Initial grain filling rate	0.16	0.67**	0.72**	0.62**
Rapid grain filling rate	0.75**	0.61**	0.76**	0.86**
Late grain filling rate	0.63**	0.12	0.30	0.46*
Average grain filling rate	0.71**	0.69**	0.85**	0.92**
Maximum grain filling rate	0.75**	0.50**	0.69**	0.80**
Onset of grain filling	0.25	-0.37*	-0.27	-0.13
Grain filling duration	-0.42*	-0.17	-0.17	-0.25
t_{max}[a]	-0.15	-0.41*	-0.34	-0.31

[a] t_{max}, the time at maximum grain filling rate.

* P < 0.05, ** P < 0.01.

Table 6-4 Phenotypic correlations between final grain dimensions and grain dry weight accumulation

Grain filling trait[a]	Grain length		Grain width		Grain height		Grain volume		Grain length/width		Grain length/height	
	2012	2013	2012	2013	2012	2013	2012	2013	2012	2013	2012	2013
Initial GFR	0.42**	-0.05	0.26*	0.60**	0.39**	0.71**	0.45**	0.53**	0.24*	-0.34	0.04	-0.64**
Rapid GFR	0.60**	0.54**	0.35**	0.37*	0.54**	0.68**	0.65**	0.75**	0.34**	0.26	0.06	-0.07
Late GFR	0.49**	0.62**	0.26*	-0.03	0.45**	0.24	0.53**	0.43*	0.30**	0.53**	0.06	0.38*
Average GFR	0.64**	0.49**	0.38**	0.46**	0.59**	0.78**	0.71**	0.80**	0.37**	0.17	0.06	-0.20
Maximum GFR	0.59**	0.60**	0.34**	0.29	0.54**	0.61**	0.64**	0.72**	0.35**	0.35	0.06	0.05
Onset of GF	0.28*	0.40*	0.27*	-0.38*	0.26*	-0.28	0.35**	-0.06	0.07	0.53**	0.01	0.61**
GF duration	0.03	-0.02	0.20	0.12	-0.03	-0.07	0.05	-0.02	-0.12	-0.07	0.06	0.06
t_{max}	0.19	0.29	0.37**	-0.19	0.12	-0.27	0.26*	-0.06	-0.09	0.34	0.08	0.50**

[a] Trait abbreviations: GFR, grain filling rate; GF, grain filling; t_{max}, the time at maximum grain filling rate.

* $P < 0.05$, ** $P < 0.01$.

6.4.3 QTL coincidences reflect the physiological relationships between grain filling traits and grain weight, and among grain filling traits

A total of 249 significant QTL were detected in the Forno × Oberkulmer mapping population across two years, including 26 QTL for final grain weight, 13 for carpel size, 81 for grain dry matter accumulation, 90 for grain water accumulation, and 39 for final grain dimensions (Fig. 6-4 and Table 6-5). These QTL were scattered on 18 chromosomes, individually explaining 6.6−39.5% of the phenotypic variation. Each parent provided about half of the increasing alleles: 122 from the bread wheat Forno and 127 from the spelt Oberkulmer.

QTL coincidence analysis revealed that each QTL for final grain weight was coincident with 2−13 traits of grain filling (Fig. 6-4 and Supplementary Table S6-2). For carpel size, 69% of the QTL were coincident with those for final grain weight on chromosomes 2A, 3B, 4A, 5A, 5DL, and 7B. Likewise, 75% of the QTL for grain dry matter accumulation, 84% for grain water accumulation, and 64% for grain dimensions at maturity were coincident with those for grain weight. All coincident QTL had the increasing alleles conferred by the same parents (Fig. 6-4). The exceptions were the QTL for the onset of grain filling on chromosome 4A (the decreasing allele desired), and one QTL for carpel size on 7B (the increasing allele conferred by Oberkulmer). These QTL coincidences explained the positive physiological relationships between final grain weight and grain filling traits.

Nine QTL for carpel size were coincident with 27 QTL for initial, rapid and average grain filling rates (Fig. 6-4 and Supplementary Table S6-3); the increasing alleles of

these QTL (except the one for carpel size on 7B) were conferred by the same parents. Similarly, 10 and 11 QTL for carpel size were coincident with 46 QTL for grain water accumulation (excluding t_{mwc}) and with 20 QTL for final grain dimensions at maturity, respectively, with the increasing alleles conferred by the same parents (except one QTL for carpel size on 7B, one for each of L/W and L/H on 5A).

QTL coincidences between grain water and dry matter accumulation occurred on seven chromosomes (2A, 3B, 4A, 4DL, 5A, 5DL, and 7B), including 71 of 85 QTL for maximum grain water content, grain water absorption and loss rates, and 60 of 78 QTL for the initial, rapid, late, average and maximum grain filling rates (Fig. 6-4). Furthermore, QTL coincidences between grain water accumulation (72 of 85 QTL) and final grain dimensions (26 of 31 QTL for length, width, height and volume) occurred on seven chromosomes (1BS, 2A, 3B, 4A, 5A, 5DL, and 7B). These coincident QTL had the same parents conferring the increasing alleles, confirming the positive physiological relationships among them (Table 6-2). Similar QTL coincidences were also observed between final grain dimensions and grain filling rates (Fig. 6-4).

Taken together, QTL coincidences among final grain weight, carpel size, grain dry matter and water accumulation, and final grain dimensions were found on 16 chromosomes, with the increasing alleles usually conferred by the same parents, indicating pleiotropy or the tight linkages of functionally related genes. This is consistent with their physiological relationships. Interestingly, a large number of coincident QTL were observed on chromosomes 2A (36 QTL for 12 traits), 3B (37 QTL for 13 traits), 4A (39 QTL for 14 traits), 5A (16 QTL for 13 traits), 5DL (20 QTL for 12 traits), and 7B (49 QTL for 12 traits).

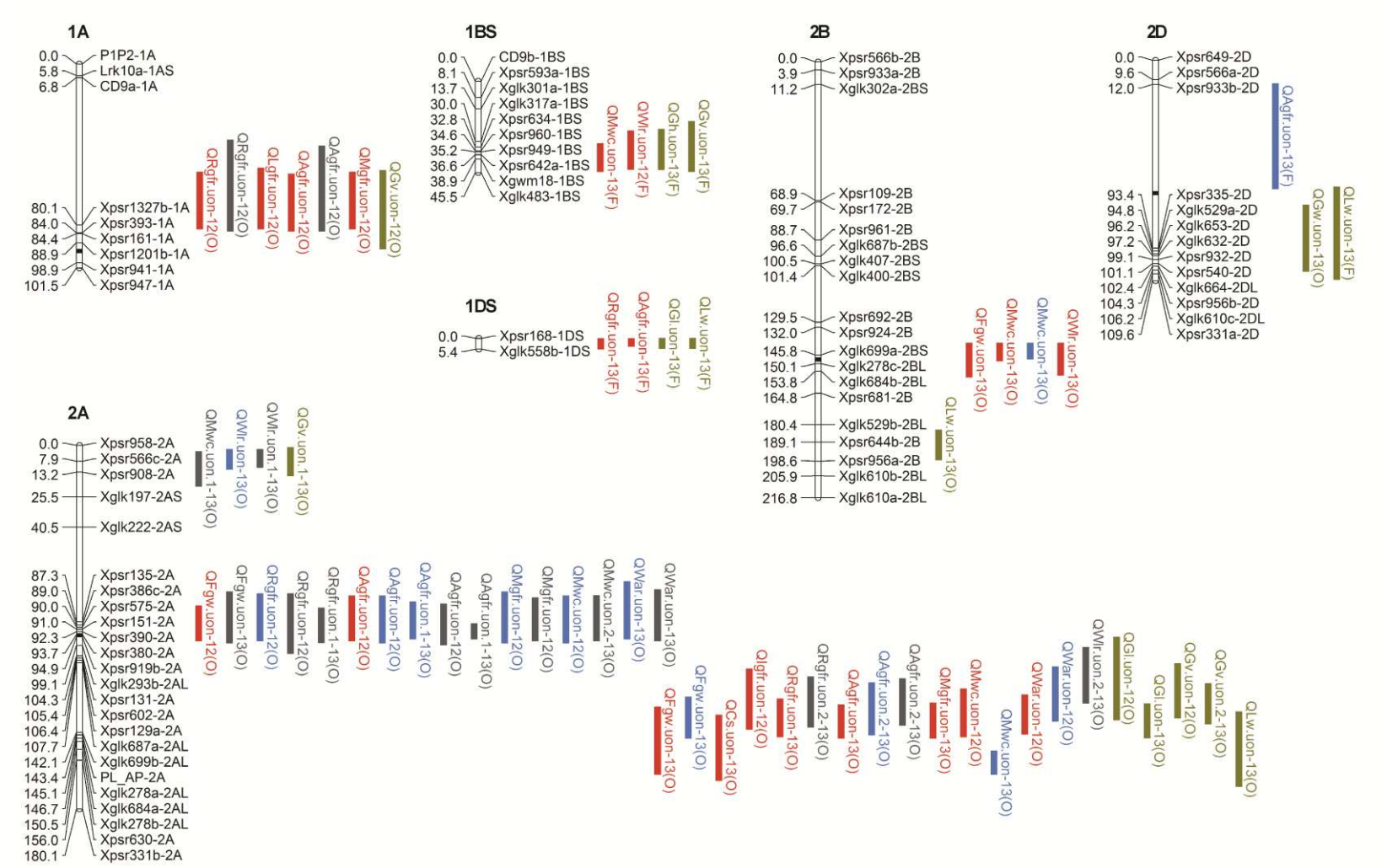

Fig. 6-4 (see the caption below)

Fig. 6-4
(continued)

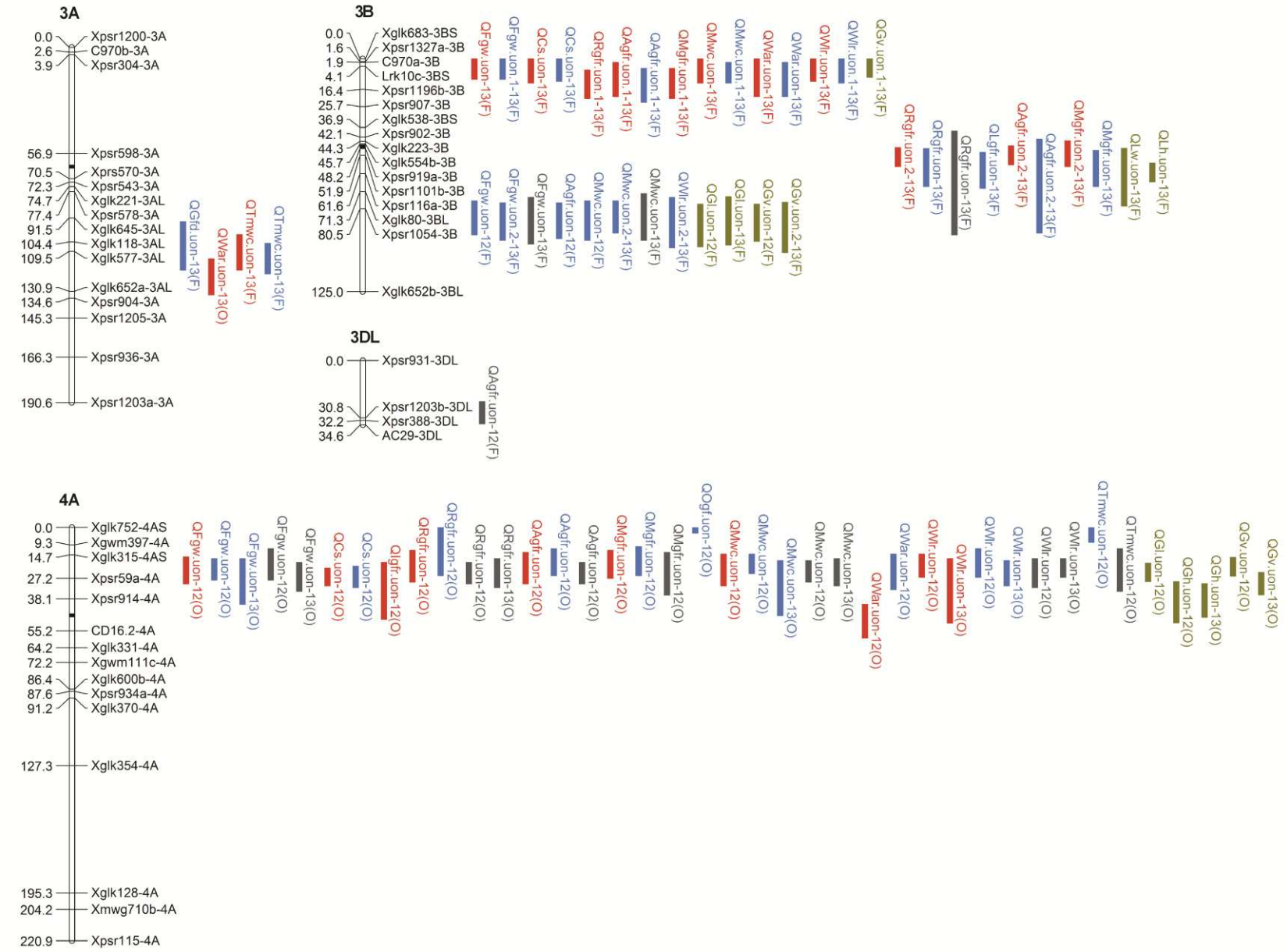

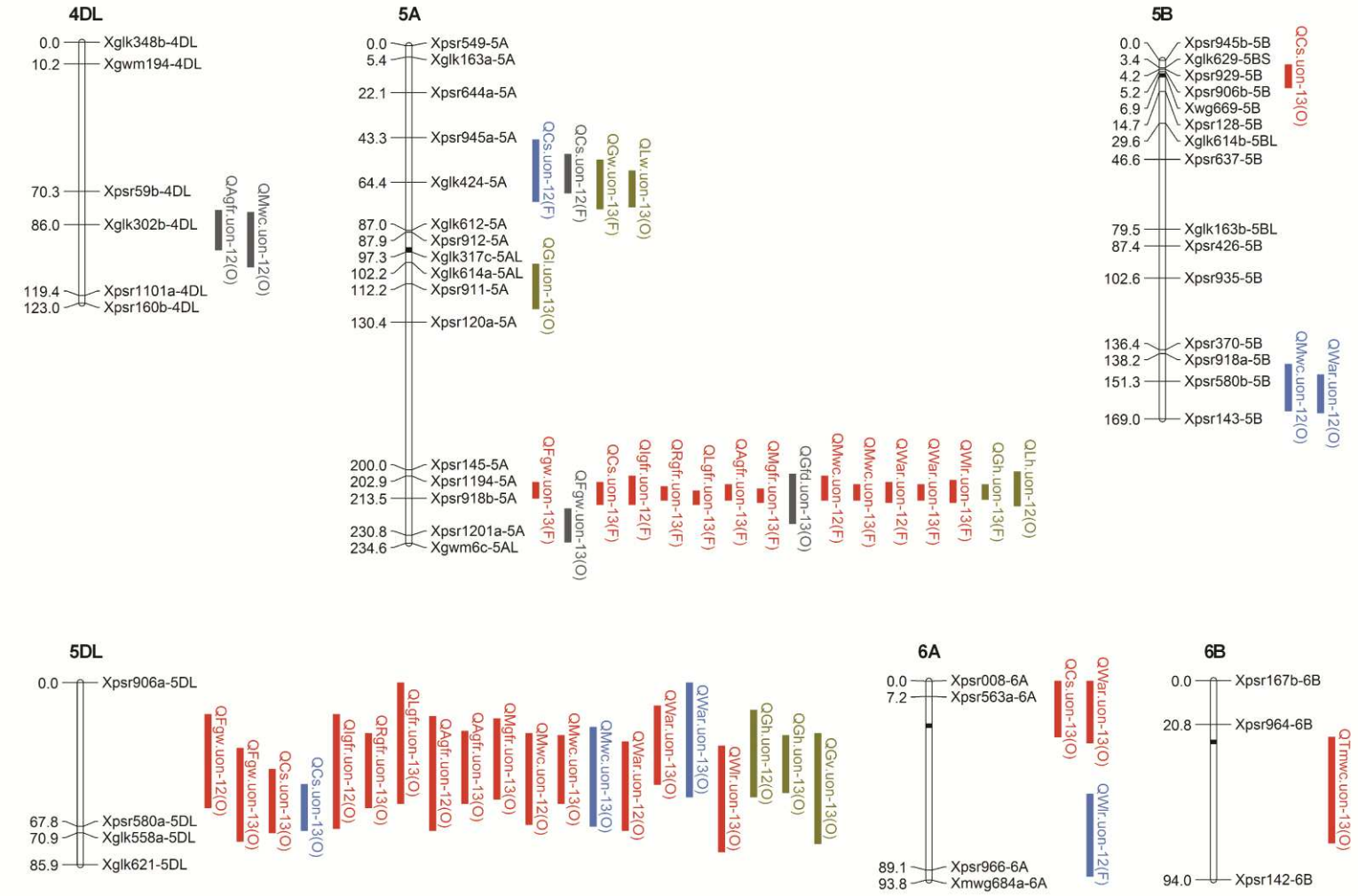

Fig. 6-4 (continued)

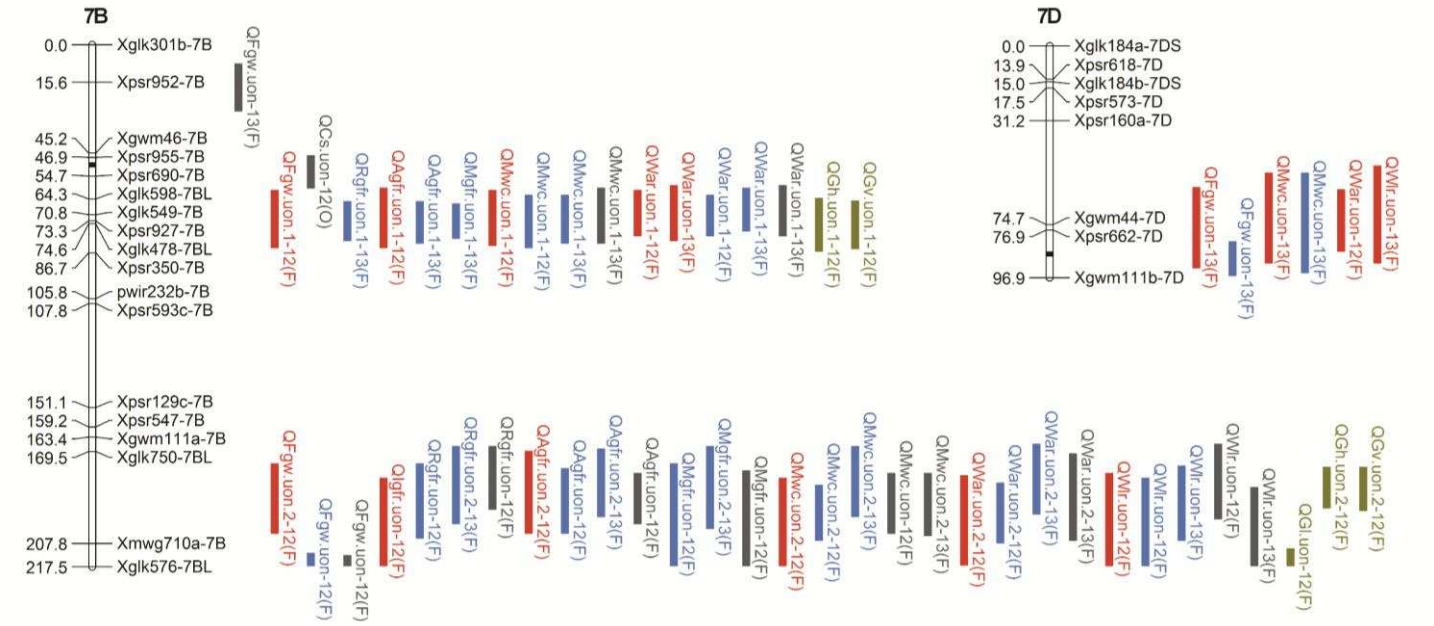

Fig. 6-4 Quantitative trait locus (QTL) identification for grain weight, carpel size, grain dry matter and water accumulation, and grain dimensions. The 1-LOD support intervals of significant QTL are indicated by red (Grain 1 or Carpel 1), blue (Grain 2 or Carpel 2), grey (Grain 3 or Carpel 3), and green (grain dimensions across different grain positions) vertical bars. A QTL symbol consists of a letter 'Q', trait abbreviation, laboratory name (uon), a serial number (if more than one QTL for the trait were detected on the same chromosome), a suffix 12 or 13 (QTL detected in 2012 or 2013), and the parentheses with the parent providing the increasing allele (increasing the value of the trait): F, bread wheat Forno; O, spelt Oberkulmer. Trait abbreviations: Fgw, final grain weight; Cs, carpel size; Igfr, initial grain filling rate; Rgfr, rapid grain filling rate; Lgfr, late grain filling rate; Agfr, average grain filling rate; Mgfr, maximum grain filling rate; Ogf, onset of grain filling; Gfd, grain filling duration; Tmax, the time at maximum grain filling rate; Mwc, grain maximum water content; War, grain water absorption rate; Wlr, grain water loss rate; Tmwc, the time at maximum grain water content; Gl, grain length; Gw, grain width; Gh, grain height; Gv, grain volume; Lw, grain length/width; Lh, grain length/height.

Table 6-5 Quantitative trait locus (QTL) identification for grain weight, carpel size, grain dry matter and water accumulation, and grain dimensions

Trait/Chromosome	Year	Position (cM)	LOD	R^{2a}	Additive effect[b]	Closest marker
Final grain weight						
Grain 1 (mg)						
2A	2012	94.9	3.14	18.7	-3.02	Xpsr919b-2A
	2013	142.1	3.14	12.3	-1.86	Xglk699b-2AL
2B	2013	145.8	3.16	12.4	-1.83	Xglk699a-2BS
3B	2013	1.0	4.76	18.1	2.36	Xpsr1327a-3B
4A	2012	21.7	5.54	30.5	-4.52	Xpsr59a-4A
5A	2013	209.9	8.70	30.5	3.37	Xpsr918b-5A
5DL	2012	36.0	3.55	20.8	-6.71	Xpsr580a-5DL
	2013	48.0	5.48	20.5	-4.45	Xpsr580a-5DL
7B	2012	70.7	3.54	20.8	3.29	Xglk549-7B
	2012	189.5	3.75	21.9	4.82	Xmwg710a-7B
7D	2013	84.8	4.06	15.6	2.45	Xpsr662-7D
Grain 2 (mg)						
2A	2013	143.4	3.20	12.6	-1.62	PL_AP-2A
3B	2012	80.5	4.17	24.0	3.49	Xpsr1054-3B
	2013	1.9	3.66	14.2	1.76	C970a-3B
	2013	80.5	5.47	20.5	2.14	Xpsr1054-3B
4A	2012	21.7	5.80	31.7	-4.53	Xpsr59a-4A
	2013	32.2	4.01	15.4	-2.10	Xpsr59a-4A
7B	2012	217.4	3.56	20.9	3.10	Xglk576-7BL
7D	2013	92.8	3.37	13.2	1.84	Xgwm111b-7D
Grain 3 (mg)						
2A	2013	90.9	4.91	18.6	-2.28	Xpsr151-2A
3B	2013	80.5	3.38	13.2	2.03	Xpsr1054-3B
4A	2012	21.7	4.16	23.9	-4.14	Xpsr59a-4A
	2013	24.7	4.72	17.9	-2.64	Xpsr59a-4A
5A	2013	227.4	3.29	12.9	-2.18	Xpsr1201a-5A
7B	2012	217.0	3.46	20.3	3.22	Xglk576-7BL
	2013	15.6	3.28	12.8	2.16	Xpsr952-7B
Carpel size						
Carpel 1 (mg)						
2A	2013	153.5	2.95	11.6	-0.04	Xglk278a-2AL
3B	2013	1.9	5.36	20.1	0.05	C970a-3B
4A	2012	27.2	4.07	23.5	-0.079	Xpsr59a-4A
5A	2013	210.9	6.20	22.9	0.06	Xpsr918b-5A
5B	2013	7.9	3.32	13.0	-0.05	Xwg669-5B
5DL	2013	67.8	4.62	17.6	-0.05	Xpsr580a-5DL
6A	2013	4.0	3.75	14.5	-0.05	Xpsr563a-6A

[a] R^2: the proportion of phenotypic variation explained by individual QTL.

[b] Positive additive effects indicate that the alleles from Forno increase the values of the traits, whereas negative additive effects indicate that the alleles from Oberkulmer increase the values of the traits.

Table 6-5 (continued)

Trait/Chromosome	Year	Position (cM)	LOD	R^2	Additive effect	Closest marker
Carpel 2 (mg)						
3B	2013	1.9	4.30	16.5	0.03	C970a-3B
4A	2012	27.2	3.78	22.0	-0.060	Xpsr59a-4A
5A	2012	58.3	3.29	19.4	0.066	Xglk424-5A
5DL	2013	67.7	3.60	14.0	-0.03	Xpsr580a-5DL
Carpel 3 (mg)						
5A	2012	62.3	4.32	24.8	0.073	Xglk424-5A
7B	2012	51.9	3.93	22.8	-0.061	Xpsr690-7B
Grain dry matter accumulation						
Grain 1						
Initial grain filling rate (mg $^{o}Cd^{-1}$)						
2A	2012	125.7	2.90	17.0	-0.0038	Xglk699b-2AL
4A	2012	33.2	3.37	19.9	-0.0032	Xpsr914-4A
5A	2012	212.9	2.90	17.3	0.0030	Xpsr918b-5A
5DL	2012	40.0	2.93	17.5	-0.0054	Xpsr580a-5DL
7B	2012	194.5	3.22	19.1	0.0039	Xmwg710a-7B
Rapid grain filling rate (mg $^{o}Cd^{-1}$)						
1A	2012	80.1	3.28	19.4	-0.0071	Xpsr1327b-1A
1DS	2013	0.1	3.38	13.2	0.0057	Xpsr168-1DS
2A	2013	142.1	3.19	12.5	-0.0055	Xglk699b-2AL
3B	2013	13.1	3.35	13.1	0.0065	Xpsr1196b-3B
	2013	51.9	3.40	13.3	0.0059	Xpsr1101b-3B
4A	2012	18.7	3.04	18.1	-0.0077	Xglk315-4AS
5A	2013	211.9	7.64	27.4	0.0092	Xpsr918b-5A
5DL	2013	40.0	5.54	20.7	-0.0147	Xpsr580a-5DL
Late grain filling rate (mg $^{o}Cd^{-1}$)						
1A	2012	80.1	3.33	19.7	-0.0020	Xpsr1327b-1A
5A	2013	213.4	4.25	16.3	0.0030	Xpsr918b-5A
5DL	2013	32.0	2.73	10.8	-0.0048	Xpsr906a-5DL
Average grain filling rate (mg $^{o}Cd^{-1}$)						
1A	2012	80.1	3.04	18.1	-0.0033	Xpsr1327b-1A
1DS	2013	0.1	3.30	12.9	0.0027	Xpsr168-1DS
2A	2012	94.9	2.90	17.1	-0.0032	Xpsr919b-2A
	2013	142.1	3.23	12.7	-0.0026	Xglk699b-2AL
3B	2013	11.1	4.01	15.5	0.0034	Xpsr1196b-3B
	2013	51.9	3.11	12.2	0.0026	Xpsr1101b-3B
4A	2012	19.7	3.86	22.4	-0.0042	Xglk315-4AS
5A	2013	210.9	9.41	32.6	0.0048	Xpsr918b-5A
5DL	2012	39.0	3.34	19.7	-0.0071	Xpsr580a-5DL
	2013	39.0	5.71	21.2	-0.0071	Xpsr580a-5DL
7B	2012	70.7	3.05	18.2	0.0034	Xglk549-7B
	2012	187.5	3.07	18.3	0.0049	Xglk750-7BL

Table 6-5 (continued)

Trait/Chromosome	Year	Position (cM)	LOD	R^2	Additive effect	Closest marker
Maximum grain filling rate (mg $^oCd^{-1}$)						
1A	2012	80.1	3.27	19.4	-0.0082	Xpsr1327b-1A
2A	2013	142.1	3.10	12.2	-0.0072	Xglk699b-2AL
3B	2013	13.1	3.10	12.2	0.0083	Xpsr1196b-3B
	2013	51.9	3.06	12.0	0.0073	Xpsr1101b-3B
4A	2012	18.7	3.35	19.8	-0.0093	Xglk315-4AS
5A	2013	213.4	7.56	27.1	0.0116	Xpsr918b-5A
5DL	2013	37.0	4.74	18.0	-0.0184	Xpsr580a-5DL
Grain 2						
Rapid grain filling rate (mg $^oCd^{-1}$)						
2A	2012	94.9	3.90	22.6	-0.0079	Xpsr919b-2A
3B	2013	56.9	4.88	18.5	0.0066	Xpsr1101b-3B
4A	2012	18.7	3.62	21.2	-0.0087	Xglk315-4AS
7B	2012	190.5	3.51	20.6	0.0112	Xmwg710a-7B
	2013	74.6	3.22	12.6	0.0052	Xglk478-7BL
	2013	184.5	3.47	13.5	0.0075	Xglk750-7BL
Late grain filling rate (mg $^oCd^{-1}$)						
3B	2013	57.9	3.26	12.8	0.0024	Xpsr116a-3B
Average grain filling rate (mg $^oCd^{-1}$)						
2A	2012	94.9	4.01	23.2	-0.0035	Xpsr919b-2A
	2013	90.6	3.75	14.5	-0.0023	Xpsr151-2A
	2013	130.6	3.38	13.2	-0.0030	Xglk699b-2AL
2D	2013	41.9	3.04	11.9	0.0048	Xpsr933b-2D
3B	2012	80.5	3.43	20.2	0.0034	Xpsr1054-3B
	2013	12.1	3.63	14.1	0.0027	Xpsr1196b-3B
	2013	77.3	4.27	16.4	0.0027	Xpsr1054-3B
4A	2012	19.7	4.70	26.6	-0.0044	Xglk315-4AS
7B	2012	190.5	4.05	23.4	0.0052	Xmwg710a-7B
	2013	76.6	3.97	15.3	0.0027	Xglk478-7BL
	2013	183.5	4.12	15.8	0.0035	Xglk750-7BL
Maximum grain filling rate (mg $^oCd^{-1}$)						
2A	2012	94.9	3.69	21.5	-0.0089	Xpsr919b-2A
3B	2013	56.9	4.80	18.2	0.0083	Xpsr1101b-3B
4A	2012	18.7	3.81	22.2	-0.0103	Xglk315-4AS
7B	2012	191.5	3.34	19.7	0.0125	Xmwg710a-7B
	2013	74.6	3.20	12.5	0.0066	Xglk478-7BL
	2013	185.5	2.90	11.4	0.0088	Xglk750-7BL
Onset of grain filling (^oCd)						
4A	2012	0.1	3.54	20.8	-15	Xglk752-4AS
Grain filling duration (^oCd)						
3A	2013	107.3	3.52	13.7	25.9	Xglk577-3AL

Table 6-5 (continued)

Trait/Chromosome	Year	Position (cM)	LOD	R^2	Additive effect	Closest marker
Grain 3						
Rapid grain filling rate (mg $^{o}Cd^{-1}$)						
1A	2012	62.8	3.26	19.3	-0.0147	Xpsr1327b-1A
2A	2012	97.9	3.05	18.2	-0.0085	Xglk293b-2AL
	2013	88.9	3.44	13.4	-0.0062	Xpsr386c-2A
	2013	127.6	4.24	16.2	-0.0099	Xglk699b-2AL
3B	2013	66.6	3.70	14.3	0.0074	Xpsr116a-3B
4A	2012	24.7	4.98	28.0	-0.0119	Xpsr59a-4A
	2013	24.7	3.19	12.5	-0.0071	Xpsr59a-4A
7B	2012	182.5	5.02	28.1	0.0146	Xglk750-7BL
Average grain filling rate (mg $^{o}Cd^{-1}$)						
1A	2012	70.8	3.07	18.3	-0.0052	Xpsr1327b-1A
2A	2012	94.9	5.01	28.1	-0.0047	Xpsr919b-2A
	2013	90.9	4.92	18.6	-0.0031	Xpsr151-2A
	2013	126.6	4.76	18.1	-0.0044	Xglk699b-2AL
3DL	2012	32.2	3.35	19.8	0.0039	Xpsr388-3DL
4A	2012	23.7	6.39	34.3	-0.0061	Xpsr59a-4A
4DL	2012	86.0	3.25	19.2	-0.0038	Xglk302b-4DL
7B	2012	189.5	5.99	32.6	0.0075	Xmwg710a-7B
Maximum grain filling rate (mg $^{o}Cd^{-1}$)						
2A	2012	87.3	4.26	24.4	-0.0187	Xpsr135-2A
4A	2012	21.7	3.61	21.1	-0.0203	Xpsr59a-4A
7B	2012	192.5	3.53	20.7	0.0249	Xmwg710a-7B
Grain filling duration (^{o}Cd)						
5A	2013	208.9	2.93	11.5	-38.3	Xpsr918b-5A
Grain water accumulation						
Grain 1						
Maximum grain water content (mg)						
1BS	2013	39.9	3.32	13.0	2.47	Xgwm18-1BS
2A	2012	132.6	3.19	18.9	-3.80	Xglk699b-2AL
2B	2013	145.8	3.22	12.6	-2.22	Xglk699a-2BS
3B	2013	8.1	5.22	19.6	3.27	Lrk10c-3BS
4A	2012	20.7	4.70	26.6	-3.84	Xglk315-4AS
5A	2012	209.9	4.36	24.9	3.83	Xpsr918b-5A
	2013	209.9	9.37	32.4	4.18	Xpsr918b-5A
5DL	2012	41.0	4.21	24.2	-6.40	Xpsr580a-5DL
	2013	40.0	6.34	23.3	-6.36	Xpsr580a-5DL
7B	2012	71.7	3.46	20.3	3.03	Xglk549-7B
	2012	193.5	3.88	22.5	4.36	Xmwg710a-7B
7D	2013	81.8	3.68	14.3	2.69	Xpsr662-7D

Table 6-5 (continued)

Trait/Chromosome	Year	Position (cM)	LOD	R^2	Additive effect	Closest marker
Water absorption rate (mg $^oCd^{-1}$)						
2A	2012	133.6	4.34	24.8	-0.0085	Xglk699b-2AL
3A	2013	123.5	3.68	14.3	-0.0071	Xglk652a-3AL
3B	2013	10.1	3.16	12.4	0.0063	Lrk10c-3BS
4A	2012	49.1	3.92	22.7	-0.0070	CD16.2-4A
5A	2012	211.9	5.27	29.3	0.0081	Xpsr918b-5A
	2013	210.9	8.42	29.7	0.0094	Xpsr918b-5A
5DL	2012	45.0	4.54	25.8	-0.0125	Xpsr580a-5DL
	2013	32.0	5.03	19.0	-0.0138	Xpsr906a-5DL
6A	2013	2.0	3.27	12.8	-0.0058	Xpsr008-6A
7B	2012	68.3	3.29	19.4	0.0059	Xglk549-7B
	2012	194.5	3.24	19.2	0.0079	Xmwg710a-7B
	2013	67.3	3.14	12.3	0.0057	Xglk598-7BL
7D	2012	74.7	3.38	19.9	0.0058	Xgwm44-7D
Water loss rate (mg $^oCd^{-1}$)						
1BS	2012	32.8	3.24	19.2	0.0060	Xpsr634-1BS
2B	2013	147.8	3.02	11.9	-0.0034	Xglk699a-2BS
3B	2013	0.1	4.85	18.4	0.0043	Xglk683-3BS
4A	2012	19.7	4.43	25.3	-0.0078	Xglk315-4AS
	2013	32.2	3.75	14.5	-0.0043	Xpsr59a-4A
5A	2013	210.9	5.31	19.9	0.0049	Xpsr918b-5A
5DL	2013	47.0	5.02	18.9	-0.0079	Xpsr580a-5DL
7B	2012	193.5	3.26	19.3	0.0085	Xmwg710a-7B
7D	2013	82.8	4.13	15.9	0.0044	Xpsr662-7D
Time at maximum grain water content (^oCd)						
3A	2013	108.3	3.51	13.7	13.7	Xglk577-3AL
6B	2013	55.7	3.12	12.2	-27.4	Xpsr964-6B
Grain 2						
Maximum grain water content (mg)						
2A	2012	94.9	3.21	19.0	-2.47	Xpsr919b-2A
	2013	156.0	3.60	14.0	-2.07	Xpsr630-2A
2B	2013	145.8	3.16	12.4	-1.90	Xglk699a-2BS
3B	2012	80.5	3.49	20.5	2.66	Xpsr1054-3B
	2013	8.1	5.50	20.6	2.89	Lrk10c-3BS
	2013	80.5	4.86	18.4	2.44	Xpsr1054-3B
4A	2012	19.7	7.02	37.0	-3.97	Xglk315-4AS
	2013	33.2	3.78	14.6	-2.44	Xpsr914-4A
5B	2012	156.2	3.02	18.0	-2.81	Xpsr580b-5B
5DL	2013	42.0	3.96	15.3	-4.35	Xpsr580a-5DL
7B	2012	71.7	3.26	19.3	2.62	Xglk549-7B
	2012	193.5	5.45	30.1	4.47	Xmwg710a-7B
	2013	68.3	5.07	19.1	2.59	Xglk549-7B
	2013	184.5	4.46	17.0	3.32	Xglk750-7BL
7D	2013	83.8	3.29	12.9	2.28	Xpsr662-7D

Table 6-5 (continued)

Trait/Chromosome	Year	Position (cM)	LOD	R^2	Additive effect	Closest marker
Water absorption rate (mg $^oCd^{-1}$)						
2A	2012	124.6	3.26	19.3	-0.0069	Xglk687a-2AL
	2013	88.3	3.09	12.1	-0.0047	Xpsr386c-2A
3B	2013	10.1	3.41	13.3	0.0059	Lrk10c-3BS
4A	2012	21.7	4.15	23.9	-0.0061	Xpsr59a-4A
5B	2012	159.2	3.49	20.5	-0.0059	Xpsr580b-5B
5DL	2013	31.0	3.05	12.0	-0.0098	Xpsr906a-5DL
7B	2012	70.7	3.85	22.4	0.0052	Xglk549-7B
	2012	193.5	4.91	27.6	0.0081	Xmwg710a-7B
	2013	67.3	5.70	21.2	0.0068	Xglk598-7BL
	2013	180.5	3.25	12.7	0.0067	Xglk750-7BL
Water loss rate (mg $^oCd^{-1}$)						
2A	2013	7.0	4.07	15.7	-0.0037	Xpsr566c-2A
3B	2013	6.1	3.39	13.2	0.0038	Lrk10c-3BS
	2013	80.5	3.36	13.1	0.0035	Xpsr1054-3B
4A	2012	20.7	5.30	29.4	-0.0091	Xglk315-4AS
	2013	21.7	7.29	26.3	-0.0058	Xpsr59a-4A
6A	2012	78.2	4.27	24.5	0.0101	Xpsr966-6A
7B	2012	195.5	3.46	20.4	0.0091	Xmwg710a-7B
	2013	190.5	3.74	14.5	0.0053	Xmwg710a-7B
Time at maximum grain water content (^oCd)						
3A	2013	112.5	3.84	14.8	15.5	Xglk577-3AL
4A	2012	0.1	3.14	18.7	-16.9	Xglk752-4AS
Grain 3						
Maximum grain water content (mg)						
2A	2013	8.9	4.03	15.5	-2.18	Xpsr566c-2A
	2013	88.9	4.18	16.1	-2.14	Xpsr386c-2A
3B	2013	80.3	3.23	12.6	2.03	Xpsr1054-3B
4A	2012	23.7	4.67	26.5	-3.55	Xpsr59a-4A
	2013	21.7	5.12	19.3	-2.87	Xpsr59a-4A
4DL	2012	95.0	3.07	18.3	-3.28	Xglk302b-4DL
7B	2012	190.5	4.45	25.4	4.41	Xmwg710a-7B
	2013	65.3	4.67	17.8	2.40	Xglk598-7BL
	2013	190.5	4.64	17.6	3.44	Xmwg710a-7B
Water absorption rate (mg $^oCd^{-1}$)						
2A	2013	88.9	3.44	13.4	-0.0041	Xpsr386c-2A
7B	2013	66.3	5.24	19.7	0.0054	Xglk598-7BL
	2013	189.5	3.19	12.5	0.0061	Xmwg710a-7B
Water loss rate (mg $^oCd^{-1}$)						
2A	2013	7.0	3.87	15.0	-0.0045	Xpsr566c-2A
	2013	117.6	4.18	16.0	-0.0061	Xglk687a-2AL
4A	2012	22.7	5.18	28.9	-0.0114	Xpsr59a-4A
	2013	21.7	6.54	24.0	-0.0068	Xpsr59a-4A
7B	2012	184.5	3.90	22.6	0.0125	Xmwg710a-7B
	2013	195.5	4.83	18.3	0.0070	Xmwg710a-7B
Time at maximum grain water content (^oCd)						
4A	2012	19.7	3.63	21.2	-34.6	Xglk315-4AS

Table 6-5 (continued)

Trait/Chromosome	Year	Position (cM)	LOD	R^2	Additive effect	Closest marker
Grain dimensions at maturity						
Grain length (mm)						
1DS	2013	0.1	3.0	6.6	0.10	Xpsr168-1DS
2A	2012	123.7	3.1	18.2	-0.26	Xglk687a-2AL
	2013	143.1	8.6	17.9	-0.16	PL_AP-2A
3B	2012	84.5	5.0	28.2	0.26	Xpsr1054-3B
	2013	79.3	6.5	13.7	0.15	Xpsr1054-3B
4A	2012	23.7	5.8	31.8	-0.27	Xpsr59a-4A
5A	2013	110.2	3.1	6.9	-0.11	Xpsr911-5A
7B	2012	215.8	3.8	22.1	0.20	Xglk576-7BL
Grain width (mm)						
2D	2013	99.1	4.3	9.4	-0.04	Xpsr932-2D
5A	2013	67.4	3.8	8.3	0.04	Xglk424-5A
Grain height (mm)						
1BS	2013	31.0	4.4	9.5	0.04	Xglk317a-1BS
4A	2012	43.1	4.6	26.1	-0.09	Xpsr914-4A
	2013	34.2	5.9	12.5	-0.06	Xpsr914-4A
5A	2013	209.9	7.4	15.5	0.07	Xpsr918b-5A
5DL	2012	35.0	3.9	22.5	-0.16	Xpsr580a-5DL
	2013	37.0	6.9	14.5	-0.12	Xpsr580a-5DL
7B	2012	79.6	3.8	22.0	0.09	Xglk478-7BL
	2012	184.5	7.6	39.5	0.15	Xglk750-7BL
Grain volume (mm^3)						
1A	2012	80.1	3.7	21.6	-2.0	Xpsr1327b-1A
1BS	2013	31.0	3.1	6.8	0.8	Xglk317a-1BS
2A	2012	122.6	3.2	18.9	-2.7	Xglk687a-2AL
	2013	6.0	3.8	8.4	-0.9	Xpsr566c-2A
	2013	126.6	6.1	13.1	-1.5	Xglk699b-2AL
3B	2012	80.5	3.8	22.0	2.1	Xpsr1054-3B
	2013	1.9	3.9	8.4	0.9	C970a-3B
	2013	85.5	4.5	9.7	1.1	Xpsr1054-3B
4A	2012	21.7	6.6	35.1	-3.0	Xpsr59a-4A
	2013	31.2	6.6	14.0	-1.3	Xpsr59a-4A
5DL	2013	41.0	4.0	8.7	-1.8	Xpsr580a-5DL
7B	2012	78.6	3.8	22.3	2.4	Xglk478-7BL
	2012	184.5	7.0	36.7	3.8	Xglk750-7BL
Grain length/width						
1DS	2013	1.0	3.7	8.1	0.04	Xpsr168-1DS
2A	2013	152.5	6.5	13.7	-0.05	Xglk278b-2AL
2B	2013	190.1	3.0	6.6	-0.04	Xpsr644b-2B
2D	2013	101.1	5.7	12.1	0.05	Xpsr540-2D
3B	2013	54.9	3.1	6.7	0.04	Xpsr1101b-3B
5A	2013	68.4	5.5	11.7	-0.06	Xglk424-5A
Grain length/height						
3B	2013	61.6	4.5	9.7	0.06	Xpsr116a-3B
5A	2012	207.9	3.5	20.4	-0.08	Xpsr1194-5A

6.4.4 Inflection points of grain filling rate, grain dimensions and flag leaf senescence occur around the time at maximum grain water content (t_{mwc})

Average grain filling rate across ten RILs and all grain positions reached its maximum first (413 DAA), followed by grain water content (500 DAA), grain length (560 DAA), grain width (603 DAA), grain height (612 DAA), and grain volume (627 DAA) (Fig. 6-5). Interestingly, flag leaf senescence (t_{msr}, 591 DAA) progressed rapidly around the time for maximum grain dimensions, and there were positive relationships between t_{msr} and the time for maximum grain dimensions (length: $r = 0.29$, $P < 0.05$; width: $r = 0.48$, $P < 0.01$; height: $r = 0.37$, $P < 0.01$; and volume: $r = 0.39$, $P < 0.01$), indicating synchrony.

Using the grain water content as a time scale, it was found that grain filling rate reached its maximum (t_{max}) just before t_{mwc} (Fig. 6-5 and Table 6-6). Grain expansion stopped just after grains started to lose water for desiccation, coinciding with rapid flag leaf senescence. All the events occurred around the time when 90% of the maximum grain water content was obtained (Fig. 6-5 and Table 6-6).

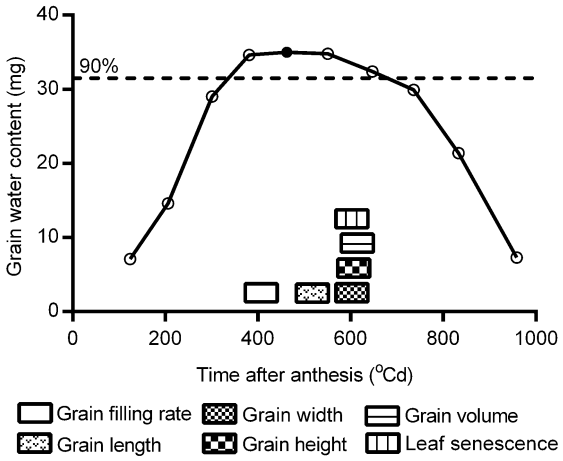

Fig. 6-5 Schematic diagram of the timing of maximum grain filling rate, maximum grain water content, maximum grain dimensions and maximum senescence rate of flag leaves. Maximum grain water content is indicated by a closed circle on the curve. The horizontal dashed line indicates 90% of the maximum grain water content. The base temperature 0°C was used to calculate the accumulated thermal time from anthesis.

Table 6-6 Relative grain water content at the inflection points of grain filling rate, grain dimensions and flag leaf senescence

Grain	RGWC at t_{max}[a]		RGWC at t_{mgl}	RGWC at t_{mgw}	RGWC at t_{mgh}	RGWC at t_{mgv}	RGWC at t_{msr}	
	2012	2013	2013	2013	2013	2013	2012	2013
Grain 1	95	96	97	94	93	92	97	88
Grain 2	95	96	98	95	93	93	97	89
Grain 3	91	95	97	94	94	91	94	91

[a] RGWC, relative grain water content (%), calculated as the proportion of grain water content at the inflection points to maximum water content; t_{max}, the time at maximum grain filling rate; t_{mgl}, the time at maximum grain length; t_{mgw}, the time at maximum grain width; t_{mgh}, the time at maximum grain height; t_{mgv}, the time at maximum grain volume; t_{msr}, the time at maximum senescence rate of flag leaves.

6.4.5 Distal and basal grains within spikelets differ in grain filling processes

As expected, G3 had lower final grain weight than G1 and G2 (Fig. 6-6). A further analysis showed that G3 had much smaller carpels and slower initial grain filling rate. The rapid grain filling rate of G3 was similar to G1, but lower than G2, whereas the late grain filling rate was fastest in G3. Maximum grain filling rates of G2 and G3 were comparable, both being higher than that of G1. In addition, G3 had slower grain water absorption rate, lower maximum grain water content, and, in general, slightly smaller maximum (final) grain dimensions.

With the exception of the onset of grain filling, which was significantly later in G3, the progress of grain filling (grain filling duration, t_{max} and t_{mwc}) was similar among grains (Fig. 6-6). Furthermore, G1, G2 and G3 reached the maximum grain dimensions at the same time (Table 6-7). In other words, the second half of grain filling process (from t_{max}) was almost synchronous among G1, G2 and G3.

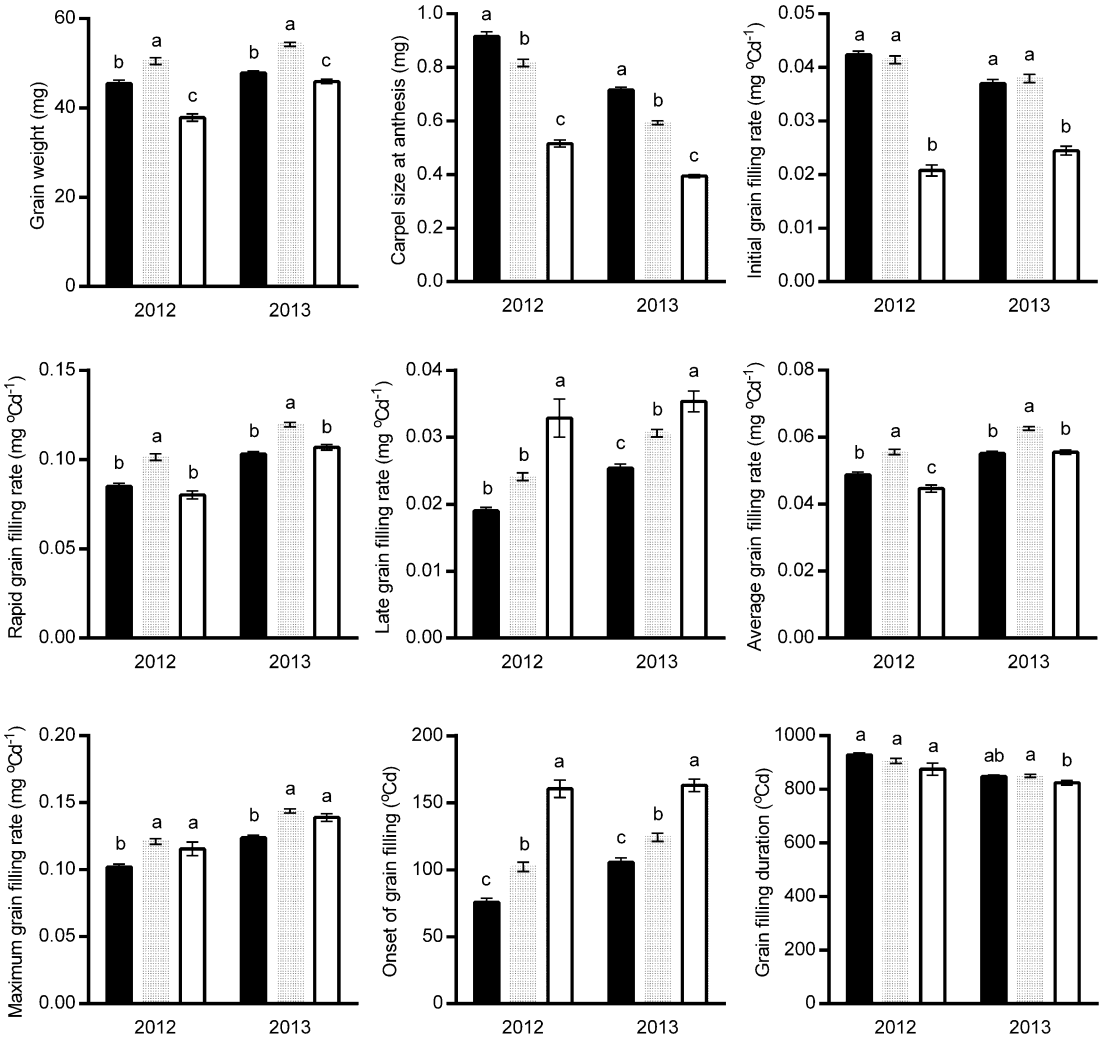

Fig. 6-6 Comparisons of grain weight and grain filling traits between Grain 1, 2 and 3 within spikelets. Black, grey and open bars (mean ± standard error of the mean) indicate Grain 1, 2 and 3, respectively. Different letters above the bars indicate significant differences between grain positions ($P < 0.01$). Trait abbreviations: t_{max}, the time at maximum grain filling rate; t_{mwc}, the time at maximum grain water content. Comparisons of maximum grain dimensions were done in 2013 only.

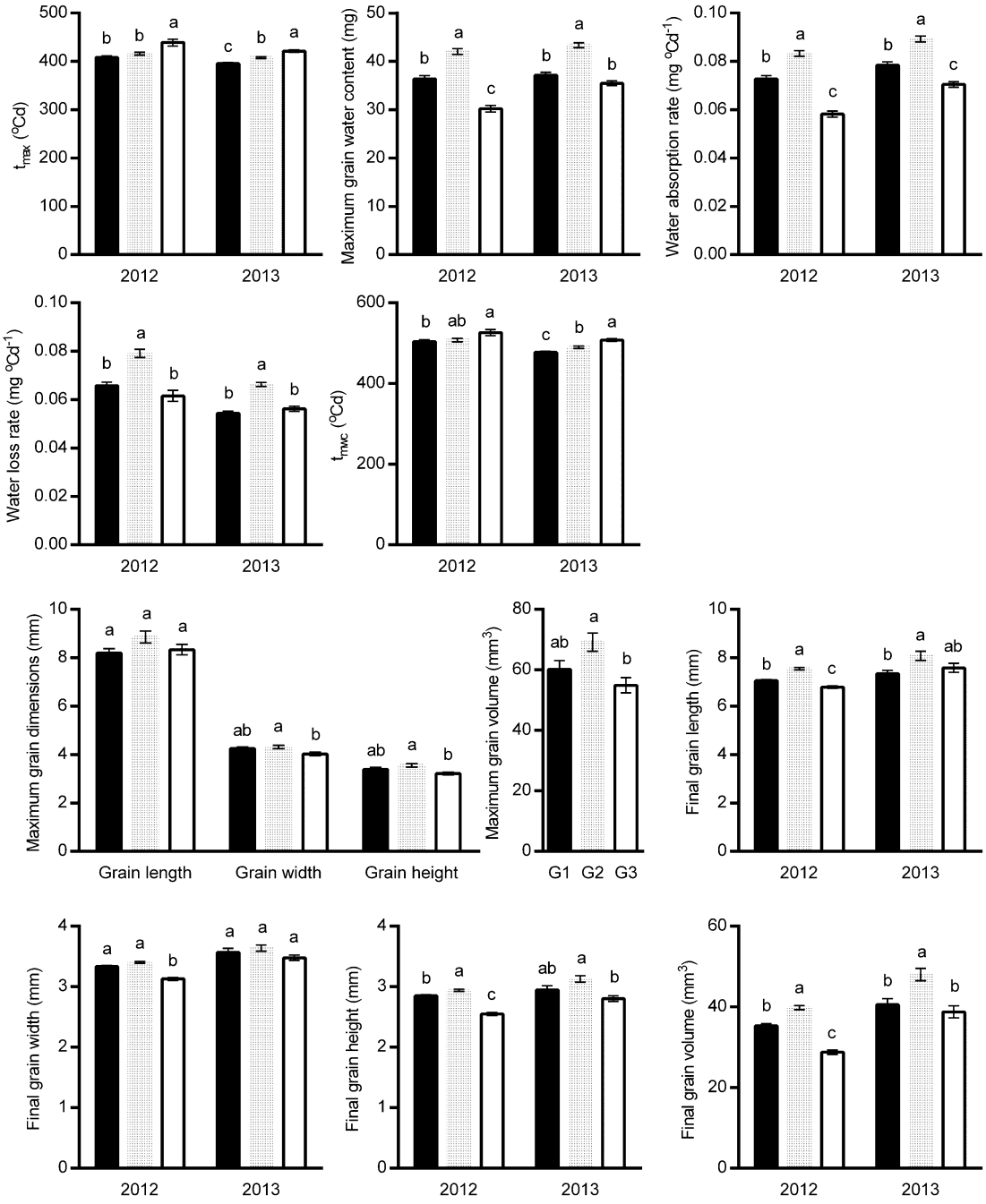

Fig. 6-6 (continued)

Table 6-7 Timing of Grain 1, 2 and 3 at maximum grain dimensions in 2013

Grain	Timing at maximum grain dimensions (^{o}Cd after anthesis)			
	Length	Width	Height	Volume
Grain 1	554	601	605	617
Grain 2	552	593	623	618
Grain 3	573	614	608	644
P-value	> 0.05	> 0.05	> 0.05	> 0.05

6.4.6 Distal and basal grains within spikelets differ in the genetic architectures of grain filling processes

G3 usually had fewer significant QTL detected for grain weight, carpel size, grain dry matter and water accumulation, than G1 and G2 (Table 6-5 and Supplementary Table S6-4). An exception was the QTL number for rapid grain filling rate, which was similar across the different grain positions. G1, G2 and G3 shared some QTL for most traits, and the most common QTL across all grain positions were located on 4A and 7B (Fig. 6-4 and Supplementary Fig. S6-2). The additive effects of the shared QTL were lower in G3 for final grain weight, maximum grain water content and water absorption rate, but higher for carpel size, and the rapid, average and maximum grain filling rates, and grain water loss rate. There were more position-specific QTL for G1 than G2 or G3 (Supplementary Fig. S6-2).

6.4.7 Distal grains respond to de-graining at anthesis

De-graining at anthesis increased the grain weight of G3 by 17% ($P < 0.05$) and G2 by 12% ($P < 0.05$) across two bread wheat cultivars Forno and Duxford. G1 did not significantly respond to de-graining, indicating that grains are more source limited from the basal to distal florets within spikelets. After de-graining, the dry weight of G3 (47.7 mg) was comparable to G1 (48.6 mg) and G2 (47.4 mg) in the intact spikes ($P > 0.05$).

6.5 Discussion

6.5.1 Close relationships between grain filling traits and final grain weight, and among the grain filling traits

Grain weight at maturity is a direct function of dry matter accumulation during grain filling. It was observed that the initial, rapid, average and maximum grain filling rates, rather than the late grain filling rate, were closely associated with final grain weight. Rapid grain filling rate was three times faster than initial and late ones, and contributed most to final grain weight. In contrast, only a weak relationship between grain filling duration and grain weight was found, indicating that the rate of synthesis of storage products is more important than its duration, consistent with the previous studies (Charmet et al., 2005; Wang et al., 2009). Stresses such as heat, drought and elevated CO_2 usually stimulate grain filling rate, but shorten its duration (Li et al., 2001; Zahedi and Jenner, 2003; Yang et al., 2004), suggesting the plasticity and central role of synthetic efficiency of storage products. In addition, earlier grain filling seems to be favourable for final grain weight, as it increased the initial grain filling rate and whole grain filling duration.

A positive relationship between carpel size at anthesis and final grain weight was found, consistent with the earlier reports in wheat (Calderini et al., 1999; Hasan et al., 2011), barley (Hordeum vulgare L.) (Scott et al., 1983), and sorghum [Sorghum bicolor (L.) Moench] (Yang et al., 2009). A further analysis in the present study revealed that larger carpels accelerated the initial and rapid grain filling rates (mainly the former), advanced the onset of grain filling, and slightly extended grain filling duration, resulting in higher grain weight. Moreover, larger carpels increased maximum grain water content, grain water absorption and loss rates, and grain dimensions. The relationships of carpels with maximum grain water content and grain dimensions were also reported by a recent study (Hasan et al., 2011). These findings indicate that final grain weight is determined during both pre- and post- anthesis periods (Calderini et al., 1999). The carpel size mediates final grain weight mainly through its effects on the initial phase of grain filling.

A strong and positive relationship between maximum grain water content and final grain weight was observed in this study, as reported earlier in wheat (Lizana et al., 2010; Hasan et al., 2011; Gonzalez et al., 2014), maize (Borras et al., 2003; Sala et al.,

2007), and sunflower (Rondanini et al., 2009). Further, grain water absorption and loss rates were also positively associated with final grain weight. These contributions likely resulted from the effects of grain water accumulation on the accelerated grain filling rates. Similarly, grain water accumulation and maximum (final) grain dimensions were positively associated. To understand the potential roles of grain water uptake and loss during grain filling, the timing of key grain growth events were compared in detail. The results showed that grain filling rate reached its maximum while grain water content levelled off, which was also observed in the reports of Laudencia-Chingcuanco et al. (2007) and Lizana et al. (2010). Considering the positive relationships between maximum grain water content and maximum grain filling rate, and between grain water absorption rate and the rates of initial and rapid grain filling, it can be deduced that grain water drives the synthesis of storage products, serving as a raw material or medium. In addition, grain length reached its maximum just after maximum grain water content. Following this, grain width, height and volume stopped expanding almost simultaneously, while the grains started to lose water. This implies that grain water may function as an incentive for grain dimension establishment. Once grain desiccation commences, the driving force disappears and grain enlargement ends. Briarty et al. (1979) reported that the endosperm and cell volume reach their maximums at the same time (35 days after anthesis), and the timing is similar to that for maximum grain water content in this study (31 days), supporting the above hypothesis. Meanwhile, the flag leaves also underwent rapid senescence, indicating synchrony. Around this critical time, rapid reduction in flag leaf and ear photosynthesis (Sofield et al., 1977) and programmed cell death in the entire endosperm of grains (Young and Gallie, 1999) occur. Taken together, it seems that there is a critical time when multiple organs (grain, ear and flag leaf) undergo rapid senescence simultaneously. Expressions of the genes for dehydrins, late embryo abundant proteins and tritins peak at this time (Laudencia-Chingcuanco et al., 2007), implying their possible roles in regulating the synchronous senescence processes.

6.5.2 QTL coincidences reflect the close relationships between carpel size, grain dry matter and water accumulation, grain morphology, and final grain weight

Grain filling is a complex but orderly process. QTL analysis revealed a large number of QTL for the grain filling traits. Of them, the QTL for carpel size, grain filling rates for different phases, and grain water uptake and loss, are reported here for the first

time in wheat. Each QTL for grain weight was coincident with 2−13 traits of grain filling; 73%, on average, of the QTL for the grain filling traits were coincident with those for grain weight, with the favourable alleles usually conferred by the same parents. The high level of QTL coincidences was also found among the grain filling traits. These QTL coincidences confirm the roles of carpel size, grain dry matter accumulation, grain water uptake and loss, and grain dimensions as the physiological determinants of final grain weight, and also explain the close relationships between the grain filling traits. The orderly processes of grain filling, therefore, result mainly from the pleiotropy or tight linkages of functionally related genes. Across the whole genome, a limited number of QTL clusters were identified on six chromosomes (2A, 3B, 4A, 5A, 5DL and 7B), and each of them harboured 16−49 QTL for more than 12 traits. They offer an opportunity to improve multiple grain filling traits simultaneously in wheat breeding.

QTL coincidences between grain filling rate and duration, and final grain weight have also been identified in an earlier study (Wang et al., 2009), in which the QTL clusters reported on 3B correspond approximately to that in the present study. In addition, the QTL coincidences between final grain dimensions and grain weight have been observed on many chromosomes (1B, 2A, 2B, 2D, 3A, 3B, 4B, 4D, 5A, 6A, and 7A) (Breseghello and Sorrells, 2007; Gegas et al., 2010; Williams et al., 2013). In this study, 16 QTL for 13 traits and 20 QTL for 12 traits (most of them for G1) were detected on homoeologous chromosomes 5AL and 5DL, respectively, suggesting homoeoalleles with the similar functions. Meanwhile, the QTL for grain threshability and glume tenacity (domestication traits) were identified on 5AL as well (data not shown). Common marker analysis showed that these QTL correspond to the domestication gene Q (Kato et al., 1998; Simonetti et al., 1999), with the bread wheat Forno providing the free-threshing allele Q. This implies that the Q allele in bread wheat may be associated with higher grain weight of G1 and other favourable traits of grain filling.

6.5.3 Late onset of grain filling and slow initial grain filling rate lead to smaller distal grains

Onset of grain filling was much later in G3 than in G1 and G2, and the subsequent progress of grain filling was almost synchronous among grains. Simultaneous termination of dry matter and water accumulation, as well as the coincidence of rapid

grain desiccation among G1, G2 and G3 have also been found in other studies (Simmons and Crookston, 1979; Millet and Pinthus, 1984). The synchrony at late grain filling is likely as a result of the whole plant senescence for maturation (as discussed above).

Compared with G1 and G2, the initial grain filling rate was much slower in G3. This may result from the late onset of grain filling, as there was a strong negative relationship between them. In contrast, G3 had the rapid grain filling rate similar to G1, and also showed fast maximum grain filling rate, indicating that G3 is capable of rapid dry matter accumulation like G1 and G2. This can be supported by the genetic evidence, which showed that G3 had similar QTL number for the rapid grain filling rate, and that the additive effects of the shared QTL for the rapid and maximum grain filling rates were even higher in G3. It has been observed that maximum starch synthetic rate and some enzyme activities are comparable or even higher in distal grains than in basal ones (Jiang et al., 2003). In addition, G3 had significantly higher late grain filling rate. Despite the capability of efficient dry matter accumulation after the initial phase of grain filling, G3 could not be fully filled because of the synchronous senescence of grains and other organs.

The combination of late onset of grain filling and slow initial grain filling rate could be responsible for smaller G3. This may be explained by a delay of 2−5 days for anthesis of distal florets compared with basal ones (Simmons and Crookston, 1979; Millet and Pinthus, 1984), and resultant later carpel growth and smaller carpel size at anthesis (Calderini et al., 1999). Moreover, a greater increase in dry weight of distal grains than that of basal ones was found after de-graining in the present and previous studies (Simmons et al., 1982; Calderini and Reynolds, 2000; Acreche and Slafer, 2009), indicating that distal grains are more source limited, whereas basal ones are more sink limited. In many cases, final grain weight can be comparable or even higher in distal grains than in basal ones after de-graining (Radley, 1978; Simmons et al., 1982; Gao et al., 1992; Calderini and Reynolds, 2000). These results thus indicate that distal grains can be improved through increased assimilate supply. As the grain filling rate is sufficient in G3 during the rapid and late phases, the increased assimilate availability after de-graining may have improved the initiation of grain filling (rate and onset). Evidence can be found from the de-graining treatment at heading, which significantly accelerates floret development of G3 and increases carpel size at anthesis

(Calderini and Reynolds, 2000). De-graining immediately after anthesis can also improve the onset and rate of initial dry matter and water accumulation, and finally produce higher dry weight of G3 (Radley, 1978; Gao et al., 1992). Limited assimilate availability for G3 during the initial grain filling phase, under normal growing conditions, probably results from the priority for assimilate partitioning to basal grains.

6.5.4 Conclusions

Individual grain weight is an important but complex trait in wheat. This study showed that the preanthesis carpel growth, and postanthesis grain dry matter and water accumulation as well as grain morphological expansion, are closely associated with each other, and with final grain weight. Genetic analysis demonstrated a high level of QTL coincidences between these traits, indicating pleiotropy or the tight linkages of functionally related genes. Frequent QTL coincidences, particularly those on chromosomes 2A, 3B, 4A, 5A, 5DL and 7B, will be useful to improve multiple grain filling traits simultaneously through marker-assisted breeding. In addition, there is a great variation in grain weight within spikelets, and smaller distal grains stem mainly from later grain filling and slower initial grain filling rate, compared with the basal grains. Although distal grains are capable of rapid dry matter accumulation thereafter, they cannot be fully filled because of the synchronous maturation or terminal plant senescence. An increase in assimilate availability around anthesis is able to improve the distal grain weight. Therefore, this study will help to understand grain weight determination in wheat. The desirable physiological traits and alleles from the relative species spelt presented here, can be used to broaden the genetic diversity of bread wheat in terms of grain weight improvement.

6.6 Acknowledgements

This work was financially supported by the grants from the China Scholarship Council and University of Nottingham. We thank Beat Keller (University of Zurich, Switzerland) for providing the mapping population, and Monika Messmer (Research Institute of Organic Agriculture, Switzerland) for providing the molecular marker data. We also thank John Alcock, Matthew Tovey and Fiona Wilkinson (University of Nottingham) for their help with field trials and laboratory work.

6.7 References

Acreche MM, Slafer GA. 2009. Grain weight, radiation interception and use efficiency as affected by sink-strength in Mediterranean wheats released from 1940 to 2005. Field Crops Research **110**, 98-105.

Barlow EWR, Lee JW, Munns R, Smart MG. 1980. Water relations of the developing wheat grain. Australian Journal of Plant Physiology **7**, 519-525.

Borras L, Slafer GA, Otegui ME. 2004. Seed dry weight response to source-sink manipulations in wheat, maize and soybean: a quantitative reappraisal. Field Crops Research **86**, 131-146.

Borras L, Westgate ME, Otegui ME. 2003. Control of kernel weight and kernel water relations by post-flowering source-sink ratio in maize. Annals of Botany **91**, 857-867.

Breseghello F, Sorrells ME. 2007. QTL analysis of kernel size and shape in two hexaploid wheat mapping populations. Field Crops Research **101**, 172-179.

Briarty LG, Hughes CE, Evers AD. 1979. The developing endosperm of wheat - a stereological analysis. Annals of Botany **44**, 641-658.

Calderini DF, Abeledo LG, Savin R, Slafer GA. 1999. Effect of temperature and carpel size during pre-anthesis on potential grain weight in wheat. Journal of Agricultural Science **132**, 453-459.

Calderini DF, Ortiz-Monasterio I. 2003. Grain position affects grain macronutrient and micronutrient concentrations in wheat. Crop Science **43**, 141-151.

Calderini DF, Reynolds MP. 2000. Changes in grain weight as a consequence of de-graining treatments at pre- and post-anthesis in synthetic hexaploid lines of wheat (Triticum durum × T. tauschii). Australian Journal of Plant Physiology **27**, 183-191.

Charmet G, Robert N, Branlard G, Linossier L, Martre P, Triboi E. 2005. Genetic analysis of dry matter and nitrogen accumulation and protein composition in wheat kernels. Theoretical and Applied Genetics **111**, 540-550.

Distelfeld A, Avni R, Fischer AM. 2014. Senescence, nutrient remobilization, and yield in wheat and barley. Journal of Experimental Botany **65**, 3783-3798.

Gao XP, Francis D, Ormrod JC, Bennett MD. 1992. Changes in cell number and cell division activity during endosperm development in allohexaploid wheat, Triticum aestivum L. Journal of Experimental Botany **43**, 1603-1609.

Gegas VC, Nazari A, Griffiths S, Simmonds J, Fish L, Orford S, Sayers L, Doonan JH, Snape JW. 2010. A genetic framework for grain size and shape variation in wheat. The Plant Cell **22**, 1046-1056.

Gillies SA, Futardo A, Henry RJ. 2012. Gene expression in the developing aleurone and starchy endosperm of wheat. Plant Biotechnology Journal **10**, 668-679.

Gonzalez FG, Aldabe ML, Terrile II, Rondanini DP. 2014. Grain weight response to different postflowering source: sink ratios in modern high-yielding Argentinean wheats differing in spike fruiting efficiency. Crop Science **54**, 297-309.

Gooding MJ, Dimmock J, France J, Jones SA. 2000. Green leaf area decline of wheat flag leaves: the influence of fungicides and relationships with mean grain weight and grain yield. Annals of Applied Biology **136**, 77-84.

Hasan AK, Herrera J, Lizana C, Calderini DF. 2011. Carpel weight, grain length and stabilized grain water content are physiological drivers of grain weight determination of wheat. Field Crops Research **123**, 241-247.

Jiang D, Cao W, Dai T, Jing Q. 2003. Activities of key enzymes for starch synthesis in relation to growth of superior and inferior grains on winter wheat (Triticum aestivum L.) spike. Plant Growth Regulation **41**, 247-257.

Kato K, Miura H, Akiyama M, Kuroshima M, Sawada S. 1998. RFLP mapping of the three major genes, Vrn1, Q and B1, on the long arm of chromosome 5A of wheat. Euphytica **101**, 91-95.

Laudencia-Chingcuanco DL, Stamova BS, You FM, Lazo GR, Beckles DM, Anderson OD. 2007. Transcriptional profiling of wheat caryopsis development using cDNA microarrays. Plant Molecular Biology **63**, 651-668.

Li AG, Hou YS, Trent A. 2001. Effects of elevated atmospheric CO_2 and drought stress on individual grain filling rates and durations of the main stem in spring wheat. Agricultural and Forest Meteorology **106**, 289-301.

Lizana XC, Riegel R, Gomez LD, Herrera J, Isla A, McQueen-Mason SJ, Calderini DF. 2010. Expansins expression is associated with grain size dynamics in wheat (Triticum aestivum L.). Journal of Experimental Botany **61**, 1147-1157.

Millet E, Pinthus MJ. 1984. The association between grain volume and grain weight in wheat. Journal of Cereal Science **2**, 31-35.

Miralles DJ, Slafer GA. 2007. Sink limitations to yield in wheat: how could it be reduced? Journal of Agricultural Science **145**, 139-149.

Radley M. 1978. Factors affecting grain enlargement in wheat. Journal of Experimental Botany **29**, 919-934.

Rondanini DP, Mantese AI, Savin R, Hall AJ. 2009. Water content dynamics of achene, pericarp and embryo in sunflower: Associations with achene potential size and dry-down. European Journal of Agronomy **30**, 53-62.

Sala RG, Westgate ME, Andrade FH. 2007. Source/sink ratio and the relationship between maximum water content, maximum volume, and final dry weight of maize kernels. Field Crops Research **101**, 19-25.

Scott WR, Appleyard M, Fellowes G, Kirby EJM. 1983. Effect of genotype and position in the ear on carpel and grain growth and mature grain weight of spring barley. Journal of Agricultural Science **100**, 383-391.

Shewry PR. 2009. Wheat. Journal of Experimental Botany **60**, 1537-1553.

Shewry PR, Mitchell RAC, Tosi P, Wan Y, Underwood C, Lovegrove A, Freeman J, Toole GA, Mills ENC, Ward JL. 2012. An integrated study of grain development of wheat (cv. Hereward). Journal of Cereal Science **56**, 21-30.

Shewry PR, Underwood C, Wan Y, Lovegrove A, Bhandari D, Toole G, Mills ENC, Denyer K, Mitchell RAC. 2009. Storage product synthesis and accumulation in developing grains of wheat. Journal of Cereal Science **50**, 106-112.

Simmons SR, Crookston RK. 1979. Rate and duration of growth of kernels formed at specific florets in spikelets of spring wheat. Crop Science **19**, 690-693.

Simmons SR, Crookston RK, Kurle JE. 1982. Growth of spring wheat kernels as influenced by reduced kernel number per spike and defoliation. Crop Science **22**, 983-988.

Simonetti MC, Bellomo MP, Laghetti G, Perrino P, Simeone R, Blanco A. 1999. Quantitative trait loci influencing free-threshing habit in tetraploid wheats. Genetic Resources and Crop Evolution **46**, 267-271.

Singh BK, Jenner CF. 1982. Association between concentrations of organic nutrients in the grain, endosperm cell number and grain dry weight within the ear of wheat. Australian Journal of Plant Physiology **9**, 83-95.

Slafer GA, Savin R. 1994. Source-sink relationships and grain mass at different positions within the spike in wheat. Field Crops Research **37**, 39-49.

Sofield I, Evans LT, Cook MG, Wardlaw IF. 1977. Factors influencing rate and duration of grain filling in wheat. Australian Journal of Plant Physiology **4**, 785-797.

Wang RX, Hai L, Zhang XY, You GX, Yan CS, Xiao SH. 2009. QTL mapping for grain filling rate and yield-related traits in RILs of the Chinese winter wheat population Heshangmai × Yu8679. Theoretical and Applied Genetics **118**, 313-325.

Williams K, Munkvold J, Sorrells M. 2013. Comparison of digital image analysis using elliptic Fourier descriptors and major dimensions to phenotype seed shape in hexaploid wheat (Triticum aestivum L.). Euphytica **190**, 99-116.

Yang JC, Zhang JH, Wang ZQ, Xu GW, Zhu QS. 2004. Activities of key enzymes in sucrose-to-starch conversion in wheat grains subjected to water deficit during grain filling. Plant Physiology **135**, 1621-1629.

Yang Z, van Oosterom EJ, Jordan DR, Hammer GL. 2009. Pre-anthesis ovary development determines genotypic differences in potential kernel weight in sorghum. Journal of Experimental Botany **60**, 1399-1408.

Young TE, Gallie DR. 1999. Analysis of programmed cell death in wheat endosperm reveals differences in endosperm development between cereals. Plant Molecular Biology **39**, 915-926.

Zahedi M, Jenner CF. 2003. Analysis of effects in wheat of high temperature on grain filling attributes estimated from mathematical models of grain filling. Journal of Agricultural Science **141**, 203-212.

6.8 Supplementary data

List of Supplementary files

Supplementary Table S6-1 Descriptive statistics on the final grain weight and grain filling traits of the parents and recombinant inbred line (RIL) mapping population.

Supplementary Table S6-2 Quantitative trait locus (QTL) coincidences between final grain weight and grain filling traits.

Supplementary Table S6-3 Quantitative trait locus (QTL) coincidences between carpel size and the other grain filling traits.

Supplementary Table S6-4 Quantitative trait locus (QTL) number detected for Grain 1, 2 and 3.

Supplementary Fig. S6-1 Grain expansion dynamics in 2013.

Supplementary Fig. S6-2 Quantitative trait locus (QTL) comparisons between different grains within spikelets.

Supplementary Table S6-1 Descriptive statistics on the final grain weight and grain filling traits of the parents and recombinant inbred line (RIL) mapping population

Trait[a]	Year	Parental lines			RILs			H^{2c}
		Forno	Oberkulmer	P-value	Mean (min; max)	P-value	SED[b]	
Final grain weight								
Grain 1 (mg)	2012	46.0	49.7	> 0.05	45.4 (30.5; 63.0)	< 0.001	3.4	0.81
	2013	57.3	45.7	< 0.01	47.8 (35.5; 60.4)	< 0.001	1.7	
Grain 2 (mg)	2012	44.1	58.8	< 0.01	50.5 (38.0; 65.1)	< 0.001	4.1	0.70
	2013	57.3	55.9	> 0.05	54.2 (45.0; 66.1)	< 0.001	2.0	
Grain 3 (mg)	2012	32.7	39.7	> 0.05	37.9 (17.8; 51.5)	< 0.001	5.7	0.67
	2013	49.2	44.8	> 0.05	45.9 (33.6; 58.3)	< 0.001	2.6	
Carpel size at anthesis								
Carpel 1 (mg)	2012	0.73	1.07	< 0.01	0.91 (0.57; 1.27)	< 0.001	0.12	0.61
	2013	0.60	0.87	< 0.01	0.72 (0.48; 1.09)	< 0.001	0.08	
Carpel 2 (mg)	2012	0.66	0.95	< 0.01	0.82 (0.57; 1.12)	< 0.001	0.10	0.41
	2013	0.46	0.67	< 0.01	0.59 (0.45; 0.80)	< 0.001	0.06	
Carpel 3 (mg)	2012	0.36	0.53	< 0.05	0.52 (0.23; 0.78)	< 0.001	0.08	0.38
	2013	0.40	0.45	> 0.05	0.39 (0.27; 0.59)	< 0.001	0.05	
Grain dry matter accumulation								
Grain 1								
Initial GFR (mg $^{o}Cd^{-1}$)	2012	0.047	0.047	> 0.05	0.042 (0.026; 0.056)	< 0.001	0.005	0.28
	2013	0.043	0.025	< 0.05	0.037 (0.011; 0.055)	< 0.001	0.008	
Rapid GFR (mg $^{o}Cd^{-1}$)	2012	0.085	0.090	> 0.05	0.085 (0.052; 0.135)	< 0.001	0.011	0.72
	2013	0.123	0.096	< 0.05	0.103 (0.064; 0.151)	< 0.001	0.011	
Late GFR (mg $^{o}Cd^{-1}$)	2012	0.018	0.020	> 0.05	0.019 (0.011; 0.035)	< 0.001	0.003	0.43
	2013	0.030	0.027	> 0.05	0.025 (0.013; 0.074)	< 0.001	0.006	
Average GFR (mg $^{o}Cd^{-1}$)	2012	0.050	0.052	> 0.05	0.049 (0.031; 0.070)	< 0.001	0.004	0.84
	2013	0.065	0.049	< 0.01	0.055 (0.040; 0.079)	< 0.001	0.003	
Maximum GFR (mg $^{o}Cd^{-1}$)	2012	0.103	0.108	> 0.05	0.102 (0.063; 0.161)	< 0.001	0.012	0.70
	2013	0.146	0.117	< 0.05	0.124 (0.081; 0.229)	< 0.001	0.014	
Onset of GF (^{o}Cd)	2012	61	76	> 0.05	76 (25; 154)	< 0.05	29	0.25
	2013	114	151	> 0.05	105 (0; 236)	< 0.001	39	
GF duration (^{o}Cd)	2012	906	943	> 0.05	928 (783; 1094)	< 0.05	70	0.21
	2013	857	883	> 0.05	847 (690; 1082)	< 0.001	63	
t_{max} (^{o}Cd)	2012	391	415	> 0.05	408 (356; 481)	< 0.01	24.7	0.52
	2013	404	437	< 0.05	395 (355; 469)	< 0.001	15	

[a] Trait abbreviations: GFR, grain filling rate; GF, grain filling; t_{max}, the time at maximum grain filling rate; t_{mwc}, the time at maximum grain water content.

[b] SED: standard error of the difference of mean.

[c] H^2: broad sense heritability.

Supplementary Table S6-1 (continued)

Trait	Year	Parental lines			RILs			H^2
		Forno	Oberkulmer	P-value	Mean (min; max)	P-value	SED	
Grain 2								
Initial GFR (mg $^oCd^{-1}$)	2012	0.042	0.050	> 0.05	0.041 (0.026; 0.056)	< 0.05	0.007	0.20
	2013	0.046	0.025	< 0.05	0.038 (0.020; 0.056)	< 0.001	0.008	
Rapid GFR (mg $^oCd^{-1}$)	2012	0.093	0.109	> 0.05	0.101 (0.063; 0.130)	< 0.001	0.014	0.71
	2013	0.124	0.123	> 0.05	0.120 (0.090; 0.147)	< 0.001	0.012	
Late GFR (mg $^oCd^{-1}$)	2012	0.022	0.025	> 0.05	0.024 (0.014; 0.035)	< 0.01	0.005	0.49
	2013	0.029	0.035	> 0.05	0.031 (0.020; 0.054)	< 0.05	0.006	
Average GFR (mg $^oCd^{-1}$)	2012	0.052	0.061	< 0.05	0.056 (0.038; 0.069)	< 0.001	0.004	0.80
	2013	0.066	0.061	> 0.05	0.063 (0.049; 0.075)	< 0.001	0.004	
Maximum GFR (mg $^oCd^{-1}$)	2012	0.111	0.130	> 0.05	0.121 (0.076; 0.155)	< 0.001	0.016	0.69
	2013	0.146	0.149	> 0.05	0.144 (0.107; 0.195)	< 0.001	0.017	
Onset of GF (^oCd)	2012	80	98	> 0.05	103 (32; 179)	< 0.001	29	0.35
	2013	104	187	< 0.05	124 (37; 202)	< 0.05	36	
GF duration (^oCd)	2012	839	953	> 0.05	906 (711; 1104)	< 0.01	79	0.24
	2013	853	874	> 0.05	850 (694; 1022)	< 0.001	62	
t_{max} (^oCd)	2012	376	432	< 0.05	416 (346; 475)	< 0.001	26	0.46
	2013	396	455	< 0.01	408 (363; 490)	< 0.001	18	
Grain 3								
Initial GFR (mg $^oCd^{-1}$)	2012	0.026	0.002	< 0.01	0.021 (0.000; 0.036)	< 0.001	0.008	0.27
	2013	0.033	0.013	< 0.05	0.025 (0.000; 0.049)	< 0.001	0.009	
Rapid GFR (mg $^oCd^{-1}$)	2012	0.070	0.070	> 0.05	0.080 (0.036; 0.118)	< 0.001	0.015	0.45
	2013	0.119	0.103	> 0.05	0.107 (0.057; 0.141)	< 0.001	0.013	
Late GFR (mg $^oCd^{-1}$)	2012	0.019	0.155	< 0.01	0.031 (0.007; 0.100)	< 0.001	0.018	0.31
	2013	0.030	0.037	> 0.05	0.035 (0.015; 0.132)	< 0.001	0.011	
Average GFR (mg $^oCd^{-1}$)	2012	0.039	0.076	< 0.01	0.044 (0.024; 0.063)	< 0.001	0.007	0.59
	2013	0.061	0.051	> 0.05	0.056 (0.039; 0.073)	< 0.001	0.005	
Maximum GFR (mg $^oCd^{-1}$)	2012	0.088	0.323	< 0.01	0.113 (0.046; 0.217)	< 0.001	0.042	0.42
	2013	0.141	0.135	> 0.05	0.139 (0.085; 0.272)	< 0.001	0.029	
Onset of GF (^oCd)	2012	92	268	< 0.01	160 (21; 291)	< 0.001	50	0.39
	2013	138	237	< 0.05	162 (0; 310)	< 0.001	46	
GF duration (^oCd)	2012	862	526	< 0.05	880 (510; 1555)	< 0.001	135	0.25
	2013	813	846	> 0.05	824 (576; 1139)	< 0.001	94	
t_{max} (^oCd)	2012	392	369	> 0.05	441 (331; 676)	< 0.01	55	0.26
	2013	401	475	< 0.01	421 (328; 501)	< 0.001	26	
Grain water accumulation								
Grain 1								
Maximum grain water content (mg)	2012	36.4	37.7	> 0.05	36.3 (22.9; 52.2)	< 0.001	2.1	0.91
	2013	48.7	31.8	< 0.01	37.1 (25.3; 56.6)	< 0.001	1.8	
Water absorption rate (mg $^oCd^{-1}$)	2012	0.079	0.067	< 0.05	0.073 (0.049; 0.104)	< 0.001	0.005	0.87
	2013	0.099	0.061	< 0.01	0.078 (0.046; 0.119)	< 0.001	0.005	
Water loss rate (mg $^oCd^{-1}$)	2012	0.055	0.081	< 0.01	0.066 (0.034; 0.092)	< 0.001	0.010	0.75
	2013	0.069	0.052	< 0.01	0.054 (0.037; 0.084)	< 0.001	0.004	
t_{mwc} (^oCd)	2012	458	565	< 0.01	503 (426; 584)	< 0.001	36	0.17
	2013	492	523	> 0.05	476 (415; 603)	< 0.001	20	

Supplementary Table S6-1 (continued)

Trait	Year	Parental lines			RILs			H^2
		Forno	Oberkulmer	P-value	Mean (min; max)	P-value	SED	
Grain 2								
Maximum grain water content (mg)	2012	38.1	47.5	< 0.01	42.0 (29.0; 54.0)	< 0.001	2.7	0.86
	2013	51.8	41.0	< 0.01	43.3 (32.1; 55.0)	< 0.001	2.3	
Water absorption rate (mg $^{o}Cd^{-1}$)	2012	0.089	0.082	> 0.05	0.083 (0.060; 0.109)	< 0.001	0.008	0.81
	2013	0.107	0.071	< 0.01	0.089 (0.059; 0.125)	< 0.001	0.006	
Water loss rate (mg $^{o}Cd^{-1}$)	2012	0.057	0.110	< 0.01	0.079 (0.047; 0.114)	< 0.001	0.013	0.70
	2013	0.073	0.076	> 0.05	0.066 (0.049; 0.086)	< 0.001	0.005	
t_{mwc} (^{o}Cd)	2012	429	582	< 0.01	508 (431; 583)	< 0.001	39	0.52
	2013	483	575	< 0.01	489 (425; 596)	< 0.001	25	
Grain 3								
Maximum grain water content (mg)	2012	26.4	43.8	< 0.01	30.1 (13.5; 41.7)	< 0.001	4.6	0.67
	2013	43.6	30.2	< 0.01	35.5 (23.5; 50.7)	< 0.001	2.8	
Water absorption rate (mg $^{o}Cd^{-1}$)	2012	0.060	0.068	> 0.05	0.058 (0.033; 0.080)	< 0.001	0.011	0.43
	2013	0.089	0.050	< 0.01	0.070 (0.043; 0.101)	< 0.001	0.008	
Water loss rate (mg $^{o}Cd^{-1}$)	2012	0.042	0.134	< 0.01	0.061 (0.019; 0.108)	< 0.001	0.015	0.65
	2013	0.062	0.062	> 0.05	0.056 (0.036; 0.115)	< 0.001	0.010	
t_{mwc} (^{o}Cd)	2012	442	647	< 0.01	525 (391; 688)	< 0.001	61	0.43
	2013	494	616	< 0.01	507 (427; 652)	< 0.001	42	
Grain dimensions at maturity								
Grain length (mm)	2012	6.5	7.8	< 0.01	7.2 (6.2; 8.2)	< 0.001	0.2	0.79
	2013	7.0	8.2	< 0.01	7.5 (6.3; 8.6)	< 0.001	0.3	
Grain width (mm)	2012	3.4	3.2	> 0.05	3.3 (3.0; 3.6)	< 0.001	0.1	0.55
	2013	3.3	3.1	> 0.05	3.2 (2.9; 3.5)	< 0.001	0.1	
Grain height (mm)	2012	2.8	2.8	> 0.05	2.8 (2.5; 3.2)	< 0.001	0.09	0.73
	2013	3.0	2.8	> 0.05	2.8 (2.5; 3.3)	< 0.001	0.1	
Grain volume (mm^3)	2012	32.4	37.8	< 0.05	35.3 (27.0; 43.9)	< 0.001	2.4	0.68
	2013	35.6	37.8	> 0.05	35.3 (26.8; 47.8)	< 0.001	2.7	
Grain length/width	2012	1.9	2.4	< 0.01	2.2 (1.9; 2.4)	< 0.001	0.07	0.81
	2013	2.1	2.6	< 0.01	2.4 (2.0; 2.9)	< 0.001	0.1	
Grain length/height	2012	2.3	2.8	< 0.01	2.6 (2.2; 2.9)	< 0.001	0.08	0.79
	2013	2.3	2.9	< 0.01	2.6 (2.2; 3.2)	< 0.001	0.1	

Supplementary Table S6-2 Quantitative trait locus (QTL) coincidences between final grain weight and grain filling traits

Chromosome	No. of QTL for Fgw[a]	No. of QTL coincident with those for Fgw																	
		Cs	Igfr	Rgfr	Lgfr	Agfr	Mgfr	Ogf	Gfd	Tmax	Mwc	War	Wlr	Tmwc	Gl	Gw	Gh	Gv	Lw	Lh
2B	1										2		1							
2A.1[b]	2			3		5	2				2	2								
2A.2	2	1	1	2		3	1				2	2	1		2			2	1	
3B.1	2	2		1		2	1				2	2	2					1		
3B.2	3					1					3		1		2			2		
4A	5	2	1	4		3	3	1			5	2	6	2	1		2	2		
5A	2	1	1	1	1	1	1		1		2	2	1				1			1
5DL	2	2	1	1	1	2	1				3	3	1				2	1		
7B.1	2	1		1		2	1				4	5					1	1		
7B.2	3		1	3		4	3				5	4	5		1		1	1		
7D	2										2	1	1							
Total coincident QTL	–	9	5	16	2	23	13	1	1	0	32	23	19	2	6	0	7	10	1	1
Total QTL detected	26	13	5	22	4	31	16	1	2	0	36	26	23	5	8	2	8	13	6	2
Proportion (%)[c]	–	69	100	73	50	74	81	100	50	–	89	88	83	40	75	0	88	77	17	50

[a] Trait abbreviations: Fgw, final grain weight; Cs, carpel size; Igfr, initial grain filling rate; Rgfr, rapid grain filling rate; Lgfr, late grain filling rate; Agfr, average grain filling rate; Mgfr, maximum grain filling rate; Ogf, onset of grain filling; Gfd, grain filling duration; Tmax, the time at maximum grain filling rate; Mwc, grain maximum water content; War, grain water absorption rate; Wlr, grain water loss rate; Tmwc, the time at maximum grain water content; Gl, grain length; Gw, grain width; Gh, grain height; Gv, grain volume; Lw, grain length/width (L/W); Lh, grain length/height (L/H).

[b] Serial number following the chromosome name indicates multiple QTL regions on the same chromosome.

[c] Percentage of the QTL coincident with those for final grain weight to the total QTL number detected for each trait.

Supplementary Table S6-3 Quantitative trait locus (QTL) coincidences between carpel size and the other grain filling traits

Chromosome	No. of QTL for Cs[a]	No. of QTL coincident with those for Cs																
		Igfr	Rgfr	Lgfr	Agfr	Mgfr	Ogf	Gfd	Tmax	Mwc	War	Wlr	Tmwc	Gl	Gw	Gh	Gv	Lw	Lh
2A	1	1	2		3	1				2	2	1		2			2	1	
3B	2		1		2	1				2	2	2					1		
4A	2	1	4		3	3	1			5	2	6	2	1		2	2		
5A.1[b]	2														1			1	
5A.2	1	1	1	1	1	1		1		2	2	1				1			1
5B	1																		
5DL	2	1	1	1	2	1				3	3	1				2	1		
6A	1										1								
7B	1		1		2	1				4	5					1	1		
Total coincident QTL	−	4	10	2	13	8	1	1	0	18	17	11	2	3	1	6	7	2	1
Total QTL detected	13	5	22	4	31	16	1	2	0	36	26	23	5	8	2	8	13	6	2
Proportion (%)[c]	−	80	45	50	42	50	100	50	−	50	65	48	40	38	50	75	54	33	50

[a] Trait abbreviations: Cs, carpel size; Igfr, initial grain filling rate; Rgfr, rapid grain filling rate; Lgfr, late grain filling rate; Agfr, average grain filling rate; Mgfr, maximum grain filling rate; Ogf, onset of grain filling; Gfd, grain filling duration; Tmax, the time at maximum grain filling rate; Mwc, grain maximum water content; War, grain water absorption rate; Wlr, grain water loss rate; Tmwc, the time at maximum grain water content; Gl, grain length; Gw, grain width; Gh, grain height; Gv, grain volume; Lw, grain length/width (L/W); Lh, grain length/height (L/H).

[b] Serial number following the chromosome name indicates multiple QTL regions on the same chromosome.

[c] Percentage of the QTL coincident with those for carpel size to the total QTL number detected for each trait.

Supplementary Table S6-4 Quantitative trait locus (QTL) number detected for Grain 1, 2 and 3

Grain	Fgw[a]	Cs	Igfr	Rgfr	Lgfr	Agfr	Mgfr	Ogf	Gfd	Tmax	Mwc	War	Wlr	Tmwc
Grain 1	11	7	5	8	3	12	7	0	0	0	12	13	9	2
Grain 2	8	4	0	6	1	11	6	1	1	0	15	10	8	2
Grain 3	7	2	0	8	0	8	3	0	1	0	9	3	6	1
Total	26	13	5	22	4	31	16	1	2	0	36	26	23	5

[a] Trait abbreviations: Fgw, final grain weight; Cs, carpel size; Igfr, initial grain filling rate; Rgfr, rapid grain filling rate; Lgfr, late grain filling rate; Agfr, average grain filling rate; Mgfr, maximum grain filling rate; Ogf, onset of grain filling; Gfd, grain filling duration; Tmax, the time at maximum grain filling rate; Mwc, grain maximum water content; War, grain water absorption rate; Wlr, grain water loss rate; Tmwc, the time at maximum grain water content.

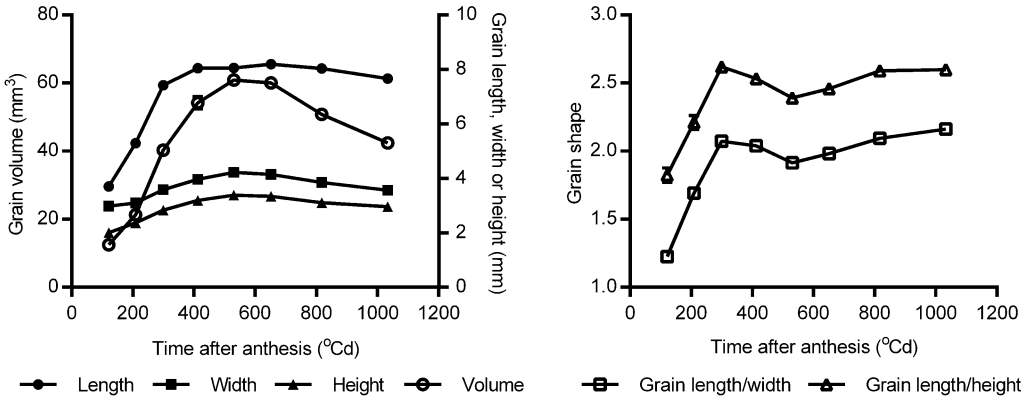

Supplementary Fig. S6-1 Grain expansion dynamics in 2013. Bars depict the standard errors of the means (SEM). The base temperature 0°C was used to calculate the accumulated thermal time from anthesis.

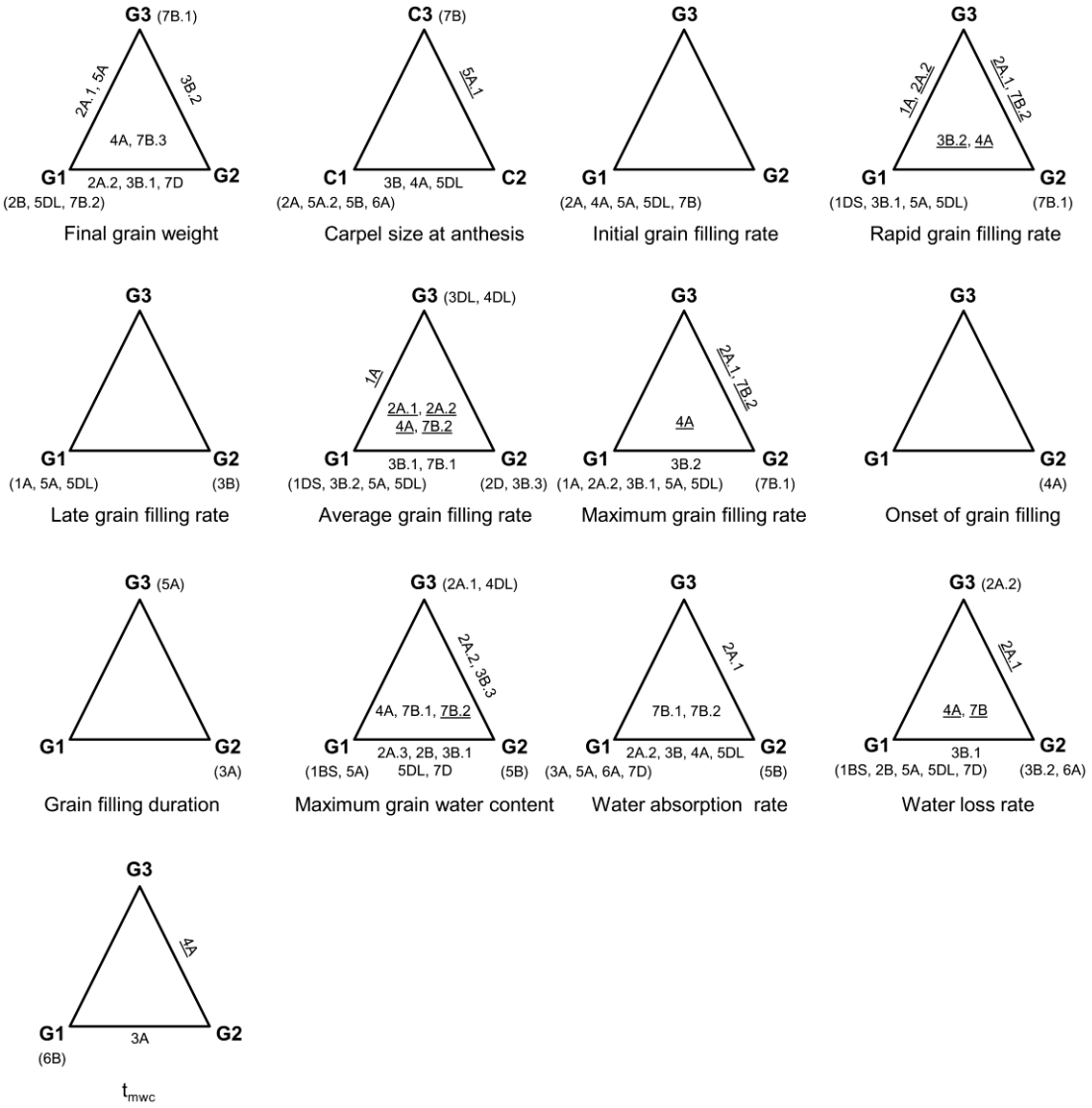

Supplementary Fig. S6-2 Quantitative trait locus (QTL) comparisons between different grains within spikelets. C1 (G1), C2 (G2) and C3 (G3) represent Carpel 1 (Grain 1), Carpel 2 (Grain 2), and Carpel 3 (Grain 3), respectively. Chromosome names following G1 (C1), G2 (C2), and G3 (C3) in the parentheses show the locations of position-specific QTL. Serial numbers after chromosome names indicate multiple QTL detected on the same chromosomes for a trait. The shared QTL with higher additive effects in G3 (C3) are marked by the underlines. The QTL shared by any two of the grains are placed at the middles outside the triangles, while these shared by all the three grains are placed inside the triangles. Trait abbreviation: tmwc, the time at maximum grain water content.

Chapter 7

General Discussion

Chapter 7 General discussion

7.1 Determination of yield and yield components

This project aimed to understand grain yield determination using an integrative approach of physiology and genetics in a bread wheat × spelt mapping population. To simplify this trait, yield was divided into a number of numerical (grain number and individual grain weight) and physiological (biomass and HI) components. Detailed analyses were done to address the physiological and genetic basis of three important components: fertile shoots (spikes) per plant (a key component of grain number), individual grain weight, and plant biomass.

It was found that grain number, individual grain weight, above-ground biomass and HI were positively associated with grain yield, as documented previously (Sayre et al., 1997; Shearman et al., 2005; Gonzalez et al., 2011; Sadras and Lawson, 2011; Bustos et al., 2013). This indicates that an increase in each component is able to improve yield indirectly, taking account of the trade-offs between them (see below). Grain number per unit land area consists of plant number per unit land area, fertile shoots (spikes) per plant, and grains per spike (further depending on spikelets per spike and grains per spikelet). Plant number per unit land area is determined by seed sown and plant establishment. Optimum plant densities are low, ranging from 62 (sown at the end of September in UK) to 140 (sown in mid-November) plants m^{-2} (Spink et al., 2000), and can be easily reached by currently high seed rates and seed quality, as well as improved sowing practices (e.g. sowing date and depth). In the field, a relatively low plant population does not lead to a loss of grain yield as a result of compensatory tillering (Sylvester-Bradley et al., 2008). Thus, the other two components, fertile shoots (spikes) per plant and grains per spike, are more critical for the genetic improvement of grain number. Detailed analysis showed that higher fertile shoot number per plant was associated with more total shoots, faster tillering rate, delayed tillering onset and cessation, and higher shoot survival. That is, genetic modification of tillering capacity, tillering timing and tiller abortion would result in more fertile shoots. In this study, QTL for these traits were identified, and QTL coincidences between them were observed, indicating the likelihood of simultaneous improvement of these traits for more fertile shoots. In addition to genetic control, tiller production and survival appear to be associated with some environmental cues, for example,

shade. Several previous reports have stated that low R:FR or far-red treatment inhibits tiller production by early tillering cessation (Evers et al., 2006; Sparkes et al., 2006; Ugarte et al., 2010; Toyota et al., 2014), consistent with the present study. Further, this study demonstrated that low R:FR after tiller initiation promoted tiller abortion. Intra-population light environment, therefore, is a key factor affecting fertile tiller production. Under low plant density, R:FR is higher (Sparkes et al., 2006; Chelle et al., 2007), leading to more total tillers per plant and higher tiller survival, which explains the compensatory role of tillering. This mechanism is valuable for yield stability across various growing conditions. In terms of the underlying physiological basis, it is proposed that an assimilate shortage for tiller buds or developing tillers, as a result of early stem elongation and enhanced stem growth induced by low R:FR, results in tillering cessation and tiller death. A similar mechanism has been reported for the determination of grain number per spike. Grains per spike were mainly associated with grains per spikelet, rather than spikelets per spike. A spikelet can initiate up to 10 florets, but many of them die just before anthesis (Kirby, 1988; González-Navarro et al., 2015). Long days increase spike growth and carbohydrate consumption, and the consequent sugar starvation triggers floret autophagy so that fertile floret number (and grains per spikelet) is defined (Ghiglione et al., 2008). Therefore, both key grain number components are affected by light signals, and maternal plants respond to them by reallocating resources within plants. It has been hypothesised that plants might use competition-like mechanisms to reallocate resources, and these processes would maximise the overall fitness of maternal plants (Sadras and Denison, 2009). In the case of wheat, tillering cessation and young tiller death would save resources for the growing stems of primary shoots in order to compete with neighbouring plants for more radiation. Distal floret abortion would also benefit the remaining florets to receive enough assimilates and set grains successfully. Plants judge these by considering the availability of environmental resources and/or capacity of resource capture. For example, increasing radiation during tiller abortion improves tiller survival (Thorne and Wood, 1987). In this study, pre-anthesis biomass, reflecting resource availability and capacity of resource capture by plants, was positively associated with grains per spike. As a major site of photosynthesis, leaf area also showed positive relationship with grains per spike. To improve tiller and floret fertility, therefore, sufficient environmental resources (e.g. radiation, water and nutrients) must be supplied; at the same time, the ability of plants to capture these

resources has to be enhanced, such as modifying plant architecture to increase radiation available for lower canopy layers, and increasing capacity of photosynthesis and nutrient uptake from soil.

For individual grain weight, it is clear that both pre- and post-anthesis periods are important. Carpels grow mainly from booting to anthesis, and carpel size at anthesis shows a positive relationship with final grain weight (Calderini et al., 1999; Hasan et al., 2011), in agreement with the present study. Apart from carpels, preanthesis biomass was positively associated with final grain weight, implying that grain weight could be determined at an early stage of maternal plant growth, at least before GS39. The physiological basis behind this may be involved in two routes. First, carpel growth responds to resources available before anthesis. This is supported by de-graining treatment at heading that increases assimilate supply for the remaining florets, leading to larger carpels at anthesis (Calderini and Reynolds, 2000). It was found in this study that QTL for biomass and carpel size were coincident on chromosomes 3B, 4A and 5A, indicating pleiotropic effects or tight gene linkages. Second, higher preanthesis biomass can accumulate more assimilates, many of which would be translocated to growing grains after anthesis. These reserves stored in vegetative organs (mainly stems, leaves and spikes) were estimated to apparently contribute 65% of grain yield, indicating the importance of preanthesis biomass. However, postanthesis biomass accumulation is also crucial, apparently contributing to 35% of grain yield, and primarily depends on green leaf persistence (stay-green) after anthesis. This study demonstrated that delayed but fast leaf senescence was associated with larger grains by increased grain filling rate, grain water absorption rate and maximum grain water content. Early anthesis had similar effects on final grain weight and grain filling processes, and also affected leaf senescence progress: the earlier anthesis, the later but faster leaf senescence. Fine-tuning of anthesis time, therefore, is important to increase postanthesis biomass accumulation and, in turn, individual grain weight.

As discussed above, the photoassimilates accumulated before and after anthesis are the sources for grain filling. A further increase in photoassimilate availability may have little effect on individual grain weight, namely sink limitation. Bread wheat is normally sink limited during grain filling (Slafer and Savin, 1994; Borras et al., 2004; Miralles and Slafer, 2007), concurring with the present study, which showed that doubling assimilate availability via the de-graining treatment at anthesis increased

grain weight by only 7.8%. Thus, a future target in wheat breeding must be removing sink limitation, i.e. increasing potential grain weight. To achieve this, the following aspects should be taken into account. In the first place, preanthesis carpel growth has been thought to set an upper limit for grain development (Calderini et al., 1999; Hasan et al., 2011). Potential carpel size can be enlarged by genetic improvement, and a number of QTL for this trait were identified in this study. As carpel size responds to preanthesis assimilate availability, an increase in plant biomass prior to anthesis through sufficient environmental resources and/or improved resource capture may stimulate carpel growth. In the second place, a filled mature grain undergoes three simultaneous processes: grain dry matter accumulation, grain water accumulation and subsequent desiccation, and grain morphological expansion. These processes interact strongly with each other, and are closely associated with final grain weight, indicating their roles as the physiological determinants. Interestingly, high level of QTL coincidences between grain filling traits were found, which enables simultaneous improvement through wheat breeding. In the third place, there is a large variation in grain weight within spikes, so increasing distal grain size would boost the average grain weight of a genotype. This study showed that smaller distal grains primarily stem from the late onset and slow initial rate of grain filling, which may be improved by increasing assimilate availability just before and/or after anthesis.

Turning to physiological components, biomass has been considered as a major target in future breeding (Fischer, 2011; Reynolds et al., 2012). Plant biomass at maturity is the sum of dry matter accumulated during different developmental intervals: from sowing to GS39, from GS39 to anthesis, and from anthesis to maturity. It was found that dry matter accumulated during each interval was positively associated with final biomass, indicating that biomass accumulation at each stage is important, even before GS39. As radiation is the main driver for dry matter synthesis, biomass can also be expressed as a function of light interception (LI) and radiation use efficiency (RUE) (Reynolds et al., 2012). To increase biomass from sowing to GS39, LI can be improved by slightly early canopy development (e.g. leaf initiation, leaf size and number, and tiller number); for example, leaf area showed a close and positive relationship with biomass at GS39. Higher RUE requires more efficient Rubisco and other Calvin cycle enzymes, reduced photoinhibition, and well-distributed light in the canopy. During the period from GS39 to anthesis, the canopy is well established

(Sylvester-Bradley et al., 2008), and most light can be intercepted, so RUE is the key determinant of biomass. After anthesis, however, both LI and RUE decrease as terminal senescence occurs (loss of green leaves reducing LI, and degradation of chlorophyll reducing RUE). The stay-green phenotype favours biomass production during grain filling (Gregersen et al., 2013). Given the weak relationship between biomass and plant height, it is possible to re-design wheat genotypes with high biomass but short stems, thereby avoiding an increased risk of lodging.

Harvest index has been largely improved in wheat breeding, currently approaching its theoretical maximum value (c. 0.64) (Foulkes et al., 2011; Reynolds et al., 2012). This study emphasises that a further increase in HI may depend on fewer infertile tillers and efficient nutrient remobilisation during grain filling and terminal senescence. As there is a net loss of dry matter from non-surviving tillers, they should be minimised to improve HI (Sharma, 1995; Berry et al., 2003; Foulkes et al., 2011). Tiller survival can be increased by increasing resource availability and optimising light environment in the canopy, as stated above. During grain filling, many preanthesis non-structural nutrients stored in stems, leaves and spikes (e.g. water soluble carbohydrates) will be translocated into growing grains (van Herwaarden et al., 1998; Rebetzke et al., 2008), which can decrease the proportions of dry matter in vegetative organs at maturity, and, in turn, increase HI. Terminal senescence ensues at late grain filling, during which chlorophyll, proteins, membrane lipids and other macromolecules in senescing organs are degraded, and the resultant nutrients can be partly remobilised to growing grains (Distelfeld et al., 2014). Higher nutrient use efficiency at terminal senescence would improve HI and yield. Regarding leaf senescence, it is proposed that delayed, short but fast senescence should be preferred for better utilisation of leaf current photosynthesis and structural nutrients: delayed leaf senescence would produce more assimilates for grain filling, and short but fast senescence would benefit nutrient use efficiency and HI.

7.2 Trade-offs between yield components to maximise yield potential

Ideally, all favourable traits (more grains, larger grains, higher biomass and HI) are assembled in new genotypes to maximise grain yield. However, this becomes difficult if there are any negative interactions between components. For two physiological components, final biomass was not significantly associated with HI, indicating that they can be increased at the same time (Garcia et al., 2013). In contrast, individual

grain weight was negatively associated with all the grain number components (grains per spike, spikelets per spike, fertile spikelets per spike, grains per spikelet, and fertile shoots per plant), resulting from pleiotropic effects or gene linkages. In other words, higher individual grain weight would lead to fewer grains. The time-courses for determination of grain number and individual grain weight are overlapped approximately from booting to anthesis, when tiller abortion, floret death, rapid accumulation of stem WSC, and carpel growth coincide. It was observed that more fertile shoots and grains per spike were associated with smaller carpels at anthesis (also less stem WSC for more fertile shoots), as supported by the genetic analysis. Therefore, wheat plants define grain number and potential grain size simultaneously during that critical time. Under favourable conditions, more grains may be defined by increasing fertile shoot and distal floret number, and then the growth of primary carpels would be limited by allocating assimilates for newly produced ones. Smaller carpels also match the reduced stem WSC available for grain filling. This mechanism might allow plants to produce uniform, viable seeds, while maintaining maternal fitness. These processes are fulfilled likely as a result of pleiotropic effects and tight linkages of functionally related genes, as presented in this study. In wheat breeding, the inverse relationship between grain number and individual grain weight can be overcome by eliminating genes with pleiotropic effects, separating linked genes and adding more independent ones.

7.3 Genetic variation as a strategy to improve yield and yield components

This work described a total of 201 traits involving yield, yield components, threshability, tillering dynamics, biomass accumulation and partitioning, phasic development, leaf senescence, and grain filling process; all of them showed large genetic variation among the RILs. Transgressive segregation was also observed for each trait. For example, 10.39 t ha^{-1} for machine-harvested grain yield were found in Line 113 in 2013, compared to 10.20 t ha^{-1} over the UK winter wheat cultivars currently recommended by HGCA. This genotype had the highest grain number m^{-2} as well (24 864 grains), 28% more than that of the high-value parent Forno. For TGW, the highest value was seen in Line 251 (52.6 g), with a relatively large individual grain volume of 40 mm^3, indicating the potential for grain size and end-use quality improvement in bread wheat. Line 177 showed the highest above-ground biomass m^{-2}

(2 428 g), 27% more than that of the high-value parent Oberkulmer, concurring with a relatively high single-shoot biomass (5.05 g). HI of the RILs, however, did not exceed the bread wheat Forno (0.51). Transgressive segregation was also determined in other physiological traits, which gives a wide range of genetic combinations to maximise grain yield and yield components.

Crossing is a traditional way to combine different desirable traits to new genotypes. After hybridisation, genetic recombinations between parental chromosomes occur since their F_1 hybrids, leading to segregating offspring with combined desirable traits. If multiple desirable traits need to be combined, a larger population of offspring has to be produced in order to obtain target lines. These lines may be backcrossed with elite varieties to eliminate detrimental traits. Conventional breeding has long been used to develop new wheat varieties, and contributed greatly to yield gain. However, this process can be accelerated with the help of marker-assisted selection (MAS). To achieve this, molecular markers associated with desirable traits have to be identified (QTL). By using these markers, a large number of segregating individuals can be screened rapidly in lab without sowing in field. In the present study, numerous molecular markers for yield, yield components and associated traits were obtained, and they would be useful for trait-based physiological and molecular breeding.

Large genetic variation in the RILs benefits from the use of spelt as a parent. Spelt Oberkulmer differed from bread wheat Forno in most of traits investigated. Compared with Forno, Oberkulmer had many desirable phenotypes to improve yield and yield components, including high individual grain weight, high tillering capacity, fast tillering rate, late tillering onset and cessation, high tiller survival and fertile tiller number, tolerance to low light quality, high biomass, large plant organs (leaf, stem and spike), high stem WSC, large leaf area, rapid preanthesis spike growth, long and lax spikes, large carpels at anthesis, large grain volume, and long grains. Furthermore, a total of 378 favourable alleles were identified from spelt, including 60 alleles for yield and yield components, 16 for tillering, 120 for biomass accumulation and partitioning, two for flowering time, 15 for leaf senescence, five for spike length and compactness, 10 for carpel size, 134 for grain dry matter and water accumulation, and 16 for grain dimensions. These indicate that spelt is a useful gene source to improve yield, yield components and associated physiological traits of bread wheat. As an ancient crop and a relative of bread wheat, spelt can be used to broaden genetic

variation in wheat breeding. While introducing desirable genes and traits from spelt to bread wheat, care must be taken to eliminate any unfavourable traits of spelt, in particular low threshability. The non-free threshing habit of spelt is mainly controlled by the Q gene on chromosome 5AL, where many favourable alleles (e.g. for long and lax spikes, grain number components, tillering capacity, tiller survival and biomass accumulation) are coincident. These alleles are difficult to use while maintaining the free-threshing habit. Most of the other favourable alleles from spelt, however, can be transferred to bread wheat without this problem.

7.4 Detection and distribution of the QTL for yield, yield components and associated physiological traits

Benefiting from the distinct genetic architecture between bread wheat and spelt, a total of 860 QTL for yield, yield components and associated physiological traits were detected in the RIL mapping population across three years. Among all the traits, thousand grain weight (19), spikelets per spike (16), grain maximum water content (15), grain volume (13), and grain threshability (12) had more QTL detected, compared with many others such as crop growth rate presenting no QTL. On average, c. four QTL were identified for each trait. A further analysis revealed that QTL number detected for a trait was positively correlated with its broad sense heritability (H^2): the higher H^2, the more QTL detectable (Fig. 7-1). In other words, it is difficult to identify QTL for the traits that are more environmentally controlled. Environmental cues during plant growth and development are various, including light signals (e.g. light quantity, light quality and photoperiod), temperature (e.g. frost and heat), and the levels of nutrients (e.g. N, P and K) and water in soil. If a trait is responsive to many of these factors, numerous genes belonging to different pathways would together determine the final phenotype, and each gene might have only a small effect, making it hard to be statistically detected. Moreover, the phenotype resulting from previous response(s) might fade at later developmental stages, so the measurement taken at a time point reflects the newest response or accumulated responses occurring before. Thus, the networks underlying different responses have to be clarified to understand the final phenotype of a trait. In wheat breeding, priority should be given to these traits with relatively high H^2.

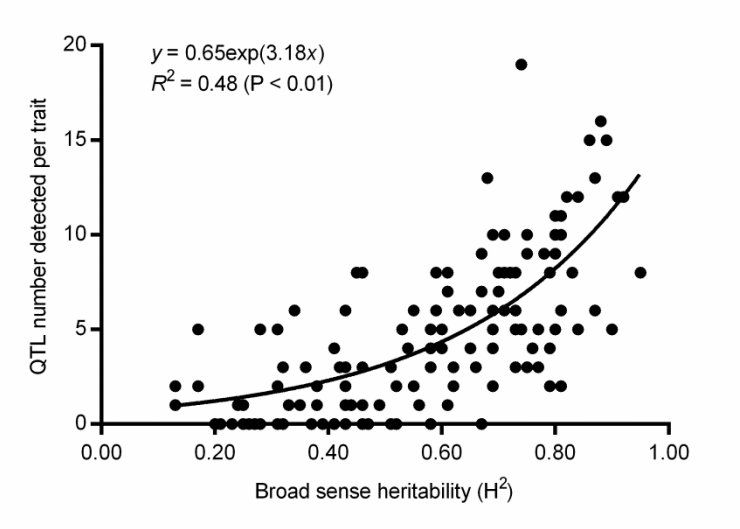

Fig. 7-1 Relationship between broad sense heritability (H^2) and quantitative trait locus (QTL) number detected per trait. Each closed cycle indicates a trait investigated.

The QTL identified here were scattered on all the chromosomes of wheat, and QTL coincidences between different traits were frequent, particularly on chromosomes 1BS, 2A, 2B, 3A, 3B, 4A, 5A, 5B, 5DL, and 7B, indicating pleiotropy or tight gene linkages. It was observed that phenotypically correlated traits usually had coincident QTL: if the phenotypic correlations were positive, their increasing alleles originated from the same parents, and vice versa. Based on this QTL cluster map, it is possible to predict trait relationships at physiological level and resultant phenotypes (e.g. for crop modelling). This is especially important in breeding when a desirable trait is targeted while avoiding other detrimental ones. The pleiotropic effects or tight gene linkages facilitate rapid initiation of multiple physiological processes, leading to systematic changes in plant growth and development. Under stressed environments, these processes might benefit trade-offs among plant organs by reallocating resources.

7.5 References

Berry PM, Spink JH, Foulkes MJ, Wade A. 2003. Quantifying the contributions and losses of dry matter from non-surviving shoots in four cultivars of winter wheat. Field Crops Research **80**, 111-121.

Borras L, Slafer GA, Otegui ME. 2004. Seed dry weight response to source-sink manipulations in wheat, maize and soybean: a quantitative reappraisal. Field Crops Research **86**, 131-146.

Bustos DV, Hasan AK, Reynolds MP, Calderini DF. 2013. Combining high grain number and weight through a DH-population to improve grain yield potential of wheat in high-yielding environments. Field Crops Research **145**, 106-115.

Calderini DF, Abeledo LG, Savin R, Slafer GA. 1999. Effect of temperature and carpel size during pre-anthesis on potential grain weight in wheat. Journal of Agricultural Science **132**, 453-459.

Calderini DF, Reynolds MP. 2000. Changes in grain weight as a consequence of de-graining treatments at pre- and post-anthesis in synthetic hexaploid lines of wheat (Triticum durum × T. tauschii). Australian Journal of Plant Physiology **27**, 183-191.

Chelle M, Evers JB, Combes D, Varlet-Grancher C, Vos J, Andrieu B. 2007. Simulation of the three-dimensional distribution of the red:far-red ratio within crop canopies. New Phytologist **176**, 223-234.

Distelfeld A, Avni R, Fischer AM. 2014. Senescence, nutrient remobilization, and yield in wheat and barley. Journal of Experimental Botany **65**, 3783-3798.

Evers JB, Vos J, Andrieu B, Struik PC. 2006. Cessation of tillering in spring wheat in relation to light interception and red:far-red ratio. Annals of Botany **97**, 649-658.

Fischer RA. 2011. Wheat physiology: a review of recent developments. Crop and Pasture Science **62**, 95-114.

Foulkes MJ, Slafer GA, Davies WJ, Berry PM, Sylvester-Bradley R, Martre P, Calderini DF, Griffiths S, Reynolds MP. 2011. Raising yield potential of wheat. III. Optimizing partitioning to grain while maintaining lodging resistance. Journal of Experimental Botany **62**, 469-486.

Garcia GA, Hasan AK, Puhl LE, Reynolds MP, Calderini DF, Miralles DJ. 2013. Grain yield potential strategies in an elite wheat double-haploid population grown in contrasting environments. Crop Science **53**, 2577-2587.

Ghiglione HO, Gonzalez FG, Serrago R, Maldonado SB, Chilcott C, Cura JA, Miralles DJ, Zhu T, Casal JJ. 2008. Autophagy regulated by day length determines the number of fertile florets in wheat. Plant Journal **55**, 1010-1024.

González-Navarro OE, Griffiths S, Molero G, Reynolds MP, Slafer GA. 2015. Dynamics of floret development determining differences in spike fertility in an elite population of wheat. Field Crops Research **172**, 21-31.

Gonzalez FG, Terrile II, Falcon MO. 2011. Spike fertility and duration of stem elongation as promising traits to improve potential grain number (and yield): variation in modern Argentinean wheats. Crop Science **51**, 1693-1702.

Gregersen PL, Culetic A, Boschian L, Krupinska K. 2013. Plant senescence and crop productivity. Plant Molecular Biology **82**, 603-622.

Hasan AK, Herrera J, Lizana C, Calderini DF. 2011. Carpel weight, grain length and stabilized grain water content are physiological drivers of grain weight determination of wheat. Field Crops Research **123**, 241-247.

Kirby EJM. 1988. Analysis of leaf, stem and ear growth in wheat from terminal spikelet stage to anthesis. Field Crops Research **18**, 127-140.

Miralles DJ, Slafer GA. 2007. Sink limitations to yield in wheat: how could it be reduced? Journal of Agricultural Science **145**, 139-149.

Rebetzke GJ, van Herwaarden AF, Jenkins C, Weiss M, Lewis D, Ruuska S, Tabe L, Fettell NA, Richards RA. 2008. Quantitative trait loci for water-soluble carbohydrates and associations with agronomic traits in wheat. Australian Journal of Agricultural Research **59**, 891-905.

Reynolds M, Foulkes J, Furbank R, Griffiths S, King J, Murchie E, Parry M, Slafer G. 2012. Achieving yield gains in wheat. Plant Cell and Environment **35**, 1799-1823.

Sadras VO, Denison RF. 2009. Do plant parts compete for resources? An evolutionary viewpoint. New Phytologist **183**, 565-574.

Sadras VO, Lawson C. 2011. Genetic gain in yield and associated changes in phenotype, trait plasticity and competitive ability of South Australian wheat varieties released between 1958 and 2007. Crop and Pasture Science **62**, 533-549.

Sayre KD, Rajaram S, Fischer RA. 1997. Yield potential progress in short bread wheats in northwest Mexico. Crop Science **37**, 36-42.

Sharma RC. 1995. Tiller mortality and its relationship to grain yield in spring wheat. Field Crops Research **41**, 55-60.

Shearman VJ, Sylvester-Bradley R, Scott RK, Foulkes MJ. 2005. Physiological processes associated with wheat yield progress in the UK. Crop Science **45**, 175-185.

Slafer GA, Savin R. 1994. Source-sink relationships and grain mass at different positions within the spike in wheat. Field Crops Research **37**, 39-49.

Sparkes DL, Holme SJ, Gaju O. 2006. Does light quality initiate tiller death in wheat? European Journal of Agronomy **24**, 212-217.

Spink JH, Whaley J, Semere T, Wade A, Sparkes D, Foulkes J. 2000. Prediction of optimum plant population in winter wheat. London: HGCA.

Sylvester-Bradley R, Berry P, Blake J, Kindred D, Spink J, Bingham I, McVittie J, Foulkes J. 2008. The wheat growth guide. London: HGCA.

Thorne GN, Wood DW. 1987. Effects of radiation and temperature on tiller survival, grain number and grain yield in winter wheat. Annals of Botany **59**, 413-426.

Toyota M, Tatewaki N, Morokuma M, Kusutani A. 2014. Tillering responses to high red/far-red ratio of four Japanese wheat cultivars. Plant Production Science **17**, 124-130.

Ugarte CC, Trupkin SA, Ghiglione H, Slafer G, Casal JJ. 2010. Low red/far-red ratios delay spike and stem growth in wheat. Journal of Experimental Botany **61**, 3151-3162.

van Herwaarden AF, Angus JF, Richards RA, Farquhar GD. 1998. 'Haying-off', the negative grain yield response of dryland wheat to nitrogen fertiliser. II. Carbohydrate and protein dynamics. Australian Journal of Agricultural Research **49**, 1083-1093.

Chapter 8

Conclusions and Future Work

Chapter 8 Conclusions and future work

8.1 Conclusions

Based on the findings in this project, the following key conclusions can be presented:

- Large genetic variation in yield, yield components and associated physiological traits exists in the bread wheat Forno × spelt Oberkulmer mapping population. Spelt has many desirable traits and alleles independent of low threshability and tenacious glumes, so it is a useful genetic resource to improve yield and yield components of bread wheat, while maintaining the free-threshing habit.
- The tillering process is under both genetic and environmental control. More fertile shoots per plant can be achieved by genetic selection for more total shoots initiated, faster tillering rate, delayed tillering onset and cessation, and higher shoot survival. Low red:far red ratio (R:FR) leads to early tillering cessation, few total shoots, high infertile shoot number and shoot abortion, probably resulting from an assimilate shortage for tiller buds or developing tillers due to early stem elongation and enhanced stem growth induced by low R:FR.
- More fertile tillers normally contribute to plant yield and grain number without reducing yield and grain set of individual shoots. However, more fertile tillers decrease individual grain weight, at least partly because of smaller carpels and fewer stem water soluble carbohydrates at anthesis, as a consequence of pleiotropic effects or tight gene linkages.
- Plant biomass accumulation during preanthesis period benefits yield and yield components at maturity.
- Slightly earlier anthesis results in delayed and faster leaf senescence, leading to faster grain filling and water absorption rates, higher maximum grain water content, and, in turn, larger grains.
- Carpel size at anthesis, grain dry matter accumulation, grain water uptake and loss, and grain morphological expansion interact strongly with each other, and play important roles in determining final grain weight. The complex but orderly grain filling processes result from high level of QTL coincidences,

which will allow simultaneous improvement of multiple grain filling traits for larger grains.

- Distal grains within spikelets are smaller than basal ones at maturity, primarily stemming from their late onset and slow initial rate of grain filling, and synchronous maturity between different grains. Distal grain size could be improved by increasing assimilate availability just before and/or after anthesis.
- These results improve our understanding of the physiological and genetic determination of yield and yield components, and provide useful information for trait-based physiological and molecular breeding in wheat.

8.2 Future work

8.2.1 Fine mapping for marker-assisted breeding and identification of candidate genes

This study presents numerous QTL for yield, yield components and associated physiological traits. However, there are still some chromosomes with only a few markers (e.g. 6A, 6B and 6D), suggesting that more QTL may be detected in these map gaps. For the QTL identified here, some markers are coincident, or closely linked with the QTL, so they might be used directly for MAS for the genotypes carrying favourable alleles. Many of the remaining QTL are flanked with relatively sparse markers, and these QTL intervals have to be fine-mapped. Fine mapping is able to find more closely linked markers for the genes of interest so that these genes can be tracked successfully in the segregating progeny. In addition, extra genes residing between markers and target genes would be reduced, and this minimises the possible detrimental effects. Apart from MAS, fine mapping is an essential step to address whether QTL coincidences are caused by pleiotropy or tight gene linkages. In this project, considerable QTL coincidences between different traits were observed, particularly on chromosomes 1BS, 2A, 2B, 3A, 3B, 4A, 5A, 5B, 5DL, and 7B, suggesting the opportunity of simultaneous selection for multiple favourable traits. These QTL regions should be saturated with a set of dense markers (e.g. single nucleotide polymorphism, SNP). A number of RILs carrying favourable alleles of the coincident QTL are selected in the mapping population, and then backcrossed with the parent conferring unfavourable alleles. Genotypes of the RILs selected should be as similar as possible to that of the recurrent parent except the QTL of interest, in order to reduce the generations of backcrossing. After a few generations of backcrossing and

selfing, phenotyping and genotyping are carried out in the new population consisting of a large number of individuals. If different QTL are detected, there are multiple genes in the region of previously coincident QTL; otherwise, it suggests pleiotropy. For the latter case, a further analysis is needed to identify the underlying candidate genes. Draft genome sequence of bread wheat is currently available by using the next generation sequencing technologies (Brenchley *et al.*, 2012; The International Wheat Genome Sequencing Consortium, 2014). Based on the information of genome sequence and SNP markers, candidate genes residing in the narrow QTL regions may be identified. This can be complemented by synteny studies with other species like rice and barley. Map-based gene cloning is to be continued, followed by functional analysis in transgenic wheat plants.

8.2.2 Responses of grain number components to changes in resource availability during stem elongation

Stem growth of primary shoots may induce tillering cessation and young tiller death due to an assimilate shortage. It can be hypothesised that a change in resource availability would reduce or intensify the competition between main stems and growing tiller buds or tillers. For example, increasing the levels of radiation and nutrients (e.g. nitrogen) just before and during stem elongation might extend tillering and reduce tiller abortion, respectively. On the other hand, partial defoliation might lead to earlier tillering cessation and higher tiller abortion. Little is known about the genetic basis of initial stem growth (from procumbent to erect stems) to date; this process may be revealed by transcriptome analysis in true stems with the help of emerging RNA sequencing technology. Similarly, transcriptome dynamics of tiller buds and young tillers that are destined to be dormant and die, respectively, can be analysed by consecutive sampling. Comparisons between transcriptome profiles of stem growth and tiller (bud) development will likely unravel their interactions. A further genetic analysis may be carried out while combing different treatments (e.g. far red, red, nutrient supply and radiation).

Strigolactones (or related compounds), recently characterised as a new class of plant hormones, respond to nitrogen and phosphorus deficiency and inhibit plant shoot branching, while stimulating symbiotic fungi in the rhizosphere to facilitate soil nutrient uptake by plants (Gomez-Roldan *et al.*, 2008; Umehara *et al.*, 2008; Umehara, 2011). These hormones probably work in wheat as well, regulating the

assimilate reallocation among plant organs as a response to environmental resource availability. This may be taken into account in the above experiments.

The other key component of grain number is grains per spike, which depend on floret fertility determined during a short period before anthesis. To test the responses of distal florets to assimilate supply, different treatments may be applied: defoliation (reducing assimilate supply), and floret removal (removing half of the spikelets of a spike or the basal florets within spikelets; increasing assimilate supply). Gene expressions in the carpels and anthers of distal florets are to be quantified by transcriptome analysis.

8.2.3 Effects of endosperm cell number, cell size, endoreduplication and cell death on grain filling

Endosperm cells are the major structure of developing grains to accumulate dry matter and water, and to drive morphological expansion. It has been reported that endosperm cell number is positively associated with grain water content and final grain weight (Brocklehurst, 1977; Gleadow *et al.*, 1982; Singh and Jenner, 1982a; Gao *et al.*, 1992; Gonzalez *et al.*, 2014). Thus, the number and size of endosperm cells may play important roles in grain filling. Cell division and expansion take place until *c*. 20 and 30 days after anthesis, respectively (Briarty *et al.*, 1979; Gleadow *et al.*, 1982; Jenner *et al.*, 1991). In this project, young grains of the subset RILs at these stages have been fixed and stored in a cold room. The endosperms can be removed, digested by pectinase, and crushed to release nuclei (Singh and Jenner, 1982b). After staining (e.g. with propidium iodide), nuclei (equal to cell number) are able to be counted with a haemocytometer or flow cytometry. For cell size, endosperm cells are spread and stained; then, images can be taken and analysed using the software Image J.

Endoreduplication is a process that an endosperm cell increases its nuclear DNA content from 3C to 24C (Chojecki *et al.*, 1986; Wegel and Shaw, 2005). An increase in nuclear DNA content is probably accompanied with more gene copies, and there is a positive relationship between endosperm DNA content and final grain weight (Chojecki *et al.*, 1986). Endoreduplication, therefore, may be crucial to determine grain filling. With the increasing use of flow cytometry in plants, quantifying cell nuclear content becomes straightforward. Even so, studies in this field are still rare, especially in wheat.

Another potentially important process during grain filling, which has long received

little attention, is endosperm cell death. It occurs from *c*. 16 days after flowering (Young and Gallie, 1999), concurring with the cessation of endosperm cell division. During this period, grain filling is fast, and early breakdown of endosperm cells may be detrimental for further accumulation of dry matter.

Grain weight determination at cell level is substantially important. Genetic basis of endosperm cell initiation, endoreduplication and cell death needs to be addressed. This information would supplement the present study regarding carpel size, grain dry matter accumulation, grain water uptake and loss, and grain morphological expansion. Potential QTL coincidences between these traits might imply the underlying gene functions (from cell initiation and death, grain filling dynamics to final grain weight). In addition, distal grains are smaller than basal ones within spikelets, and removing basal grains likely increases distal ones significantly. Comparisons of the transcriptomes between control and treated distal grains may reveal key genes and pathways for grain filling.

8.3 References

Brenchley R, Spannagl M, Pfeifer M, et al. 2012. Analysis of the bread wheat genome using whole-genome shotgun sequencing. Nature **491**, 705-710.

Briarty LG, Hughes CE, Evers AD. 1979. The developing endosperm of wheat - a stereological analysis. Annals of Botany **44**, 641-658.

Brocklehurst PA. 1977. Factors controlling grain weight in wheat. Nature **266**, 348-349.

Chojecki AJS, Bayliss MW, Gale MD. 1986. Cell production and DNA accumulation in the wheat endosperm, and their association with grain weight. Annals of Botany **58**, 809-817.

Gao XP, Francis D, Ormrod JC, Bennett MD. 1992. Changes in cell number and cell division activity during endosperm development in allohexaploid wheat, Triticum aestivum L. Journal of Experimental Botany **43**, 1603-1609.

Gleadow RM, Dalling MJ, Halloran GM. 1982. Variation in endosperm characteristics and nitrogen content in six wheat lines. Australian Journal of Plant Physiology **9**, 539-551.

Gomez-Roldan V, Fermas S, Brewer PB, et al. 2008. Strigolactone inhibition of shoot branching. Nature **455**, 189-194.

Gonzalez FG, Aldabe ML, Terrile II, Rondanini DP. 2014. Grain weight response to different postflowering source: sink ratios in modern high-yielding Argentinean wheats differing in spike fruiting efficiency. Crop Science **54**, 297-309.

Jenner CF, Ugalde TD, Aspinall D. 1991. The physiology of starch and protein deposition in the endosperm of wheat. Australian Journal of Plant Physiology **18**, 211-226.

Singh BK, Jenner CF. 1982a. Association between concentrations of organic nutrients in the grain, endosperm cell number and grain dry weight within the ear of wheat. Australian Journal of Plant Physiology **9**, 83-95.

Singh BK, Jenner CF. 1982b. A modified method for the determination of cell number in wheat endosperm. Plant Science Letters **26**, 273-278.

The International Wheat Genome Sequencing Consortium. 2014. A chromosome-based draft sequence of the hexaploid bread wheat (Triticum aestivum) genome. Science **345**, 1251788.

Umehara M. 2011. Strigolactone, a key regulator of nutrient allocation in plants. Plant Biotechnology **28**, 429-437.

Umehara M, Hanada A, Yoshida S, et al. 2008. Inhibition of shoot branching by new terpenoid plant hormones. Nature **455**, 195-200.

Wegel E, Shaw PJ. 2005. Chromosome organization in wheat endosperm and embryo. Cytogenetic and Genome Research **109**, 175-180.

Young TE, Gallie DR. 1999. Analysis of programmed cell death in wheat endosperm reveals differences in endosperm development between cereals. Plant Molecular Biology **39**, 915-926.

Appendices

Appendices

Field trial 2011−2012: agronomy

Title		Wheat x Spelt
Researcher		Quan Xie - Debbie Sparkes
	Date	**Details**
Field		S24
Previous crop		Winter Oats
SNS N Index	2012/2/23	18.9 kg/ha, SNS Index 0
Soil Indices		P:4, K:4, Mg:4, pH:7.6
Cultivations	2011/9/13	Plough
	2011/9/22	Powerharrow
	2011/10/19	Roll after drilling
Crop/variety		Various (see seedrates tab)
TGW (g)		Various (see seedrates tab)
Sowing	2011/10/19	
Seed rate (m^{-2})		250 seeds m^{-2}
Drill type		Wintersteiger
Row width (cm)		12.5
Plot length (m)		6
Plot width (m)		1.625
Fertiliser	2012/2/24	2.0 l/ha Headland Jet
	2012/3/8	116 kg/ha 34.5% Nitram (40kg/ha N)
	2012/3/20	Headland Jett @ 2l/ha
	2012/4/11	116 kg/ha 34.5% Nitram (40kg/ha N)
	2012/4/30	Manganese 15% @1.5l/ha
	2012/5/10	174 kg/ha 34.5% Nitram (60kg/ha N)
	2012/5/23	Magnor @ 1l/ha
	2012/5/25	Magnor @ 1l/ha
Herbicide	2011/11/9	Liberator @ 0.6l/ha
	2012/3/20	Lorate @ 25g/ha
	2012/4/24	Foxtrot @ 1l/ha + Toil @ 1l/ha
	2012/5/23	Spitfire @ 1l/ha
Fungicide	2012/3/20	Instinct @ 0.4l/ha + Bravo @ 1l/ha + Opus @ 0.75l/ha
	2012/4/30	Cortez @ 0.75l/ha + Phoenix @ 1.3l/ha
	2012/5/23	Opus @ 0.75l/ha + Phoenix @ 1.3l/ha
	2012/6/25	Orius @ 0.85l/ha + Vegas @ 0.15l/ha
Insecticide	2011/11/9	Permasect @ 0.25l/ha
	2012/6/25	Aphox @ 0.28kg/ha
PGR	2012/3/20	Moddus @ 0.2l/ha
	2012/4/30	Moddus @ 0.2l/ha + Chlormequat @ 1.5l/ha

Field trial 2011−2012: experimental design

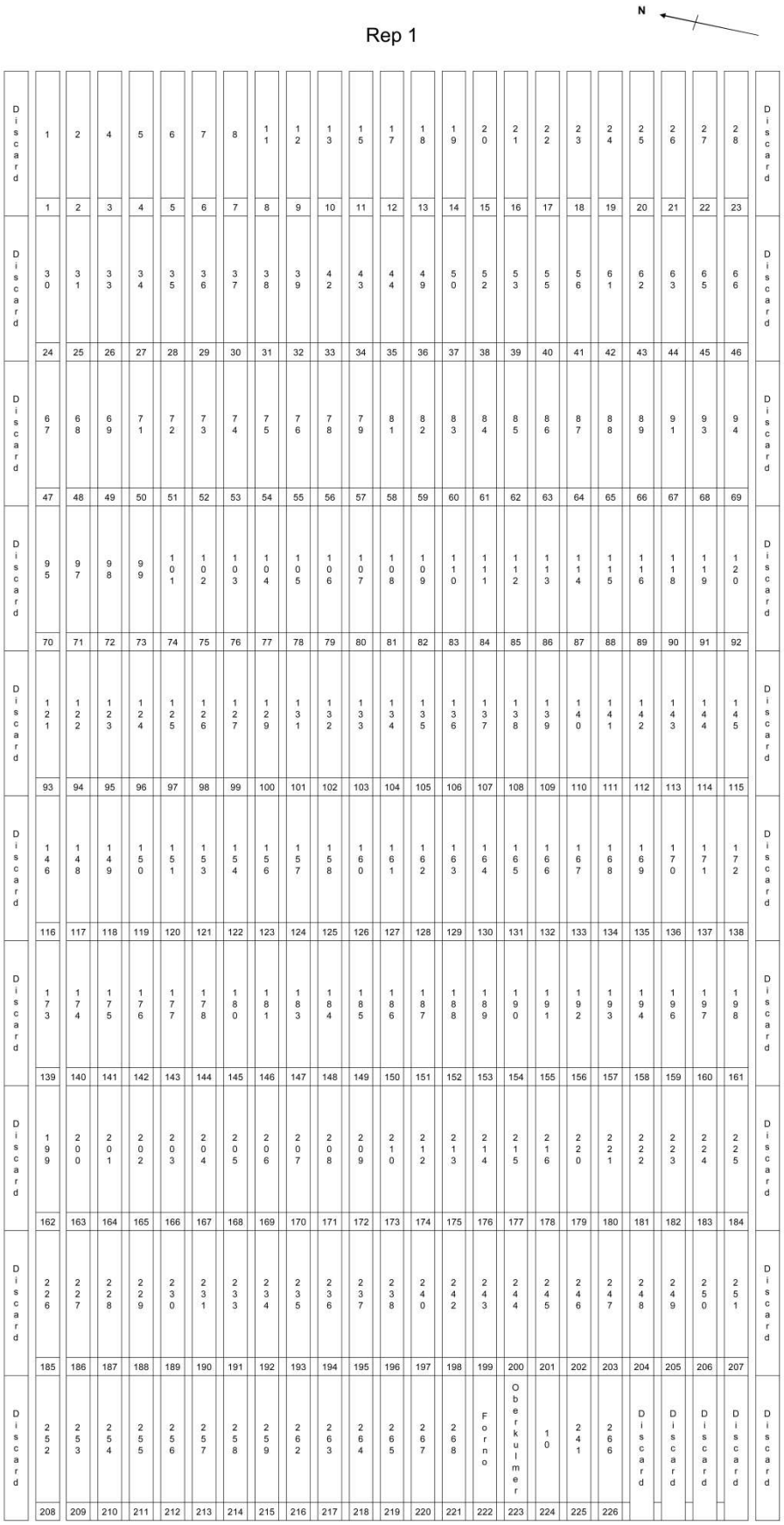

N

Rep 2

Discard	66	19	234	203	165	33	255	190	154	106	85	258	149	120	209	199	228	174	111	Forno	223	180	150	Discard
	227	228	229	230	231	232	233	6	234	235	236	237	238	239	240	241	242	243	244	245	246	247	248	249	
Discard	246	156	121	268	98	216	118	63	264	125	17	1	245	160	84	250	173	42	222	105	208	22	267	Discard
	250	251	252	253	254	255	256	1	257	258	259	260	261	262	263	264	265	266	267	268	269	270	271	272	
Discard	231	163	83	13	164	131	104	141	55	198	82	110	215	53	153	6	72	189	256	97	178	233	124	Discard
	273	274	275	276	277	278	279	6	280	281	282	283	284	285	286	287	288	289	290	291	292	293	294	295	
Discard	122	224	151	214	61	230	188	144	244	140	227	81	243	35	221	103	202	108	27	143	187	123	62	Discard
	296	297	298	299	300	301	302	6	303	304	305	306	307	308	309	310	311	312	313	314	315	316	317	318	
Discard	204	252	95	79	107	142	7	23	213	116	34	52	207	186	196	94	148	86	56	240	12	11	161	Discard
	319	320	321	322	323	324	325	6	326	327	328	329	330	331	332	333	334	335	336	337	338	339	340	341	
Discard	109	201	162	36	242	73	194	2	212	138	102	229	39	175	67	65	172	249	139	129	18	69	119	Discard
	342	343	344	345	346	347	348	6	349	350	351	352	353	354	355	356	357	358	359	360	361	362	363	364	
Discard	259	71	193	127	28	238	158	134	93	171	265	253	87	170	263	37	21	197	166	91	235	168	78	Discard
	365	366	367	368	369	370	371	6	372	373	374	375	376	377	378	379	380	381	382	383	384	385	386	387	
Discard	76	114	177	43	210	26	205	74	183	31	257	112	Oberkulmer	99	50	157	24	4	133	115	135	8	30	Discard
	388	389	390	391	392	393	394	6	395	396	397	398	399	400	401	402	403	404	405	406	407	408	409	410	
Discard	145	248	101	5	262	137	251	88	38	236	113	247	225	25	200	185	167	169	191	176	132	44	181	Discard
	411	412	413	414	415	416	417	418	419	420	421	422	423	424	425	426	427	428	429	430	431	432	433		
Discard	20	220	226	49	192	184	68	237	146	254	206	126	15	89	136	75	241	Discard	Discard	Discard	Discard	Discard	Discard	Discard	
	434	435	436	437	438	439	440	441	442	443	444	445	446	447	448	449	450								

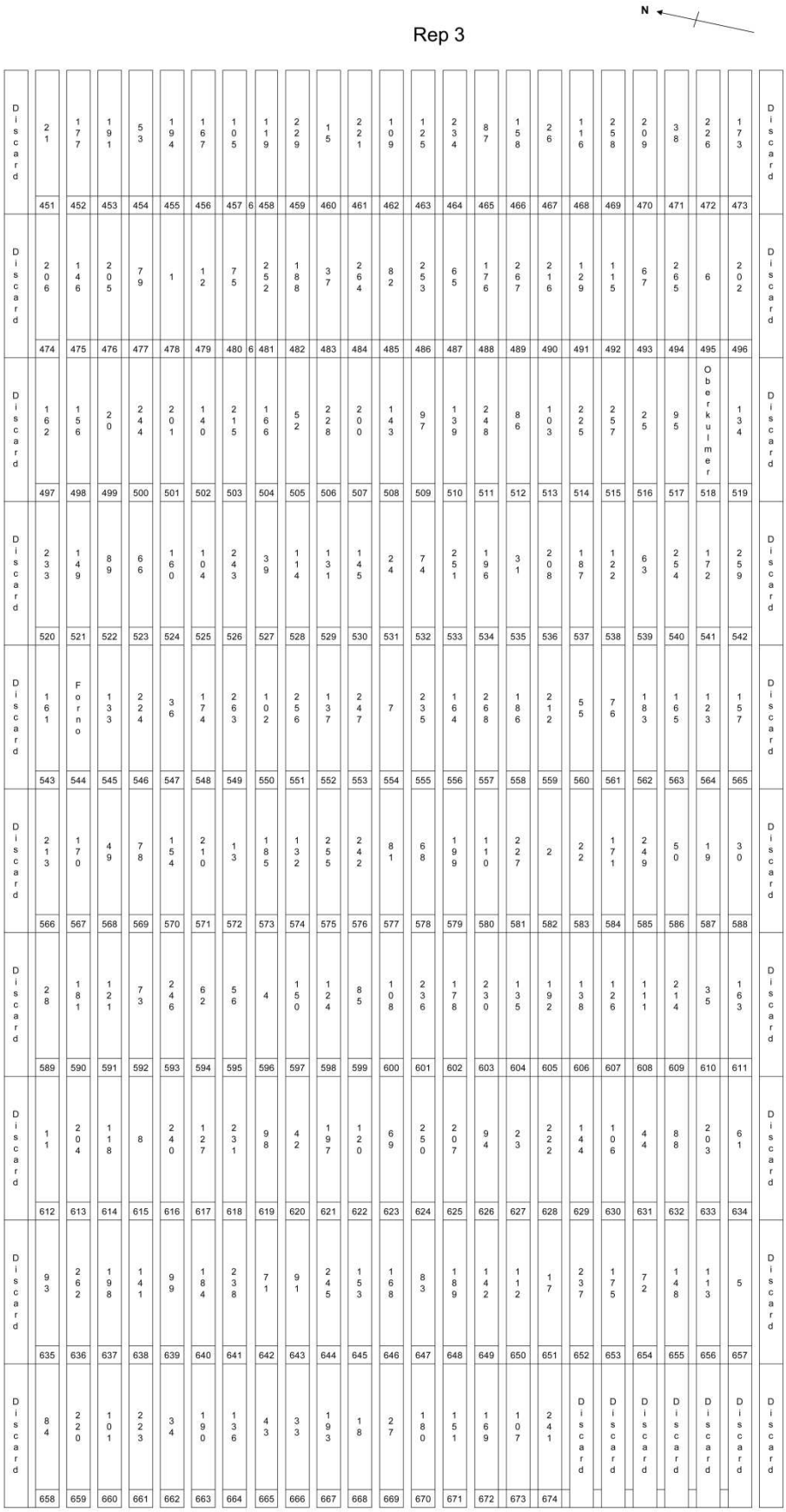
N
Rep 3
Discard
21 451
177 452
191 453
53 454
194 455
167 456
105 457
6
119 458
229 459
15 460
221 461
109 462
125 463
234 464
87 465
158 466
26 467
116 468
258 469
209 470
38 471
226 472
173 473
206 474
146 475
205 476
79 477
1 478
12 479
75 480
6
252 481
188 482
37 483
264 484
82 485
253 486
65 487
176 488
267 489
216 490
129 491
115 492
67 493
265 494
6 495
202 496
162 497
156 498
20 499
244 500
201 501
140 502
215 503
166 504
52 505
228 506
200 507
143 508
97 509
139 510
248 511
86 512
103 513
225 514
257 515
25 516
95 517
Oberkulmer 518
134 519
233 520
149 521
89 522
66 523
160 524
104 525
243 526
39 527
114 528
131 529
145 530
24 531
74 532
251 533
196 534
31 535
208 536
187 537
122 538
63 539
254 540
172 541
259 542
161 543
Forno 544
133 545
224 546
36 547
174 548
263 549
102 550
256 551
137 552
247 553
7 554
235 555
164 556
268 557
186 558
212 559
55 560
76 561
183 562
165 563
123 564
157 565
213 566
170 567
49 568
78 569
154 570
210 571
13 572
185 573
132 574
255 575
242 576
81 577
68 578
199 579
110 580
227 581
2 582
22 583
171 584
249 585
50 586
19 587
30 588
28 589
181 590
121 591
73 592
246 593
62 594
56 595
4 596
150 597
124 598
85 599
108 600
236 601
178 602
230 603
135 604
192 605
138 606
126 607
111 608
214 609
35 610
163 611
11 612
204 613
118 614
8 615
240 616
127 617
231 618
98 619
42 620
197 621
120 622
69 623
250 624
207 625
94 626
23 627
222 628
144 629
106 630
44 631
88 632
203 633
61 634
93 635
262 636
198 637
141 638
99 639
184 640
238 641
71 642
91 643
245 644
153 645
168 646
83 647
189 648
142 649
112 650
17 651
237 652
175 653
72 654
148 655
113 656
5 657
Discard
84 658
220 659
101 660
223 661
34 662
190 663
136 664
43 665
33 666
193 667
18 668
27 669
180 670
151 671
169 672
107 673
241 674
Discard
Discard
Discard
Discard
Discard
Discard

Field trial 2011−2012: the subset population (72 lines + parents)

Line	Flowering time (dd/mm/yy)		Line	Flowering time (dd/mm/yy)	
	2010	2011		2010	2011
2	21/06/10	05/06/11	134	21/06/10	05/06/11
4	21/06/10	07/06/11	135	25/06/10	07/06/11
6	25/06/10	07/06/11	136	21/06/10	05/06/11
7	25/06/10	07/06/11	145	21/06/10	05/06/11
12	21/06/10	05/06/11	153	25/06/10	07/06/11
13	21/06/10	05/06/11	156	25/06/10	07/06/11
21	21/06/10	07/06/11	157	21/06/10	07/06/11
28	25/06/10	07/06/11	169	21/06/10	07/06/11
31	25/06/10	07/06/11	174	21/06/10	07/06/11
34	21/06/10	07/06/11	177	21/06/10	07/06/11
35	21/06/10	05/06/11	180	21/06/10	05/06/11
43	25/06/10	07/06/11	185	21/06/10	07/06/11
49	25/06/10	07/06/11	186	21/06/10	05/06/11
53	21/06/10	05/06/11	189	21/06/10	07/06/11
56	21/06/10	05/06/11	190	21/06/10	07/06/11
63	21/06/10	05/06/11	191	21/06/10	07/06/11
67	25/06/10	07/06/11	196	21/06/10	07/06/11
69	21/06/10	07/06/11	197	21/06/10	07/06/11
72	21/06/10	07/06/11	200	21/06/10	05/06/11
75	21/06/10	05/06/11	202	25/06/10	05/06/11
76	21/06/10	07/06/11	207	21/06/10	07/06/11
79	21/06/10	05/06/11	210	25/06/10	07/06/11
83	21/06/10	05/06/11	214	21/06/10	07/06/11
84	21/06/10	07/06/11	215	25/06/10	07/06/11
89	21/06/10	05/06/11	230	21/06/10	05/06/11
91	25/06/10	07/06/11	231	25/06/10	07/06/11
93	25/06/10	07/06/11	234	25/06/10	07/06/11
97	25/06/10	07/06/11	236	21/06/10	07/06/11
98	21/06/10	07/06/11	238	21/06/10	05/06/11
99	21/06/10	07/06/11	242	25/06/10	07/06/11
101	21/06/10	07/06/11	247	25/06/10	05/06/11
103	21/06/10	05/06/11	248	25/06/10	07/06/11
116	25/06/10	07/06/11	249	21/06/10	07/06/11
118	21/06/10	07/06/11	256	21/06/10	07/06/11
122	21/06/10	07/06/11	257	21/06/10	07/06/11
123	21/06/10	05/06/11	Forno	15-06-10	02-06-11
124	21/06/10	07/06/11	Oberkulmer	25-06-10	10-06-11

Field trial 2012−2013: agronomy

Title		Wheat x Spelt
Researcher		Quan Xie - Debbie Sparkes
	Date	**Details**
Field		S26
Previous crop		Winter Oats
SNS N Index	2013/3/2	30 kg/ha, SNS Index 0
Soil Indices		P:5, K:4, Mg:4, pH:7.3
Cultivations	2012/9/17	Plough + Press
	2012/10/31	Roll after drilling
Crop/variety		Various (see seedrates tab)
TGW (g)		Various (see seedrates tab)
Sowing	2012/10/31	
Seed rate (m^{-2})		250
Drill type		Wintersteiger
Row width (m)		0.125
Plot length (m)		12.0
Plot width (m)		1.625
Fertiliser	2013/2/27	Manganese 15% @1l/ha
	2013/3/6	116 kg/ha 34.5% Nitram (40kg/ha N)
	2013/3/21	Manganese 15% @ 2l/ha
	2013/4/17	174 kg/ha 34.5% Nitram (60kg/ha N)
	2013/5/2	Manganese 15% @ 2l/ha
	2013/5/13	Manganese 15% @ 1l/ha
	2013/5/21	174 kg/ha 34.5% Nitram (60kg/ha N)
	2013/6/3	Magnor @ 1.0 l/ha
Herbicide	2012/10/2	Round-up @ 2.5 l/ha (Pre-drilling)
	2012/10/30	Round-up @ 2.5 l/ha (Pre-drilling)
	2013/4/10	Hatra @ 1l/ha + Charge @ 2l/ha + Liberator @ 0.3l/ha + Zeal @ 0.3l/ha
	2013/6/3	Lorate @ 25g/ha
Fungicide	2013/5/2	Kestrel @ 1l/ha + Phoenix @ 1l/ha + Flexity @ 0.14l/ha
	2013/6/3	Brutus @ 1.25 l/ha + Amistar Opti @ 1.0 l/ha + Vegas @ 0.15 l/ha
	2013/6/26	Brutus @ 1l/ha + Bravo @ 1l/ha + Instinct @ 0.5l/ha
Insecticide		
PGR	2013/5/2	Chlormequat @ 1.4l/ha
	2013/5/13	Moddus @ 0.2l/ha
	2013/6/3	Terpal @ 0.5 l/ha

Field trial 2012−2013: experimental design

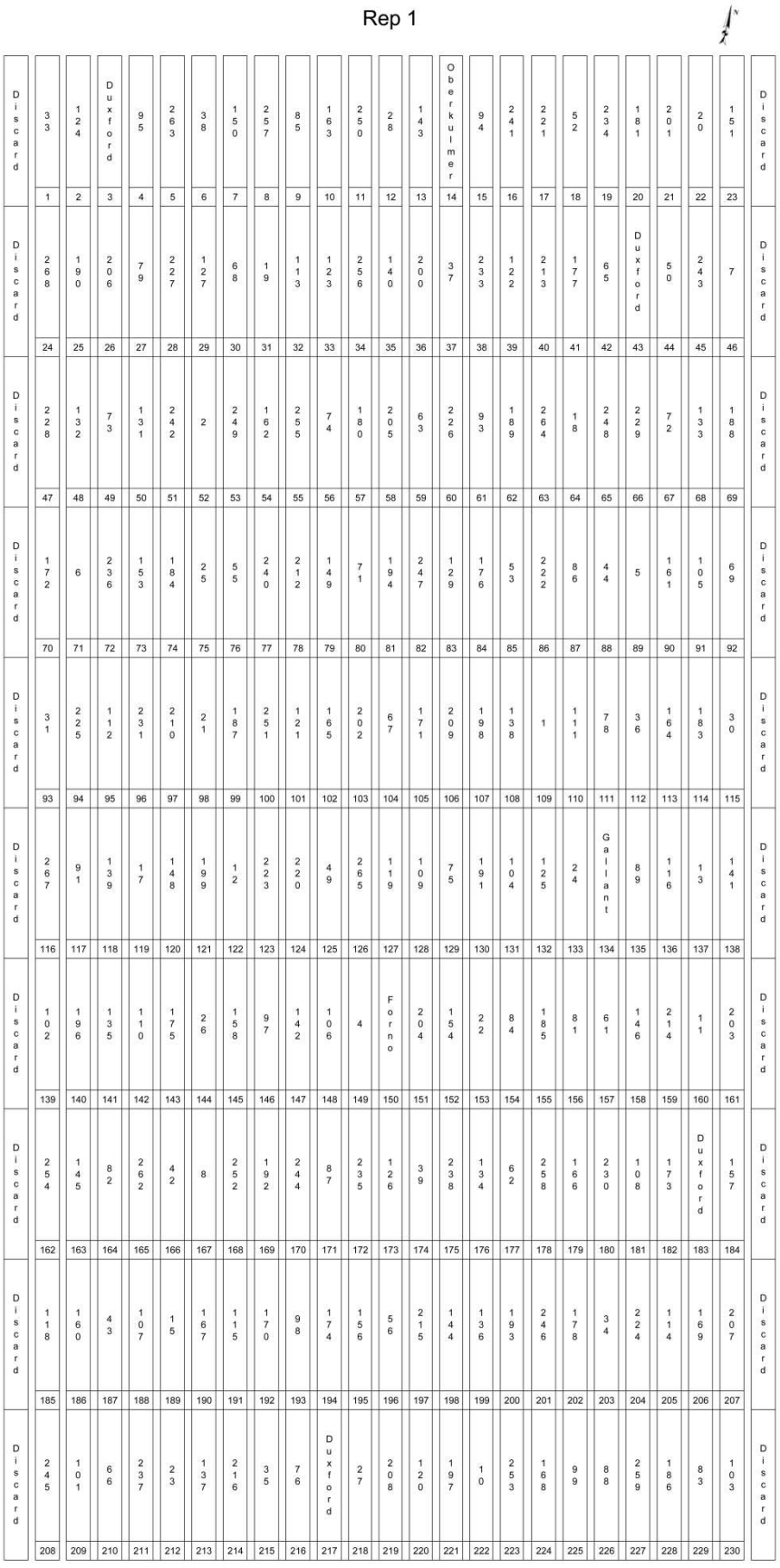

Rep 2

26	139	227	67	157	103	63	198	10	185	87	42	174	241	36	122	137	168	22	95	149	78	49	Discard
231	232	233	234	235	236	237	238	239	240	241	242	243	244	245	246	247	248	249	250	251	252	253	
183	148	173	39	17	221	167	264	76	144	213	233	83	66	197	Duxford	110	240	162	253	136	231	143	Discard
254	255	256	257	258	259	260	5 261	262	263	264	265	266	267	268	269	270	271	272	273	274	275	276	
238	91	212	138	33	237	172	99	Gallant	56	225	131	252	38	263	11	242	156	226	84	15	102	210	Discard
277	278	279	280	281	282	283	5 284	285	286	287	288	289	290	291	292	293	294	295	296	297	298	299	
120	192	37	4	111	234	109	186	127	Forno	21	154	268	206	55	184	27	8	75	105	254	65	220	Discard
300	301	302	303	304	305	306	5 307	308	309	310	311	312	313	314	315	316	317	318	319	320	321	322	
164	101	255	158	116	82	196	243	176	104	25	Duxford	123	35	199	171	191	88	115	244	175	142	30	Discard
323	324	325	326	327	328	329	5 330	331	332	333	334	335	336	337	338	339	340	341	342	343	344	345	
249	133	44	202	12	53	209	181	89	257	187	18	166	251	2	129	Duxford	150	256	73	204	180	31	Discard
346	347	348	349	350	351	352	5 353	354	355	356	357	358	359	360	361	362	363	364	365	366	367	368	
141	190	71	28	259	161	215	7	112	222	62	228	193	126	50	135	214	23	140	114	69	230	121	Discard
369	370	371	372	373	374	375	5 376	377	378	379	380	381	382	383	384	385	386	387	388	389	390	391	
262	94	245	20	200	79	5	265	68	Oberkuimer	203	106	43	248	177	85	235	207	13	258	224	108	246	Discard
392	393	394	395	396	397	398	5 399	400	401	402	403	404	405	406	407	408	409	410	411	412	413	414	
170	151	247	24	86	132	145	223	118	74	229	93	188	97	72	169	163	194	201	81	250	178	208	Discard
415	416	417	418	419	420	421	5 422	423	424	425	426	427	428	429	430	431	432	433	434	435	436	437	
134	205	61	98	124	Duxford	19	107	267	52	216	165	34	1	189	113	160	146	6	153	236	119	125	Discard
438	439	440	441	442	443	444	5 445	446	447	448	449	450	451	452	453	454	455	456	457	458	459	460	

129	63	235	95	89	106	184	27	250	143	262	84	126	36	240	173	5	149	255	Duxford	249	136	13	Discard
461	462	463	464	465	466	467	468	469	470	471	472	473	474	475	476	477	478	479	480	481	482	483	
220	193	12	180	154	Duxford	259	208	62	268	52	234	161	135	94	44	122	162	221	25	201	101	256	Discard
484	485	486	487	488	489	490	5	491	492	493	494	495	496	497	498	499	500	501	502	503	504	505	506	
114	248	99	26	200	83	215	167	23	247	185	71	Oberkulmer	254	75	183	141	66	82	174	56	186	111	Discard
507	508	509	510	511	512	513	5	514	515	516	517	518	519	520	521	522	523	524	525	526	527	528	529	
187	55	165	43	253	224	121	267	28	153	241	49	258	172	238	35	229	166	110	127	6	131	151	Discard
530	531	532	533	534	535	536	5	537	538	539	540	541	542	543	544	545	546	547	548	549	550	551	552	
33	206	150	93	171	148	7	Duxford	233	199	125	65	212	115	74	42	91	24	188	168	107	216	11	Discard
553	554	555	556	557	558	559	5	560	561	562	563	564	565	566	567	568	569	570	571	572	573	574	575	
263	181	72	243	192	37	228	163	236	79	204	194	15	222	1	246	156	88	144	53	210	68	207	Discard
576	577	578	579	580	581	582	5	583	584	585	586	587	588	589	590	591	592	593	594	595	596	597	598	
124	17	176	85	257	116	Gallant	102	189	145	231	30	139	105	242	61	226	132	8	251	118	21	175	Discard
599	600	601	602	603	604	605	5	606	607	608	609	610	611	612	613	614	615	616	617	618	619	620	621	
213	87	78	22	142	134	252	10	245	73	264	169	97	50	227	196	230	4	198	Duxford	140	244	103	Discard
622	623	624	625	626	627	628	5	629	630	631	632	633	634	635	636	637	638	639	640	641	642	643	644	
67	202	112	197	157	34	108	214	Forno	18	205	98	160	223	138	178	190	39	31	120	237	158	76	Discard
645	646	647	648	649	650	651	5	652	653	654	655	656	657	658	659	660	661	662	663	664	665	666	667	
177	19	170	104	191	2	137	265	119	38	209	164	86	225	69	133	146	81	203	123	20	113	109	Discard
668	669	670	671	672	673	674	5	675	676	677	678	679	680	681	682	683	684	685	686	687	688	689	690	

Field trial 2012−2013: the subset population (110 lines + parents)

These lines were also used in the glasshouse experiment in 2013−2014.

Line	Flowering time (dd/mm/yy)		Line	Flowering time (dd/mm/yy)		Line	Flowering time (dd/mm/yy)	
	2010	2011		2010	2011		2010	2011
2	21/06/10	05/06/11	101	21/06/10	07/06/11	192	18/06/10	07/06/11
4	21/06/10	07/06/11	103	21/06/10	05/06/11	193	18/06/10	07/06/11
5	25/06/10	05/06/11	107	28/06/10	07/06/11	196	21/06/10	07/06/11
7	25/06/10	07/06/11	110	25/06/10	05/06/11	197	21/06/10	07/06/11
12	21/06/10	05/06/11	111	18/06/10	05/06/11	202	25/06/10	05/06/11
13	21/06/10	05/06/11	113	18/06/10	05/06/11	207	21/06/10	07/06/11
21	21/06/10	07/06/11	118	21/06/10	07/06/11	208	25/06/10	05/06/11
22	18/06/10	05/06/11	122	21/06/10	07/06/11	209	28/06/10	07/06/11
23	28/06/10	05/06/11	123	21/06/10	05/06/11	210	25/06/10	07/06/11
24	28/06/10	07/06/11	124	21/06/10	07/06/11	212	18/06/10	05/06/11
25	28/06/10	07/06/11	134	21/06/10	05/06/11	214	21/06/10	07/06/11
26	28/06/10	05/06/11	135	25/06/10	07/06/11	215	25/06/10	07/06/11
27	25/06/10	05/06/11	136	21/06/10	05/06/11	216	18/06/10	07/06/11
28	25/06/10	07/06/11	138	28/06/10	07/06/11	220	28/06/10	07/06/11
31	25/06/10	07/06/11	145	21/06/10	05/06/11	224	18/06/10	05/06/11
34	21/06/10	07/06/11	146	18/06/10	05/06/11	228	18/06/10	05/06/11
36	28/06/10	07/06/11	148	18/06/10	05/06/11	230	21/06/10	05/06/11
42	28/06/10	07/06/11	153	25/06/10	07/06/11	231	25/06/10	07/06/11
43	25/06/10	07/06/11	156	25/06/10	07/06/11	234	25/06/10	07/06/11
49	25/06/10	07/06/11	157	21/06/10	07/06/11	236	21/06/10	07/06/11
53	21/06/10	05/06/11	161	28/06/10	07/06/11	237	21/06/10	07/06/11
56	21/06/10	05/06/11	164	25/06/10	05/06/11	238	21/06/10	05/06/11
63	21/06/10	05/06/11	166	25/06/10	05/06/11	242	25/06/10	07/06/11
67	25/06/10	07/06/11	167	18/06/10	05/06/11	245	28/06/10	07/06/11
69	21/06/10	07/06/11	168	25/06/10	05/06/11	247	25/06/10	05/06/11
72	21/06/10	07/06/11	169	21/06/10	07/06/11	248	25/06/10	07/06/11
76	21/06/10	07/06/11	174	21/06/10	07/06/11	249	21/06/10	07/06/11
79	21/06/10	05/06/11	176	18/06/10	07/06/11	251	18/06/10	07/06/11
83	21/06/10	05/06/11	177	21/06/10	07/06/11	253	28/06/10	07/06/11
84	21/06/10	07/06/11	178	28/06/10	07/06/11	255	18/06/10	05/06/11
85	28/06/10	07/06/11	180	21/06/10	05/06/11	256	21/06/10	07/06/11
86	21/06/10	07/06/11	184	18/06/10	05/06/11	257	21/06/10	07/06/11
89	21/06/10	05/06/11	185	21/06/10	07/06/11	262	25/06/10	05/06/11
91	25/06/10	07/06/11	186	21/06/10	05/06/11	263	28/06/10	05/06/11
93	25/06/10	07/06/11	187	25/06/10	07/06/11	Forno	15-06-10	02-06-11
97	25/06/10	07/06/11	189	21/06/10	07/06/11	Oberkulmer	25-06-10	10-06-11
98	21/06/10	07/06/11	190	21/06/10	07/06/11			
99	21/06/10	07/06/11	191	21/06/10	07/06/11			

Views of the field and glasshouse experiments

Field trial view

Glasshouse experiment view